

# COOL-COLOR ROOFING MATERIAL ATTACHMENT 11: TASK 2.7.1 REPORTS - TECHNOLOGY TRANSFER



Arnold Schwarzenegger  
Governor

## PIER FINAL PROJECT REPORT

*Prepared For:*  
**California Energy Commission**  
Public Interest Energy Research Program

*Prepared By:*  
**Lawrence Berkeley National Laboratory  
and Oak Ridge National Laboratory**



ERNEST ORLANDO LAWRENCE  
BERKELEY NATIONAL LABORATORY

June 2006  
CEC-500-2006-067-AT11



***Prepared By:***

Lawrence Berkeley National Laboratory  
Hashem Akbari  
Berkeley, California  
Contract No. 500-01-021

Oak Ridge National Laboratory  
William Miller  
Oak Ridge, Tennessee

***Prepared For:***

California Energy Commission  
Public Interest Energy Research (PIER) Program

Chris Scruton  
***Contract Manager***

Ann Peterson  
***Building End-Use Energy Efficiency Team Leader***

Nancy Jenkins  
***PIER Energy Efficiency Research Office Manager***

Martha Krebs, Ph.D.  
***Deputy Director***  
**ENERGY RESEARCH AND DEVELOPMENT  
DIVISION**

B. B. Blevins  
***Executive Director***

**DISCLAIMER**

This report was prepared as the result of work sponsored by the California Energy Commission. It does not necessarily represent the views of the Energy Commission, its employees or the State of California. The Energy Commission, the State of California, its employees, contractors and subcontractors make no warrant, express or implied, and assume no legal liability for the information in this report; nor does any party represent that the uses of this information will not infringe upon privately owned rights. This report has not been approved or disapproved by the California Energy Commission nor has the California Energy Commission passed upon the accuracy or adequacy of the information in this report.

**Reports included in this attachment:**

- Effects of soiling and cleaning on the reflectance and solar heat gain of a light-colored roofing membrane
- Experimental analysis of the natural convection effects observed within the closed cavity of tile roof systems
- Cool metal roofing is topping the building envelope with energy efficiency and sustainability
- Special infrared reflective pigments make a dark roof reflect almost like a white roof
- Cool colored materials for roofs
- Cool colored roofs to save energy and improve air quality
- Cool metal roofing tested for energy efficiency and sustainability
- PVDF coatings with special IR reflective pigments
- Cool color roofs with complex inorganic color pigments
- Potentials of urban heat island mitigation
- Aging and weathering of cool roofing membranes
- Cooler tile-roofed buildings with near-infrared-reflective nonwhite coatings
- Cooling down the house: residential roofing products will soon boast “cool” surfaces
- Solar spectral optical properties of pigments
- Cool colors: a roofing study is developing cool products for residential roofs



# Effects of soiling and cleaning on the reflectance and solar heat gain of a light-colored roofing membrane

Ronnen Levinson<sup>a,\*</sup>, Paul Berdahl<sup>a</sup>, Asmeret Asefaw Berhe<sup>b</sup>, Hashem Akbari<sup>a</sup>

<sup>a</sup>Heat Island Group, Lawrence Berkeley National Laboratory, 1 Cyclotron Road, Berkeley, CA 94720, USA

<sup>b</sup>Ecosystem Sciences Division, University of California at Berkeley, Berkeley, CA 94720, USA

Received 24 May 2005; received in revised form 24 August 2005; accepted 24 August 2005

## Abstract

A roof with high solar reflectance and high thermal emittance (e.g., a white roof) stays cool in the sun, reducing cooling power demand in a conditioned building and increasing summertime comfort in an unconditioned building. The high initial solar reflectance of a white membrane roof (circa 0.8) can be lowered by deposition of soot, dust, and/or biomass (e.g., fungi or algae) to about 0.6; degraded solar reflectances range from 0.3 to 0.8, depending on exposure. We investigate the effects of soiling and cleaning on the solar spectral reflectances and solar absorptances of 15 initially white or light-gray polyvinyl chloride membrane samples taken from roofs across the United States. Black carbon and organic carbon were the two identifiable strongly absorbing contaminants on the membranes. Wiping was effective at removing black carbon, and less so at removing organic carbon. Rinsing and/or washing removed nearly all of the remaining soil layer, with the exception of (a) thin layers of organic carbon and (b) isolated dark spots of biomass. Bleach was required to clear these last two features. At the most soiled location on each membrane, the ratio of solar reflectance to unsoiled solar reflectance (a measure of cleanliness) ranged from 0.41 to 0.89 for the soiled samples; 0.53 to 0.95 for the wiped samples; 0.74 to 0.98 for the rinsed samples; 0.79 to 1.00 for the washed samples; and 0.94 to 1.02 for the bleached samples. However, the influences of membrane soiling and cleaning on roof heat gain are better gauged by fractional variations in solar absorptance. Solar absorptance ratios (indicating solar heat gain relative to that of an unsoiled membrane) ranged from 1.4 to 3.5 for the soiled samples; 1.1 to 3.1 for the wiped samples; 1.0 to 2.0 for the rinsed samples; 1.0 to 1.9 for the washed samples; and 0.9 to 1.3 for the bleached samples.

© 2005 Elsevier Ltd. All rights reserved.

**Keywords:** Roofing; Single-ply membrane; Polyvinyl chloride (PVC); Black carbon; Organic carbon; Biomass; Fungi; Algae; Solar spectral reflectance; Solar reflectance; Solar absorptance; Absorption; Optical depth; Soiling; Cleaning; Wiping; Washing; Rinsing; Bleaching

## 1. Introduction

A roof with high solar reflectance and high thermal emittance (e.g., a white roof) stays cool in

the sun, reducing cooling energy use in a conditioned building and increasing comfort in an unconditioned building. Prior research has indicated that savings are greatest for buildings located in climates with long cooling seasons and short heating seasons, particularly those buildings that have distribution ducts in the plenum, distribution ducts on the roof, and/or low rates of plenum

\*Corresponding author. Tel.: +1 510 486 7494;  
fax: +1 510 486 6658.

E-mail address: [RMLevinson@LBL.gov](mailto:RMLevinson@LBL.gov) (R. Levinson).



<b>Nomenclature</b>		$\delta Z$	variation in thickness of soil layer
<i>English symbols</i>		$\delta\tau$	absolute decrease in spectral optical depth of soil layer
$A$	solar absorptance of membrane	$\eta$	average pathlength parameter
$c$	coefficient	$\lambda$	wavelength of light (in air)
$f$	fraction of membrane area covered by soil layer	$\tau$	spectral optical depth of soil layer
$r$	spectral reflectance of membrane	<i>Subscripts and superscripts</i>	
$R$	solar reflectance of membrane	0	unsoiled
$t$	spectral transmittance of soil layer	$n$	state $n$ , or cleaning process that begins from state $n$ states: 5 = soiled, 4 = wiped, 3 = rinsed, 2 = washed, 1 = bleached, 0 = unsoiled
$z$	position in soil layer (height above membrane's surface)	$N$	soiled (state 5)
$Z$	soil layer thickness	'	of nonuniform thickness
<i>Greek symbols</i>			
$\alpha$	spectral absorption coefficient		
$\gamma$	fraction remaining of initial spectral optical depth of soil layer		

ventilation (Abkari, 1998; Akbari et al., 1999; Konopacki and Akbari, 1998). Widespread use of cool roofs can also reduce summertime urban air temperatures by 1 to 2K (Akbari and Konopacki, 1998; Young, 1998; Pomerantz et al., 1999; Akbari et al., 1999).

The high initial solar reflectance of a white roof (not less than 0.7 for products meeting California's Title-24 energy code for nonresidential buildings with low-slope roofs (CEC, 2005)) can be degraded by deposition of soot, dust, and/or biomass (e.g., fungi or algae) to about 0.6, depending on exposure. Some materials have higher initial solar reflectance; white polyvinyl chloride (PVC) membranes, for example, typically have initial solar reflectances exceeding 0.8. Simulations indicate that replacing a roof of solar reflectance 0.20 (e.g., a weathered medium-gray roof) on a typical California commercial building by a roof of solar reflectance 0.55 (e.g., a weathered white roof) can yield net energy savings (cooling energy savings – heating energy penalties) with a 15-year net present value (NPV) of about \$1 to \$7/m<sup>2</sup> of roof area (Levinson et al., 2005a). The energy savings achieved by replacing a less reflective roof with a more reflective roof are linearly proportional to the change in the solar reflectance (Konopacki et al., 1997). Hence, a cleaning regimen that maintains the solar reflectance of a white roof at its initial value of 0.70 can increase the 15-year

NPV of net energy savings by over 40%, worth an additional \$0.5 to \$3/m<sup>2</sup>.

Slightly over two years of exposure at an outdoor test facility in eastern Tennessee reduced the typical solar reflectance of eight white latex coatings applied to low-slope roofing to 0.56 from 0.84 (Wilkes et al., 2000). Three and a half years of exposure at the same facility decreased the average solar reflectance of four low-slope, single-ply, white PVC roofing membranes to 0.49 from 0.86, and reduced the solar reflectance of a low-slope metal roofing panel with a white polyvinylidene fluoride (PVDF) coating to 0.62 from 0.64 (Roodvoets et al., 2004a). Solar reflectances stabilized after about two years in both studies.

A simple gauge of the cleanliness of an initially reflective surface bearing contaminants that absorb but do not scatter light is the ratio of its solar reflectance after exposure to its solar reflectance before exposure. This value approaches zero for heavily soiled surfaces and is one for clean surfaces. The solar reflectance ratios for the PVC membranes and the adjacent PDVF-coated metal panel were 0.57 and 0.97, respectively, indicating that the PVC was much more soiled.

Thermal cycling can drive liquid plasticizers to the surface of a PVC membrane, rendering it tacky (Griffin, 2002) and hence prone to collect contaminants. Roodvoets et al. (2004a) detected significant

growth of biomass (primarily fungi) on the PVC membranes exposed at the test facility. They hypothesized that airborne microorganisms attached to and possibly fed on the leached plasticizers, establishing a net-like growth on the surface that accelerated soiling by trapping dirt. The cleanliness of the PVDF-coated metal panel was attributed to its smoother and thus more difficult to colonize surface (Miller et al., 2002).

Washing the soiled PVC membranes with water or with one of several commercially available cleaning agents—trisodium phosphate, a household cleaner/degreaser, or a chlorine solution—removed most of the contaminants, raising typical solar reflectance to 0.80–0.85 (Roodvoets et al., 2004b) and typical solar reflectance ratio to 0.93–0.99.

Our earlier investigation of the effects of weathering on the solar spectral reflectances of two roofing surfaces—a light-gray PVC roofing membrane and a steel panel with a zinc-aluminum coating—concluded that their reflectances were decreased primarily by the deposition of soot (Berdahl et al., 2002). Washing with a mild soap solution removed the carbon from the PVC membrane, but not from the steel panel.

In North America, visible light (400–700 nm) conveys 43% of the power in the air-mass 1.5 global solar irradiance spectrum (300–2500 nm); the

remainder arrives as near-infrared (700–2500 nm, 52%) or ultraviolet (300–400 nm, 5%) radiation (ASTM, 2003) (Fig. 1). We noted in our earlier study that most of the minerals found in atmospheric dust and soil are either nonabsorbing in the visible and near infrared ranges (quartz, ammonium sulfate, sodium chloride) or have a definite absorption spectrum (hematite [iron oxide red], hydrated clays). Soot—particulate matter emitted from fossil fuel combustion—is a notable exception. Soot is primarily “black carbon,” though it can also include “organic carbon” (Kirchstetter and Novakov, 2004). Black carbon is refractory, elemental in composition (i.e., presents with a low ratio of hydrogen to carbon), and is insoluble in water (and other solvents); organic carbon is that contained in a typically complex mixture of organic compounds, and is generally taken to be the difference between total carbon and black carbon (Turpin and Lim, 2001; Turpin et al., 2000; Kirchstetter et al., 2005). Black carbon has strong absorption with a nearly featureless spectrum. The strong optical absorption by black carbon also means that it can be a minor component of the accumulated dust but still be the dominant source of reflectance change.

Spectral features in absorption by the “soil” layer on a roofing surface can identify contaminants. Fig. 2 shows typical spectral absorption coefficients

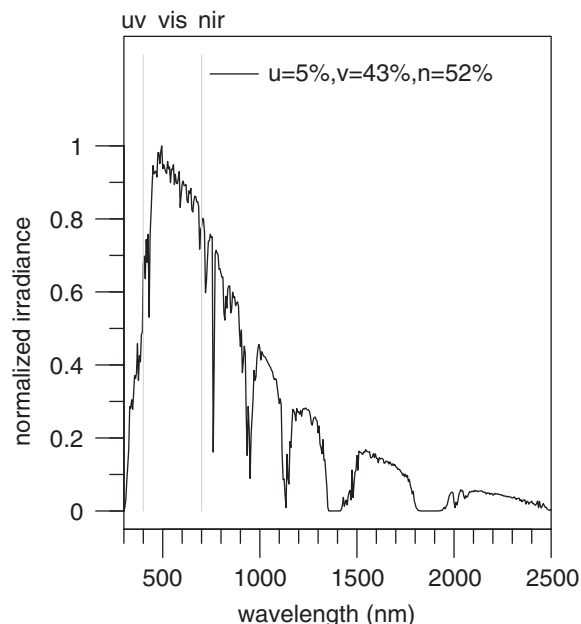


Fig. 1. Air-mass 1.5 global solar spectral irradiance typical of North American insolation (5% ultraviolet, 43% visible, 52% near-infrared) (ASTM, 2003).

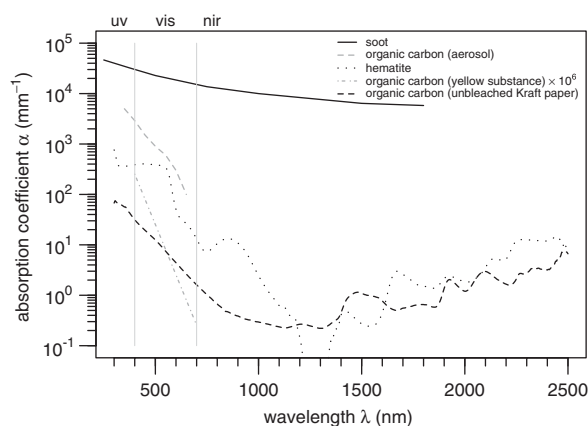


Fig. 2. Typical spectral absorption coefficients  $\alpha(\lambda)$  of propane soot (Lindberg et al., 1993), hematite (Levinson et al., 2005c), and three sources of organic carbon: vehicle-exhaust and wood-smoke aerosols (Kirchstetter and Novakov, 2004), organic matter dissolved in seawater (“yellow substance”) (Kirchstetter and Novakov, 2004), and unbleached brown Kraft paper. Absorption coefficient values for the yellow substance are multiplied by  $10^6$  to fit the scale.

of propane soot (Lindberg et al., 1993), an acrylic paint film pigmented with hematite (red iron oxide; mean particle size  $0.3\ \mu\text{m}$ ; pigment volume concentration 3%) (Levinson et al., 2005c), and three samples of organic carbon. The first specimen of organic carbon was extracted from aerosols, namely vehicle exhaust and wood smoke (Kirchstetter and Novakov, 2004); we converted the absorption efficiency ( $\text{m}^2\text{g}^{-1}$ ) presented in this reference to an absorption coefficient ( $\text{mm}^{-1}$ ) by assuming a nominal density of  $1\text{ g cm}^{-3}$  for organic carbon. The second specimen was organic matter dissolved in seawater, commonly referred to as “yellow substance” (Kirchstetter and Novakov, 2004). The third specimen was a sheet of unbleached, brown Kraft paper, characterized following the methodology of Levinson et al. (2005b). We obtained a spectral reflectance curve similar to that of the brown Kraft paper when we characterized a brown dead leaf.

Featureless absorption wherein magnitude is inversely proportional to wavelength (declining by about half an order of magnitude between 400 and 1500 nm) signifies the presence of black carbon. Rapid, exponential decay of about two to three orders of magnitude across the visible spectrum is characteristic of absorption by organic carbon. Hematite has strong, uniform absorption in the blue and green spectra (400–600 nm); rapid, roughly exponential decay of absorption between 600 and 1200 nm; and an absorption peak between 800 and 900 nm. The absorption features in the 1300–2500 nm range shown for paper-derived organic carbon and for hematite may originate from vibrations of hydrogen atoms (in groups such as C–H,  $\text{H}_2\text{O}$ , and OH) in the paper and in the polymer binder of the red paint.

The current study examines the effects of exposure and cleaning on the solar spectral reflectances and solar absorptances of 15 initially white or light-gray membrane samples taken from roofs across the United States. Particular attention is paid to spectral characterization of the extents to which various laboratory representations of roof cleaning processes (e.g., rinsing to simulate rain) can reduce light absorption by surface contaminants and thereby increase roof reflectance. Specifically, we seek to answer the following questions:

1. What contaminants reduce the reflectance of the membranes, and by what processes are they removed?

2. To what extent does soiling degrade and cleaning improve the reflectance of a light-colored membrane?
3. How do soiling and cleaning affect the solar heat gain of a light-colored membrane roof?

## 2. Theory

### 2.1. Spectral optical depth of soil layer

We consider a very simple optical model for the soil layer. Our goal is to define “spectral optical depth,” a parameter that can be used to examine spectral absorption features in soil layers. Since the light-colored membrane substrate is highly reflective (at wavelengths longer than 400 nm), the scattering by the soil layer itself is not expected to have a large effect on the reflectance of the soil/membrane composite. We therefore neglect soil scattering, and focus on the effect of soil absorptance. A more sophisticated optical model, while desirable, would introduce a level of complexity that we wish to avoid in this study.

Consider a flat, uniform, and opaque membrane. An absorbing and nonscattering soil layer of uniform thickness  $Z_n$  will have spectral optical depth

$$\tau_n(\lambda) \equiv \int_0^{Z_n} \alpha(z, \lambda) dz, \quad (1)$$

where  $\alpha(z, \lambda)$  is the soil’s spectral absorption coefficient (assumed cross-section invariant) at height  $z$  above the membrane’s surface. Applying Beer’s law (Incropera and DeWitt, 1985), the soil layer has spectral transmittance

$$t_n(\lambda) = \exp[-\eta \tau_n(\lambda)], \quad (2)$$

where the average pathlength parameter  $\eta$ , or ratio of light pathlength to layer thickness, is 1 for surface-normal collimated light and 2 for perfectly diffuse light.

The soil layer reduces the spectral reflectance of the membrane by the square of its spectral transmittance. That is, the spectral reflectance of the soiled membrane is

$$r_n(\lambda) = r_0(\lambda) \exp[-2\eta \tau_n(\lambda)], \quad (3)$$

where  $r_0(\lambda)$  is the spectral reflectance of the unsoiled membrane. Rearranging, the spectral optical depth of the soil layer can be estimated from the ratio of the spectral reflectance of the soiled membrane to

that of the unsoiled membrane as

$$\tau_n(\lambda) = -\frac{1}{2\eta} \ln \left[ \frac{r_n(\lambda)}{r_0(\lambda)} \right]. \quad (4)$$

If the soil layer is normally illuminated with collimated light and the membrane reflects diffusely, the effective value of  $\eta$  in Eqs. (3) and (4) is  $\frac{3}{2}$ .

We compute the spectral optical depth  $\tau_n(\lambda)$  of the soil layer in each state  $n$  to identify soil constituents, and to determine the extents to which these contaminants are removed by each cleaning process. The values of spectral optical depth  $\tau_n(\lambda)$  measured in this study should be typical of any light-colored PVC membranes exposed to similar soiling and cleaning processes. However, our assumption that the soil layer is nonscattering may be unsuited to describing the effects of soiling on the spectral and solar reflectances of an initially dark surface. For example, a scattering-induced reflectance rise of several hundredths may represent a large *fractional* increase in the reflectance of a black membrane whose initial reflectance is about 0.05 across the entire solar spectrum. Hence, any model of the effect of soiling on the reflectance of a dark membrane should consider both absorption and scattering in the soil layer.

Nonuniformities in the thickness of the soil layer (e.g., bare patches alternating with heavily soiled spots) tend to attenuate peaks in the spectral optical depth curve (Appendix A; see also Berdahl et al. (2002)). This can mask spectral features that would otherwise identify contaminants. For simplicity, we will not try to quantify the magnitudes of these nonuniformities and their effects on spectral optical depth. However, we will note in our analysis when a soil layer appears particularly nonuniform.

## 2.2. Effects of cleaning on spectral optical depth

The effects of cleaning on spectral absorption can be gauged by changes in spectral optical depth. Let  $n = N$  denote the state of the membrane after soiling, but before cleaning. Consider a sequence of cleaning processes—in this study, wiping, rinsing, washing, and bleaching—that raise the spectral reflectance of the soiled membrane from  $r_N(\lambda)$  to  $r_{N-1}(\lambda)$ ,  $r_{N-2}(\lambda)$ , ..., and finally  $r_1(\lambda)$ . We model the cleaning process  $n$  that increases the membrane's spectral reflectance from  $r_n(\lambda)$  to  $r_{n-1}(\lambda)$  as removing a soil sublayer of spectral optical depth

$$\delta\tau_n(\lambda) \equiv \tau_n(\lambda) - \tau_{n-1}(\lambda) = -\frac{1}{2\eta} \ln \left[ \frac{r_n(\lambda)}{r_{n-1}(\lambda)} \right]. \quad (5)$$

Spectral features in  $\delta\tau_n(\lambda)$  can indicate the removal of specific contaminants, such as black carbon, hematite or organic carbon.

The fraction of the spectral optical depth of the initial soil layer  $\tau_N(\lambda)$  remaining in state  $n$  is

$$\gamma_n(\lambda) \equiv \tau_n(\lambda)/\tau_N(\lambda). \quad (6)$$

## 2.3. Effects of soiling and cleaning on solar reflectance and solar heat gain

One measure of the influences of soiling and cleaning on solar reflectance is  $R_n/R_0$ , the ratio of a membrane's solar reflectance in state  $n$  to that in its unsoiled state 0. The geometric relationship among the spectral reflectances of the unsoiled, soiled, and cleaned membranes generally precludes any simple theoretical relationship among their solar reflectances (Appendix B). Hence, the solar reflectance ratio  $R_n/R_0$  is just an empirical measure of cleanliness, equalling one when the membrane is unsoiled, and approaching zero when the membrane is covered with an opaque, nonscattering soil layer. (We note that the first-surface reflectance induced by the passage of light from air [real refractive index 1] to the soil layer [real refractive index  $>1$ ] will prevent  $R_n$  and hence the ratio  $R_n/R_0$  from equalling zero (Levinson et al., 2005b).)

Since the solar heat gain of an opaque surface is proportional to its solar absorptance ( $1 - \text{solar reflectance}$ ), the influence of membrane cleaning on building heat gain is better gauged by fractional variations in solar absorptance than by those in solar reflectance. For example, a cleaning process that raises solar reflectance from 0.8 to 0.9 increases solar reflectance by only one part in eight, but decreases solar absorptance and hence solar heat gain by a factor of two. Two particularly useful metrics for evaluating the influences of soiling and cleaning on building energetics are (a) solar absorptance,  $A_n$ ; and (b) the ratio  $A_n/A_0$  of solar absorptance in state  $n$  to solar absorptance in the unsoiled state. The latter indicates the factor by which the roof's solar heat gain has increased.

## 3. Experiment

### 3.1. Roofing membrane samples

Soiled and unsoiled light-colored, single-ply PVC membrane samples were taken from 15 five-to-eight-year-old low-slope roofs, all in good

Table 1

Sources and ages of 15 membrane samples taken from light-colored, low-slope PVC membrane roofs in 10 US cities

Sample	City	Building	Years exposed
1	Springfield, MA	Building a	5
2	Springfield, MA	Building b	6
3	Lancaster, OH	Building c	6
4	Heath, OH	Building d	6
5	West Hampton, NJ	Building e	6
6	West Hampton, NJ	Building f	8
7	Plantation, FL	Building g	6
8	Plantation, FL	Building g	6
9	Gardena, CA	Building h	5
10	Gardena, CA	Building h	6
11	Solano Beach, CA	Building i	8
12	Solano Beach, CA	Building i	8
13	Alpharetta, GA	Building j	6
14	Bethesda, MD	Building k	6
15	Fredericksburg, VA	Building l	5

mechanical condition, covering 12 buildings in 10 US cities in eight states (Table 1). Since roofs were chosen based on availability for sampling, the soiling experienced by these samples may or may not be representative of that experienced by any larger population of roofs. All membranes were manufactured by the same firm. At least one 0.5 m<sup>2</sup> membrane sample containing a membrane seam (hot-air welded overlap) was removed from each roof. The non-welded area of the flap on the underside of a seam served as the unexposed, “unsoiled” surface (Fig. 3).

### 3.2. Reflectance measurements

Small coupons (4 cm × 4 cm) were extracted from a representative portion of each unsoiled sample and a heavily soiled portion of each soiled sample. The near-normal-hemispherical solar spectral reflectance (300–2500 nm @ 5-nm intervals; hereafter, simply “spectral reflectance”) and corresponding reflectance to air-mass 1.5 global solar radiation (ASTM, 2003) (hereafter, simply “solar reflectance”) of a 10 mm<sup>2</sup> area at the center of each coupon were measured via ASTM Standard E903 (ASTM, 1996) using a PerkinElmer Lambda 900 UV/Visible/NIR Spectrometer with Labsphere 150-mm Integrating Sphere. The surface-average solar reflectance of each membrane was estimated as the mean of ASTM Standard C1549 air-mass 1.5 solar reflectances (ASTM, 2002) measured with a Devices

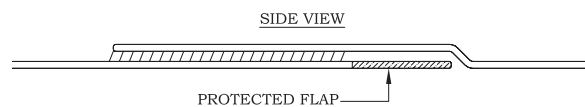


Fig. 3. Side view of a membrane sample containing a seam. The “soiled” coupon was extracted from the exposed top layer, while the “unsoiled” coupon was taken from the unexposed underside of the seam.

& Services Solar Spectrum Reflectometer (model SSR-ER) at several 2.5-cm diameter spots (five per soiled membrane, three per unsoiled membrane) over a 17 cm × 17 cm area.

### 3.3. Cleaning

The spectral reflectance of each soiled coupon was remeasured followed each of four sequential laboratory processes—wiping, rinsing, washing, and bleaching—intended to simulate various natural and artificial cleaning mechanisms (Table 2). Each cleaning technique was applied vigorously until the appearance of the membrane stabilized. This yielded six states of exposure for each membrane: (5) soiled; (4) soiled and wiped; (3) soiled, wiped, and rinsed; (2) soiled, wiped, rinsed, and washed; (1) soiled, wiped, rinsed, washed, and bleached; and (0) unsoiled. For brevity, each state is named by its final condition—i.e., soiled, wiped, rinsed, washed, bleached, or unsoiled.

We note again that the unsoiled sample was extracted from the underside of the seam and was neither exposed nor cleaned.

## 4. Results

### 4.1. Presence and removal of soil-layer contaminants

The sample images in Fig. 4a,b suggest that the soil layer includes (a) loosely bound material that can be wiped off, as seen on soiled sample 13; (b) tightly bound material (possibly the same) that can be removed by rinsing or washing, such as that remaining on wiped sample 13; and (c) biological growth, possibly fungi or dead algae, that is especially visible on samples 7, 8, and 11, and that disappears entirely only after the application of bleach.

The measured spectral reflectances  $r_n(\lambda)$  of the 15 samples in each of the six states—soiled, wiped, rinsed, washed, bleached, and unsoiled—are charted



Table 2  
Laboratory simulations of roof cleaning processes

Procedure	Laboratory technique	Mechanism(s) simulated
Wiping	Wiping with dry cloth	Wind, sweeping
Rinsing	Rinsing with running water; air drying	Rain
Washing	Scrubbing with phosphate-free dishwashing detergent and water; air drying	Washing with detergent
Bleaching	Scrubbing with bleach-based algae cleaner (solution of sodium hypochlorite and sodium hydroxide) and water; air drying	Washing with algae cleaner

in Fig. 5. Analogous graphs of spectral reflectance ratio  $r_n(\lambda)/r_0(\lambda)$ , spectral optical depth  $\tau_n(\lambda)$ , and optical depth fraction  $\gamma_n(\lambda) \equiv \tau_n(\lambda)/\tau_N(\lambda)$  are shown in Figs. 6–8. The spectral optical depths  $\delta\tau_n(\lambda) \equiv \tau_n(\lambda) - \tau_{n-1}(\lambda)$  of sublayers removed by each process are shown in Fig. 9.

In their soiled states, the optical depth curves of all samples except 5 and 6 exhibit the broad, slowly declining absorption spectrum characteristic of black carbon, decreasing by a factor of about two from 400 to 1500 nm (Fig. 7). The swifter spectral decline in the optical depths of soiled samples 5 and 6 (decreasing by a factor of 20 over the same range), coupled with the presence of dark spots (biomass) on their surfaces, suggests that they are coated primarily with organic carbon. We rule out hematite as the dominant contaminant on samples 5 and 6 because no strong absorption peak is seen in the range 800–900 nm.

Again excepting samples 5 and 6, wiping removed a sublayer of black carbon from each membrane, as indicated by the broad, slowly declining spectra of the optical depth reductions induced by wiping (Fig. 9). However, black carbon remained on all wiped samples except 3, 10, 5, and 6. Wiping appears to have removed the black carbon from samples 3 and 10, leaving behind only organic carbon (compare to the optical depth spectra of soiled samples 5 and 6).

Rinsing removed much of the remaining black carbon from samples 7, 8, 9, 11, and 15, but little black carbon from samples 1, 2, 4, 12, 13, and 14. Very weak absorption at wavelengths longer than 1500 nm indicate that washing removed the remaining black carbon from all samples but 2, 4, 7 and 12. The optical depths of washed samples 12, 14, and 15 increased with wavelength in the near-

infrared, suggesting that the washing process may have left a residue.

Samples 5–12 are each covered to various extents by biomass. The images indicate that wiping and rinsing each removed some of the growth. While wiping was not particularly effective, rinsing removed about half of the biomass present on wiped samples 7, 8, 11, and 12, and washing removed nearly all of the biomass remaining on those samples. Bleaching was required to clear isolated dark spots of growth remaining on samples 5–9 and 11–12. We note that bleach does not actually remove biomass, but instead renders colorless the light-absorbing chromophores in organic material.

#### 4.2. Effects of soiling and cleaning on reflectance

Soiling attenuated the reflectance of membranes more strongly at shorter wavelengths, consistent with the absorption spectra of black carbon and organic carbon (Fig. 2). The reflectance ratios  $r_n(\lambda)/r_0(\lambda)$  of soiled samples covered with biomass (e.g., 7, 8, and 11) were about 0.3 in the visible spectrum, and 0.3–0.8 in the near-infrared. The ratios for samples not covered with biomass were typically 0.6–0.8 in the visible, and 0.8–0.9 in the near-infrared (Fig. 6).

Gauging by the optical depth fractions  $\gamma_n(\lambda)$  shown in Fig. 8, wiping was a highly effective cleaning process on biomass-free membranes. In the 300–1500 nm spectrum bearing 90% of the power in ground-level sunlight (Fig. 1), wiping removed about 50–80% of the initial optical depth  $\tau_N(\lambda)$  on biomass-free samples. Wiping removed about 20–40% of the initial optical depth in that spectrum on biomass-covered samples 7, 8, and 11, and only about 10% on samples 5 and 6, which appear to

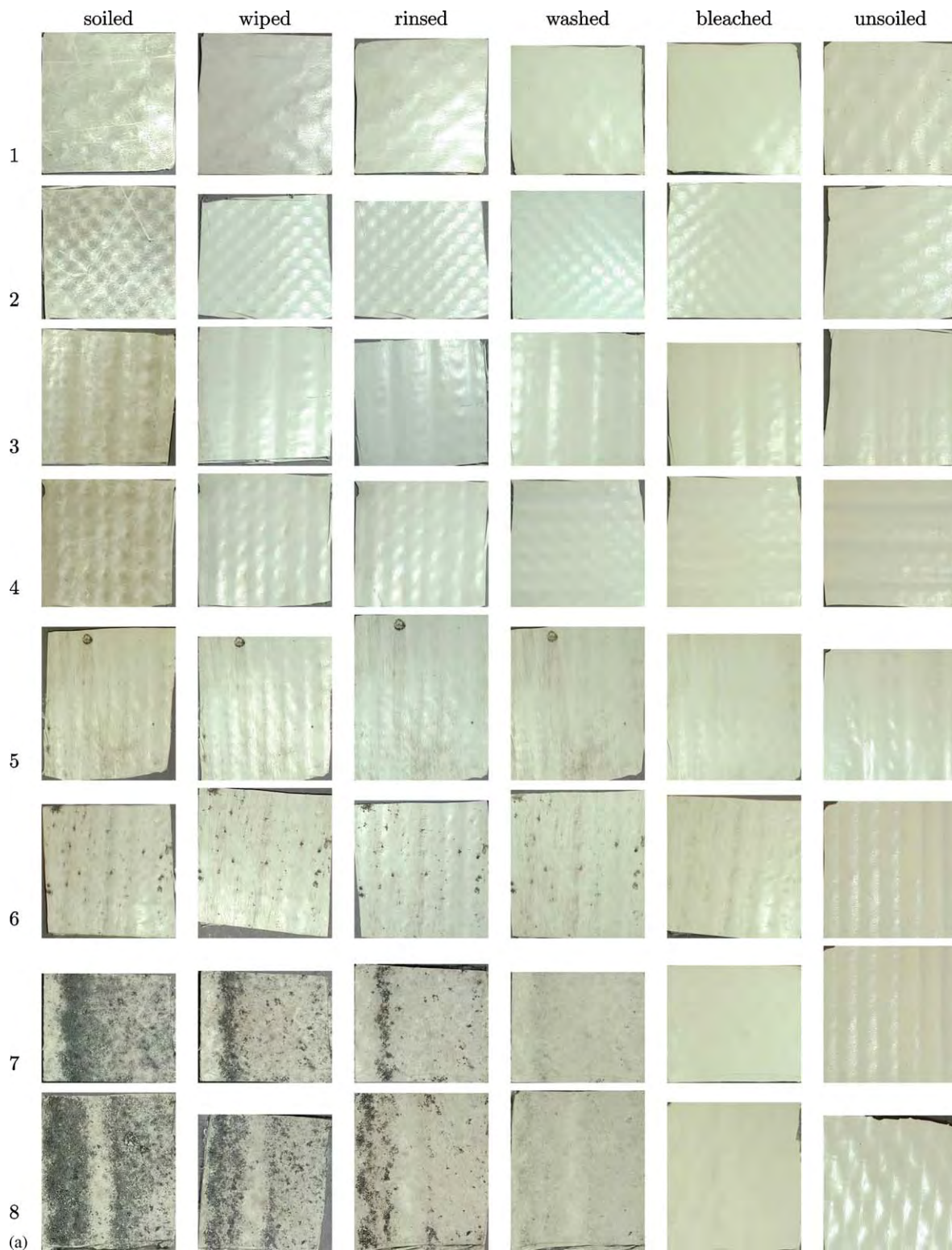


Fig. 4. Images of coupons from (a) membranes 1–8 and (b) membranes 9–15 in their soiled, wiped, rinsed, washed, bleached, and unsoiled states.

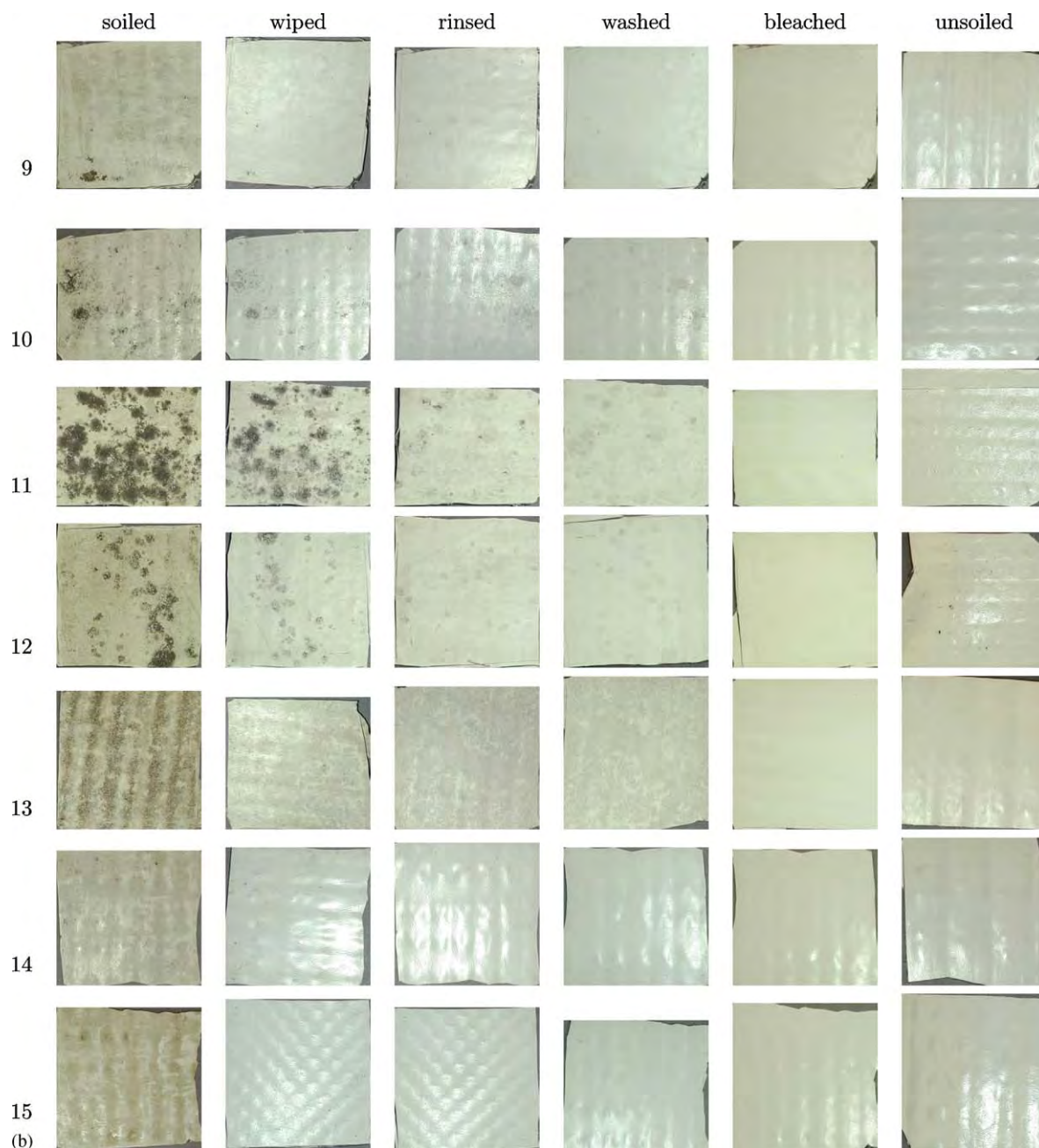


Fig. 4. (Continued)

have been covered with a thin layer of organic carbon.

Rinsing and washing were very effective on biomass-covered samples 7, 8, and 11, removing another 10–50% and 10–25% (respectively) of the initial optical depth  $\tau_N(\lambda)$  in the 300–1500 nm spectrum. Washing and/or rinsing removed most

of the remaining soil on all samples other than 5 and 6. On these two lightly soiled samples, bleaching was much more effective than wiping, rinsing, or washing.

The effect of bleaching on reflectance is largest at short wavelengths (like the effect of the black carbon), diminishing at wavelengths greater than



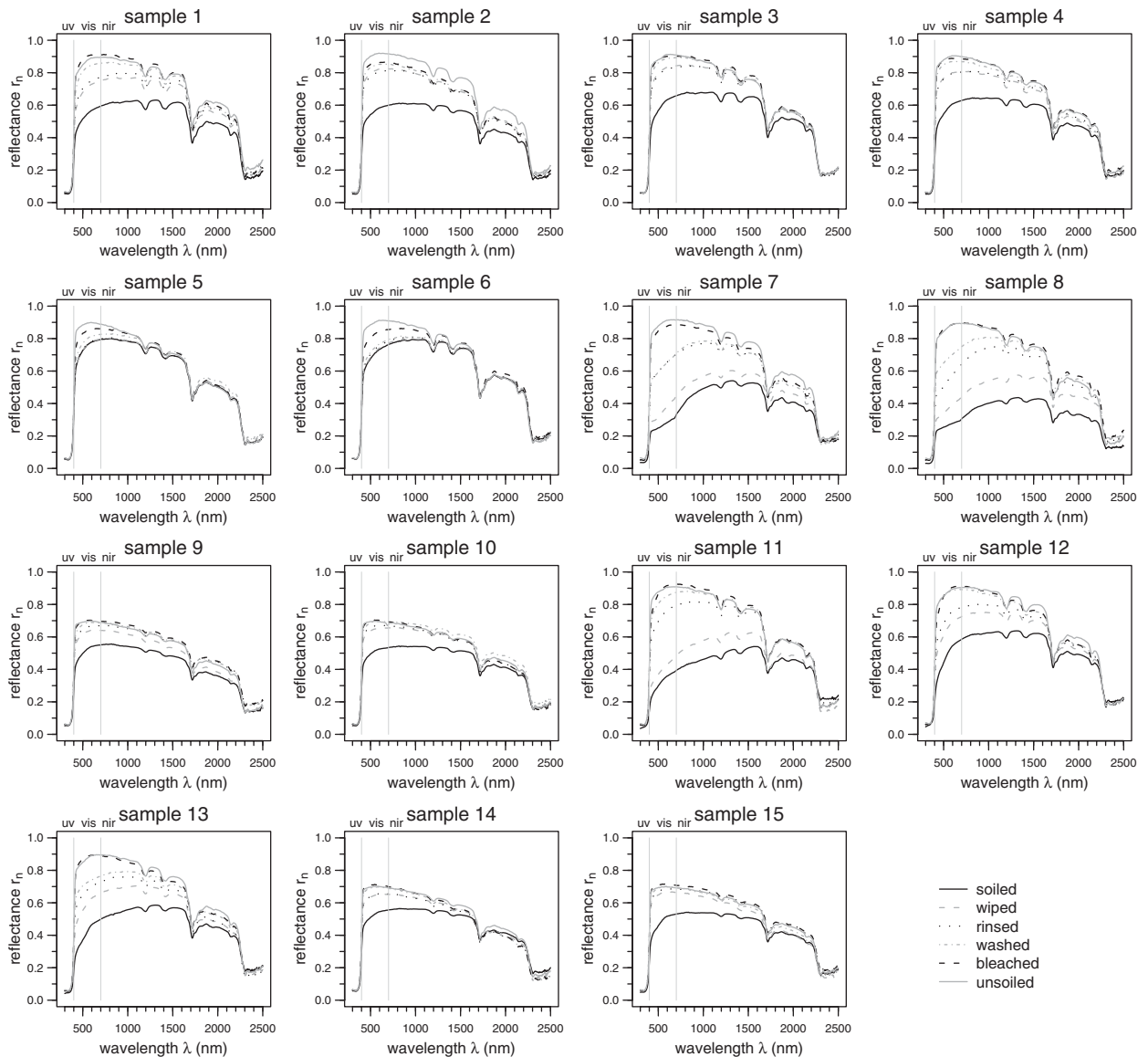


Fig. 5. Spectral reflectances  $r_n(\lambda)$  of 15 membranes in their soiled, wiped, rinsed, washed, bleached, and unsoiled states.

1200 nm. After wiping, rinsing, washing, and bleaching, the optical depth of the remaining soil layer was negligible on all samples.

The ratio of solar reflectance to unsoiled solar reflectance,  $R_n/R_0$ , ranged from 0.41 to 0.89 for the soiled samples; 0.53 to 0.95 for the wiped samples; 0.74 to 0.98 for the rinsed samples; 0.79 to 1.00 for the washed samples; and 0.94 to 1.02 for the bleached samples (Table 3). In the soiled and wiped states, the solar reflectance ratios of the biomass-covered samples (7, 8, and 11) were significantly

lower than those of the other samples. Washing closed most of the gap; after bleaching, the influence of the initial biomass cover vanished.

#### 4.3. Effects of soiling and cleaning on solar heat gain

The solar absorptances  $A_n$  and ratios  $A_n/A_0$  of solar absorptance to unsoiled solar absorptance of the 15 samples in each state are presented in Tables 4 and 5, respectively. The latter metric, indicating solar heat gain relative to that of an

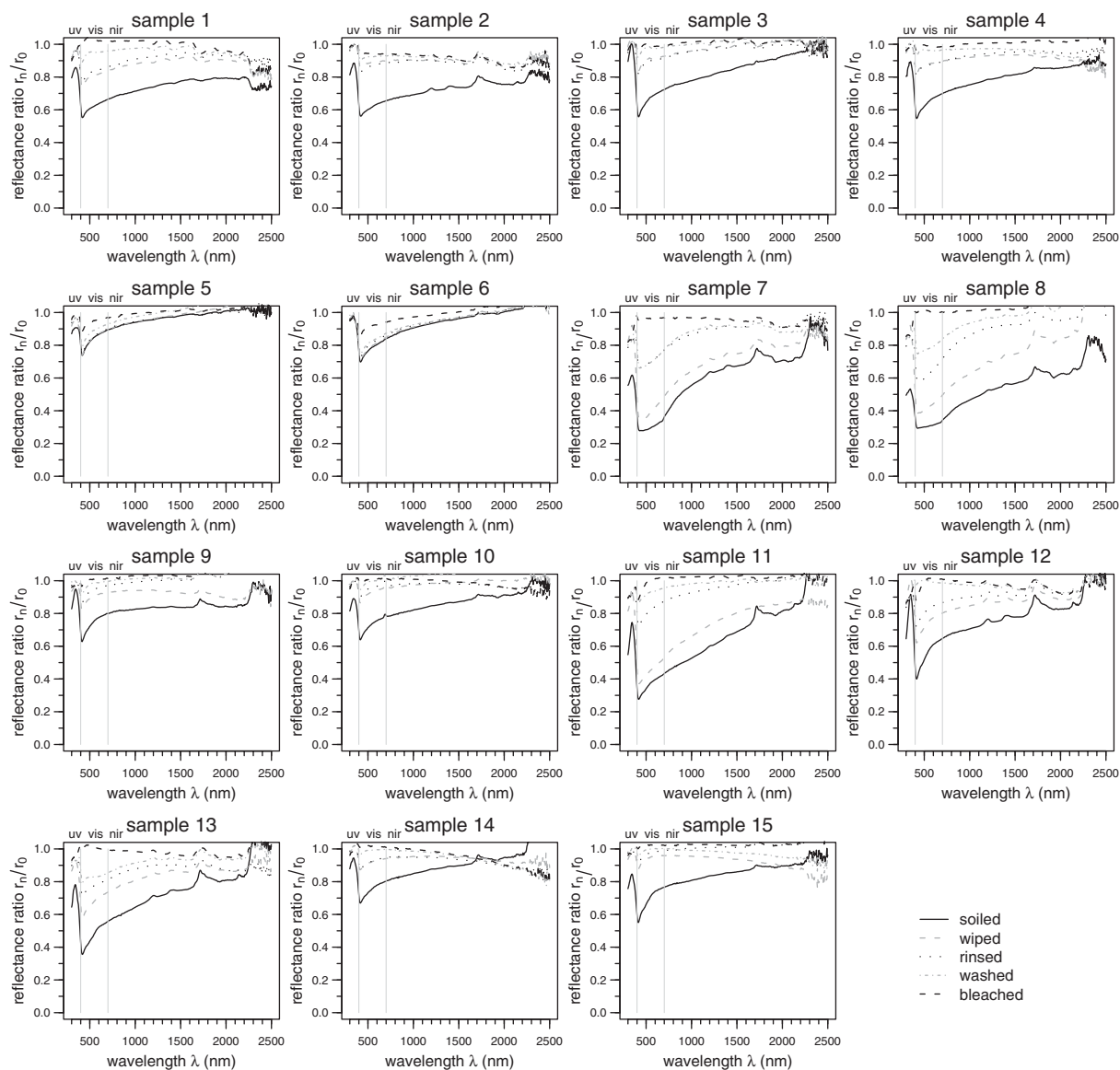


Fig. 6. Ratios  $r_n(\lambda)/r_0(\lambda)$  of the spectral reflectances of 15 membranes in their soiled, wiped, rinsed, washed, and bleached states to their spectral reflectances in their unsoiled states.

unsoiled membrane, ranged from 1.4 to 3.5 for the soiled samples; 1.1 to 3.1 for the wiped samples; 1.0 to 2.0 for the rinsed samples; 1.0 to 1.9 for the washed samples; and 0.9 to 1.3 for the bleached samples.

## 5. Discussion

Black carbon and organic carbon were the two identifiable absorbing contaminants on the mem-

branes. Wiping was effective at removing black carbon (a strong absorber) and less so at removing organic carbon (a weaker absorber). Rinsing and/or washing removed nearly all of the remaining soil layer, with the exceptions of (a) thin layers of organic carbon and (b) isolated dark spots of biomass. Bleach was required to clear the last two features.

Peaks in the measured spectral optical depth of a soil layer may be attenuated by variations in the

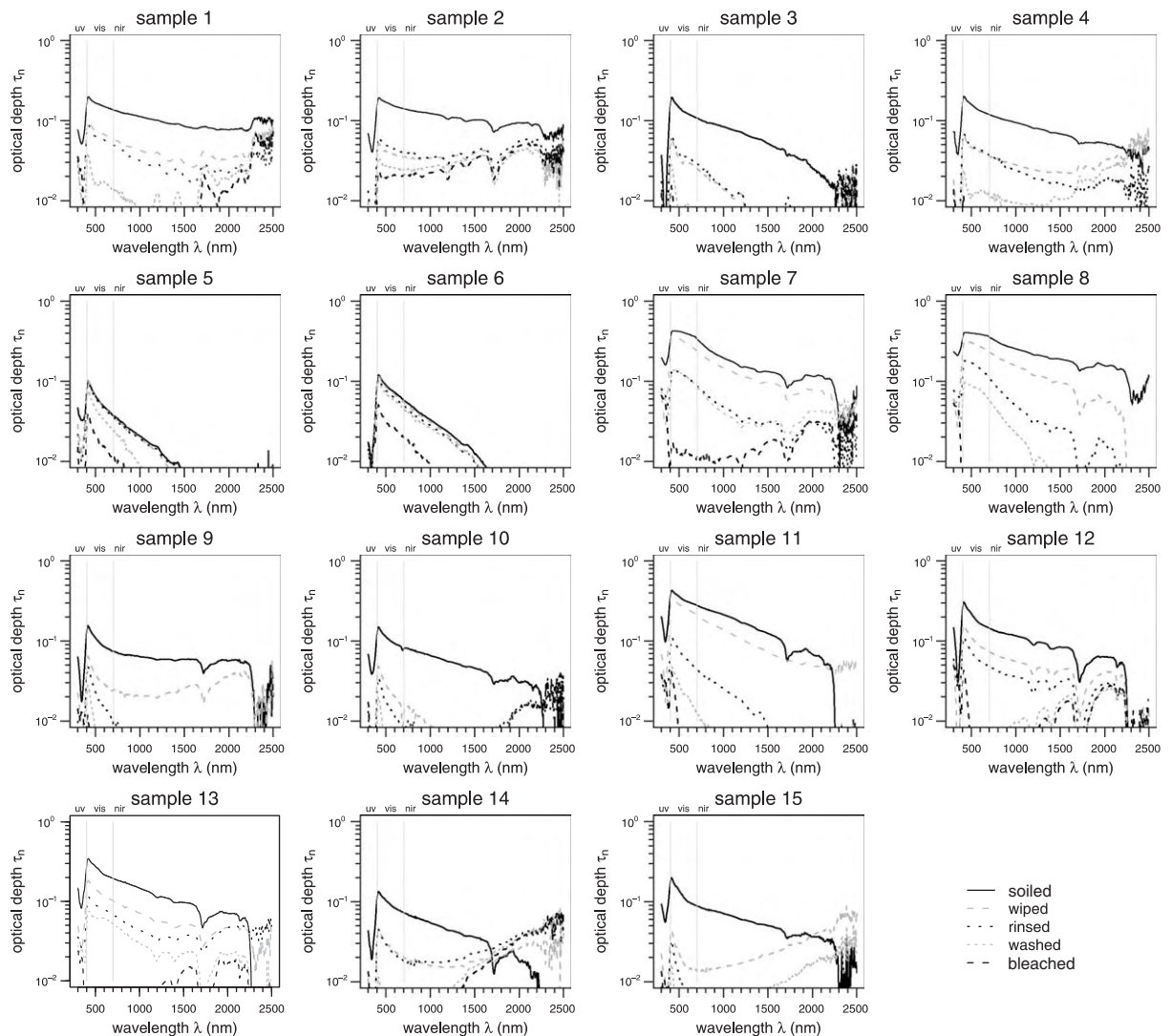


Fig. 7. Spectral optical depths  $\tau_n(\lambda)$  of soil layers present on the 15 membranes in their soiled, wiped, rinsed, washed, and bleached states.

layer thickness (Appendix A). However, with the exception of a few visible-spectrum optical depths of up to 0.3 for the most heavily (but non-uniformly) soiled samples (7, 8, and 11), the measured optical depths in the visible and near-infrared spectra were generally too small (typically not exceeding order 0.1) to be significantly affected by this phenomenon (cf. Fig. A.1).

The solar reflectance of a light-colored membrane thickly coated with black carbon and/or biomass to the point where it appears brown or black can drop to about half that of the unsoiled membrane. Wiping restores some of the initial reflectance, but

rinsing and/or washing are more effective. Bleaching can remove aesthetically undesirable dark spots, but in most cases does not greatly increase the solar reflectance of a washed roof.

The spectral optical depth fractions  $\gamma(\lambda)$  in each state varied too much from sample to sample (e.g., compare wiped samples 1, 6, 7 and 10 in Fig. 8) to expect this property to have a particular spectral shape for each cleaning technique. This is unsurprising, since the efficacy of a cleaning process depends on the nature of the contaminants, and on how tightly they are bound to the membrane. Hence, we do not expect to be able to

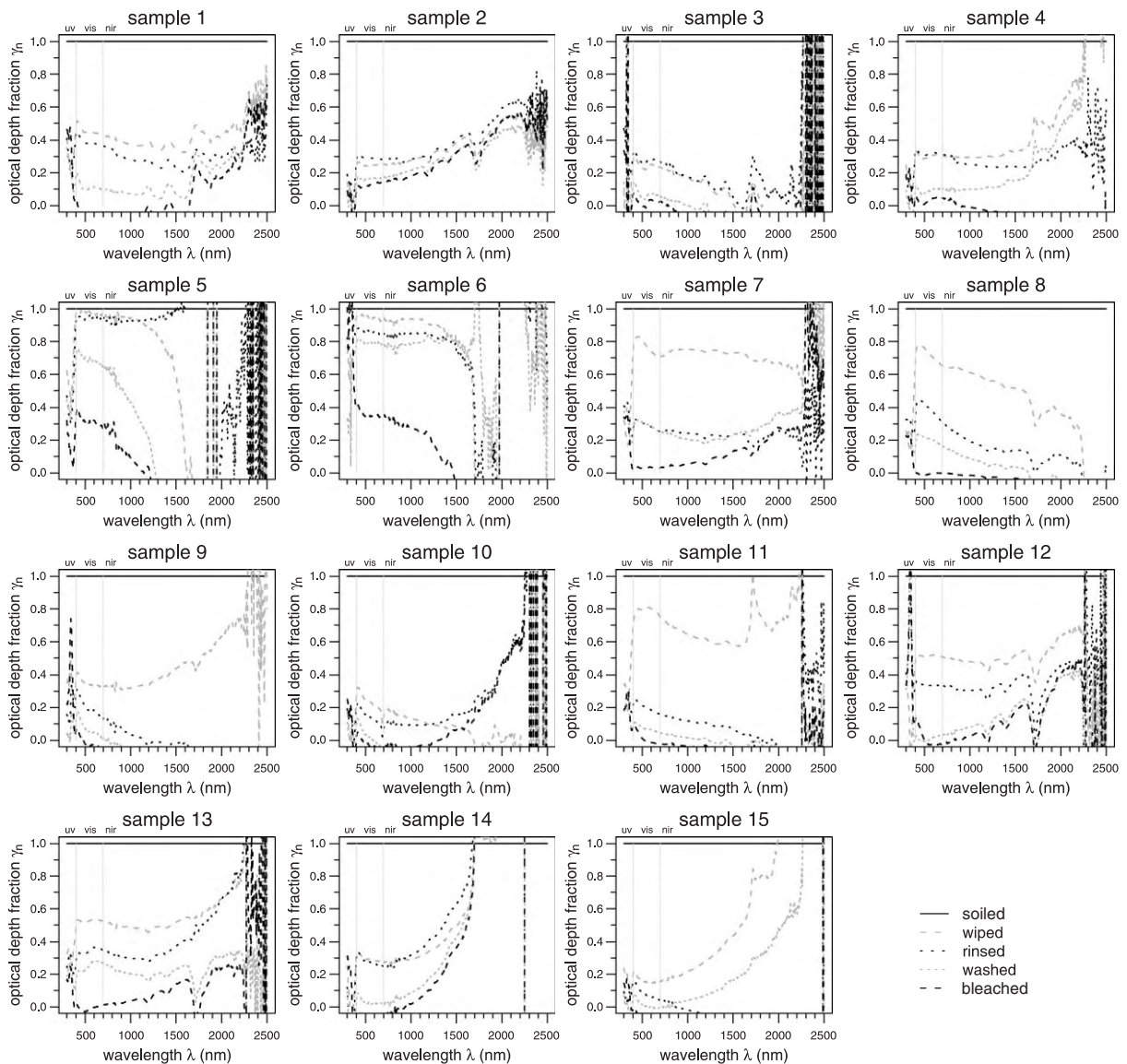


Fig. 8. Fractions  $\gamma_n(\lambda)$  of the initial soil layer's spectral optical depth remaining on each of the 15 membranes in their soiled, wiped, rinsed, washed, and bleached states.

predict the spectral reflectance of a cleaned membrane from its spectral reflectances in its soiled and unsoiled states.

Solar absorptance ratio, rather than solar reflectance ratio, is the proper indicator of the effects of soiling and cleaning on roof heat gain. Since the solar absorptance of an unsoiled white roof is typically about 0.2, heavy soiling can easily triple its solar absorptance, and hence triple its solar gain. For example, the soiled, wiped,

rinsed, washed, and bleached solar absorptance ratios of biomass-laden sample 7 (unsoiled solar absorptance 0.18) are 3.5, 3.1, 2.0, 1.9, and 1.2, respectively. Thus even after washing, the membrane's solar gain is 90% higher than in its unsoiled state.

We note that the solar absorptance of the most heavily soiled membrane (sample 8; soiled solar absorptance 0.68) is still much lower than that of a clean black membrane (about 0.95).

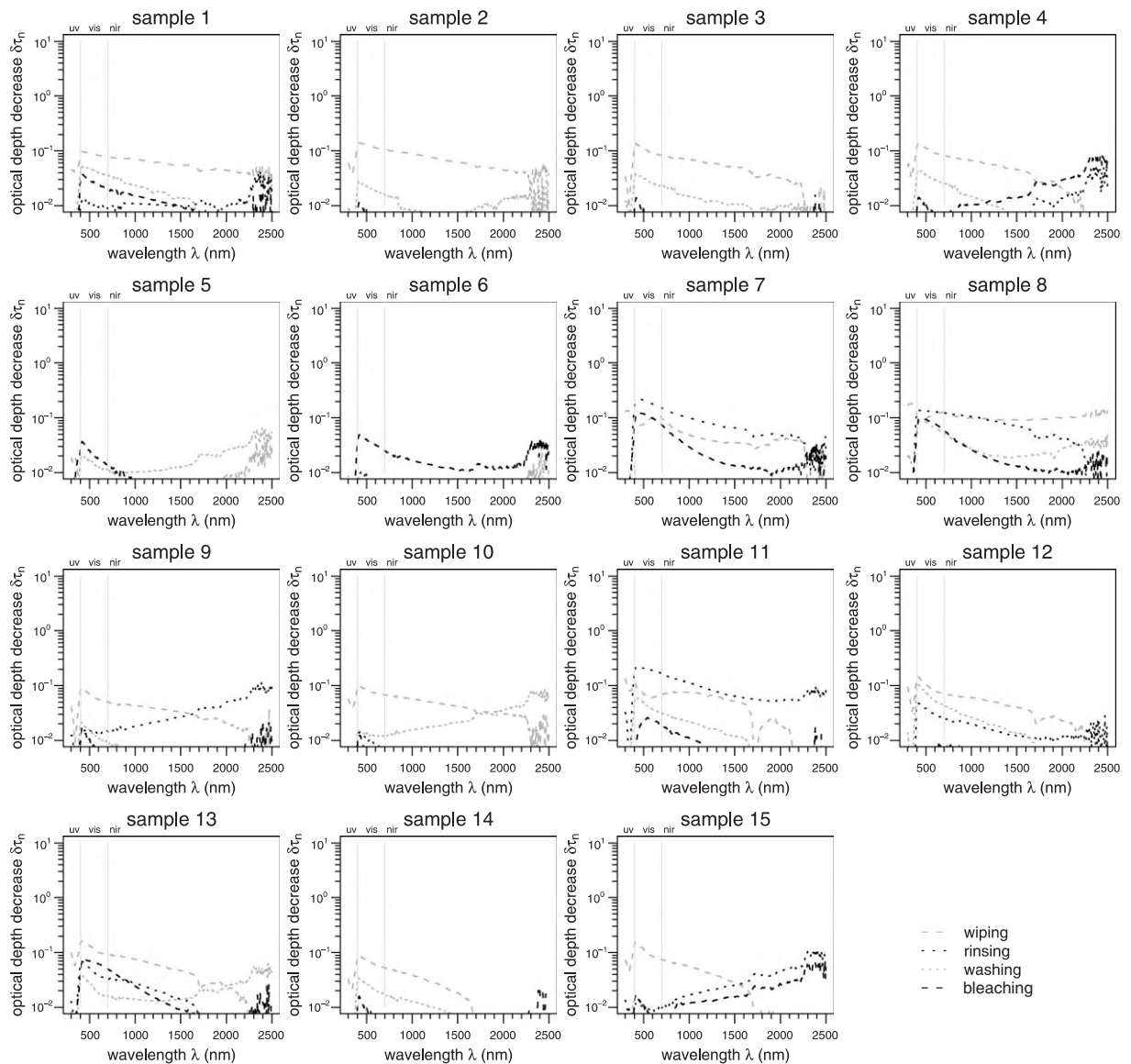


Fig. 9. Absolute reductions  $\delta\tau_n(\lambda)$  in soil-layer spectral optical depth on the 15 membranes achieved by wiping, rinsing, washing, and bleaching.

## 6. Conclusions

Black carbon and to a lesser extent organic carbon significantly reduced the solar spectral reflectances of 15 light-colored PVC membrane samples taken from roofs across the United States. Wiping removed much of the black carbon, but was less effective at removing the (relatively weakly absorbing) organic carbon. Rinsing and/or washing removed nearly all of the remaining soil

layer, though bleach was required to clear isolated dark spots of biomass. The ratio of solar reflectance to unsoiled solar reflectance (a measure of cleanliness) ranged from 0.41 to 0.89 for the soiled samples; 0.53 to 0.95 for the wiped samples; 0.74 to 0.98 for the rinsed samples; 0.79 to 1.00 for the washed samples; and 0.94 to 1.02 for the bleached samples.

The influences of membrane soiling and cleaning on roof heat gain are better gauged by fractional

Table 3

Solar reflectance  $R_0$  of unsoiled membranes and solar reflectance ratio  $R_n/R_0$  of membranes in each exposure state  $n$ . All solar reflectances in this table were measured via ASTM Standard E903

Sample	Solar reflectance $R_0$	Solar reflectance ratio $R_n/R_0$					
	Unsoiled	Soiled	Wiped	Rinsed	Washed	Bleached	Unsoiled
1	0.80	0.68	0.85	0.87	0.96	1.02	1.00
2	0.82	0.67	0.90	0.88	0.93	0.94	1.00
3	0.81	0.73	0.93	0.92	0.99	1.00	1.00
4	0.80	0.71	0.90	0.90	0.97	0.99	1.00
5	0.79	0.89	0.89	0.89	0.93	0.97	1.00
6	0.81	0.85	0.85	0.87	0.88	0.94	1.00
7	0.82	0.43	0.53	0.79	0.79	0.96	1.00
8	0.79	0.41	0.53	0.74	0.86	1.01	1.00
9	0.63	0.79	0.92	0.95	0.98	1.00	1.00
10	0.63	0.78	0.95	0.97	1.00	1.01	1.00
11	0.81	0.46	0.58	0.88	0.96	1.00	1.00
12	0.81	0.64	0.80	0.86	0.99	0.99	1.00
13	0.80	0.57	0.75	0.83	0.87	0.99	1.00
14	0.63	0.79	0.94	0.94	0.99	1.01	1.00
15	0.63	0.76	0.95	0.98	1.00	1.02	1.00

Table 4

Membrane solar absorptances  $A_n$  in each exposure state  $n$  based on solar reflectances measured via ASTM Standards E903 and C1549. E903 absorptances were measured at the dirtiest spot on the membrane and were thus generally higher than the C1549 values, which are averages of measurements made at three to five locations

Sample	C1549 Unsoiled	±	C1549 Soiled	±	E903 Soiled	E903 Wiped	E903 Rinsed	E903 Washed	E903 Bleached	E903 Unsoiled
1	0.19	0.01	0.39	0.05	0.46	0.32	0.30	0.23	0.18	0.20
2	0.16	0.00	0.37	0.04	0.45	0.27	0.28	0.24	0.23	0.18
3	0.16	0.00	0.39	0.00	0.41	0.24	0.25	0.20	0.19	0.19
4	0.19	0.01	0.39	0.04	0.43	0.28	0.28	0.22	0.21	0.20
5	0.19	0.00	0.23	0.02	0.29	0.29	0.29	0.27	0.23	0.21
6	0.16	0.00	0.21	0.04	0.31	0.31	0.29	0.28	0.23	0.19
7	0.17	0.00	0.48	0.12	0.65	0.57	0.36	0.35	0.21	0.18
8	0.17	0.01	0.46	0.11	0.68	0.58	0.41	0.32	0.20	0.21
9	0.35	0.00	0.53	0.09	0.50	0.42	0.40	0.38	0.37	0.37
10	0.34	0.00	0.47	0.01	0.51	0.40	0.39	0.37	0.37	0.37
11	0.17	0.00	0.52	0.05	0.62	0.53	0.29	0.22	0.18	0.19
12	0.16	0.01	0.47	0.09	0.48	0.35	0.31	0.20	0.20	0.19
13	0.17	0.00	0.52	0.04	0.55	0.41	0.34	0.31	0.21	0.20
14	0.34	0.00	0.49	0.03	0.50	0.41	0.41	0.37	0.36	0.37
15	0.34	0.00	0.51	0.03	0.52	0.40	0.38	0.37	0.36	0.37

variations in solar absorptance. Solar absorptance ratios (indicating solar heat gain relative to that of an unsoiled membrane) ranged from 1.4 to 3.5 for the soiled samples; 1.1 to 3.1 for the wiped samples; 1.0 to 2.0 for the rinsed samples; 1.0 to 1.9 for the

washed samples; and 0.9 to 1.3 for the bleached samples.

Further research is required to quantify the effects of soiling and cleaning on the solar spectral reflectances of *dark* roofing surfaces.



Table 5

Ratio  $A_n/A_0$  of solar absorptance in exposure state  $n$  to unsoiled solar absorptance, based on membrane solar reflectances measured via ASTM Standard E903

Sample	Soiled	Wiped	Rinsed	Washed	Bleached	Unsoiled
1	2.3	1.6	1.5	1.2	0.9	1.0
2	2.5	1.5	1.5	1.3	1.3	1.0
3	2.2	1.3	1.3	1.1	1.0	1.0
4	2.2	1.4	1.4	1.1	1.0	1.0
5	1.4	1.4	1.4	1.3	1.1	1.0
6	1.7	1.6	1.6	1.5	1.2	1.0
7	3.5	3.1	2.0	1.9	1.2	1.0
8	3.3	2.8	2.0	1.5	1.0	1.0
9	1.4	1.1	1.1	1.0	1.0	1.0
10	1.4	1.1	1.1	1.0	1.0	1.0
11	3.3	2.8	1.5	1.2	1.0	1.0
12	2.5	1.8	1.6	1.1	1.0	1.0
13	2.7	2.0	1.7	1.5	1.0	1.0
14	1.4	1.1	1.1	1.0	1.0	1.0
15	1.4	1.1	1.0	1.0	1.0	1.0

## Acknowledgements

This work was supported by Sarnafil Incorporated, and by the Assistant Secretary for Renewable Energy under Contract No. DE-AC03-76SF00098. We would like to thank Stanley Graveline and Kevin Foley of Sarnafil and Thomas Kirchstetter of Lawrence Berkeley National Laboratory for their technical assistance.

## Appendix A. Attenuation of features in spectral optical depth of soil layer by spatial variations in thickness

The spatial mean reflectance of a membrane soiled by a layer with nonuniform thickness of mean value  $Z_n$  will always exceed that of the same membrane soiled by a layer of uniform thickness  $Z_n$ . To see this, consider a membrane half covered by a soil layer of thickness  $Z_n - \delta Z$ , and half covered by a soil layer of thickness  $Z_n + \delta Z$ . If the soil has a spatially invariant spectral absorption coefficient  $\alpha(\lambda)$ , the spatial mean reflectance of the nonuniformly soiled membrane (superscript prime) will be

$$r'_n(\lambda) = r_0(\lambda)(0.5 \exp[-2\eta \alpha(\lambda)(Z_n - \delta Z)] + 0.5 \exp[-2\eta \alpha(\lambda)(Z_n + \delta Z)]). \quad (\text{A.1})$$

The reflectance of a membrane soiled with a layer of uniform thickness  $Z_n$  is

$$r_n(\lambda) = r_0(\lambda) \exp[-2\eta \alpha(\lambda) Z_n]. \quad (\text{A.2})$$

For any  $\delta Z > 0$ ,

$$\frac{r'_n(\lambda)}{r_n(\lambda)} = \cosh[2\eta \alpha(\lambda) \delta Z] > 1. \quad (\text{A.3})$$

Applying Eq. (4), the change in optical depth induced by nonuniformity is

$$\begin{aligned} \tau'_n(\lambda) - \tau_n(\lambda) &= -\frac{1}{2\eta} \ln \left[ \frac{r'_n(\lambda)}{r_n(\lambda)} \right] \\ &= -\frac{1}{2\eta} \ln \cosh[2\eta \alpha(\lambda) \delta Z] < 0. \end{aligned} \quad (\text{A.4})$$

Hence, nonuniform soil layer thickness decreases spectral optical depth. This effect grows stronger as the spectral absorption coefficient  $\alpha(\lambda)$  rises, attenuating peaks in the spectral absorption curve.

One particularly interesting case is that of an otherwise uniform soil layer with holes. Consider a nonuniform layer of mean thickness  $Z_n$  that covers a fraction  $f$  of the membrane with thickness  $Z_n/f$  and leaves the rest of the membrane bare. If the spectral optical depth of a soil layer of the same composition and uniform thickness  $Z_n$  is  $\tau_n(\lambda)$ , the spectral optical depth of the nonuniform layer—i.e., that computed from its spectral mean reflectance via Eq. (4)—will be

$$\tau'_n(\lambda) = -\frac{1}{2\eta} \ln([1 - f] + f \exp[-2\eta \tau_n(\lambda)/f]). \quad (\text{A.5})$$

The holes in the soil layer act as a low-pass filter on spectral optical depth. That is, when the spectral optical depth  $\tau_n(\lambda)$  of the uniform layer is small, the spectral optical depth  $\tau'_n(\lambda)$  of the nonuniform layer is close to that of the uniform layer; when  $\tau_n(\lambda)$  is large,  $\tau'_n(\lambda)$  saturates at a much lower value (Fig. A.1).

## Appendix B. Predicting solar reflectance of a cleaned membrane

The solar reflectance  $R$  of a surface with spectral reflectance  $r(\lambda)$  is

$$R = I^{-1} \int_{\infty}^0 i(\lambda) r(\lambda) d\lambda, \quad (\text{B.1})$$

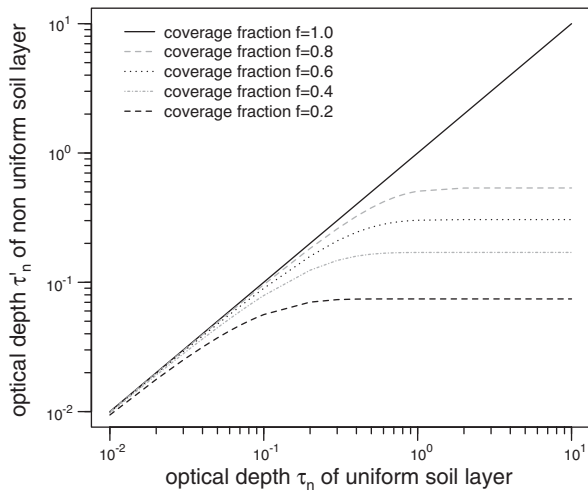


Fig. A.1. Variation with coverage fraction  $f$  of the optical depth  $\tau'_n$  of a nonuniform soil layer vs. optical depth  $\tau_n$  of a uniform soil layer of the same composition and equal mean thickness.

where  $i(\lambda)$  is solar spectral irradiance (power per unit area per unit wavelength; see Fig. 1), and

$$I \equiv \int_{\infty}^0 i(\lambda) d\lambda \quad (\text{B.2})$$

is solar irradiance (power per unit area). A *linear* relationship among the observed spectral reflectances of the cleaned, soiled, and unsoiled membranes will propagate to their solar reflectances. That is, if

$$r_n(\lambda) = c_1 r_0(\lambda) + c_2 r_N(\lambda), \quad (\text{B.3})$$

then it follows from Eq. (B.1) that

$$R_n = c_1 R_0 + c_2 R_N. \quad (\text{B.4})$$

However, should the observed spectral reflectances of the cleaned, soiled, and unsoiled samples exhibit a *nonlinear* relationship, their corresponding solar reflectances will lack any obvious closed-form relationship unless the spectral reflectances are constant. The relationship among the spectral reflectances derived from a Beer's law model of exponential light attenuation [cf. Eq. (3)] is geometric:

$$r_n(\lambda) = [r_0(\lambda)]^{(1-\gamma_n(\lambda))} \times [r_N(\lambda)]^{\gamma_n(\lambda)}, \quad (\text{B.5})$$

where spectral optical depth fraction  $\gamma_n(\lambda) \equiv \tau_n(\lambda)/\tau_N(\lambda)$ . Hence, we do not expect to find a closed-form relationship among the *solar* reflectances of the cleaned, soiled, and unsoiled membranes.

## References

- Abkari, H., 1998. Cool roofs save energy. *ASHRAE Transactions* 104 (1B), 783–788.
- Akbari, H., Konopacki, S.J., 1998. The impact of reflectivity and emissivity of roofs on building cooling and heating energy use. In: *Proceedings of the Thermal Performance of the Exterior Envelopes of Building*, vol. VII, Clearwater Beach, FL, 6–8 December.
- Akbari, H., Konopacki, S., Pomerantz, M., 1999. Cooling energy savings potential of reflective roofs for residential and commercial buildings in the United States. *Energy* 24, 391–407.
- ASTM, 1996. ASTM E 903-96: standard test method for solar absorptance, reflectance, and transmittance of materials using integrating spheres. Technical Report, American Society for Testing and Materials.
- ASTM, 2002. ASTM C 1549-02: standard test method for determination of solar reflectance near ambient temperature using a portable solar reflectometer. Technical Report, American Society for Testing and Materials.
- ASTM, 2003. ASTM G 173-03: standard tables for reference solar spectral irradiance at air mass 1.5: direct normal and hemispherical on 37° tilted surface. Technical Report, American Society for Testing and Materials.
- Berdahl, P., Akbari, H., Rose, L.S., 2002. Aging of reflective roofs: soot deposition. *Applied Optics* 41 (12), 2355–2360.
- CEC, 2005. Building Energy Efficiency Standards for Residential and Nonresidential Buildings. Publication P400-03-001F, California Energy Commission, Sacramento, CA, September 2004.
- Griffin, E.R., 2002. Building a better PVC: introducing stability at the molecular level. *Roofing Technology Magazine* 2 (2), 19–21.
- Incropera, F.P., DeWitt, D.P., 1985. *Fundamentals of Mass and Heat Transfer*. Wiley, New York.
- Kirchstetter, T.W., Novakov, T., 2004. Evidence that the spectral dependence of light absorption by aerosols is affected by organic carbon. *Journal of Geophysical Research* 109, D21208.
- Kirchstetter, T.W., Novakov, T., Aguiar, J., Haesloop, O., Boone, A.A., 2005. Evaluation of the aethalometer for measuring real-time black carbon concentrations, in preparation.
- Konopacki, S., Akbari, H., 1998. Simulated impact of roof surface solar absorptance, attic, and duct insulation on cooling and heating energy use in single-family new residential buildings. Technical Report LBNL-41834, Lawrence Berkeley National Laboratory, Berkeley, CA.
- Konopacki, S., Akbari, H., Pomerantz, M., Gabersek, S., Gartland, L., 1997. Cooling energy savings potential of light-colored roofs for residential and commercial buildings in 11 U.S. metropolitan areas. Technical Report LBNL-39433, Lawrence Berkeley National Laboratory, Berkeley, CA.
- Levinson, R., Akbari, H., Konopacki, S., Bretz, S., 2005a. Inclusion of cool roofs in nonresidential Title 24 prescriptive requirements. *Energy Policy* 33, 151–171.
- Levinson, R., Berdahl, P., Akbari, H., 2005b. Solar spectral optical properties of pigments—Part I: model for deriving scattering and absorption coefficients from transmittance and



- reflectance measurements. *Solar Energy Materials & Solar Cells* 89 (4), 319–349.
- Levinson, R., Berdahl, P., Akbari, H., 2005c. Solar spectral optical properties of pigments—Part II: survey of common colorants. *Solar Energy Materials and Solar Cells* 89 (4), 351–389.
- Lindberg, J.D., Douglass, R.E., Garvey, D.M., 1993. Carbon and the optical properties of atmospheric dust. *Applied Optics* 32, 6077–6081.
- Miller, W.A., Cheng, M.-D., Pfiffner, S., Byars, N., 2002. The field performance of high-reflectance single-ply membranes exposed to three years of weathering in various U.S. climates. Technical Report, Single-Ply Roofing Institute, Needham, MA.
- Pomerantz, M., Akbari, H., Konopacki, S.J., Taha, H., Rosenfeld, A.H., 1999. Reflective surfaces for cooler buildings and cities. *Philosophical Magazine B* 79 (9), 1457–1476.
- Roodvoets, D., Miller, W.A., Desjarlais, A.O., 2004a. Long term reflective performance of roof membranes. In: *Proceedings of the 19th International RCI Convention and Trade Show*, Reno, NV.
- Roodvoets, D., Miller, W.A., Desjarlais, A.O., 2004b. Saving energy by cleaning reflective thermoplastic low-slope roofs. In: *Proceedings of Thermal Performance of the Exterior Envelopes of Buildings*, vol. IX, Clearwater, FL.
- Turpin, B.J., Lim, H.-J., 2001. Species contributions to PM<sub>2.5</sub> mass concentrations: revisiting common assumptions for estimating organic mass. *Aerosol Science and Technology* 35, 602–610.
- Turpin, B.J., Saxena, P., Andrews, E., 2000. Measuring and simulating particulate organics in the atmosphere: problems and prospects. *Atmospheric Environment* 34, 2983–3013.
- Wilkes, K.E., Petrie, T.W., Atchley, J.A., Childs, P.W., 2000. Roof heating and cooling loads in various climates for the range of solar reflectances and infrared emittances observed for weathered coatings. In: *Proceedings of the 2000 ACEEE Summer Study on Energy Efficiency in Buildings*, American Council for an Energy-Efficient Economy, vol. 3, Washington, DC, pp. 3.361–3.372.
- Young, R., 1998. Cool roofs: light-colored coverings reflect energy savings and environmental benefits. *Building Design and Construction* 39 (2), 62–64.

# **Experimental Analysis of the Natural Convection Effects Observed within the Closed Cavity of Tile Roof Systems**

by

William A. Miller, Ph.D., P.E.  
André Desjarlais, P.E.  
Jerry Atchley

Majid Keyhani, Ph.D.  
Wes MacDonald

Rick Olson  
Jerry Vandewater

*Oak Ridge National Laboratory*

*University of Tennessee*

*Tile Roofing Institute*

“Cool Roofing... Cutting through the Glare”  
Atlanta, GA  
May 12-13, 2005

## **ABSTRACT**

High reflectance roof tile formulated with infrared reflective color pigments and buoyancy driven airflow on the underside of roof tile are key strategies for providing cool roof products that reduce both the heat transfer across the roof and the whole house energy consumption.

A field study is in progress to demonstrate and document the thermal benefits of clay and concrete tile roofs. The reflectance and emittance of the roof tiles, the bulk air temperatures underneath the tiles, the deck temperatures and the deck heat flux at specific distances from the roof's soffit to its ridge are being measured on an outdoor attic test assembly. The attic assembly has asphalt shingles and roof tiles directly nailed to the roof deck, and roof tile attached to batten and counter-batten systems adhered to the deck. Field data are reviewed to better understand the synergism observed from the tile's solar reflectance and the venting occurring between the roof deck and the underside of the tile.

## **INTRODUCTION**

The Tile Roofing Institute (TRI) and the Oak Ridge National Laboratory (ORNL) are working together to quantify and report the potential energy savings for concrete and clay tile roofs. The TRI and its affiliate members are very interested in specifying tile roofs as cool roof products and they want to know the effect of the tile's solar reflectance and the effect of venting the underside of a roof tile. Parker et al., (2002) demonstrated that a Florida home with a “white reflective” barrel-shaped concrete tile roof reduced the annual cooling energy by 22% of the energy consumed by an identical and adjacent home having an asphalt shingle roof. The cost savings due to the reduced use of comfort cooling energy was about US \$120 or about 6.7¢ per square foot per year.

The venting of the underside of a roof tile covering also provides thermal benefits for comfort cooling. Residential roof tests by Beal and Chandra (1995) demonstrated a 45% reduction in the daytime heat flux penetrating a counter-batten tile roof as compared to a direct nailed shingle roof. Parker et al., (2002) observed that a moderate solar reflectance

terra cotta barrel-shaped tile reduced the home's annual cooling load by about 8% of the base load measured for an identical home with an asphalt shingle roof that was adjacent to the home with terra cotta tile. These reported energy savings are in part attributed to the venting that occurs on the underside of the roof tile although it is difficult to quantify this benefit.

The reduced heat flow occurs because of a thermally driven airflow within the air gap formed between the tile and the roof deck. Wood furring strips, counter-battens, are laid vertically (soffit-to-ridge) against the roof deck, and a second batten running parallel to the roof's ridge is laid horizontally across the vertical counter-battens (Figure 1). The bottom surface of the inclined channel is formed by the roof deck and 30# felt and is relatively in-plane and smooth. The underside of the roof tiles establish the upper surface of the inclined vent, and the tile overlaps are designed to be air porous to allow pressure equalization and reduce the wind uplift on the tiles (Figure 1). The design may further complicate a solution of the heat transfer, because an accurate prediction of the airflow is required to predict the heat transfer crossing the roof boundary.

The airflow in the inclined vent is driven by both buoyancy and wind-driven forces. The air gap also provides an improvement in the insulating effect of the roof system. However, measuring and correctly describing the heat flow within the vent cavity of a tile roof is a key hurdle for predicting the roof's thermal performance. The heat transfer within the channel can switch from conduction to single-cell convection to Bénard cell convection dependent on the channel's aspect ratio, the roof slope and the season of the year. The co-existence and competition of the various modes of heat transfer requires experimental measurements and numerical simulations.

Therefore, a combined experimental and analytical approach is in progress with field data just coming available, some of which we are reporting to show the potential energy savings for residential homes having concrete and clay tile roofs.



Figure 1. Batten and Counter-Batten Assembly Showing Inclined Air Cavity for the Slate Tile Roof.

## FIELD DEMONSTRATION

Members of the TRI installed clay and concrete tile on a fully instrumented attic test assembly at the ORNL campus (Figure 2). High-profile clay and concrete tile, medium-profile concrete and a concrete slate tile are directly nailed to the roof deck, installed on batten or on batten and counter-batten systems. The sixth lane (see furthestmost left lane in Figure 2) has a standard production asphalt shingle roof for comparing energy savings. The tile roofs are approximately 4 feet wide with 16 feet of footprint. Table 1 lists the salient features of the concrete and clay tiles being field tested on the Envelope Systems Research Apparatus (ESRA). All tiles, whether direct nailed or installed on battens, have a venting occurring from the soffit to the ridge and transversely along the width of the

test roofs. Parapet partitions with channel flashing were installed between lanes to restrict transverse airflows between test roofs (Figure 1). The ridge vent for each test roof was closed to mimic conventional construction.

**Table 1: Clay and Concrete Tile Placed on the ESRA**

<b>Roof Cover</b>	<b>Roof System</b>	<b>Reflectance</b>	<b>Emittance</b>
		SR <sub>xx</sub> E <sub>yy</sub> <sup>1</sup>	
S-Mission Clay	Direct to Deck	SR54E90	
Medium-Profile Concrete	Direct to Deck	SR10E93	
S-Mission Concrete	Spot Adhered to Deck using Foam	SR26E86	
Slate Concrete	Counter-Batten/Batten	SR13E83	
S-Mission Concrete	Batten	SR34E83	
Asphalt Shingle	Direct to Deck	SR10E89	

<sup>1</sup>SR<sub>xx</sub> states the solar reflectance of a new sample. E<sub>yy</sub> defines the thermal emittance of the new sample. As an example, the asphalt-shingle roof is labeled SR10E89; its freshly manufactured surface properties are therefore 0.10-reflectance and 0.89-emittance.

Each test roof has its own attic cavity with 11 inches of expanded polystyrene insulation installed between adjacent cavities. This reduces the heat leakage between cavities to less than 0.5% of the solar flux incident at solar noon on a test roof. Therefore, each lane can be tested as a stand-alone entity. Salient features of the ESRA facility are fully discussed by Miller et al., (2002).

Roof surface temperature, oriented strand board (OSB) temperature on both the upper and lower surfaces, and the heat flux transmitted through the roof deck are directly measured. Prior to installing the heat flux transducers, they were placed in a guard made of the same material used in construction, and calibrated using a FOX 670 Heat Flow Meter Apparatus to correct for shunting effects (i.e., distortion due to three-dimensional heat flow). Thermocouples are also stationed from the soffit to the ridge to measure the bulk air temperatures in the air channel. The attic cavities also have an instrumented area in the ceiling for measuring the heat flows into the conditioned space. The ceiling consists of a metal deck, a 1 inch thick piece of wood fiberboard lying on the metal deck, and a ½ inch thick piece of wood fiberboard placed atop the 1 inch thick piece. The heat flux transducer for measuring ceiling heat flow is embedded between the two pieces of wood fiberboard. It too was calibrated in a guard made of wood fiberboard before put in field service.

## REFLECTANCE AND EMITTANCE OF TILE

The solar reflectance and the thermal emittance of a roof surface are important surface properties affecting the roof temperature which, in turn, drives the heat flow through the roof. The solar reflectance ( $\rho$ ) determines the fraction of radiation incident from all directions that is diffusely reflected by the surface. The thermal emittance ( $\varepsilon$ )

describes how well the surface radiates energy away from itself as compared to a blackbody operating at the same roof temperature.

Solar reflectance measures of the clay and concrete tile roofs exposed at ORNL are collected quarterly; these data are shown in Figure 3. Each tile roof is identified by the SRxxEyy nomenclature described in Table 1. After two years of exposure, the S-Mission tiles (SR54E90, SR26E86 and SR34E83) show little drop in solar reflectance. The medium-profile concrete (SR10E93) and the slate (SR13E83) tiles actually show slight increases in solar reflectance as does the asphalt shingle roof due to the accumulation of airborne contaminants. Dust tend to lighten these darker colors. Data for clay tile are also shown for field exposure testing in three of the sixteen climatic zones of California. The clay samples are identical to those tested at ORNL. They show a loss of solar reflectance that occurs, because of climatic soiling. The worst soiling observed occurs in the urban area of Colton and the desert area of El Centro (Figure 4). However, the crisp and clear alpine climate of McArthur shows the lowest loss of solar reflectance, because less contaminants pollute the air. Roof slope appears to affect the loss of solar reflectance (Figure 4). Testing at the slope of 8 inches of rise per 12 inches of run (33.7° slope) has less reflectance loss compared to testing at 2 inches of rise per 12 inches of run (9.5°) for all three exposure sites (Figure 4). Precipitation is not believed to be the dominant player, especially when one considers that El Centro has less than 3 inches of annual rainfall! Rather, wind may be causing the differences in loss of solar reflectance as roof slope changes from 9.5° to 33.7°. The results in Figures 3 and 4 also show that exposure testing differed between the western and mid-eastern climates of the United States. Samples from the two regions show California has more airborne dust than does Tennessee, which causes the greater loss of reflectance in California.

The clay tile (SR54E90) tested at ORNL and California exceeds the solar reflectance of all the other tile (Figure 3), because it contains complex inorganic color pigments that boost its reflectance in the infrared spectrum. A slurry coating process is used to add color to the surface of a clay tile. Once coated, the clay is kiln-fired, and the firing temperature, the atmosphere and the pigments affect the final color and solar reflectance Akbari, et al., (2004a). The complex inorganic color pigments, termed here as cool roof color materials (CRCMs), are of paramount importance and will literally revolutionize the roofing industry. The energy and cost savings reported by Parker et al., (2002) for white reflective concrete tile are promising; however, in the residential market, the issues of aesthetics and durability will limit the acceptance of “white” residential roofing. To homeowners, dark roofs simply blend better with the surroundings than their counterpart, a highly reflective “white” roof. What the public is not aware of, however, is that the aesthetically pleasing dark roof can be made to reflect like a “white” roof in the near infrared spectrum. Miller et al., (2004), Akbari et al., (2004b) and Levinson et al., (2004a and 2004b) provide further details about the potential energy benefits and identification, and characterization of dark yet highly reflective color pigments.

Coating tile with CRCMs has been successfully demonstrated by American Rooftile Coatings which applied its COOL TILE IR COATING™ to several samples of concrete tiles of different colors (Figure 5). The solar reflectance for all colors tested exceeded 0.40. Most dramatic is the effect of the dark colors. The black coating increased the solar reflectance from 0.04 to 0.41, while the chocolate brown coating increased from 0.12 to 0.41, a 250% increase in solar reflectance! Because solar heat gain is

proportional to solar absorptance, the COOL TILE IR COATING™ reduces the solar heat gain by roughly 33%, of the standard color, which is very promising. The coating application is a significant advancement for concrete tile, because the alternative is to add the CRCMs to the cement and sand mixture, which requires too much pigment and makes the product too expensive. The coating can certainly help tile roof products pass California's Title 24 and the Environmental Protection Agency's Energy Star 0.25 solar reflectance criteria for steep-slope roofing.

The thermal emittance of the clay and concrete tile has not changed much after two years of exposure in California. It remains relative constant at about 0.85.

## EXPERIMENTAL RESULTS

The multiple hazard protection provided by concrete and clay tile from fire and wind and the superior aesthetics and durability of tile are making these roof materials the preference of homeowners in the western and some southern states. Thermal performance data collected from the attic test assembly at ORNL show tile to be an energy-efficient roof product. The clay S-Mission tile (SR54E90), the S-Mission tile spot adhered with foam (SR26E86) and the S-Mission tile on battens (SR34E83) had the least amount of heat penetrating into their respective roof decks (Figure 6). The roof heat flux data are for two consecutive days of exposure during August 2004 in East Tennessee's hot and humid climate. All three tiles have venting occurring along the underside of the tile's barrel from soffit to ridge. Of these three roof systems, the clay tile (SR54E90) had the lowest heat flux through the deck due primarily to the tile's high solar reflectance. The clay tile reduced the peak heat transfer penetrating the roof deck at solar noon by about 70% of the energy penetrating through the deck of the attic covered with an asphalt shingle roof. Subsequently, the heat penetrating the ceiling of the attic assembly was reduced by about 60% of that entering through the ceiling of the attic assembly with asphalt shingles.

The solar reflectance and thermal emittance of the slate roof (SR13E83) and the medium-profile tile (SR10E93) are very similar to that of the asphalt shingle (SR10E89) but the heat transfer through the roof and ceiling of the attic with the slate roof and the medium-profile tile roof are only half that measured for the asphalt shingle roof. The reduction must be due to buoyancy and wind force effects occurring in the inclined air channel that dissipates heat away from the deck. The slate tiles are attached to batten and counter-batten strips, which form a vent cavity that is about 1½ inches deep. The medium-profile tile forms its own half-cylindrical channel of about 0.5 inch radius. It is very interesting that these two dark tile systems (SR13E83 and SR10E93) as compared to the shingle roof (SR10E89) significantly reduce the heat penetrating their respective ceilings. The data in Figure 6 clearly show the benefit derived from venting the roof deck based solely on the direct comparison of the percent reduction of peak loads (i.e., ~45% reduction for the SR13E83 or SR10E93 and a 70% reduction for the SR54E90 tile as compared to the shingle roof). By proportioning the heat reduction due solely to venting (SR10E93 vs SR10E89) to the heat reduction due to solar reflectance and venting (SR54E90 vs SR10E89):

$$\frac{\overbrace{45\% \text{ due to venting}}^{\text{heat reduction}}}{70\% \text{ due to venting and SR}} \cdot [SR_{54}^{\text{Clay Tile}} - SR_{10}^{\text{Shingle}}]$$

The benefit of venting at solar noon is equivalent to roughly 30 points of surface reflectance! Hence, the data at peak loading imply that “cool roofing” credits are obtainable through venting the underside of a tile or similarly constructed roof system. The data also clearly show the synergism gained by both the solar reflectance of CRCMs (Figure 6) and the deck venting used by all tile roofs.

Demonstration homes located in Fair Oaks, California are also under field study to further document the effects of CRCMs and roof venting (Akbari et al., 2004). A pair of homes are adjacent to one another, and have the same identical floor plan and roof orientation. Both homes have the same medium-profile tile with chocolate brown color (SR10E93) as being tested on the ESRA at ORNL; however, one of the two homes was coated with CRCMs and has a measured solar reflectance of about 0.41 (see the chocolate brown color tile in Figure 5). The field data show that the higher reflectance roof reduced the attic temperature about 5°F to 15°F around solar noon. The reduction in attic temperature is a direct result of the reduction in heat penetrating the roof. Heat flux transducers embedded in the west facing roofs of both homes show that the roof with Cool Tile IR Coating™ had less heat penetrating the roof compared to the roof with standard color tile. As result, there is a lower temperature driving force from attic to the conditioned space and, therefore, the heat penetrating the ceiling at solar noon is reduced about 70% of that measured for the standard production tile roof (Figure 7). Integrating the heat flows over the three-day daytime period shows a 25% reduction in the heat load that is due solely to the higher reflectance of the medium-profile tile. Therefore, CRCMs and roof venting are key strategies for providing cool roof products that can reduce whole house energy consumption.

## PHYSICS OF THE HEAT FLOW IN THE INCLINED CHANNEL

The transfer of heat across the roof tile and roof deck has similar physics to the problem associated with the heat transfer across the inclined air channel formed by roof-mounted solar collectors. Comprehensive reviews of both experimental and theoretical results are available in the literature, Hollands et al., (1976), Arnold et al., (1976) and most recently Brinkworth (2000) studied this situation as applied to flat-plate photovoltaic cladding.

All residential roofs are sloped and make an angle  $\theta$  with the horizontal plane that ranges from 2 inches of rise per 12 inches of run (9.5° slope) to a steep-sloped roof of 45°. During winter exposure, a roof deck is warmer than the tile and in the inclined air channel the heated surface is positioned below the cooler tile surface much like the solar panel application studied by Hollands et al. (1976). Here, a more dense air layer near the tile overlays a lighter air adjacent the roof deck (see  $\theta = 0$ , Figure 8). Hollands observed that the heat transfer across the air channel can switch from conduction to single-cell convection to Bénard cell convection depending on the strength of a non-dimensional parameter called the Rayleigh (Ra) Number. For Rayleigh numbers less than

$1708/\cos(\theta)$ , there is no naturally induced airflow within the cavity, and the heat transfer occurs exclusively by conduction. However, a flow of air occurs if buoyancy forces

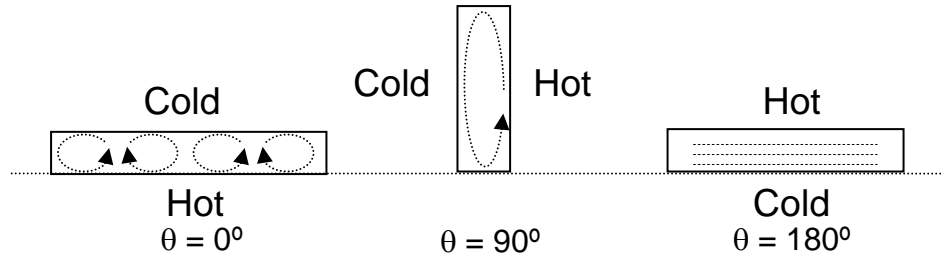


Figure 8. Heat Transfer Phenomena Occurring on the Underside of Roof Tile.

overcome the resistance imposed by the viscous or frictional forces. As the flow increases due to buoyancy, the heat transfer within the channel switches to Bénard cell convection, which has hexagonal cells with flow ascending in the center and descending along the sides of the air channel (see  $\theta = 0$ , Figure 8). Arnold et al., (1976) observed that the channel's aspect ratio and the slope of the solar panel (for our application a roof) had a major impact on the flow and heat transfer within the air channel. They observed that if the channel was rotated from  $\theta = 180^\circ$  (summer exposure for a roof) all the way to  $\theta = 0^\circ$  (winter exposure), the heat transfer rises to a maximum at  $\theta = 90^\circ$  and then as  $\theta$  decreases below  $90^\circ$  the heat transfer rate first decreases and passes through a local minimum at  $\theta^*$  (Bejan 1984). However, as  $\theta$  decreases below  $\theta^*$ , the heat transfer rate again rises because of the inception of Bénard cell convection. Arnold et al., (1976) also observed that the aspect ratio of the channel changed the critical angle  $\theta^*$  where the heat transfer across the channel was minimal. The information may be very useful for designing tile to limit ice damming in predominantly cold climates.

During summer exposure, the tile is hotter than the roof deck and Bénard cell convection does not occur within the inclined channel, because the lighter air layer is now atop the denser air layer near the roof deck. The air heated by the underside of the tile tends to rise, and natural convection begins within a boundary layer formed along the underside of the tile ( $\theta = 180$ , Figure 8). Brinkworth (2000) studied this situation as applied to flat-plate photovoltaic cladding, and it is this configuration and heat transfer mechanism that is evident in the field experiments shown for the ESRA tile roof systems.

## NUMERICAL SIMULATIONS

Computer simulations for thermally induced airflow and heat transfer across an inclined air channel were conducted for several different constant temperature wall boundary conditions and several different inclinations with the horizontal plane to better understand the strength of natural convection forces occurring within the heated channel. The channel was modeled for three conditions (Table 2) with the top plate always held at a higher temperature than the bottom plate to simulate summer exposure of the tile roof. The bottom and the two side surfaces of the channel were held at  $68^\circ\text{F}$ , and the top surface was held at  $68^\circ\text{F} + \Delta T$  listed in Table 2. All channel surfaces were assumed smooth and solid. The aspect ratio of the duct was fixed at 0.01.



Table 2: Channel Inclinations and Temperature Gradients used in Simulations.

Channel Inclination	Top Plate to Bottom Plate $\Delta T$ (°F)
0°	27
5°	1.8
35°	27

The simulations in Figures 9 and 10 are plotted in terms of the isotherms (constant temperature lines shown in color) and streamlines (lines of constant velocity). The results depicted in Figure 9a show that with no inclination, natural convection flow does not occur within the channel. Rather, a plume of heated air forms above the heated top surface. Because no net airflow occurs within the channel, the heat transfer across the two plates is conduction dominated. In Figure 9b with only five degrees of inclination and the top plate held just 1.8°F above the lower plate, there is a distinct flow moving within a boundary layer on the underside of the top plate. The flow field is laminar, which is most probably the same flow occurring in the inclined air channels of the tiles being field tested on the ESRA. These simulations indicate that naturally induced flow can be expected at very low inclination angles and very low temperature differences, well below those experienced in roofing systems. The induced flow causes a net flow from soffit to ridge that carries heat away from the attic. Parker et al., (2001) tested the white tile roof at 5 inches of rise per 12 inches of run (35° slope). They measured during July exposure a temperature gradient from the tile to the roof deck of about 14°F, (Figure 10). A numerical simulation is superimposed onto the roof for the roof slope studied by Parker et al., (2001) to help show the strength of the natural convection flows. The flow patterns are similar to those described in Figure 9; however, the exit jet is more in line with the duct axis indicating the momentum of the flow has increased (see Figure 10). Hence, the numerical results help to show qualitatively that the venting occurring on the underside of the roof tile can be very significant for dissipating heat away from the roof deck, making the tile roof system cooler than conventional direct nailed systems.

The numerical results do not take into account the effect of a forced flow component, which may aid or oppose the naturally induced flow nor is air leakage between the tile overlaps considered. Mixed convection (forced convection driven by wind effects that are accompanied by buoyancy effects) is an additional confounding variable that must be mathematically described a priori the prediction of the heat transfer across the roof deck. The key to the problem is to predict accurately the airflow within the cavity. Once known, the portions of heat penetrating the roof deck and that convected away through the ridge vent can be derived from energy balances.

## CONCLUSION

The tile roofs exposed to East Tennessee's climate have maintained their solar reflectance after two full years of exposure. Dust and urban pollution in California's urban areas soil the materials more so than in the less populated sections of the state, and the loss of reflectance is most severe for samples exposed at the slope of 2 inches of rise

per 12 inches of run. Increasing the slope reduced the soiling because the dust is probably blown away by the strong California winds.

The addition of complex inorganic pigments to clay and concrete tile significantly increased the solar reflectance and reduced the heat penetrating into the conditioned space. Applying a coating with CRCMs to medium-profile concrete tile reduced the heat penetrating the ceiling of a demonstration home by about 70% of that measured for an identical home with the same standard production medium-profile tile.

The venting occurring beneath a roof tile and the addition of CRCMs yields a synergistic improvement in the thermal performance of clay and concrete tile roofs. Field data collected at peak solar loading for clay and concrete tile roofs at ORNL demonstrate that venting is roughly equivalent to about 30 points of solar reflectance. Therefore, venting offers a significant 50% reduction in the heat penetrating the conditioned space compared to direct nailed roof systems that are in direct contact with the roof deck.

The combination of tile venting and improved solar reflectance offers excellent credits that clay and concrete tile can claim for cool roof steep-slope roof products as specified by the EPA and many state energy offices.

Numerical simulations of the inclined air channel formed by tile roof systems demonstrated that naturally induced flow can be expected at very low roof slopes and very low temperature differences, well below those experienced in roofing systems.

## **ACKNOWLEDGEMENTS**

Funding for this project was provided by the California Energy Commission's Public Interest Energy Research program through the U. S. Department of Energy under contract DE-AC03-76SF00098. The PIER project "Cool Roofs" has team players Steve Weil, Hashem Akbari, Ronnen Levinson and Paul Berdahl from LBNL and André Desjarlais and William Miller from ORNL working together to make CRCMs a market reality in tile, metal and shingles by 2006.

## **REFERENCES**

- Akbari, H., R. Levinson, P. Berdahl. 2004a. "A Review of Methods for the Manufacture of Residential Roofing Materials." Report to the California Energy Commission. To be published.
- Akbari, H., P. Berdahl, R. Levinson, R. Wiel, A. Desjarlais, W. Miller, N. Jenkins, A. Rosenfeld, C. Scruton. 2004b. "Cool Colored Materials for Roofs," *ACEEE Summer Study on Energy Efficiency in Buildings*. Proceedings of American Council for an Energy Efficient Economy, Asilomar Conference Center in Pacific Grove, CA, August.
- Arnold, J.N., I. Catton, D.K. Edwards. 1976. "Experimental Investigation of Natural Convection in Inclined Rectangular Regions of Differing Aspect ratios." *Journal of Heat Transfer*. (February) 67-71.

- Beal, D. and S. Chandra. 1995. "The Measured Summer Performance of Tile Roof Systems and Attic Ventilation Strategies in Hot Humid Climates." *Thermal Performance of the Exterior Envelopes of Buildings VI*, U.S. DOE/ORN/BETEC, December 4-8, Clearwater, FL.
- Bejan A. 1984. *Convection Heat Transfer*. New York: John Wiley & Sons, Inc.
- Brinkworth, B.J. 2000. "A Procedure for the Routine Calculation of Laminar Free and Mixed Convection in Inclined Ducts." *International Journal of Heat and Fluid Flow* 21: 456-462.
- Hollands K.G.T., T.E. Unny, G.D. Raithby and L. Konicek. 1976. "Free Convection Heat Transfer Across Inclined Air Layers." *Journal of Heat Transfer*. (May) 189-193.
- Levinson R., P. Berdahl and H. Akbari. 2004a. "Solar spectral optical properties of pigments, Part I: model for deriving scattering and absorption coefficients from transmittance and reflectance measurements." Submitted to *Solar Energy Materials & Solar Cells*.
- . 2004b. "Solar spectral optical properties of pigments, Part II: survey of common colorants." Submitted to *Solar Energy Materials & Solar Cells*.
- Miller, W.A., M-D. Cheng, S. Pfiffner and N. Byars. 2002. "The Field Performance of High-Reflectance Single-Ply Membranes Exposed to Three Years of Weathering in Various U.S. Climates." Final Report to SPRI, Inc., August.
- Miller W. A., K.T. Loyle, A.O. Desjarlais, H. Akbari, R. Levenson, P. Berdahl, S. Kriner, S. Weil, and R.G. Scichile. 2004. "Special IR Reflective Pigments Make a Dark Roof Reflect Almost Like a White Roof." *Thermal Performance of the Exterior Envelopes of Buildings, IX*. Proceedings of ASHRAE THERM IX, December, Clearwater, FL.
- Parker, D.S., J.K. Sonne, and J.R. Sherwin. 2002. "Comparative Evaluation of the Impact of Roofing Systems on Residential Cooling Energy Demand in Florida." *ACEEE Summer Study on Energy Efficiency in Buildings*. Proceedings of American Council for an Energy Efficient Economy, Asilomar Conference Center in Pacific Grove, CA, August.
- Parker, D.S., J.K. Sonne, J.R. Sherwin and N. Moyer. 2001. "Comparative Evaluation of the Impact of Roofing Systems on Residential Cooling Energy Demand in Florida." Final Report FSEC-CR-1220-00, prepared for the Florida Power and Light Company, May.



Figure 2: Clay and Concrete Tile being Field Tested on the Steep-Slope Attic Assembly at ORNL. (From right-to-left the test roofs are: direct nailed S-Mission Clay, direct nailed Medium-Profile Concrete, spot adhered foam S-Mission Concrete, batten and counter-batten Flat Concrete Slate, batten S-Mission Concrete and the direct nailed asphalt shingle roof.)

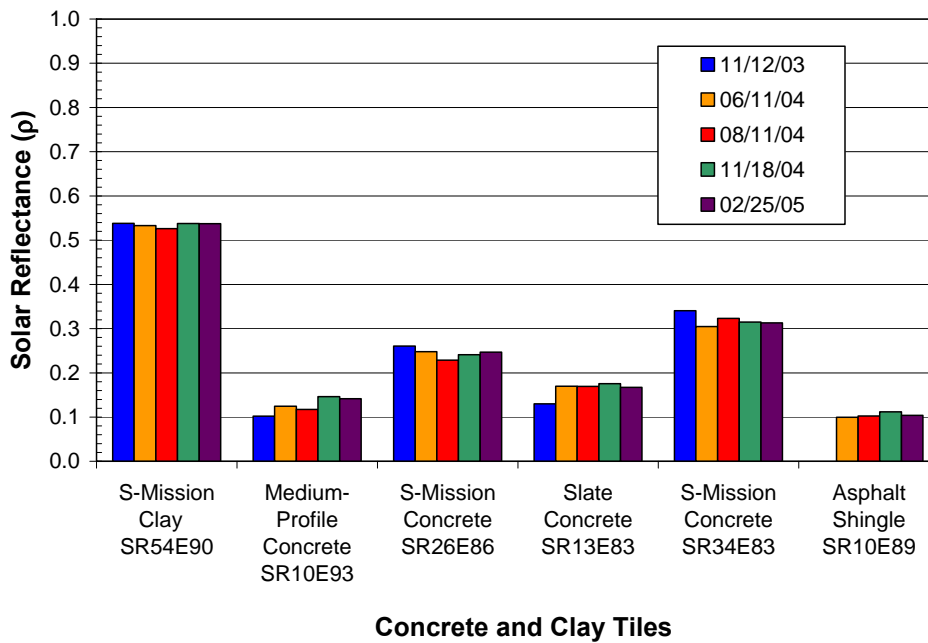


Figure 3: Solar Reflectance Measurements for the Tile Exposed on the Attic Assembly at ORNL. SRxxEyy values are solar reflectance and thermal emittance measures taken 11/12/03.

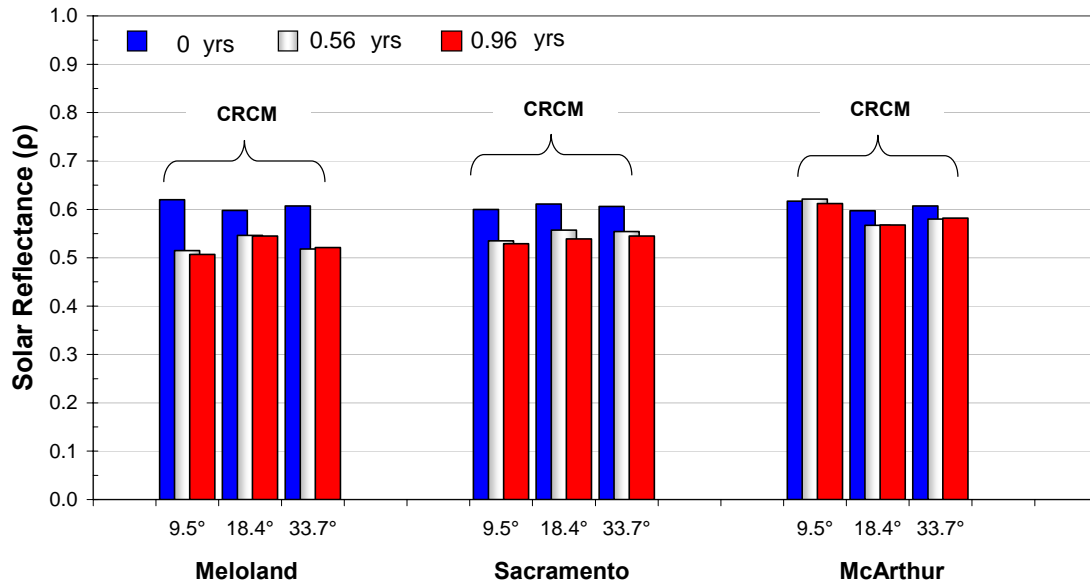


Figure 4: Clay Tile Field Tested on Exposure Racks in California at the slopes of 9.5°, 18.4°, and 33.7° which Represent Roof Slope Settings of 2, 4, and 8 inches of Rise per 12 inches of Run.

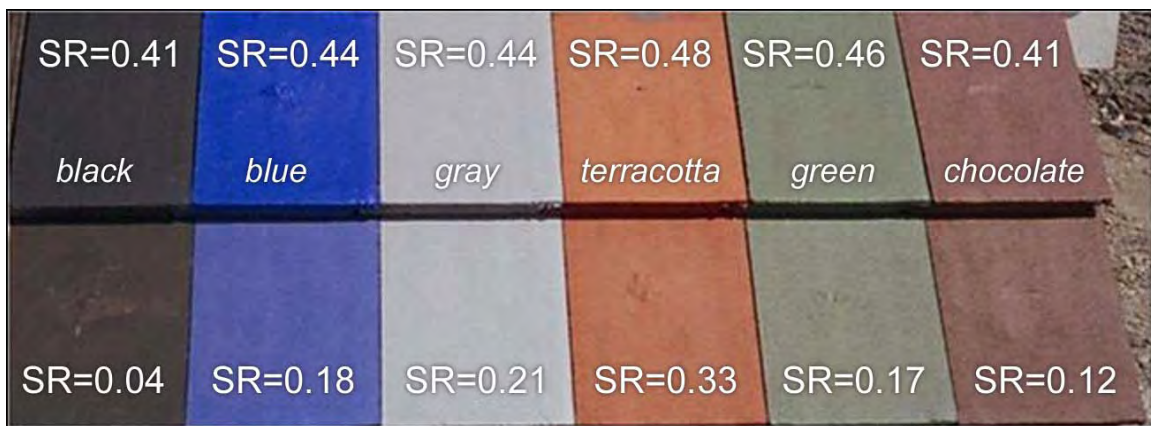


Figure 5: Solar Reflectance of Concrete Tile Roofs with CRCMs (top row) and Without CRCMs (bottom row). (The COOL TILE IR COATING™ technology was developed by Joe Reilly of American Rooftile Coating).

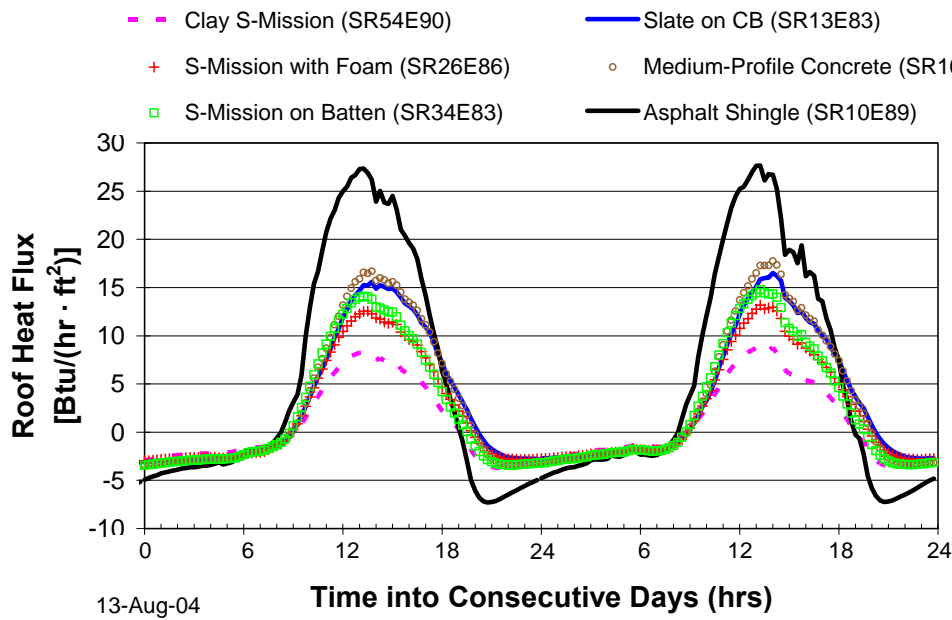


Figure 6: Heat Penetrating the Roof of each Attic Assembly being Field Tested on the ESRA.

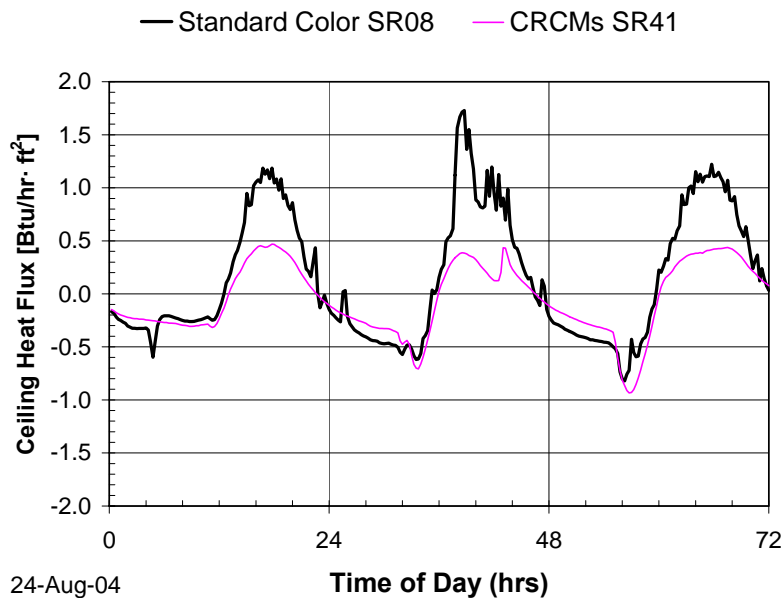


Figure 7: The Heat Penetrating the Ceiling of Two Homes Having Identical Footprint and Orientation in Fair Oaks, CA. (Roofs Are the Same as the Medium-Profile Concrete Tile Tested at ORNL.)

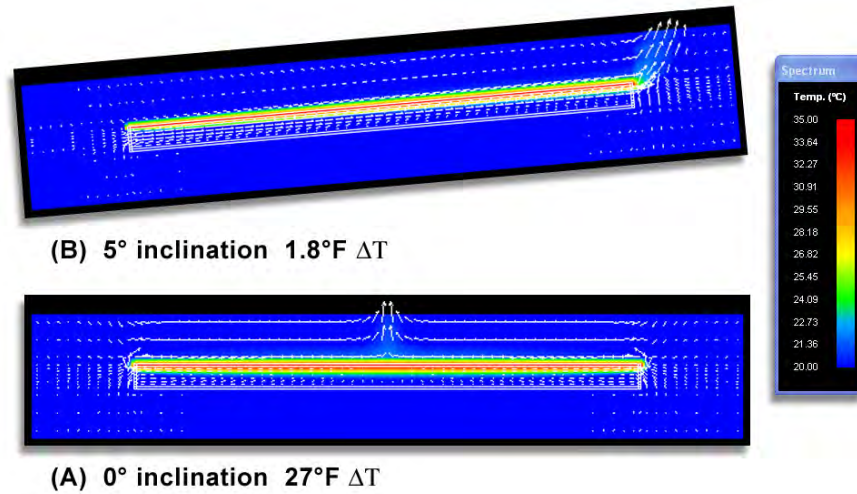


Figure 9: Naturally Induced Flow Observed at Low Inclinations and at Low Temperature Gradients from the Top Plate to the Lower Plate.

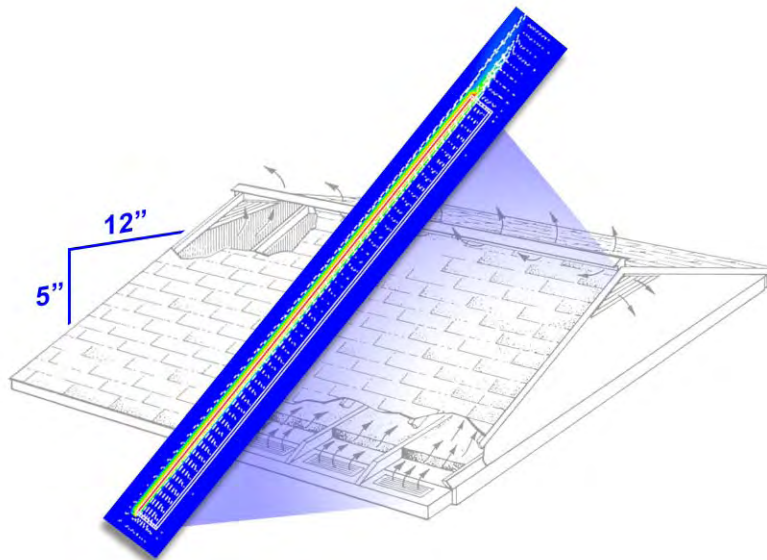


Figure 10: Naturally Induced Flow Observed at Typical Roof Slope and Temperature Gradients Observed in the work of Parker et al., (2002).



# PROFESSIONAL ROOFING

## Cooling down the house

### Residential roofing products soon will boast "cool" surfaces

by **Hashem Akbari and André Desjarlais**

Energy-efficient roofing materials are becoming more popular, but most commercially available products are geared toward the low-slope sector. However, research and development are taking place to produce "cool" residential roofing materials.

In 2002, the California Energy Commission asked Lawrence Berkeley National Laboratories (LBNL), Berkeley, Calif., and Oak Ridge National Laboratories (ORNL), Oak Ridge, Tenn., to collaborate with a consortium of 16 manufacturing partners and develop "cool" non-white roofing products that could revolutionize the residential roofing industry.

The commission's goal is to create dark shingles with solar reflectances of at least 0.25 and other nonwhite roofing products—including tile and painted metal—with solar reflectances not less than 0.45. The manufacturing partners have raised the maximum solar reflectance of commercially available dark products to 0.25-0.45 from 0.05-0.25 by reformulating their pigmented coatings. (For a list of the manufacturers, see "[Manufacturing partners](#)," page 36.)

Because coatings colored with conventional pigments tend to absorb invisible "near-infrared" (NIR) radiation that bears more than half the power of sunlight (see Figure 1), replacing conventional pigments with "cool" pigments that absorb less NIR radiation can yield similarly colored coatings with higher solar reflectances. These cool coatings lower roof surface temperatures, reducing the need for cooling energy in conditioned buildings and making unconditioned buildings more comfortable.

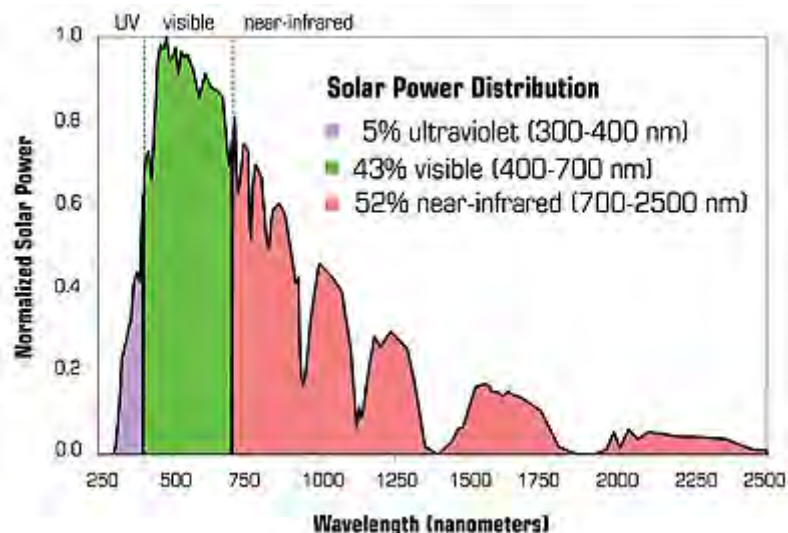


Figure courtesy of the Lawrence Berkeley National Laboratories, Berkeley, Calif.

**Figure 1: Peak-normalized solar spectral power—more than half of all solar power arrives as invisible, "near-infrared" radiation**

Cool, nonwhite roofing materials are expected to penetrate the roofing market within the next three years to five years. Preliminary analysis by LBNL and ORNL suggests the materials may cost up to \$1 per square meter more than conventionally colored roofing materials. However, this would raise the total cost of a new roof system only 2 percent to 5 percent.

### Cool, nonwhite colors

Developing the colors to achieve the desired solar reflectances involves much research and development. So far, LBNL has characterized the optical properties of 87 common and specialty pigments that may be used to color architectural surfaces. Pigment analysis begins with measurement of the reflectance— $r$ —and transmittance— $t$ —of a thin coating, such as paint film, containing a single pigment, such as iron oxide red. These "spectral," or wavelength-dependent, properties of the pigmented coating are measured at 441 evenly spaced wavelengths spanning the solar spectrum (300 nanometers to 2,500 nanometers).

Inspection of the film's spectral absorbance (calculated as  $1-r-t$ ) reveals whether a pigmented coating is "cool" (has low NIR



absorptance) or "hot" (has high NIR absorptance). The spectral reflectance and transmittance measurements also are used to compute spectral rates of light absorption and backscattering (reflection) per unit depth of film. The spectral reflectance of a coating colored with a mixture of pigments then can be estimated from the spectral absorption and backscattering rates of its components.

LBNL has produced a database detailing the optical properties of the 87 characterized pigmented coatings (see Figure 2). Its researchers are developing coating formulation software intended to minimize NIR absorptance (and maximize the solar reflectance) of a color-matched pigmented coating. The database and software will be shared with the consortium manufacturers later this year.

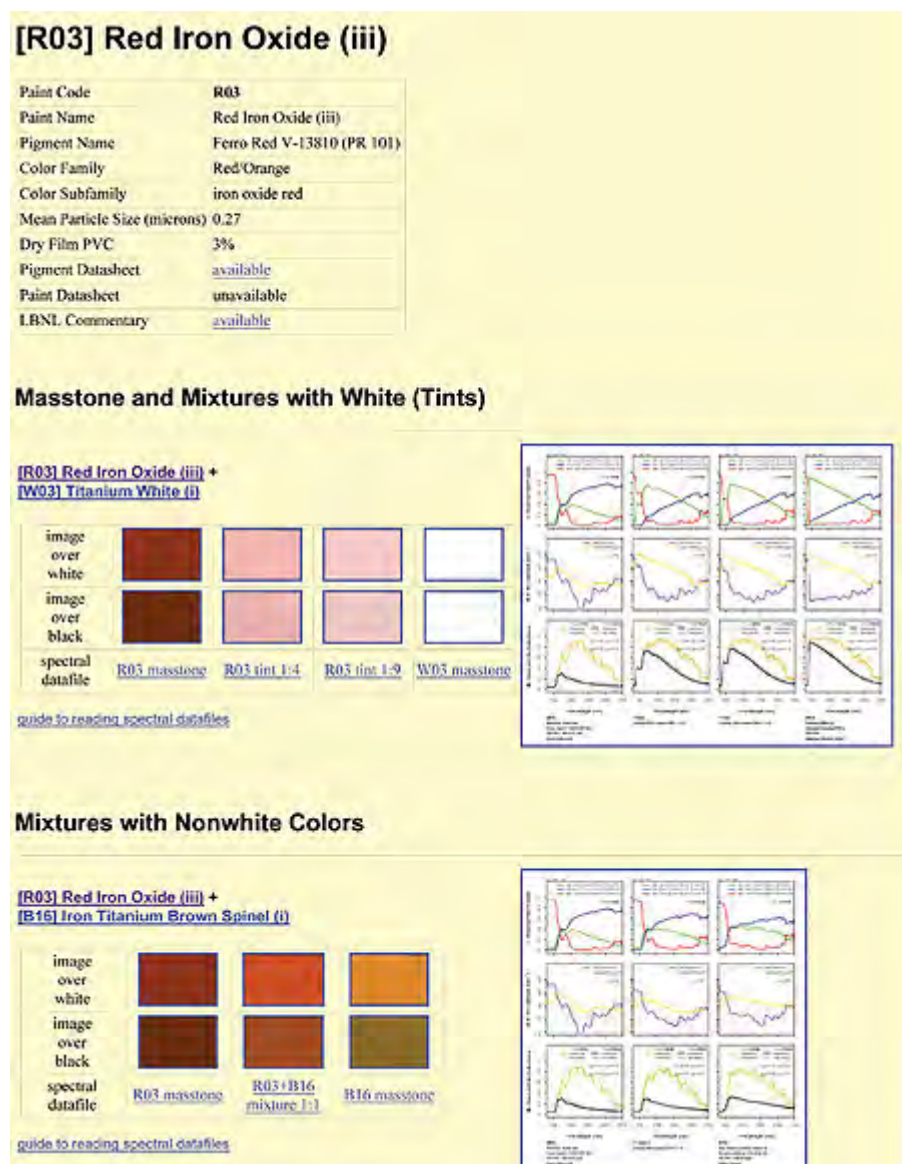


Figure courtesy of Lawrence Berkeley National Laboratories, Berkeley, Calif.

**Figure 2: Description of a red iron oxide pigment in the Lawrence Berkeley National Laboratory pigment database**

## Shingles

A new shingle's solar reflectance is dominated by the solar reflectance of its granules, which cover more than 97 percent of its surface. Until recently, the way to produce granules with high solar reflectance has been to use a coating pigmented with titanium dioxide (TiO<sub>2</sub>) white. Because a thin TiO<sub>2</sub>-pigmented coating is reflective but not opaque in NIR, multiple layers are needed to obtain high solar reflectance. Thin coatings colored with cool, nonwhite pigments also transmit NIR radiation. Any NIR light transmitted through the pigmented coating will strike the granule aggregate where it will be absorbed (typical dark rock) or reflected (typical white rock).

Multiple color layers, a reflective undercoating and/or reflective aggregate can increase granules' solar reflectances, thereby increasing shingles' solar reflectances.

Figure 3 shows the iterative development of a cool black shingle prototype by ISP Minerals Inc., Hagerstown, Md. A conventional black roof shingle has a reflectance of about 0.04. Replacing the granule's standard black pigment with a cool NIR-scattering black pigment (prototype 1) increases the solar reflectance of the shingle to 0.12. Incorporating a thin white sublayer (prototype 2) raises the shingle's solar reflectance to 0.16; using a thicker white sublayer (prototype 3) increases the shingle's reflectance to 0.18. The figure also shows an approximate performance limit (solar reflectance 0.25) obtained by applying 25-micron NIR-reflective black topcoat over an opaque white background.

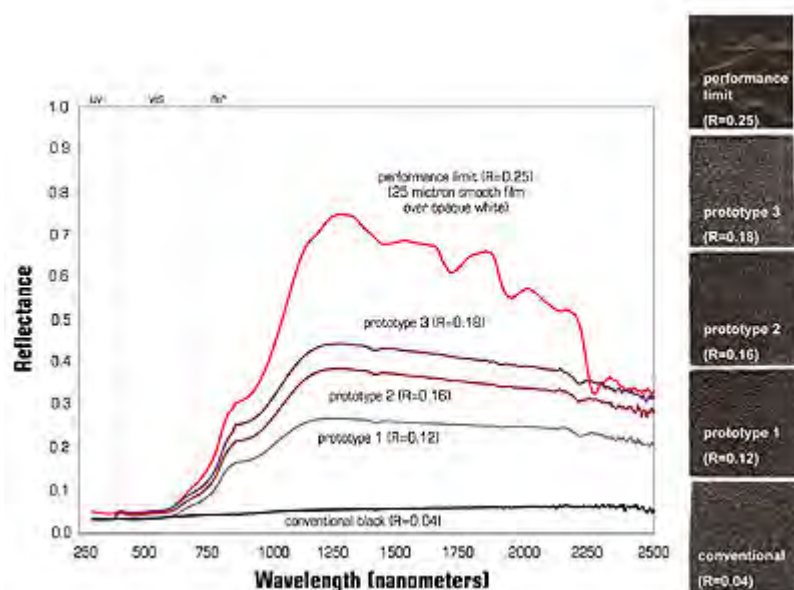


Figure courtesy of Lawrence Berkeley National Laboratories, Berkeley, Calif.

**Figure 3: ISP Minerals Inc., Hagerstown, Md., is developing a cool, black shingle. Shown are the solar spectral reflectances, images and solar reflectances (R) of a conventional black shingle; three prototype cool, black shingles; and smooth, cool, black film over an opaque white background.**

## Tile

There are three ways to improve solar reflectances of colored tiles: use clay or concrete with low concentrations of light-absorbing impurities, such as iron oxides and elemental carbon; color tile with cool pigments contained in a surface coating or mixed integrally; and/or include an NIR-reflective sublayer, such as a white sublayer, beneath an NIR-transmitting colored topcoat.

American Rooftile Coatings, Fullerton, Calif., has developed a palette of cool, nonwhite coatings for concrete tiles. Each of its COOL TILE IR COATINGS™ shown in Figure 4 has a solar reflectance greater than 0.40. The solar reflectance of each cool coating exceeds that of a color-matched, conventionally pigmented coating by 0.15 (terra cotta) to 0.37 (black).

## Metal

Cool, nonwhite pigments can be applied to metal with or without a white sublayer. If a metal is highly reflective, the sublayer may be omitted. The polymer coatings on metal panels are kept thin to withstand bending. This restriction on coating thickness limits pigment loading (pigment mass per unit surface area).

## Performance research

ORNL naturally is weathering various types of conventionally pigmented and cool-pigmented roofing products at seven California sites. Each "weathering farm" has three south-facing racks for exposing samples of roofing products at typical roof slopes. Sample weathering began in August 2003 and will continue for three years—until October 2006. Solar reflectance and thermal emittance are measured twice per year; weather data are available continuously. Solar spectral reflectance is measured annually to gauge soiling and document imperceptible color changes.

ORNL and the consortium manufacturers also are exposing roof samples to 5,000 hours of xenon-arc light in a weatherometer, a laboratory device that accelerates aging via exposure to ultraviolet radiation and/or water spray. ORNL will examine the naturally weathered samples for contaminants and biomass to identify the agents responsible for soiling. This may help manufacturers produce roofing materials that better resist soiling and retain high solar reflectance. Changes in reflectance will be correlated to exposure.

The labs and manufacturing partners also have established residential demonstration sites in California. The first, in Fair Oaks

(near Sacramento), includes two pairs of single-family, detached homes. One pair is roofed with color-matched conventional and cool-painted metal shakes supplied by Custom-Bilt Metals, South El Monte, Calif., and the other features color-matched conventional and cool low-profile concrete tiles supplied by Hanson Roof Tile, Charlotte, N.C. The second site, in Redding, is under construction and by summer will have a pair of homes roofed with color-matched conventional and cool asphalt shingles.

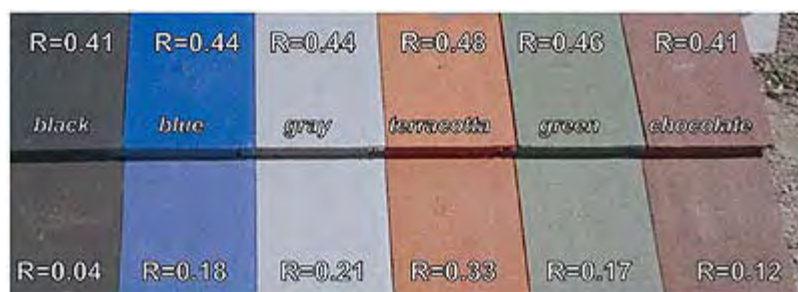


Figure courtesy of American Rooftile Coatings.

**Figure 4:** This is a palette of color-matched cool (top row) and conventional (bottom row) roof tile coatings developed by American Rooftile Coatings, Fullerton, Calif. Shown on each coated tile is its solar reflectance.

The homes in Fair Oaks are adjacent and share the same floor plan, roof orientation and level of blown ceiling insulation (19 hr•ft<sup>2</sup>•°F/Btu). The homes in Fair Oaks and Redding will be monitored through at least summer 2006.

One of the Fair Oaks homes roofed with low-profile concrete tile was colored with a conventional chocolate brown coating (solar reflectance 0.10), and the other was colored with a matching cool chocolate brown (an American Rooftile Coatings COOL TILE IR COATING™ with solar reflectance 0.41). The attic air temperature beneath the cool brown tile roof has been measured to be 3 K to 5 K cooler than that below the conventional brown tile roof during a typical hot summer afternoon (273.15 K equals 0 C).

The results for the pair of Fair Oaks homes roofed with painted metal shakes are just as promising. There, the attic air temperature beneath the cool brown metal shake roof (solar reflectance 0.31) was measured to be 5 K to 7 K cooler than that below the conventional brown metal shake roof.

These reductions in attic temperature are solely the result of the application of cool, colored coatings. The use of these cool, colored coatings also decreased the total daytime heat influx (solar hours are from 8 a.m.-5 p.m.) through the west-facing concrete tile roof by 4 percent and the south-facing metal shake roof by 31 percent (see Figure 5).

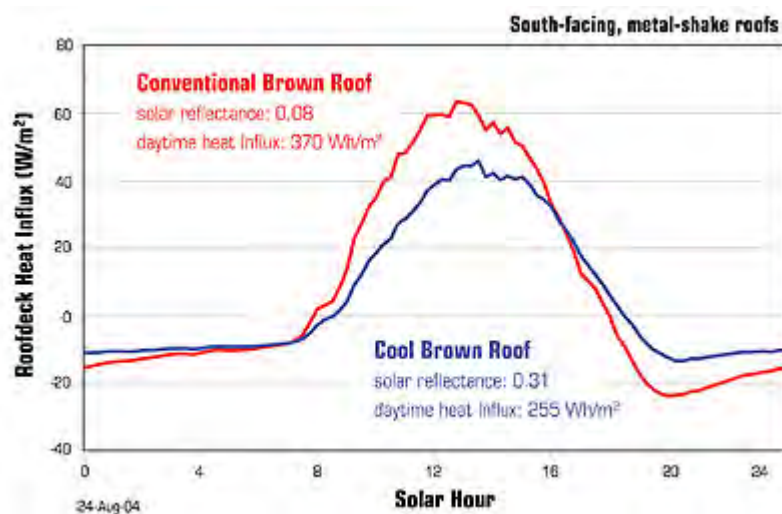


Figure courtesy of Oak Ridge National Laboratory, Oak Ridge, Tenn.

**Figure 5:** Heat flows through the roof decks of an adjacent pair of homes during the course of a hot summer day. The total daily heat influx through the cool brown metal shake roof (solar reflectance 0.31) between the solar hours of 8 a.m. and 5 p.m. is 31 percent lower than through the conventional brown metal shake roof (solar reflectance 0.08).

ORNL also is testing several varieties of concrete and clay tile on a steep-slope roof to further investigate the individual and combined effects of cool, colored coatings and subtile ventilation on the thermal performance of a cool roof system.

## Results to date

The two laboratories and their industrial partners have achieved significant success in developing cool, colored materials for

concrete tile, clay tile and metal roofs.

Since the inception of this program, the maximum solar reflectances of commercially available dark roofing products has increased to 0.25-0.45 from 0.05-0.25. Bi-layer coating technology (a color topcoat over a white or other highly reflective undercoat) is expected to soon yield several cost-effective cool, colored shingle products with solar reflectances in excess of the U.S. Environmental Protection Agency's ENERGY STAR® threshold of 0.25. Early monitoring results indicate using cool, colored roofing products measurably reduces heat flow into conditioned homes with code-level ceiling insulation.

As homeowners continue to seek energy-efficient products, the roofing industry's research into residential roofing products that offer energy-efficient features naturally will continue to evolve.

Provided energy-efficient products continue to perform satisfactorily, we expect cool, nonwhite metal, tile and shingle products to penetrate the roofing market within the next three to five years.

*Hashem Akbari leads LBNL's Heat Island Group. André Desjarlais leads ORNL's Building Envelope Group.*

**Editor's note:** Ronnen Levinson, scientist, Paul Berdahl, staff scientist, and Stephen Wiel, staff scientist, of LBNL; William Miller senior research engineer of ORNL; and Nancy Jenkins, program manager, Arthur Rosenfeld, commissioner, and Chris Scruton, project manager, of the California Energy Commission contributed to this article.

---

## Manufacturing partners

### 3M

St. Paul, Minn.

[www.scotchgard.com/roofinggranules](http://www.scotchgard.com/roofinggranules)

### Akzo Nobel

Felling, United Kingdom

[www.akzonobel.com](http://www.akzonobel.com)

### American Rooftile Coatings

Fullerton, Calif.

[www.americanrooftilecoatings.com](http://www.americanrooftilecoatings.com)

### BASF Industrial Coatings

Florham Park, N.J.

[www.ultra-cool.basf.com](http://www.ultra-cool.basf.com)

### CertainTeed Corp.

Valley Forge, Pa.

[www.certainteed.com](http://www.certainteed.com)

### Custom-Bilt Metals

South El Monte, Calif.

[www.custombiltmetals.com](http://www.custombiltmetals.com)

### Elk Corp.

Dallas

[www.elkcorp.com](http://www.elkcorp.com)

### Ferro Corp.

Cleveland

[www.ferro.com](http://www.ferro.com)

### GAF Materials Corp.

Wayne, N.J.

[www.gaf.com](http://www.gaf.com)

### Hanson Roof Tile

Charlotte, N.C.

[www.hansonrooftile.com](http://www.hansonrooftile.com)

### ISP Minerals Inc.

Hagerstown, Md.

### MCA Tile

Corona, Calif.

[www.mca-tile.com](http://www.mca-tile.com)

**MonierLifetile LLC**

Irvine, Calif.

[www.monierlifetile.com](http://www.monierlifetile.com)

**Owens Corning**

Toledo, Ohio

[www.owenscorning.com/around/roofing/Roofhome.asp](http://www.owenscorning.com/around/roofing/Roofhome.asp)

**Shepherd Color Co.**

Cincinnati

[www.shepherdcolor.com](http://www.shepherdcolor.com)

**Steelscape Inc.**

Kalama, Wash.

[www.steelscape-inc.com](http://www.steelscape-inc.com)

---

**Web-exclusive information** — [Study about the development of cool, colored roofing materials](#)

[© Copyright 2006 National Roofing Contractors Association](#)

# **COOL METAL ROOFING IS TOPPING THE BUILDING ENVELOPE WITH ENERGY EFFICIENCY AND SUSTAINABILITY**

by

Scott Kriner, Akzo Nobel Coatings, Inc.  
William A. Miller, Ph.D., P.E., Oak Ridge National Laboratory  
Danny S. Parker, Florida Solar Energy Center

“Cool Roofing...Cutting through the Glare”  
Atlanta, GA  
May 12-13, 2005

## **INTRODUCTION**

Evaluating the weathering effects on solar reflectance and thermal emittance of metal roofing is important in determining the cooling and heating energy loads on a building. Akbari and Konopacki (1998) found that annually about \$0.75 billion can be saved by widespread implementation of light-colored roofs in cooling dominant climates. Their simulations based on both old and new residential and commercial construction having respectively R-11 and R-19 levels of ceiling insulation also showed that thermal emittance affects both cooling and heating energy use. In cooling dominant climates, a low-emittance roof yields a higher roof temperature and in turn, increases the cooling load imposed on the building. Their simulations showed that changing the thermal emittance from 0.90 to 0.25 caused a 10% increase in the annual utility bill. However, in cold climates, a low-emittance roof adds resistance to the passage of heat leaving the roof, which results in savings in heating energy. Akbari and Konopacki (1998) showed that in very cold climates with little or no summertime cooling, the heating energy savings resulting from decreasing the roof emittance almost reached 3% of the buildings annual energy consumption.

The durability or retention of the solar reflectance and thermal emittance is of paramount importance for sustained thermal performance of a roof. Painted metal roofing is commonly offered with 30 year product warranties because field exposures have shown it retains almost 95% of its initial solar reflectance even after 30 years of climatic exposure (Miller and Rudolph 2004). Hence, the aged radiative properties are very similar to initial values, and therefore should be considered when sizing the comfort conditioning equipment or projecting the energy cost savings as compared to other roofing products that soil and lose reflectance.

## **METAL ROOFING**

According to 2004 F.W. Dodge reports, metal's share of the residential steep-slope roofing market has reached 8%. This is a three-fold increase in the past six years, and



more and more residential and steep-slope architectural roofing projects are demanding pre-painted metal roofing. Ducker Worldwide study (2002) showed that metal's overall share of the commercial roofing market is 15%, and in steep-slope commercial applications, metal has a 33% market share. Its finishes are colorful, inert, and do not pose a health risk. Metal roofing is code compliant and tested for fire, wind, hail resistance and is non-combustible which reduces the spread of fire in and among buildings.

Metal roofing is available in a wide variety of textures, colors, surface finishes, and formed profiles. Linear roll-formed panels as well as modular press-formed shingle, shake or tile facsimiles are possible with unpainted or pre-painted metal. Given the diversity of the family of metal roofing products, the material can be engineered for optimum energy efficiency depending on the climate and microenvironment. For example, unpainted metal roofing such as 55% Al-Zn coated steel<sup>1</sup> sheet or hot dip galvanized steel<sup>2</sup> has a relatively high solar reflectance but a low thermal emittance. In cold climates where heating loads dominate, this type of roofing product is desirable to minimize annual energy consumption, because the low thermal emittance retains heat that would otherwise radiate to the night-sky. In contrast, a light-colored, or specially a pre-painted metal roof can have a high solar reflectance and a high thermal emittance. In warmer climates where cooling loads dominate, that type of roof is desirable for reducing annual energy costs. In both cases, metal can be chosen as an energy-efficient roof product.

## **PRE-PAINTED METAL ROOFING**

Premium industrial paint finishes are applied to metal substrates using a controlled continuous coil coating process at speeds of up to 700 feet per minute. Paint systems are oven-baked in this process and are warranted for up to 30 years for chalk and fade resistance. Paint suppliers who offer these warranties do so based on real-time outdoor performance data obtained from weathering farms. Polyvinylidene fluoride (PVDF) paint resin systems have become the premier metal roofing finish owing to its superior resistance to color fade. Color fade is measured in  $\Delta E$  Hunter units per ASTM D 2244-02 (ASTM 2002). One  $\Delta E$  unit is the slightest color difference perceptible to the human eye. PVDF-painted metal roofing material typically displays no more than 5  $\Delta E$  units of fade over 20 years.

The PVDF resin chemistry was patented and licensed by Pennwalt Corp. in the 1960's and is now available from Arkema under the Kynar 500® trademark and from Solvay Solexis under the Hylar 5000® trademark. The chemistry is from the same organic film bonding that is responsible for Teflon®, making it extremely chemical resistant and

---

<sup>1</sup> This steel is exposed to a molten bath composed of 55% Al-43.5% Zn -1.5% Si at a temperature of 1100°F (593°C). The coating is solidified rapidly to enhance both the microstructure and the corrosion resistance.

<sup>2</sup> A zinc-coated steel sheet manufactured by the steel being dipped in continuous coil form through a molten bath of zinc.

dirt shedding. Years of testing show that PVDF resin is most durable when it comprises 70% of the total resin component in a paint film. The Kynar or Hylar type coatings have superior resistance to color fade, chalk, gloss change and corrosion.

Table 1 shows examples of some typical radiative properties of different types of metal roof products that are listed on the Energy Star<sup>®</sup> roof products directory. Metal and metal paint finishes comprise 65% of the products on the Energy Star<sup>®</sup> roofing directory.

Table 1: Energy Star<sup>®</sup> Radiative Properties of Listed Metal Roofing

Surface	Initial Solar Reflectance	3-year Aged Solar Reflectance
Unpainted 55% Al-Zn	0.78	0.58
Acrylic coated 55% Al-Zn	0.68	0.57
Painted White	0.77	0.74
Painted Beige	0.67	0.67
Painted Off-White	0.56	0.52
Painted Almond	0.51	0.52
Painted Silver	0.45	0.43
Painted Copper	0.42	0.39
Painted Green	0.32	0.31
Painted Red	0.31	0.31
Note: Thermal emittance of unpainted metal surfaces is 0.08 – 0.10. Thermal emittance of painted surfaces is typically 0.84 - 0.87		

## FSEC EXPERIMENTAL PROGRAMS

In the summer of 2000, the Florida Solar Energy Center (FSEC), in co-operation with Florida Power and Light (FPL) and Habitat for Humanity (HFH), instrumented seven side-by-side homes in Fort Myers, Florida with identical floor plans, construction, and orientation, but with different roofing systems designed to reduce attic heat gain (Parker et al., 2002). Six houses had R-19 ceiling insulation, and the seventh house had an unvented attic with insulation on the underside of the roof deck rather than the ceiling. Identical two-ton split system air conditioners with 5 kW strip heaters were installed in each of the seven homes. The houses underwent a series of tests to ensure that the construction and mechanical systems performed similarly.

A three-letter identification code is used to identify each roof product, and the initial solar reflectance and thermal emittance of new material are shown below.

Description of Test Roof on each HFH House	Label	Solar Reflectance	Thermal Emittance
• Dark Gray Fiberglass Shingles	RGS	0.082	0.89
• White Barrel-Shaped Tile	RWB	0.742	0.89
• White Fiberglass Shingle	RWS	0.240	0.91

Description of Test Roof on each HFH House	Label	Solar Reflectance	Thermal Emittance
• Flat White Tile	RWF	0.773	0.89
• Terra Cotta Barrel-Shaped Tile	RTB	0.346	0.88
• White 5-Vee Metal	RWM	0.662	0.86
• Dark Gray Fiberglass Shingles on a Sealed Attic having Insulation on the Roof Plane	RSL	0.082	0.89

The relative performance of the seven homes was evaluated for one month in the summer of 2000 under unoccupied and carefully controlled conditions. Parker et al., (2001) set the temperature controls on the air conditioning thermostats of all the houses at a constant 77° F (25°C). Table 2 summarizes the measured attic temperatures, cooling loads and savings for the seven homes over the unoccupied monitoring period; the data are ranked in descending order of total daily energy consumption. The average interior air temperature near the thermostat in all homes was within 1°F (0.56°C) of each other. However, because of the large influence of the thermostat temperature, the monitored cooling results in Table 1 are adjusted to account for set point differences among houses, (Parker et al., 2001). All thermostats were adjusted up 1°F (0.56°C) for four consecutive days and the data was used to map correction factors for power consumption by the air conditioner as effected by the variation in thermostat setpoint.

Not surprisingly, the control home (RGS) had the highest consumption (17.0 kWh/day). The true white roofing types (> 60% reflectance) had the lowest energy use. Both the white barrel (RWB) and white flat tile (RWF) roofs averaged a consumption of 13.3 kWh/day for respectively a 18.5% and 21.5% cooling energy reduction. The white metal roof (RWM) showed the largest impact with a 12.0 kWh/day July consumption, yielding a 24% reduction in cooling energy consumption.

**TABLE 2: Cooling Performance\* During Unoccupied Period: July 8 – 31, 2000**

Site	Total kWh/d	Savings kWh/d	Thermostat		Mean Attic (°F)	Mean Attic (°C)	Max Attic (°F)	Max Attic (°C)	Temp. Adjust %	Field EER	Final Saving %
			(°F)	(°C)							
RGS	17.0	0.00	77.2	25.11	90.8	32.7	135.6	57.5	0.0	8.30	0.0
RTB	16.0	1.01	77.0	25.0	87.2	30.7	110.5	43.6	-1.6	8.12	7.7
RWS	15.3	1.74	77.0	25.0	88.0	31.1	123.5	50.8	-1.2	9.06	10.6
RSL	14.7	2.30	77.7	25.4	79.0	26.1	87.5	30.8	5.4	8.52	7.8
RWB	13.3	3.71	77.4	25.2	82.7	28.2	95.6	35.3	2.8	8.49	18.5
RWF	13.2	3.83	77.4	25.2	82.2	27.9	93.3	34.1	2.1	7.92	21.5
RWM	12.0	5.00	77.6	25.3	82.9	28.3	100.7	38.2	4.9	8.42	24.0
Note:											
* Final savings are corrected for the differences in the interior temperature and the performance of the air conditioner among houses.											

It is noteworthy that the average July outdoor ambient air temperature during the monitoring period (82.6°F [28.1°C]) was very similar to the 30-year average for Fort Myers (82°F [27.7°C]). Thus, the current data are representative of typical South Florida weather conditions. Relative to the standard control home, the data show two distinct groups in terms of performance.

- Terra Cotta tile, white shingle and sealed attic constructions produced approximately an 8% to 11% cooling energy reduction.
- Reflective white roofing yielded a 19% to 24% reduction in the consumed cooling energy.

White flat tile performed slightly better than the white barrel due to its higher solar reflectance. The better performance of white metal is believed due to the effect of thermal mass. The metal roof incurred lower nighttime and early morning attic temperatures than did the tile or shingles, leading to lower nighttime cooling demand. According to FPL, this study showed that a white painted galvanized metal roof should save a customer who lives in an average-size 1,770 square foot home approximately \$128 or 23% to 24% annually in cooling costs, compared with a dark gray shingle roof on the same home. It should be noted, however, that this estimation is based on the assumption that the initial reflectance performance remains unchanged over time.

### **Peak Day Performance**

July 26 was one of the hottest and brightest days in the data collection period and was used to view the effects of maximum solar irradiance on the candidate roofing systems and to also evaluate peak influences on utility demand (Table 3). The average solar irradiance was 371 W/m<sup>2</sup> and the maximum outdoor ambient air temperature was 93.0°F (33.8°C).

The roof decking temperature (Figure 1), measured just underneath the respective roof covers, were highest for the sealed attic construction (RSL) since the insulation under the decking forced much of the collected solar heat to migrate back out through the shingles. The sealed attic construction experienced measured deck temperatures that were 20°F (11.1°C) higher than the control house during the sunlight hours. The (RGS) dark gray shingle had the next highest deck temperature; it reaching a peak high of 143.5°F (62°C). Increasing the solar reflectance of the (RGS) shingle from 0.082 to 0.24 for the white fiberglass shingle (RWS) dropped the peak deck temperature about 14°F (7.9°C). The white roofing systems (RWM, RWB and RWF) experienced peak deck temperatures approximately 40°F (22°C) cooler than the darker shingles on the control house (RGS in Figure 1). The terra cotta barrel tile was about 29°F (16°C) cooler on this July 26 day of peak solar irradiance.

The measured mid-attic air temperatures above the ceiling insulation further revealed the impact of the white reflective roofs with max attic temperatures about 35 to 40°F (19.2 to 22.2°C) cooler than the control home (RGS), with the exception of white fiberglass shingles (Table 2). The white metal, white clay tile and the white shingle roofs did better at controlling demand than did the sealed attic on this very hot day. However,

the white metal roof performed best showing peak savings of 33% over the RGS control (Table 3).

**TABLE 3: Summer Peak Day Cooling Performance for July 26, 2000**

Site	Cooling Energy	Savings		Peak Period*		
		kWh	Percent	Demand (kW)	Savings (kW)	Percent
RGS	18.5 kWh		----	1.631	0.000	----
RTB	17.2 kWh	1.3	7%	1.570	0.061	3.7
RSL	16.5 kWh	2.0	11%	1.626	0.005	0.3
RWS	16.5 kWh	2.0	11%	1.439	0.192	11.8
RWF	14.2 kWh	4.3	23%	1.019	0.612	37.5
RWB	13.4 kWh	5.1	28%	1.073	0.558	34.2
RWM	12.4 kWh	6.1	33%	0.984	0.647	39.7
* Peak utility load occurred from 4 to 6 PM						

#### **ORNL EXPERIMENTAL PROGRAMS**

The Buildings Technology Center (BTC) of ORNL evaluated pre-painted and unpainted metal roof systems for the Cool Metal Roof Coalition (CMRC), a consortium of metal roofing industries. The American Iron and Steel Institute (AISI), the GALVALUME Sheet Producers of North America (NamZAC), the Metal Building Manufacturers Association (MBMA), the Metal Construction Association (MCA), and the National Coil Coaters Association (NCCA) are keenly interested in documenting whether their products can reduce the energy used for comfort cooling and heating of both residential and commercial buildings.

The study found that PVDF painted metal sheds dirt, retains its initial solar reflectance very well, resists the growth of biomass, resists corrosion, and performs similarly in different climates. Compared to some non-metallic roofing products, such as single-ply membrane which showed a drop in solar reflectance of 40% in a three-year period, painted metal retained 95% of its initial solar reflectance over the same time period (Miller, et al., 2004).

The BTC instrumented and field tested steep-slope and low-slope roof test sections of pre-painted and unpainted metals for three years on a test building called the Envelope Systems Research Apparatus (ESRA). The test assembly included white-painted PVDF galvanized steel, off-white polyester, 55% Al-Zn coated steel painted with a clear acrylic dichromate layer, unpainted galvanized steel, and unpainted 55% Al-Zn-coated steel. Five painted metal panels were tested on a steep-slope assembly. Three panels of white-painted PVDF galvanized steel, three panels of 55% Al-Zn-coated steel painted with a clear acrylic dichromate layer, six panels of bronze-painted PVDF aluminum, and three panels of black-painted PVDF galvanized steel were also exposed to East Tennessee's weather. An asphalt-shingle roof section was included as the base of comparison. It is warranted for a 15-year lifetime and has both Underwriter Laboratory and American

Society for Testing Materials (ASTM) approval for residential roofing. Salient features of the ESRA facility are fully discussed by Miller and Kriner (2001).

Reflectance measurements were made every three months on the ESRA's steep- and low-slope metal roofs. Each metal roof was described generically using an SR<sub>xx</sub>E<sub>yy</sub> designation. SR<sub>xx</sub> states the solar reflectance of a new sample, 1.0 being a perfect reflector. E<sub>yy</sub> defines the thermal emittance of the new sample, 1.0 being blackbody radiation. For example, the asphalt-shingle roof is labeled SR09E91 in Figure 2. Its freshly manufactured surface properties are therefore 0.09-solar reflectance and 0.91-thermal emittance. Miller and Kriner (2001) identify the SR<sub>xx</sub>E<sub>yy</sub> designations for the different painted and unpainted test metals tested at ORNL.

After 3.5 years of exposure, the white and bronze painted PVDF metal roofs, SR64E83 and SR07E87 respectively, lost less than 5% of their original reflectance. The coated steel painted with a clear acrylic dichromate layer, SR64E08, showed a 12% loss in reflectance. In comparison the asphalt shingle roof, SR09E91, had a measured reflectance of about 10% (Figure 2). The reflectance comparison is very important, because both SR64E83 and SR64E08 roofs reflected about 50% more solar energy away from these test roofs than did the asphalt shingle. Even more promising is the observed durability of the surface of the painted metals; reflectance remained fairly level. Less heat is therefore absorbed by the "cool" painted metal roofs and the building load and the peak utility load are reduced as compared to darker more absorptive roofs (i.e., SR09E91). The urban heat content is also reduced because the "cool" painted metal roofs would not convect as much heat to the ambient wind blowing across the "cool" roof.

Testing conducted at the roof slopes of 4 inches of rise per 12 inches of run (i.e., steep slope-roof [SSR] in Figure 2) and at ¼ inch of rise per 12 inches of run (i.e., low-slope roof [LSR] in Figure 2) further show that the slope of the roof has little effect on the loss of reflectance for the painted metal roofing having the PVDF finish. The painted metal appears to have excellent corrosion resistance. Its surface opacity have limited any photochemical degradation caused by ultraviolet light present in sunlight over the three years of testing. All painted metal roofs have maintained their original manufactured appearance. After 3.5 years of exposure, acid rains with a measured pH of 4.3 in East Tennessee (National Atmospheric Deposition Program) have not etched the metal finish. ORNL scientists detected evidence of biological growth on some of the test roofs (Miller et al., 2002); however, the PVDF surface finish does not appear to allow the growth to attach itself and atmospheric pollution is washed off by rain.

Most dramatic are the trends observed in the solar reflectance and the thermal emittance of the painted metal roofs tested at different exposure sites across the country. Similar reflectance was measured in the hot, moist climate of Florida as compared to the predominantly cold climate of Nova Scotia (Figure 3). Solar reflectance and thermal emittance measures collected from the test fence exposure sites in Florida, Nova Scotia, Pennsylvania and also at Oak Ridge (Figure 3) are very similar to the reflectance and emittance measures recorded for the test roofs exposed on the ESRA in Oak Ridge (Figure 1). The changes in solar reflectance and thermal emittance of the painted PVDF metals are independent of climate. The results show that fence exposure data are a viable alternative for certifying the painted PVDF metal roofs as Energy Star® compliant,



because they yielded very similar trends as the identical roofs exposed on the ESRA steep-slope assembly.

The emittance of the painted metal roofs did not change much after 3.5 years of weathering. In fact, the data in Figure 3 show that the emittance increased slightly over time.

#### AGED REFLECTANCE PERFORMANCE

Codes and standards organizations often specify only initial solar reflectance and thermal emittance values but no specific aged criteria. Instead, a standard rate of degradation is commonly assumed and applied to the initial values to predict aged values. For example, in the California state energy code Title 24, 2005 version, the prescriptive criteria for a “cool roof” specifies a minimum initial solar reflectance of 0.70 and thermal emittance of 0.75. The aged solar reflectance ( $\rho_{\text{Aged}}$ ) value is calculated using the following equation:

$$\rho_{\text{Aged}} = 0.2 + 0.7 * [\rho_{\text{initial}} - 0.2]$$

Using the minimum initial solar reflectance ( $\rho_{\text{initial}}$ ) of 0.70 prescribed by the 2005 version of Title 24, the calculation yields an assumed aged reflectance value of 0.55 or a 21.4% drop in initial solar reflectance for white-painted PVDF metal (Figure 3). Here the loss of solar reflectance is clearly overestimated. However, the prescriptive criteria fairly depict the loss of reflectance for the coated steel painted with a clear acrylic dichromate layer, SR64E08 (Figure 4).

Similarly, in the ASHRAE 90.1 commercial roofing standard, the insulation credits apply to cool roofs defined as having an initial solar reflectance of 0.70. The insulation adjustment factors are based on an aged solar reflectance value of 0.55 for the calculations. The white-painted PVDF metal appears to be unduly penalized because it retains its solar reflectance based on the three year results of the ORNL study. To further prove metal’s superior retention of reflectance the metal industry collected data from the thousands of pre-painted metal samples routinely tested by suppliers for outdoor weathering. Outdoor exposure data from over a variety of time periods showed that PVDF paint systems, exposed in a variety of southern Florida weathering farms, retained approximately 95% of its initial solar reflectance (Figure 5). The data clearly demonstrates that the initial solar reflectance of pre-painted metal drops less than 5% from aging even after 30 years of exposure.

Therefore present codes and standards are unduly penalizing pre-painted metal roof systems. As an example, a light-colored painted metal roof product with a solar reflectance of 0.68 would not qualify as a “cool roof” in Title 24 or in the ASHRAE 90.1 standard even though its aged solar reflectance drops to only 0.65. In comparison, other types of non-metallic roofing that meet the initial “cool roof” solar reflectance criteria of 0.70, would be expected to degrade to a solar reflectance of about 0.55 after three years of climatic exposure. Hence, a painted metal roof may not be classed as a cool roof initially by some standards, but over time it could actually display a higher solar reflectance and provide greater energy efficiency than some “cool roofs” that meet the initial requirements but show significant degradation over time. In situations like these,

the painted metal roofing is actually disadvantaged in some code and standards with regard to the expected degradation over time.

Much of the cool roof initiative to date has focused on low-slope, large commercial roofing applications. This is true in Title 24, ASHRAE, IECC, and other codes or standards. As regulatory bodies begin to consider similar cool roof incentives for steep-slope and residential roofing applications, metal is poised to capitalize on its attractive surface properties. In steep-slope and residential roofing the aesthetics of color durability and retention of solar reflectance are expected to become more important in the selection of energy-efficient roofing materials. Codes and standards bodies should therefore take into consideration painted metal's excellent retention of solar reflectance when predicting energy savings beyond the three-year mark.

## CONCLUSION

Cool metal roofing is durable in its appearance and properties, which includes its retention of initial solar reflectance. The initial value solar reflectance for pre-painted metal may not be as important as the aged value given the excellent retention of this property. This is due to the fact that the surface of this roofing material does not retain dirt or support growth of biomass. The tight tenacious bonding of the paint resin makes for a tough yet resistant surface. It has become a favorite choice of architects designing for a long lasting product with energy-efficient properties. Due to its demonstrated retention of initial solar reflectance, the standard rates of degradation cited in some codes and standards should be reconsidered for painted metal roofing products.

## REFERENCES

- Akbari, H. and S.J. Konopacki. 1998. "The Impact of Reflectivity and Emissivity of Roofs on Building Cooling and Heating Energy Use." *Thermal Performance of the Exterior Envelopes of Buildings*. Proceedings of ASHRAE THERM VII, Clearwater, FL, December.
- American Society for Testing and Materials (ASTM). 2002. Designation D2244-02: Standard Practice for Calculation of Color Tolerances and Color Differences from Instrumentally Measured Color Coordinates. West Conshohocken, PA.: American Society for Testing and Materials.
- Ducker Worldwide. 2002. "2002 Metal Roofing Industry Profile and Analysis." Ducker Research Company Inc. and Metal Construction Association.
- Miller, W. and B. Rudolph. 2004 "Exposure Testing Of Painted PVDF Metal Roofing." Report prepared for the Cool Metal Roof Coalition.
- Miller, W.A. and S. Kriner. 2001. "The Thermal Performance of Painted and Unpainted Structural Standing Seam Metal Roofing Systems Exposed to One Year of Weathering." *Thermal Performance of the Exterior Envelopes of Buildings*. Proceedings of ASHRAE THERM VIII, Clearwater, FL, December.

Miller, W.A., A. Desjarlais, D.S. Parker and S. Kriner. 2004. "Cool Metal Roofing Tested for Energy Efficiency and Sustainability." Proceedings of CIB World Building Congress, Toronto, Ontario, May 1-7, 2004.

Parker, D.S., J.K. Sonne, J.R. Sherwin, and N. Moyer. 2001, "Comparative Evaluation of the Impact of Roofing Systems on Residential Cooling Energy Demand in Florida." Final Report FSEC-CR-1220-00, prepared for the Florida Power and Light Company, May.

Parker, D.S., J.K. Sonne, J.R. Sherwin. 2002, "Comparative Evaluation of the Impact of Roofing Systems on Residential Cooling Energy Demand in Florida." *ACEEE Summer Study on Energy Efficiency in Buildings*. Proceedings of American Council for an Energy Efficient Economy, Asilomar Conference Center in Pacific Grove, CA, August.

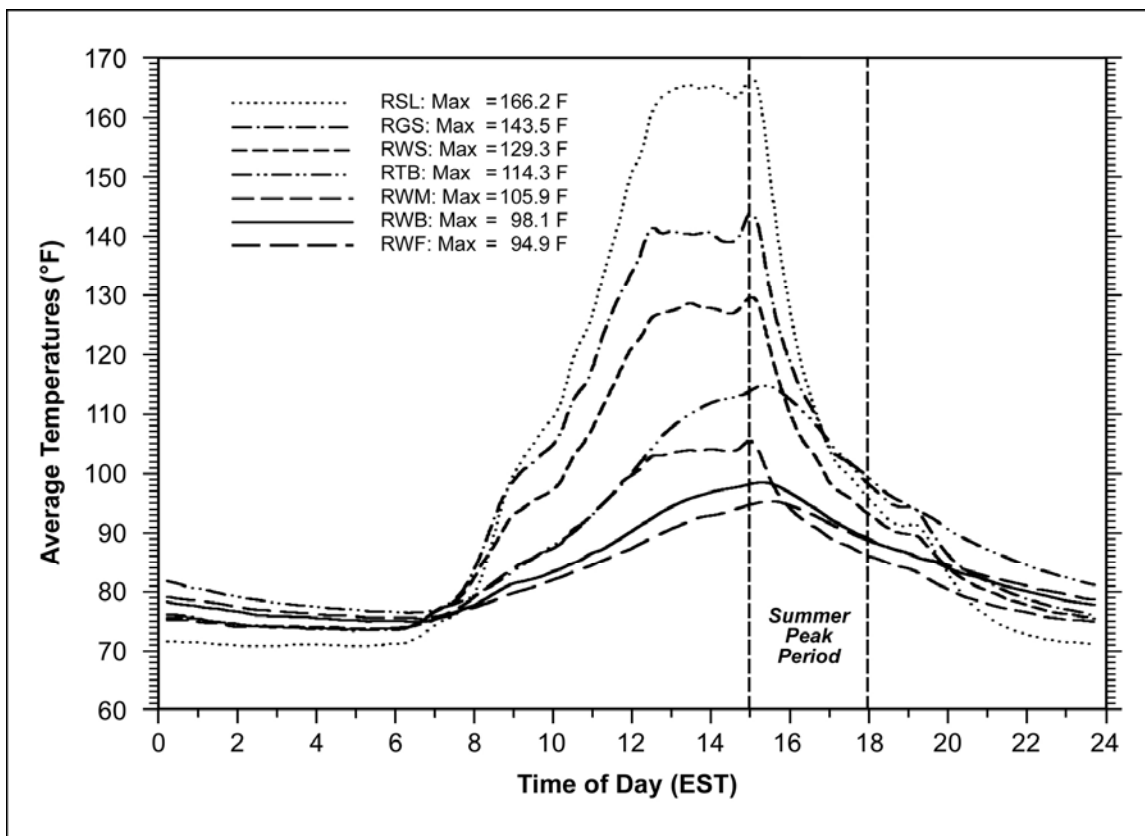


Figure 1. Roof surface temperatures for the demonstration homes tested by FSEC in Ft. Myers, FL.

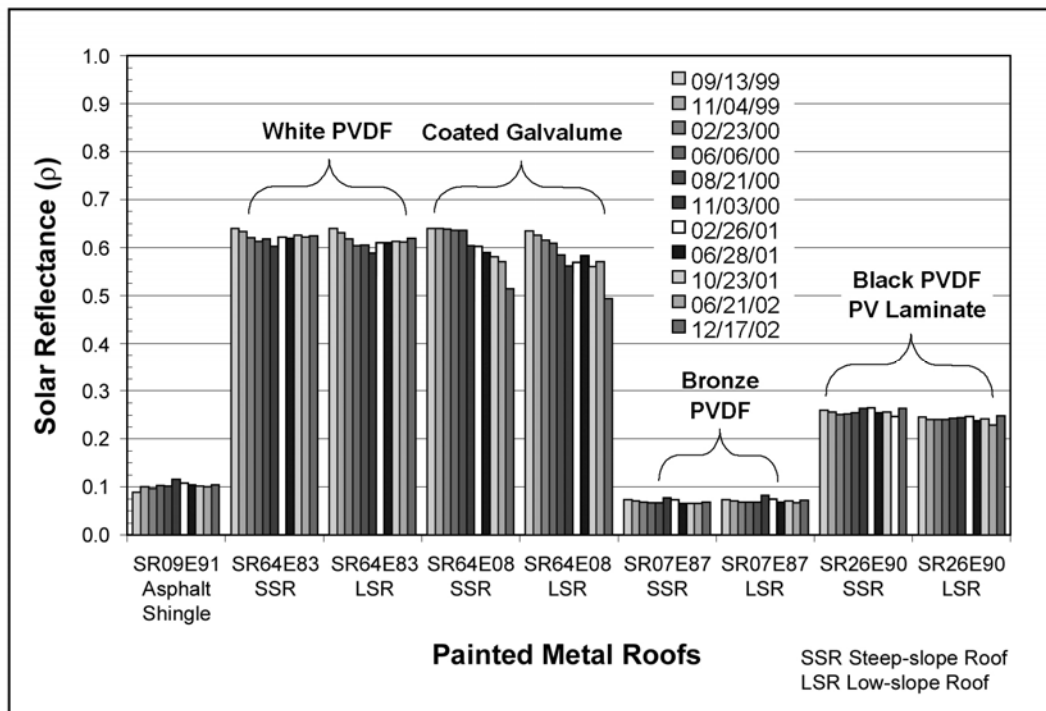


Figure 2. Solar reflectance of painted metal exposed to weathering on ESRA at Oak Ridge, TN.

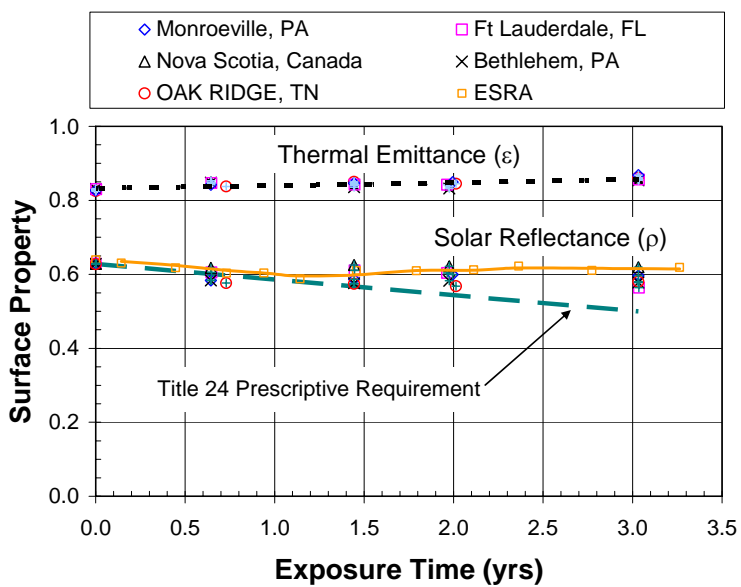
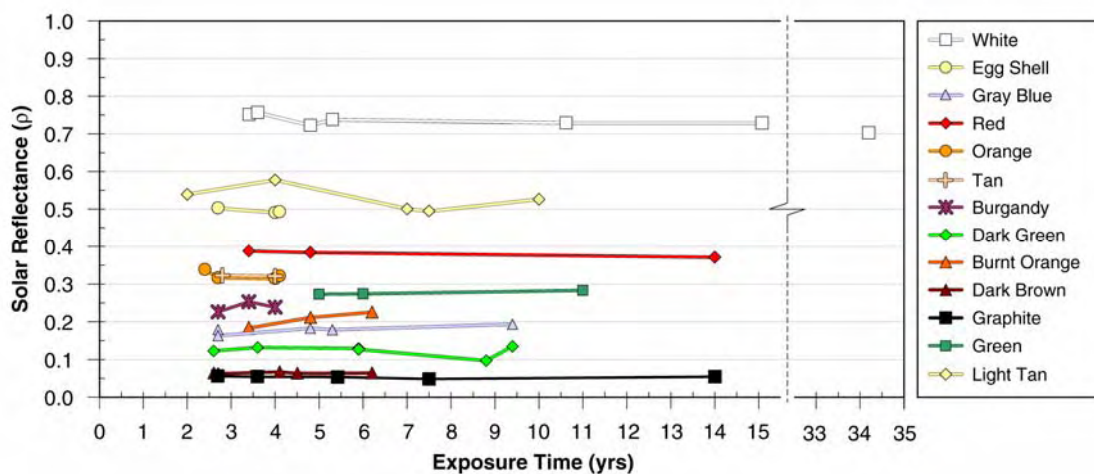
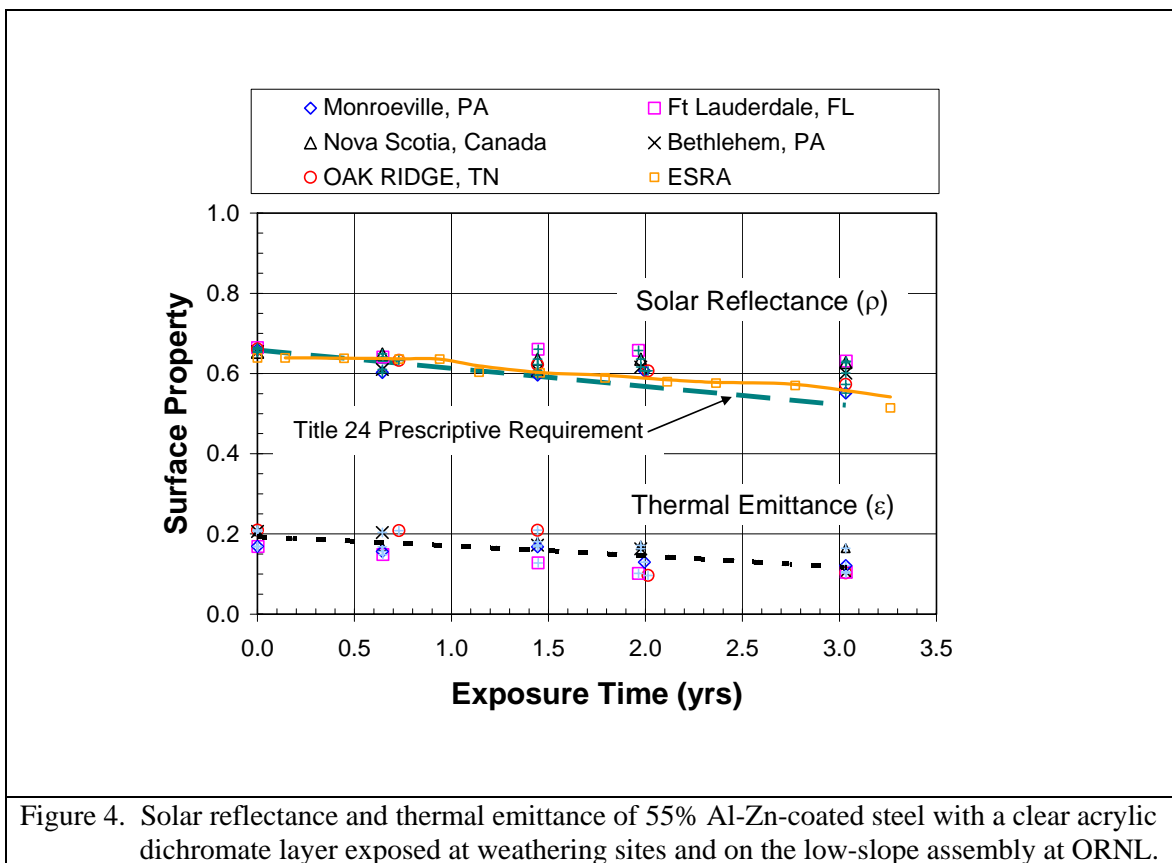


Figure 3. Solar reflectance and emittance of white PVDF painted metal (SR64E83) exposed at weathering sites and on the low-slope assembly at ORNL



# Special Infrared Reflective Pigments Make a Dark Roof Reflect Almost Like a White Roof

**William (Bill) Miller<sup>1</sup>, Ph.D.**  
Oak Ridge National Laboratory  
Member ASHRAE

**Kenneth T. Loye**  
FERRO Corporation

**Andre Desjarlais**  
Oak Ridge National Laboratory  
Member ASHRAE

**Hashem Akbari, Ph.D.**  
Lawrence Berkeley National Laboratory  
Member ASHRAE

**Scott Kriner**  
Metal Construction  
Association

**Stephen Wiel, Ph.D.**  
Lawrence Berkeley National Laboratory

**Ronnen Levinson, Ph.D.**  
Lawrence Berkeley National Laboratory

**Robert G. Scichili**  
BASF Corp

**Paul Berdahl, Ph.D.**  
Lawrence Berkeley National Laboratory

## ABSTRACT

*Pigment colorant researchers are developing new complex inorganic color pigments that exhibit dark color in the visible spectrum and high reflectance in the near-infrared portion of the electromagnetic spectrum. The new pigments increase the near infrared reflectance of exterior finishes and paints thereby dropping the surface temperatures of roofs and walls, which in turn reduces the cooling-energy demand of the building. However, determining the effects of climate and solar exposure on the reflectance and the variability in color over time is of paramount importance for promoting these energy efficiency benefits and for accelerating the market penetration of products using the new color pigments.*

## INTRODUCTION

A new roofing product is about to revolutionize the building industry, bringing relief to homeowners and utilities alike. Cool Roof Color Materials (CRCMs) made from complex inorganic color pigments (CICPs) will reduce the amount of energy needed to cool buildings, helping the power utilities reduce hot-weather strain on the electrical grids. The new technology will help mitigate carbon dioxide emissions, reduce the impacts of metropolitan heat buildups and urban smog, and support conservation of water resources otherwise used to clean and process fuel consumed by fossil-fuel driven power plants Gipe (1995).

The California Energy Commission (CEC) has two sister laboratories' Oak Ridge (ORNL) and Lawrence Berkeley (LBNL) working collaboratively on a 3-year, \$2 million project with the roofing industry to develop and produce new reflective, colored roofing products. The CEC aims to make CRCMs a market reality in the California homebuilding industry within 3 to 5 years. For tile, painted metal, and wood shake, the CEC's goal is products with about 0.50 solar reflectance. For residential shingles, the goal is a solar reflectance of at least 0.30.

The Florida Power & Light Company sponsored a field project in Fort Myers, FL that compared the energy performance of six identically constructed, side-by-side homes built with various reflective roof products. Parker, Sonne and Sherwin (2002) showed that a white galvanized metal roof and a white S-

---

<sup>1</sup> Dr. William Miller is a research scientist working at the Oak Ridge National Laboratory (ORNL). Kenneth Loye is the Technical Manager of the Pigments Group at FERRO Corporation. André Desjarlais is manager of ORNL's Building Envelope Group. Scott Kriner is Chairman of the Metal Construction Association. Robert Scichili is the Industrial Coatings Manager at BASF. Dr. Hashem Akbari, Dr. Ronnen Levinson and Dr. Paul Berdahl are research scientists working at Lawrence Berkeley National Laboratory. Steve Weil is retired from LBNL and serves as acting Director of the Cool Roof Project sponsored by the CEC.



shaped cement tile roof caused the respective Fort Myers' homes to use 4.2 to 3.0 kilowatt-hours per day less air-conditioning energy than an otherwise identical home with a dark gray asphalt shingle roof. The measurements showed that the white reflective roofs reduced cooling energy consumption by 18-26% and peak demand by 28-35%. The resultant annual savings for comfort cooling the two homes with white reflective roofs was reported at roughly \$120 or about 6.7¢ per square foot per year, which is very promising. However, in the residential market, the issues of aesthetics and durability are more important to the homeowner than are the potentials for reduced air-conditioning loads and reduced utility bills. To homeowners, dark roofs simply look better than their counterpart, a highly reflective "white" roof. What the public does not know, however, is that the aesthetically pleasing dark roof can be made to reflect like a "white" roof in the near infrared spectrum.

Therefore a combined experimental and analytical approach is in progress with field data just coming available, some of which we are reporting along with preliminary results of computer simulations showing the potential energy savings throughout the U.S. for residential homes having CRCMs roofs. A roof covered with CRCMs absorbs less solar energy and we believe can reduce home air-conditioning energy ~20%, which in turn reduces the national primary energy consumption by ~0.5 quads per year.

### **COOL ROOF COLORED MATERIALS (CRCMs)**

Dark roofing can be formulated to reflect like a highly reflective "white" roof in the near infrared (NIR) portion of the solar spectrum (700 to 2,500 nm). For years the vinyl siding industry has formulated different colors in the same polyvinyl chloride base by incorporating titanium dioxide ( $\text{TiO}_2$ ) and black NIR-reflective paint pigments to produce dark siding that is cool in temperature (Ravinovitch and Summers 1984). Researchers discovered that a dark color is not necessarily dark in the infrared. Brady and Wake (1992) found that 10  $\mu\text{m}$  particles of  $\text{TiO}_2$  when combined with colorants such as red and yellow iron oxides, phthalocyanine blue, and palygen black, could be used to formulate fairly dark colors with near-infrared reflectances of 0.3 and higher. Researchers working with the Department of Defense added complex inorganic color pigments (CICPs) to paints used for military camouflage and matched the reflectance of background foliage in the visible and NIR spectra. At 750 nm the chlorophyll<sup>2</sup> in foliage naturally boosts the reflectance of a plant leaf from 0.1 to about 0.9, which explains why a dark green leaf remains cool on a hot summer day. Tailoring CICPs for high NIR reflectance similar to that of chlorophyll provides an excellent passive energy saving opportunity for exterior residential surfaces such as walls and roofs. A CICP consisting of a mixture of the black pigments chromic oxide ( $\text{Cr}_2\text{O}_3$ ) and ferric oxide ( $\text{Fe}_2\text{O}_3$ ) increases the solar reflectance of a standard black pigment from 0.05 to 0.26 (Sliwinski, Pipoly & Blonski 2001).

### **Identification and Characterization of Pigments**

We are working with pigment manufacturers to optimize the solar reflectance of a pigmented surface by identifying and characterizing pigments with optical properties suitable for cool roof color materials (CRCMs). LBNL characterized some 83 single-pigment paints as reported by Levinson, Berdahl and Akbari (2004b), and used the data to formulate and validate an algorithm for predicting the spectral irradiative properties Levinson, Berdahl and Akbari (2004a). LBNL also characterized various coating additives such as "transparent" mineral fillers (e.g., mica, clay, silica, talc) and binders (e.g., polymeric resins, silicates) to identify deleterious absorptions in the near infrared. The maximum amount of each material is then determined so that it will not impair the near-infrared reflectance of the pigmented surface. The spectral solar reflectance and transmittance; pigment chemistry, name, and measured film thickness; computed absorption and backscattering coefficients; and many ancillary values are planned for public dissemination for the 83 single-pigment paints from the Cool Roof web site (<http://coolcolors.lbl.gov>). Further discussion of the pigment identification and characterization work is reported by Akbari et al. 2004.

### **Application of Pigments to Roof Products**

Identifying, characterizing and then optimizing the reflectance of a pigmented coating is only part of the job for making dark yet highly reflective roof products. The application of the CRCMs varies among the different roof products, and we are working with industry to develop engineering methods for successfully applying them to the sundry roof systems. Each roofing type has its own specific challenges.

---

<sup>2</sup> Chlorophyll, the photosynthetic coloring material in plants, naturally reflects near-IR radiation.

For composition shingles, the application of pigmented coatings to roofing granules appears to be the critical process because the solar reflectance is predominately determined by the granules, which cover ~97% of a shingle's surface. Coating the granules with CRCMs helps increase reflectance, but some pigments are partly transparent to NIR light and therefore any NIR light not reflected by the cool pigment is transmitted to the dark substrate, where it is absorbed as heat. Multiple layers of coatings can be applied to increase reflectance; however, each additional coating increases cost. A two-step, two-layer process has proven more cost effective. In the first step, the granule is pre-coated with an inexpensive white pigment that is highly reflective to NIR light. In the second step, the cool-colored pigment is applied to the pre-coated granules.

A slurry coating process is used to add color to the surface of a clay tile. Once coated the clay is kiln-fired, and the firing temperature, the atmosphere and the pigments affect the final color and solar reflectance. However, for concrete tile the colorants are included throughout the bulk of the tile or are applied as a slurry coat to the surface. The addition of CRCMs to the material bulk requires too much pigment and makes the process too expensive. Coating the tile has been successfully demonstrated by American Rooftile Coatings who applied their COOL TILE IR COATING™ to several samples of concrete tiles of different colors (Fig. 1). The solar reflectance for all colors tested exceeded 0.40. Most dramatic is the effect of the dark colors. The black coating increased the solar reflectance from 0.04 to 0.41, while the chocolate brown coating increased from 0.12 to 0.41, a 250% increase in solar reflectance! Because solar heat gain is proportional to solar absorptance, the COOL TILE IR COATING™ reduces the solar heat gain roughly 33% of the standard color, which is very promising. The coating can certainly help tile roof products pass the Environmental Protection Agency's Energy Star 0.25 solar reflectance criterion as well as California's Title 24 pending criterion<sup>3</sup> for steep-slope roofing.

Premium coil coated metal roofing probably has the best opportunity for applying CRCMs because the paint coating is reasonably thick (~25 micron) and because the substrate has high NIR reflectance ( $\rho_{\text{nir}} \sim 0.55$  to  $0.7$ ). The coatings for metal shingles are durable polymer materials, and many metal roof manufacturers have introduced the CRCM pigments in their complete line of painted metal roof products. The additional cost of the pigments is only about 5¢ per square foot of finished metal product (Chiovare 2002). Success of the new CRCM metal products is evident in the market share recently captured by the metal roof industry. Historically metal roofs have had a smaller share of only about 4% in the residential market. The architectural appeal, flexibility, and durability, due in part to the CIPs pigments, has steadily increased the sales of painted metal roofing, and as of 2002 its sales volume has doubled since 1999 to 8% of the residential market, making it the fastest growing residential roofing product (F. W. Dodge 2002).

## FADE RESISTANCE OF ROOF PRODUCTS WITH CRCMs

The color of a roof product must remain fade resistant or the product will not sell. Industry judges fade resistance by measuring the spectral reflectance and transmittance of a painted surface and converting the measures to color-scale values based on the procedures in ASTM E308-02 (ASTM 2001). The color-scale values are compared to standard colors and the color differences ( $\Delta L$ ,  $\Delta a$ , and  $\Delta b$ ), which represent the luminance of color, are calculated from:

- $\Delta L = L_{\text{Batch}} - L_{\text{Standard}}$ , where  $\Delta L > 0$  is lighter and a  $\Delta L < 0$  is darker;
- $\Delta a = a_{\text{Batch}} - a_{\text{Standard}}$ , where  $\Delta a > 0$  is redder and a  $\Delta a < 0$  is greener; and
- $\Delta b = b_{\text{Batch}} - b_{\text{Standard}}$ , where  $\Delta b > 0$  is more yellow and  $\Delta b < 0$  is bluer.

Manufacturers of premium coil coated metal use a total color difference ( $\Delta E$ ) to specify the permissible color change between a test specimen and a known standard. The total color difference value is described in ASTM D 2244-02 (ASTM 2002), and is a method adopted by the paint industry to numerically identify variability in color over periods of time; it is calculated by the formula:

$$\Delta E = \left[ (\Delta L)^2 + (\Delta a)^2 + (\Delta b)^2 \right]^{1/2} \quad (1)$$

<sup>3</sup> Title 24 has legislation pending approval that will require new steep-slope roofs to have a reflectance exceeding the 0.25 Energy Star threshold after 2008.

Typically, premium coil-coated metal roofing is warranted for 20 years or more to have a  $\Delta E$  of 5 units or less for that period.  $\Delta E$  color changes of 1 unit or less are almost indistinguishable from the original color, and depending on the hue of color,  $\Delta E$  of 5 or less is considered very good.

### Fade Resistance Results for Painted PVDF Roofing

To evaluate color changes of CRCMs as compared to standard colors, we used a three-year exposure test to natural sunlight in Florida following ASTM G7-97 (ASTM 1997). Test data showed excellent light fastness of the CRCM masstones<sup>4</sup> exposed in the field (Fig. 2). The three color pairs labeled in Figure 2 are identified with their respective unweathered solar reflectance values (e.g., SR40 designation represents a solar reflectance of 0.40 for the CRCM green-painted PVDF metal). Differences in the masstone discoloration occur after two years of exposure for the green and brown CRCM coil-coated metals. However, both the green and brown CRCM colors have faded less than their counterpart standard colors. After three years of exposure the standard black has a  $\Delta E \sim 3.5$  as compared to the CRCM black with only a 0.5  $\Delta E$ . Four years of exposure were also available for the standard colors, and the green and brown masstones were stable, while the black showed a  $\Delta E$  of 21 (Fig. 2). The Florida exposure data is promising and shows that over the three-year test period the CRCMs fade less than do the standard masstone colors with known performance characteristics. For the CRCM black masstone the fade resistance is much improved over the standard color. Tints, especially the blue tints are well known to fade; however, 50/50 tints of the CRCMs field tested in Florida also show excellent fade resistance (Table 1). The highest total color change was observed for the CRCM black tint, which is still indistinguishable from the original color.

**Table 1. Color Difference for 50/50 tints of the CRCMs exposed to natural sunlight for three years in Florida. ( $\Delta E$  based on International Commission on Illumination (CIE L\*A\*B) Index)**

Years	Total color difference ( $\Delta E$ )				
	Green	Yellow	Brown	Black	Marine Blue
1	0.55	0.21	0.47	0.19	0.46
2	0.42	0.25	0.70	0.67	0.50
3	0.53	0.14	0.99	1.51	0.76

The xenon-arc accelerated weathering tests were previously reported by Miller et al. (2002) and showed that after 5000 hours of xenon-arc exposure all CRCMs were clustered together with  $\Delta E < 1.5$ , which is considered a very good result.

### FIELD TESTING OF ROOFS WITH CRCMs

Experimental field studies are in progress to catalog temperature, heat transmission, solar reflectance, thermal emittance and color fastness data for CRCMs applied to tile, metal, wood shake and composition shingle roofs. We are using the data to formulate and validate design tools for predicting the roof energy load during the cooling and heating seasons for residential buildings that use CRCM roof products. A demonstration site in Sacramento, California has two pair of identical homes, one pair roofed with concrete tile with and without the CRCMs and the other pair roofed with painted metal shakes with and without CRCMs. All roofs have the same visible dark brown color. A coating was applied to one of the two homes having concrete tile roofs; solar reflectance for the coated roof was a measured 0.41 as compared to the other base house with tile reflectance of only 0.08. Solar reflectance of the painted metal roof with CRCMs was 0.31 versus the roof with standard color metal shingles having 0.08 reflectance.

We are also exposing samples of metal, clay and concrete tile materials at weathering farms in seven different climate zones of California and are conducting thermal performance testing of several tile roofs of different profile on a fully instrumented roof assembly to help quantify the potential energy savings as compared to asphalt shingles. The Tile Roof Institute (TRI) and its affiliate members are keenly interested in specifying tile roofs as cool roof products using CRCMs. TRI is also keenly interested in knowing the effect of venting the underside of concrete and clay roof tiles. Beal and Chandra (1995) demonstrated a 45% daytime reduction in heat flux for a counter-batten tile roof as compared to a direct nailed shingle roof. The reduced heat flow occurs because of a thermally driven airflow within a channel that is formed by the tile nailed to a counter-batten roof deck. Typically, stone-coated metal and tile coverings are placed on

<sup>4</sup> Masstones represents the full color of the pigment while tints are blends of colors.

batten and counter batten supports, yielding complex air flow patterns through the supports. Correctly modeling the heat flow across the air channel is a key hurdle for predicting the thermal performance of tile roofs.

The data for these field studies are just coming online and will be reported in future publications. However, for the present work the results of simulations are presented for quantifying the potential energy savings for residential roofs with CRCMs. The data acquired from the demonstration homes and from the tile roof assemblies will be used to further formulate and validate our simulation tool, AtticSim.

## THERMAL PERFORMANCE OF ROOFS WITH CRCMs

The ultimate goal of the pigment identification, characterization and application work is to increase the solar reflectance of roofing materials upwards of 0.50. Present CRCMs pose an excellent opportunity for raising roof reflectance from a typical value of 0.1 – 0.2 to an achievable 0.4 without compromising the home's exterior décor. The adoption of CRCMs into the roofing market can therefore significantly reduce the 2.0 quadrillion BTUs (quads) of primary electrical energy consumed for the comfort cooling of residential homes (Kelso and Kinzey 2000). To estimate these energy savings we conducted simulations using AtticSim based on two scenarios:

1. energy savings for CRCM metal products already on the open market, and
2. energy savings for dark roof products achieving the 0.50 solar reflectance goal.

The Cool Metal Roof Coalition (CMRC) provided measurements of solar reflectance and thermal emittance of painted PVDF metal products. These values are used by AtticSim to answer the first question regarding potential energy savings for available CRCM products. The surface properties are as follow:

**Table 2. Reflectance and emittance values\* for PVDF metal roofs with and without CRCMs.**

	Regal White	Surrey Beige	Colonial Red	Chocolate Brown
CRCM	SR75E80	SR65E80	SR45E80	SR30E80
Standard	SR70E80	SR52E80	SR27E80	SR08E80
*The roof colors are described generically using a SRxxEyy designation. "SRxx" states the solar reflectance; "Eyy" defines the thermal emittance. Thus, labeling the standard regal white color as SR70E80 indicates that it has a solar reflectance of 0.70 and an emittance of 0.80.				

The Table 2 reflectance data were verified by a coatings manufacturer (Scichili 2004), and show that the darker the color the greater is the increase in reflectance induced by the CRCMs. ORNL used an emissometer to measure the emittance for several samples of the Table 2 colors and found the emittance to be  $0.82 \pm 0.02$ . The pigments in the CRCMs do not affect the emittance and at the request of the CMRC, we fixed emittance at 0.80 for all the simulations.

## AtticSim SIMULATIONS

AtticSim is a computer tool for predicting the thermal performance of residential attics. It mathematically describes the conduction through the gables, eaves, roof deck and ceiling; the convection at the exterior and interior surfaces; the radiosity heat exchange between surfaces within the attic enclosure; the heat transfer to the ventilation air stream; and the latent heat effects due to sorption and desorption of moisture at the wood surfaces. Solar reflectance, thermal emittance and water vapor permeance of the sundry surfaces are input. The model can account for different insulation R-values and/or radiant barriers attached to the various attic surfaces. It also has an algorithm for predicting the effect of air-conditioning ducts placed in the attic (Petrie et al. 2004). The code reads the roof pitch, length and width and the ridge orientation (azimuth angle with respect to north) and calculates the solar irradiance incident on the roof. Conduction heat transfer through the two roof decks, two gables and vertical eaves are modeled using the thermal response factor technique (Kusuda 1969), which requires the thermal conductivity, specific heat, density and thickness of each attic section for calculating conduction transfer functions.

Heat balances at the interior surfaces (facing the attic space) include the conduction, the radiation exchange with other surfaces, the convection and the latent load contributions. Heat balances at the exterior

surfaces balance the heat conducted through the attic surface to the heat convected to the air, the heat radiated to the surroundings and the heat stored by the surface. Iterative solution of the simultaneous equations describing the heat balances yields the interior and exterior surface temperatures and the attic air temperature at one-hour time steps. The heat flows at the attic's ceiling, roof sections, gables and eaves are calculated using the conduction transfer function equations. The tool was validated by Wilkes (1991) against field experiments, and is capable of predicting the ceiling heat flows integrated over time to within 10% of the field measurement. AtticSim can predict the thermal performance of attics having direct nailed roof products but it has not been used to predict the heat flow across a tile roof having a venting occurring on the underside of the roof, between the roof deck and exterior roof cover.

**Ventilation In Attic Space.** An important issue in our study is the effect of venting the attic. CRCMs are best suited to hot and moderate climates and in hot climates the primary reason for ventilating an attic is to keep it cool and lessen the burden on the comfort cooling system. Ledger (1996) reported that some roof warranties insist on attic ventilation to protect their roof products against excessive temperatures. CRCMs can help improve the durability and extend the longevity of certain roof products, and the CRCMs will help lower the attic air temperature thereby reducing the heat penetrating the house.

The AtticSim simulations assumed equal soffit and ridge vent openings with a net free vent area of 1:300<sup>5</sup>. Using a constant ventilation rate is the simple approach to simulating the attic convective heat flows; however, thermal buoyancy affects the surface temperatures of the attic enclosure, which in turn causes error in the calculated attic heat flows. This is especially true in climates where there is little to no wind to force air in and out of the vents. Buoyancy, termed by many as stack effects, then becomes the sole driving force for attic ventilation.

AtticSim was exercised for a moderately insulated (R-19 h•ft<sup>2</sup>•°F/Btu) attic exposed in both hot and cold climates in the U.S. Roof pitch was set at 4-in of rise per 12-in of run and the ridge vent was oriented east–west. The soffit and ridge vent areas were made equal and yielded a net free vent area of 1:300. We conducted a regression analysis to derive a correlation of AtticSim's computed attic ventilation air changes per hour (ACH) as function of the wind velocity and the computed attic-air-to-outdoor ambient air temperature gradient; results depicted in Figure 3. Summer (June, July and August) and winter (December, January and February) seasonal averages were used to fit the correlation. The regression coefficients for the correlation show a stronger dependence on stack effect than on the wind driven forces. Note that the correlation was not used for computing ACH, rather it was derived to better view both stack and wind effects in a simple two-dimensional plot and for comparing AtticSim's computations to published literature data. The ordinate of Figure 3 is scaled by the regression parameter  $1.1\{V^{0.04}\}$ . The curve fit  $\{\Delta T\}^{0.33}$  is superimposed onto AtticSim's computed ACH values, which as stated are scaled by  $1.1\{V^{0.04}\}$ . The resultant graph allows direct comparison of the data by Burch and Treado (1979) and by Walker (1993) to AtticSim's output. Burch and Treado (1979) listed field data for soffit and ridge venting of a Houston, Texas house. A tracer gas technique using sulfur-hexafluoride was released at six-inch levels above the ceiling insulation at eight different attic locations. Sixteen air samples were collected at different attic locations and the dilution of the gas yielded the ACH. They stated the attic ventilation measurements were probably somewhat on the high side; however, their field data for soffit and ridge venting compares well to the results computed by AtticSim. Walker (1993) studied attic ventilation in Alberta, Canada. His results showed large variations in ventilation rates. We culled his data by selecting some of the measured ACH values for wind speeds not exceeding 4.5 mph (2 m/s). Further, Parker, Fairey and Gu (1991) also measured attic ventilation rates using short term sulfur hexafluoride tracer gas. Their results under normal summer wind and thermal conditions in Cape Canaveral, Florida yielded an average of 2.7 ACH over a three-day period with variation from 0.5 to 4.5 ACH. The AtticSim simulations yielded an annual average of 2.9 ACH with variation from 0.2 to 10 ACH. Therefore, the AtticSim code appears consistent with literature data, and yields reasonable values of attic ventilation for the soffit and ridge venting being exercised in this report.

**SIMULATION PROCEDURE.** Simulations generated the heat flux entering or leaving the conditioned space for a range of roof insulation levels, exterior roof radiation properties, and climates derived from the TMY2 database (NREL 1995). Roof insulation levels ranged from no ceiling insulation

<sup>5</sup> Ventilation area is defined as the ratio of the net free vent area to the footprint of the attic floor area.

through R-49. Simulations assumed painted PVDF metal roofs with and without CRCMs. The roof's solar reflectance and thermal emittance were chosen based on the state-of-the art CRCMs on the open market and also based on our ultimate goal for optimizing solar reflectance (see Table 2). The roofs are assumed direct nailed to the roof deck having only a direct conduction path through the material of the roof deck. The hourly averages of the outdoor ambient dry bulb and specific humidity, the cloud amount and type, the wind speed and direction and the total horizontal and direct beam solar irradiance were read from the TMY2 database for the climates of Miami, FL; Dallas, TX; Burlington, VT; and Boulder, CO. The hourly ceiling heat flux predicted by AtticSim was used to generate annual cooling and heating loads for the attic and roof combinations. An annual cooling load  $[Q_{Cool}]$  was defined as the time integrated heat flux entering the conditioned space through the ceiling when the outdoor air temperature exceeded 75°F (24°C). Similarly, the annual heating load  $[Q_{Heat}]$  was defined as the time integrated heat flux moving upward through the ceiling if the outdoor air temperature dropped below 60°F (16°C).

The output from AtticSim can be coupled to the DOE-2.1E program to model the effect of the ceiling heat flux from the perspective of the whole house energy consumption. However, the multiplicity of residential homes, the diversity of occupant habits, the broad range of exterior surface area-to-house volume, and the internal loading can confound the interpretation of results developed for reflective roofing. Therefore, the reported results center on the heat flows entering and leaving the ceiling of the house. Further analysis of the whole house will be conducted as the data become available from the demonstrations sites to validate our results.

**SIMULATION RESULTS** The annual energy savings due to the change in heat penetrating the ceiling is displayed in Figure 4 for the various painted PVDF metals whose solar reflectance and thermal emittance properties are listed in Table 2. The reductions in energy (cooling savings) are based on the difference in ceiling heat flux for the same color roof with and without CRCMs. Potential savings are also shown for a popular chocolate brown roof whose solar reflectance is increased from 0.08 to our ultimate reflectance goal of 0.50.

A chocolate brown color roof with 30% reflective CRCMs decreased the consumed cooling energy by 15% of that used for a roof with standard colors exposed in Miami and Dallas; the cooling savings are respectively 623 and 884 Btu per yr per square foot of ceiling for an attic having R-19 insulation<sup>6</sup> (Fig. 4). We believe the pigment optimizations can increase reflectance to the 0.50 mark. In that case, the heat penetrating the ceiling would drop by 30% of that computed for the same standard color roof exposed in Miami and Dallas.

Notice that as the roof color lightens, the CRCMs produce less energy savings as compared to the same standard pigmented color because the lighter colored standard materials have higher solar reflectance to start with (Fig. 4). The increase in solar reflectance caused by CRCMs diminishes as the visible color of the roof lightens from black to brown to a white painted PVDF metal (Fig. 4). The CRCMs induce about a 0.05 reflectance point increase for white-painted metal (SR70E80) while a darker chocolate brown roof (SR08E80) increases 0.22 points (Table 2), which is the benefit of the CRCMs. People prefer the darker color roof and the dark colors yield the higher gain in reflectance. The data in Figure 4 therefore show the level of achievable energy savings with roof color for existing CRCMs being marketed as cool roof products. However further improvements are achievable! We have successfully demonstrated concrete tile coatings (Fig. 1) with reflectances slightly above 0.40 and continue to develop prototype coatings to achieve our solar reflectance goal of 0.50, a ~0.40 increase in solar reflectance over a standard brown color!

Figure 4 compares materials of the same color. However, the lighter the color of the roof, the greater are the energy savings due to less heat penetrating the roof. If the comparison is made between different colors, one can judge the thermal advantage gained by selecting a lighter roof décor. As example, if the surrey beige with CRCM (SR65E80) is compared to the standard chocolate brown (SR08E80), then the surrey beige reduces the ceiling heat flux 42% of that predicted for the standard brown SR08E80 roof exposed in Dallas with R-19 attic insulation. In comparison the same chocolate brown color (SR30E80) saved 15% as compared to the same color SR08E80.

<sup>6</sup> The International Energy Conservation Code's recommended ceiling R-value for Dallas is R-19 and for Miami it is R-13 for a home having windows covering 12% of the exterior walls.

**CRCMs IN VARIOUS CLIMATES** Simulations for attics with R-19 insulation (Fig. 5) show the tradeoffs between the heating and cooling season. In the more moderate climates there is a heating load penalty that offsets the cooling energy savings and because higher levels of insulation are required in moderate to cold climates CRCMs do not yield an energy savings. Burlington VT is a cold climate and incurs an annual penalty for roofs with CRCMs (Fig. 5) regardless of the level of attic insulation. A slight benefit is observed for the climate of Boulder exposing brown and surry biege colored roofs having CRCMs (Fig. 5). Obviously the hotter the climate the better is the performance of the CRCMs. In Miami, the net savings are almost 900 Btu per year per square foot for a chocolate brown CRCM covering an attic with R-19 ceiling insulation (Fig. 5).

**CEILING INSULATION EFFECTS** The most obvious trend shown in Figure 4 is the effect of the ceiling insulation on the reduction of heat penetrating into the conditioned space. The level of attic insulation directly affects the ceiling's thermal load. As example, for Dallas TX, a chocolate brown metal roof (SR30E80) saves about 4902 Btu per year per square foot for an attic having no ceiling insulation (Fig. 4). Increasing the insulation to R-19 drops the savings to 623 Btu per year per square foot. R-49 further drops the savings to only 250 Btu per year per square foot. Table 3 lists the International Energy Conservation Code's recommended attic R-value based on the number of heating degree-days ( $HDD_{65}$ ). The number of cooling degree days ( $CDD_{65}$ ) and the average daily solar flux are also listed in Table 3. We included our predictions of the attic heat penetrating the ceiling of a house having the chocolate brown painted PVDF metal roof with and without CRCM. The calculations used the recommended attic insulations from the IECC (2000) for each city (Table 3).

In Burlington, VT a house with R-49 attic insulation does not yield enough cooling benefit from the CRCMs to merit their use. In Bolder the cooling benefit is about 164 Btu per year per square ft, and it exceeds the heating penalty by only 23 Btu per yr per square ft. In Dallas, TX the recommended R-19 attic with SR30E80 chocolate brown CRCM dropped the heat flux entering the ceiling by 623 Btu per yr per square ft of ceiling. In the still hotter climate of Miami, the CRCM SR30E80 incurs 15% less energy penetrating the ceiling for an R-13 attic. Using the SR60E80 CRCM the performance improves and about 31% less energy penetrated from the attic into the house.

**Table 3. Ceiling insulation minimum R-values recommended by the International Energy Conservation Code (IECC, 2000) for homes with windows covering 12% of the exterior wall.**

	Burlington, VT	Boulder, CO	Dallas, TX	Miami, FL
Recommended R-Value	<b>R-49</b>	<b>R-38</b>	<b>R-19</b>	<b>R-13</b>
$HDD_{65}$	7903	6012	2304	141
$CDD_{65}$	407	623	2415	4127
Solar flux <sup>1</sup> [Btu/(h·ft <sup>2</sup> )]	1194	1467	1559	1557
SR08 Annual Cooling [Btu/yr·ft <sup>2</sup> ]	335	920	4017	8450
SR50 Annual Cooling [Btu/yr·ft <sup>2</sup> ]	215	596	2798	5860

<sup>1</sup> Average daily global flux incident on a horizontal surface.

<sup>2</sup> Annual cooling represents the annual energy transfer by attic heat penetrating through the ceiling into the living space.

It is interesting that both Burlington and Boulder, which have moderate cooling demands also have incident solar irradiance that is almost as much as that for Dallas and Miami (Table 3). Despite the low energy savings in Boulder or Burlington as compared to the hotter climates, the high summer irradiance affects peak demand loads on the electric utility seen in urban areas. CRCMs will help alleviate the demand load as homeowners replace their roof, which they are more apt to do than adding attic insulation.

## THE ECONOMICS OF ROOFS WITH CRCMs

We estimated the value of energy savings using the electric and natural gas prices published at the Energy Information Administration's web site <http://www.eia.doe.gov/>. An electricity cost of \$0.10 per



kWh and natural gas cost of \$10.00 per 1000 ft<sup>3</sup> (about 10<sup>6</sup> Btu or 10 Therm) are slightly above the 2001 national average for these energy sources and are assumed for estimating the value of energy savings.

**ALGORITHM FOR ESTIMATING SAVINGS** The coefficient of performance (COP) describes the performance of the HVAC system in terms of the ratio of the machine's cooling capacity to the power needed to produce the cooling effect. To estimate the value of the electrical energy savings requires systems performance data for the HVAC unit:

$$\text{COP}_{\text{HVAC}} = \frac{\text{Cooling Capacity}}{\text{Power}_{\text{HVAC}}} \quad (2)$$

Because the HVAC unit meets the house load, the heat penetrating the ceiling [ $Q_{\text{Cool}}$ ] can substitute for the "Cooling Capacity" term of Eq. 2 to estimate the power needed to meet the attic's portion of the building load. Cost savings (\$cool) follow from the formula:

$$\text{\$cool} = \frac{Q_{\text{cool}} \cdot \text{\$elec}}{\text{COP}_{\text{HVAC}}} \quad (3)$$

The annual heating energy cost savings (\$heat) require the efficiency of the furnace and are calculated by the formula:

$$\text{\$heat} = \frac{Q_{\text{heat}} \cdot \text{\$fuel}}{\eta_{\text{heat}}} \quad (4)$$

The efficiency of the furnace ( $\eta$ ) was set at 0.85 and is relatively constant; however, the cooling COP of HVAC equipment typically drops as the outdoor air temperature increases, as the heat exchangers foul, as mechanical wear occurs on the compressor valves and especially as the unit leaks refrigerant charge. Hence what COP should one use to fairly judge cost savings? A conservative approach would be to use the average COP of 2.5 for new HVAC equipment reported by Kelso and Kinzey (2000).

**PREDICTED SAVINGS FOR CRCMS AND INSULATION** The more insulation in the attic the lower is the ceiling heat flow, and the less is the benefit of more reflective roofing. Conversely, it is also true that the higher the solar reflectance of the roof the lower is the ceiling heat flow, and the less is the benefit of additional ceiling insulation in cooling dominant climates. There can therefore be a tradeoff between the level of ceiling insulation and the solar reflectance of the roof, and the tradeoff is constrained by material costs and the value of energy saved by the CRCMs and by the ceiling insulation.

In Miami the recommended ceiling insulation for a house with about 12% exterior window coverage is R-13 (IECC 2000). Dallas requires R-19 ceiling insulation. Typically a dark residential roof has a solar reflectance of about 0.08. We therefore assumed these recommended insulations levels and used SR08E80 as the base for computing the savings in operating energy for incremental increases in both CRCMs and additional insulation for roofs exposed in Miami and Dallas.

We looked at the energy savings from the perspective of increasing the amount of blanket insulation in the ceiling while holding the solar reflectance constant at 0.08 and also at the higher value of 0.45 (plots SR08 and SR45 in Figure 6). R-values 19, 30, 38 and 49 are displayed to help the reader pick off the savings data listed on the abscissa of Figure 6. The savings are based on the incremental gains over an SR08E80 roof with R13 insulation in Miami and R-19 insulation in Dallas. An SR08E80 roof in Miami saves ~5 cents per year per square ft if blanket insulation is increased from R13 to R19 (see SR08 plot for Miami). For CRCMs having 0.45 solar reflectance, the savings are ~4 cents per year per square ft. The installed cost for R-19 insulation is about \$0.36 per square ft in new construction and is \$0.41 for existing construction (R.S. Means 2002). From these data, the additional insulation (R-13 to R-19) is paid for in

about 7 years for new construction and in about 8 years for existing construction for an SR08 roof. In Dallas going from the recommended R-19 to R-38 yields savings of ~\$0.05 per year per square ft, which for new construction pays for itself in ~7 years.

Figure 6 also shows the energy savings from the perspective of increasing roof reflectance while holding the ceiling insulation constant at the recommended code level and at the higher level of R-38. The R-13 plot for Miami (Fig. 6) shows the cost savings for CRCMs on an attic with R-13 ceiling insulation (SR values are labeled from 0.08 to 0.75). Results show that CRCMs yield savings of about 2.2 cents per year per square foot for the identical color SR30E80 roof as compared to the SR08E80 roof with R-13 insulation. As stated earlier, the incremental cost for adding CRCMs to coil-applied metal roofing is ~5 cents per square foot. Hence, the savings in Miami pay for the CRCM technology in about 2½ years. Increasing solar reflectance to 0.50 increases the cost premium and the CRCMs pay for themselves in just 1 year! In Dallas with R-19 recommended insulation, the SR30E80 roof pays for the added cost of the CRCMs in about 5 years; at 0.50 solar reflectance the premium shortens to ~2½ years. If the ceiling insulation is increased to R-38, the incremental increases in solar reflectance are not as economically effective as seen by the slopes of the R-13 vs R-38 plots for Miami (Fig. 6). The savings in Miami are ~\$0.10 per year per square ft for the SR08E80 roof (R-13 vs R-38) and diminish to about \$0.06 per year per square ft for a SR75E80 roof (again, R-13 vs R-38). The comparable savings in Dallas are about half those predicted for Miami (Fig. 6).

For the earlier stated fuel prices and the energy savings, the annual cost savings per square foot of ceiling can be as high as \$0.07 per year per square ft in Miami, FL for a house with R-13 ceiling insulation. In Dallas the savings can be as high as \$0.03 per year per square ft for a house with R-19 ceiling insulation. Therefore the CRCMs have an affordable premium; energy savings easily pay for the roughly 5¢ added expense of the pigments in a CRCM metal roof.

## SUMMARY

We have identified and characterized some 83 different complex inorganic pigments and are developing engineering methods to apply them with optimum solar reflectance for the various roof products. Coatings have been developed and demonstrated that match a tile's color and increase the solar reflectance from about 0.08 to over 0.40, a 5-fold jump in reflectance. The solar reflectance of painted PVDF metals available on the open market are about 3 times better with the addition of CRCMs, and we expect further gains as more pigments are identified and new engineering applications are adopted for the production of the metal roof products. Work continues to improve the solar reflectance to our 0.50 goal for tile and painted PVDF metal roofing.

Accelerated weather testing using natural sunlight and xenon-arc weatherometer exposure are proving the CRCMs retain their color. After three years of natural sunlight exposure in southern Florida, the CRCMs show excellent fade-resistance and remain colorfast. The CRCMs have excellent discoloration resistance, as proven by the three-years of field exposure and the 5000 hours of xenon-arc exposure. Their measure of total color difference was an  $\Delta E$  value less than 1.5. CRCM 50/50 tints field tested in Florida also showed excellent fade resistance. The highest total color change was observed for the CRCM black tint, which is still indistinguishable from the original color. Therefore, color changes in many of the CRCMs are indistinguishable from their original color.

CRCMs reflect much of the NIR heat and therefore reduce the surface temperature of the roof. The lower exterior temperature leads to energy savings. A chocolate brown color roof with 30% reflective CRCMs decreases the consumed cooling energy by 15% of that used for a roof with standard chocolate brown color exposed in Miami and Dallas. If we achieve reflectance measures of 0.50 the energy savings increase to ~30% of the heat flow through an attic having recommended ceiling insulation and the same color roof. The CRCMs also provide an ancillary benefit in older existing houses that have little or no attic insulation and poorly insulated ducts in the attic because the cooler attic temperature in turn leads to reduced heat gains to the air-conditioning ductwork.

The cost to the homeowner to achieve this efficiency improvement for coil-applied metal roofing is the incremental cost of about 5¢ per square foot. The CRCMs being sold in coil-applied metal roofing yield

savings of about 2.2¢ per year per square foot for the identical color SR30E80 roof as compared to the SR08E80 roof with R-13 insulation. Hence, the savings in Miami pay for the CRCM technology in about 2½ years. Increasing solar reflectance to 0.50 increases the cost premium and the CRCMs would pay for themselves in just 1 year!

## REFERENCES

- Akbari, H., Berdahl, P., Levinson, R., Wiel, S., Desjarlais, A., Miller, W., Jenkins, N., Rosenfeld, A., Scruton, C. 2004. "Cool Colored Materials for Roofs," in ACEEE Summer Study on Energy Efficiency in Buildings, proceedings of American Council for an Energy Efficient Economy, Asilomar Conference Center in Pacific Grove, CA., Aug. 2004.
- American Society for Testing and Materials (ASTM). 2002. Designation D2244-02: Standard Practice for Calculation of Color Tolerances and Color Differences from Instrumentally Measured Color Coordinates. West Conshohocken, Pa.: American Society for Testing and Materials.
- . 1997b. Designation G7-97: Standard Practice for Atmospheric Environmental Exposure Testing of Nonmetallic Materials. West Conshohocken, Pa.: American Society for Testing and Materials.
- . 2001. Designation E 308-02: Standard Practice for Computing the Colors of Objects by using the CIE System. West Conshohocken, Pa.: American Society for Testing and Materials.
- Beal, D. and Chandra, S., 1995. "The Measured Summer Performance of Tile Roof Systems and Attic Ventilation Strategies in Hot Humid Climates," Thermal Performance of the Exterior Envelopes of Buildings VI, U.S. DOE/ORNL/BETEC, December 4-8, 1995, Clearwater, FL.
- Brady, R. F., and L. V. Wake. 1992. "Principles and Formulations for Organic Coatings with Tailored Infrared Properties." *Progress in Organic Coatings* 20:1–25.
- Burch, D.M. and Treado, S.J. 1979. "Ventilating Residences and Their Attics for Energy Conservation—An Experimental Study." NBS Special Publication 548: Summer Attic and Whole House Ventilation. Washington, D.C.: National Bureau of Standards.
- Chiovare, Tony CEO of Custom-Bilt Metals, personal communications with ORNL and LBNL on cost premiums for painted metal roofs having CRCMs.
- Gipe, P. 1995. *Wind Energy Comes of Age*, John Wiley & Sons.
- F.W. Dodge. 2002. *Construction Outlook Forecast*, F.W. Dodge Markert Analysis Group, 24 Hartwell Avenue, Lexington, MA 02421. Telephone 800-591-4462, FAX 781-860-6884, URL:www.FWDodge.com.
- International Energy Conservation Code, 2000, p. 81.
- Kelso, J., and Kinzey, B., 2000, "BTS Core Data Book," DOE's Office of Building Technology, State and Community Programs, U.S. Department of Energy, Washington, DC.
- Kusuda, T. 1969. "Thermal Response Factors for Multi-Layer Structures of Various Heat Conduction Systems," *ASHRAE Transactions*, Vol. 75, Part 1, pp. 246-271.
- Ledger, G. 1996. "Building Hot Roofs." *House Magazine*, Patric Gass and Company, Inc.
- Levinson, R., and Berdahl, P., and Akbari, H. 2004a. "Solar Spectral Optical Properties of Pigments, Part II: Survey of Common Colorants." in review at LBNL.
- Levinson, R., and Berdahl, P., and Akbari, H. 2004b. "Solar Spectral Optical Properties of Pigments, Part I: Model for Deriving Scattering and Absorption Coefficients from Transmittance and Reflectance Measurements." in review at LBNL.
- Miller, W.A., Loye, K. T., Desjarlais, A. O., and Blonski, R.P. 2002. "Cool Color Roofs with Complex Inorganic Color Pigments," in ACEEE Summer Study on Energy Efficiency in Buildings, proceedings of American Council for an Energy Efficient Economy, Asilomar Conference Center in Pacific Grove, CA., Aug. 2002.
- NREL, 1995, "TMY2s. Typical Meteorological Years Derived from the 1961–1990 National Solar Radiation Database," Data Compact Disk. National Renewable Energy Laboratory, Golden, CO.
- Parker, D.S., Fairey, P.W., and Gu, L. 1991. "A Stratified Air Model for Simulation of Attic Thermal Performance," pp. 44-69, *Insulation Materials: Testing and Applications*, 2nd Volume, ASTM STP 1116, R.S. Graves and D.C. Wysocki, Eds. Philadelphia, PA: American Society for Testing and Materials.

- Parker, D.S., Sonne, J. K., Sherwin, J. R. 2002. "Comparative Evaluation of the Impact of Roofing Systems on Residential Cooling Energy Demand in Florida," in ACEEE Summer Study on Energy Efficiency in Buildings, proceedings of American Council for an Energy Efficient Economy, Asilomar Conference Center in Pacific Grove, CA., Aug. 2002.
- Petrie, T.W., Stovall, T.K., Wilkes, K.E. and Desjarlais, A.O. 2004. "Comparison of Cathedralized Attics to Conventional Attics: Where and When Do Cathedralized Attics Save Energy and Operating Costs?," to be published in Thermal Performance of the Exterior Envelopes of Buildings, IX, proceedings of ASHRAE THERM VIII, Clearwater, FL., Dec. 2004.
- Ravinovitch, E. B., and J. W. Summers. 1984. "Infrared Reflecting Vinyl Polymer Compositions." U.S. Patent 4,424,292. January 3.
- R. S. Means Company, Means CostWorks 2002, R. S. Means Company, Inc., Kingston, MA, Version 6.0
- Robert G. Scichili, BASF Industrial Coatings, personal communications with ORNL on reflectance of painted PVDF metals containing CRCMs, April 2004.
- Sliwinski, T. R., R. A. Pipoly, and R. P. Blonski. 2001. "Infrared Reflective Color Pigment." U.S. Patent 6,174,360, January 16.
- Walker, I. S. May 1993. "Prediction of Ventilation, Heat Transfer and Moisture Transport in Attics." Ph.D. dissertation, Edmonton, Alberta, Canada.
- Wilkes, K.E. 1991. *Thermal Model of Attic Systems with Radiant Barriers*. ORNL/CON-262. Oak Ridge, Tenn.: Oak Ridge National Laboratory.

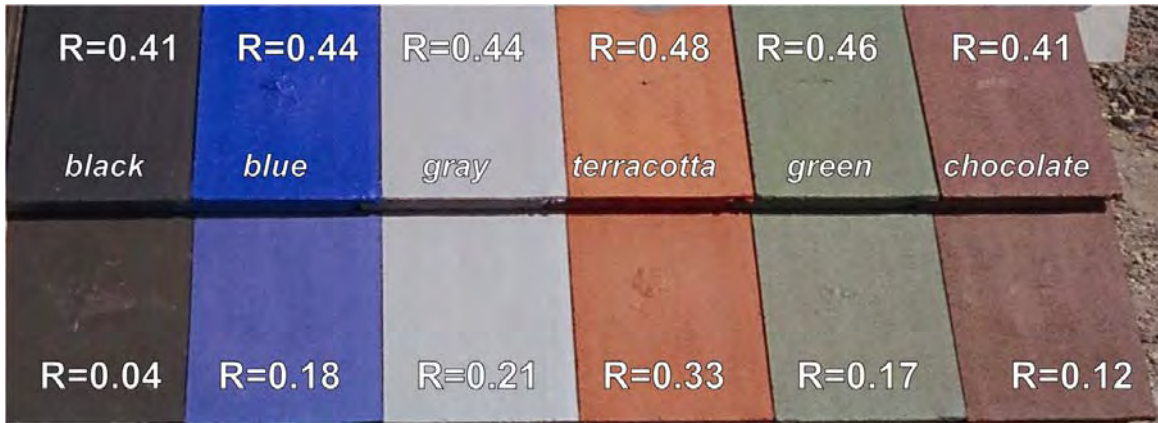


**Figure 1.** Solar reflectance of concrete tile roofs with CRCMs (top row) and without CRCMs (bottom row). The COOL TILE IR COATING™ technology was developed by Joe Riley of American Rooftile Coating.

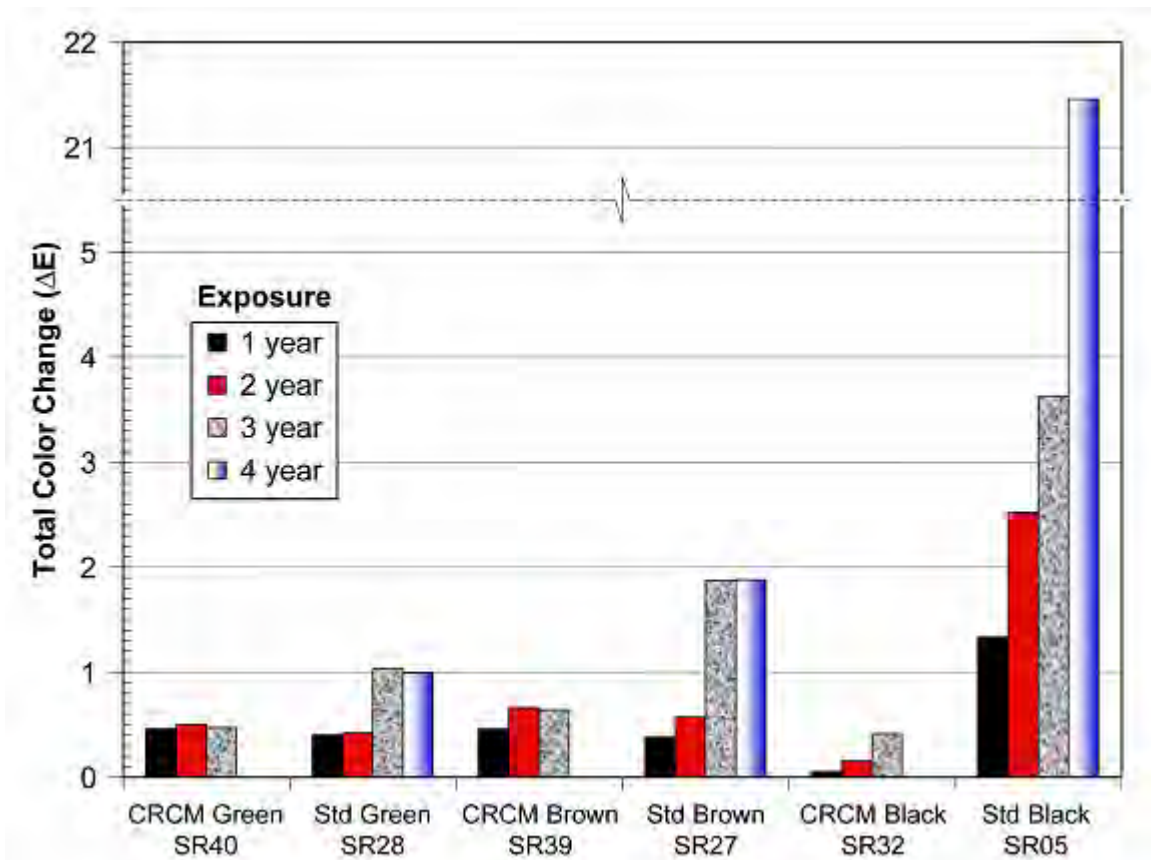


**Figure 2.** Three years of natural sunlight exposure in Florida shows that the CRCMs have improved the fade resistance of the painted PVDF metals.

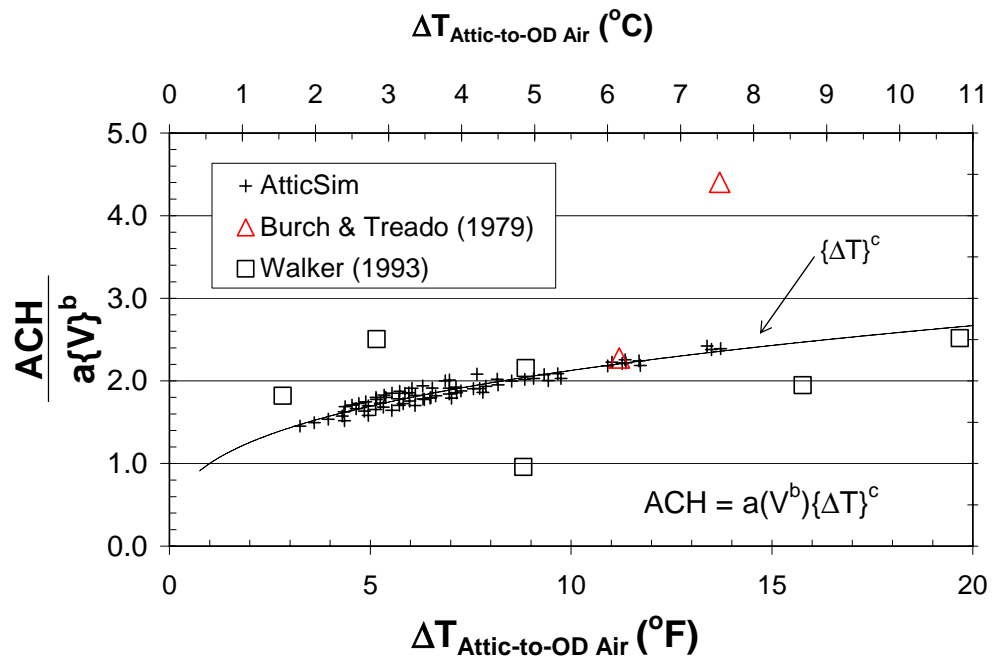


**Figure 3.** The air changes per hour (ACH) computed by AtticSim are compared to literature data and show the reasonableness of the predicted ventilation rate.

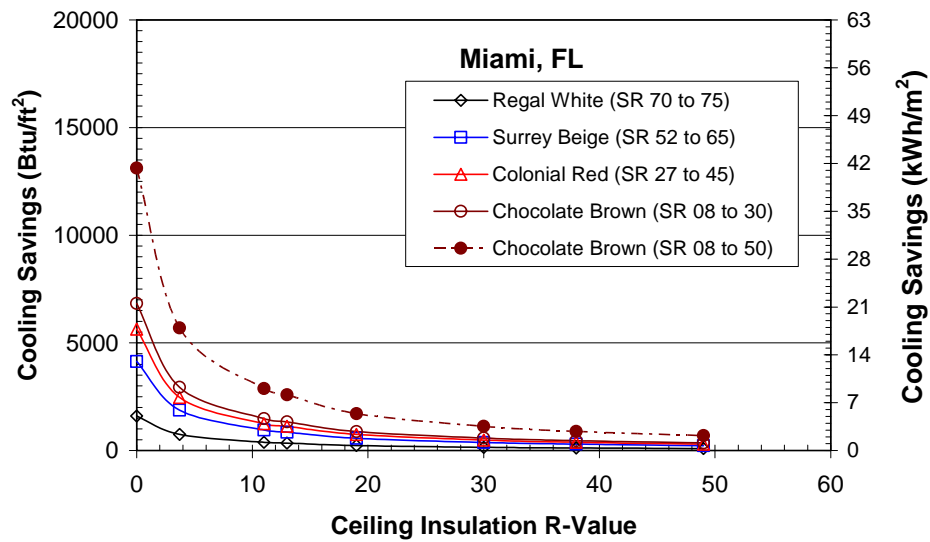
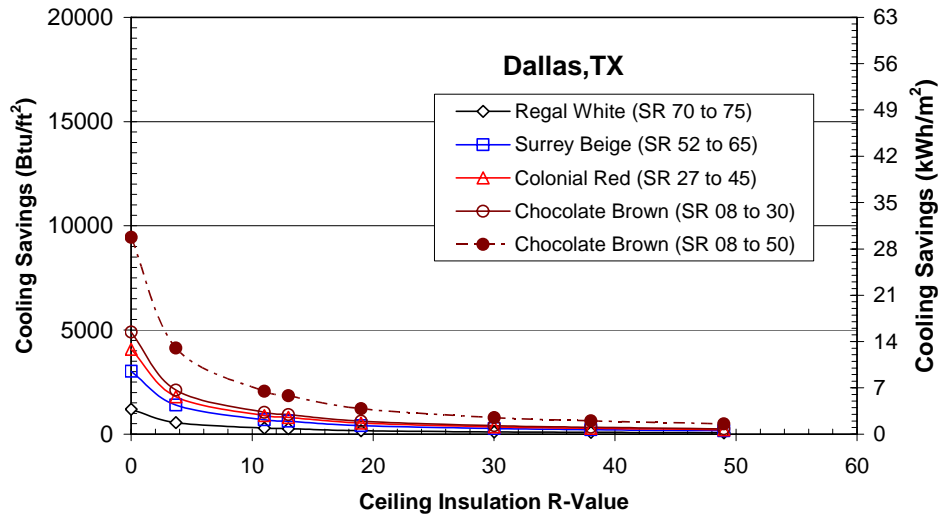


**Figure 4.** The reduction in the ceiling heat produced by CRCMs as compared to the same standard color roof.



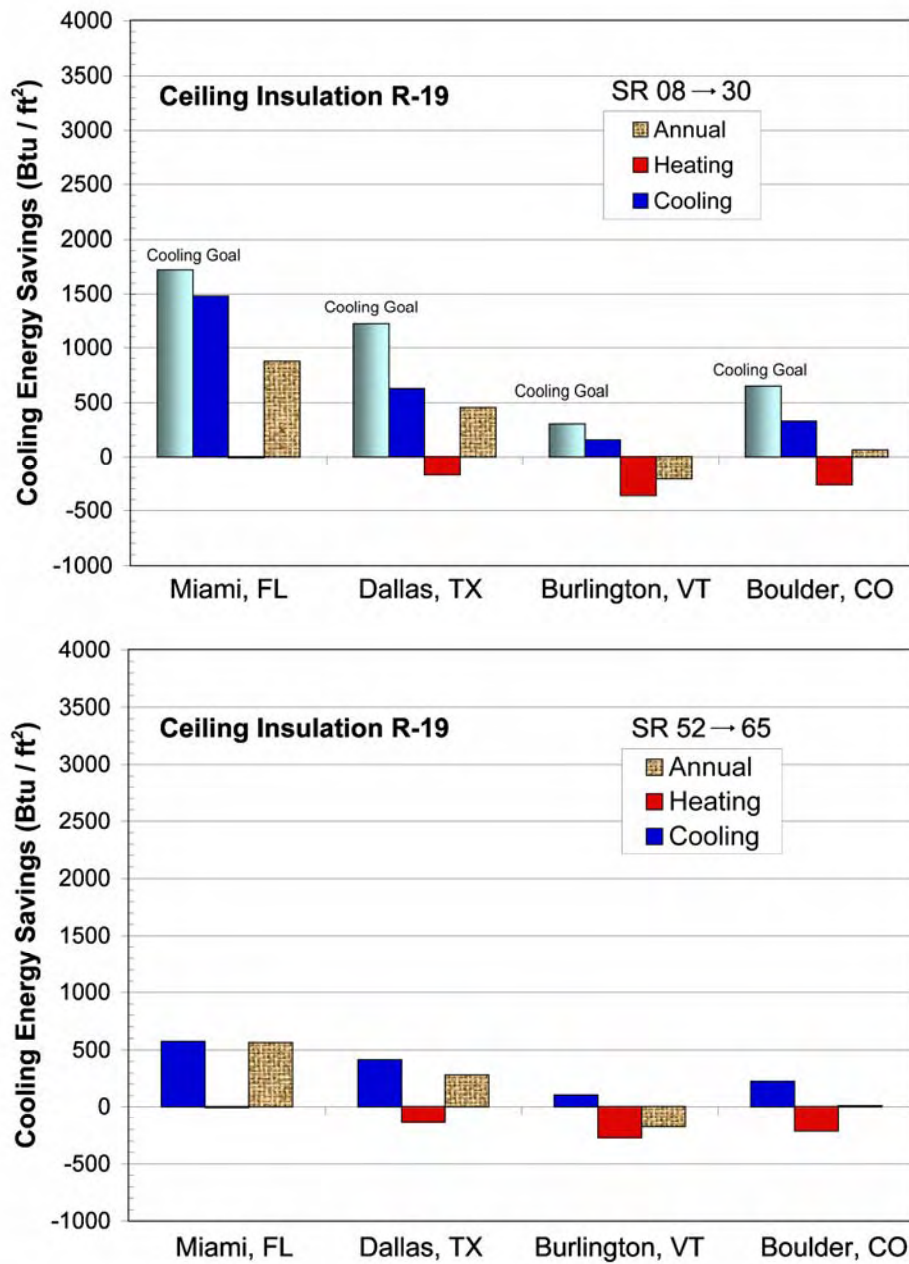


**Figure 5.** The cooling, heating and net annual energy savings achieved by CRCMs as compared to the same standard color roof with R-19 attic insulation.  
 $\text{kWh} = 0.00315 \times [\text{Btu} / \text{ft}^2]$

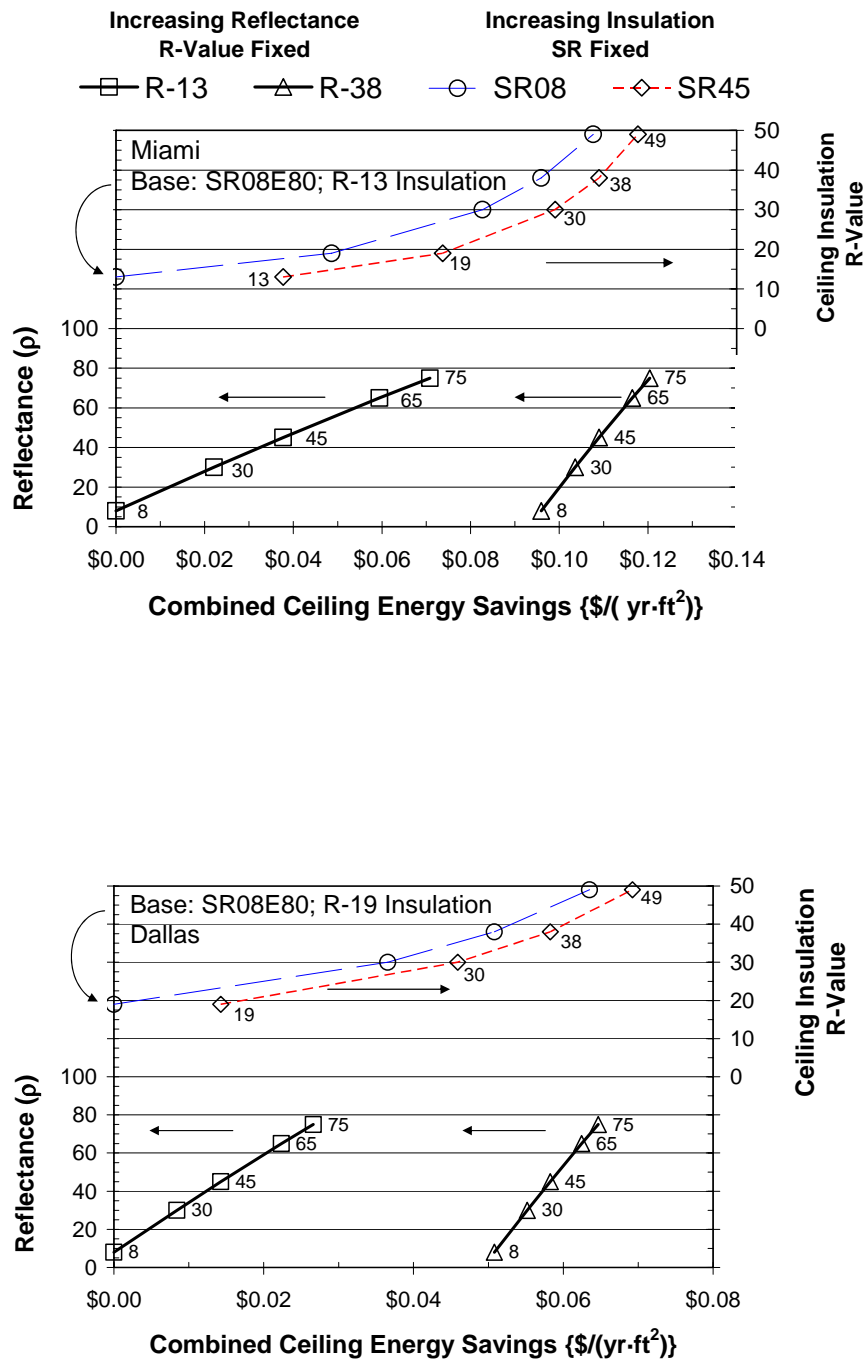


**Figure 6.** The energy savings estimates for the combined effects of CRCMs and ceiling insulation. Base of comparisons based on recommended insulation levels and a roof having SR08E80 radiation properties.  
 $\$/(\text{yr} \cdot \text{m}^2) = 10.764 * \$/(\text{yr} \cdot \text{ft}^2)$

# Cool Colored Materials for Roofs

*H. Akbari, P. Berdahl, R. Levinson, and S. Wiel, Lawrence Berkeley National Laboratory*

*A. Desjarlais and W. Miller, Oak Ridge National Laboratory*

*N. Jenkins, A. Rosenfeld, and C. Scruton, California Energy Commission*

## ABSTRACT

Raising the solar reflectance of a roof from a typical value of 0.1 – 0.2 to an achievable 0.6 can reduce cooling-energy use in buildings by more than 20%. Cool roofs also reduce ambient outside air temperature, thus further decreasing the need for air conditioning and retarding smog formation.

We are collaborating with pigment manufacturers to characterize colorants, and with manufacturers of roofing materials to produce cool colored products, including asphalt shingles, tiles, metal roofing, wood shakes, membranes, and coatings. Significant efforts are being devoted to the identification and characterization of pigments suitable for cool-colored coatings, and to the development of engineering methods for applying cool coatings to roofing materials. We are also measuring and documenting the laboratory and in-situ performances of roofing products. Demonstration of energy savings can accelerate the market penetration of cool-colored roofing materials. Early results from this program have yielded colored concrete, clay, and metal roofing products with solar reflectances exceeding 0.4. Obtaining equally high reflectances for roofing shingles is more challenging, but we expect manufacturers to soon have several cost-effective colored shingles with reflectances of at least 0.25.

## Introduction

### Benefits of Cool Roofs

Building-energy monitoring studies in California and Florida have demonstrated cooling-energy savings in excess of 20% upon raising the solar reflectance of a roof to 0.6 from a prior value of 0.1 - 0.2 (Konopacki and Akbari, 2001; Konopacki *et al.*, 1998; Parker *et al.*, 2002). Energy savings are particularly pronounced in older houses that have little or no attic insulation, especially if the attic contains the air distribution ducts. Our research estimates U.S. potential energy savings in excess of \$750 million per year in net annual energy bills (cooling-energy savings minus heating-energy penalties) (Akbari *et al.*, 1999). Cool roofs also significantly reduce peak electric demand in summer (Akbari *et al.*, 1996; Levinson *et al.*, 2004a). The widespread installation of cool roofs can lower the ambient air temperature in a neighborhood or city, decreasing the need for air conditioning, retarding smog formation, and improving environmental comfort. These “indirect” benefits of reduced ambient air temperatures have roughly the same economic value as the direct energy savings (Rosenfeld *et al.*, 1997).

Lower surface temperatures may also increase the lifetime of roofing products (particularly asphalt shingles), reducing replacement and disposal costs. Our preliminary analysis suggests that there may be a surcost of up to \$1 per square meter for cool roofing materials. This represents 2 to 5% of the cost of installing a new residential roof.

## Availability of Cool Roofing Materials

Cool (solar-reflective) roofing products currently available in the market, such as single-ply membranes and elastomeric coatings, are applied almost exclusively to commercial buildings with low-sloped roofs. Cool products for pitched residential roofs are generally limited to tile and metal. Asphalt shingles dominate the residential roofing market, comprising 47% of 2004 sales in the western state residential market (Western Roofing, 2004). Assuming that the cost per unit roof area of asphalt shingles is about half that of other residential roofing products, we estimate the fraction by surface area is over 60%. Most commercially available asphalt shingles are optically dark, with solar reflectance ranging from 0.05 to 0.25, depending on color. With the exception of one “ultra-white” product, even nominally “white” shingles appear gray, and have a solar reflectance of about 0.25—much lower than the solar reflectance of 0.7 achieved by a white tile or a white metal panel. It is possible to produce a truly white shingle with a solar reflectance of about 0.55 by increasing the amount of white pigment (titanium dioxide rutile) on its granules. However, since many homeowners desire nonwhite roofs, we seek to develop and promote cool colored roofing products, especially shingles.

## Development of Nonwhite Cool Roofing Materials

Currently, suitable cool *white* materials are available for most roofing products, with the notable exception of asphalt shingles. Cool nonwhite materials are needed for all types of roofing. Industry researchers have developed complex inorganic color pigments that are dark in color but highly reflective in the infrared portion of the solar spectrum. The high near-infrared reflectance of coatings formulated with these and other “cool” pigments—e.g., chromium oxide green, cobalt blue, phthalocyanine blue, Hansa yellow—can be exploited to manufacture roofing materials that reflect more sunlight than conventionally pigmented roofing products.

The California Energy Commission (CEC) has engaged Lawrence Berkeley National Laboratory (LBNL) and Oak Ridge National Laboratory (ORNL) on a three-year project to (a) work with the roofing industry to develop and produce colored roofing products with high solar reflectance, and (b) encourage the homebuilding industry to use these products. The intended outcome of this project is to make nonwhite cool roofing materials commercially available within three to five years. Specifically, we aim to produce nonwhite shingles with solar reflectances not less than 0.3, and other types of nonwhite roofing products (e.g., tiles) with solar reflectances not less than 0.45. The reflectance goal for shingles is lower than that for other products because (a) the roughness of a shingle’s surface reduces its reflectance, and (b) manufacturing constraints typically limit the reflectance of coatings applied to granules.

We are collaborating with pigment manufacturers to characterize colorants, and with manufacturers of roofing materials to produce cool colored products, including asphalt shingles, tiles, metal roofing, wood shakes, membranes, and coatings. Significant efforts are being devoted to the identification and characterization of pigments suitable for cool-colored coatings, and to the development of engineering methods for applying cool coatings to roofing materials. We are also measuring and documenting the laboratory and in-situ performance of roofing products. The latter, including demonstrations of building energy savings, can accelerate the market penetration of cool-colored roofing materials.

## Research & Marketing Issues

Our activities are designed to address the following six topics.

1. *Formulation of Cool Colored Coatings.* How can we maximize the total solar reflectance of a pigmented coating while matching a desired color?
2. *Development of Cool Colored Roofing Prototypes.* What is the relationship between the optical properties of a simple pigmented coating and the optical properties of a pigmented coating applied to roofing materials (e.g., granules, tiles)?
3. *Durability of Cool Colored Coatings.* How do cool colored coatings weather and age?
4. *Longevity of Cool Colored Roofing Materials.* Does higher solar reflectance increase the lifetime of cool colored roofing materials?
5. *Demonstration of Energy Savings.* What are the building-energy savings yielded by use of cool colored roofing materials?
6. *Market Introduction.* How can we promote the use of cool colored roofing materials?

## Formulation of Cool Colored Coatings

In order to determine how to optimize the solar reflectance of a pigmented coating matching a particular color, and how the performance of cool-colored roofing products compares to that of a standard material, we (a) have identified and characterized the optical properties of over 100 pigmented coatings; (b) have created a preliminary database of pigment characteristics; and (c) are developing a computer model to maximize the solar reflectance of roofing materials for a choice of visible color.

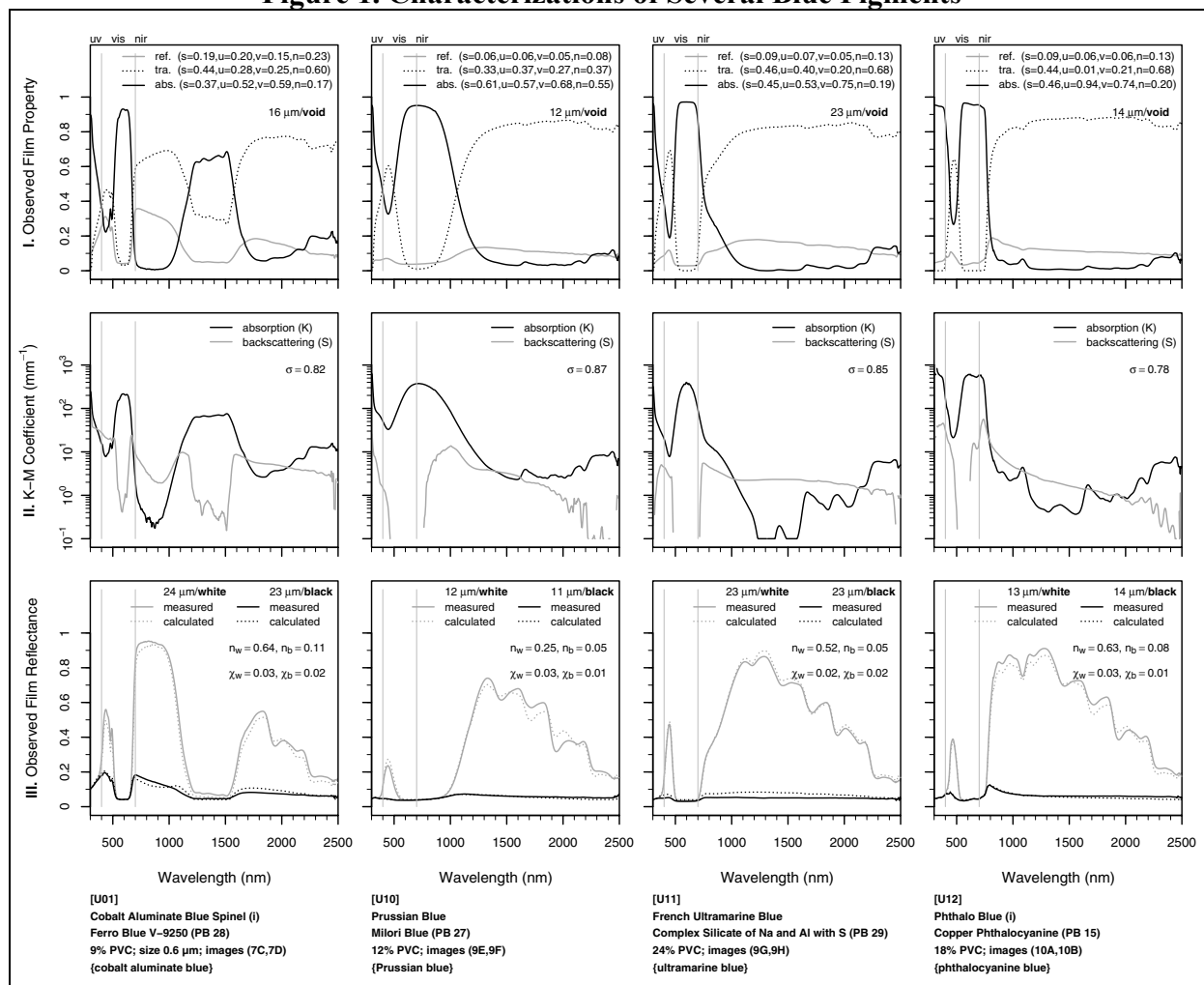
### Pigment Characterization

We have measured the spectral optical properties of many individual pigments and have used these data to develop a method to predict the spectral radiative properties of materials fabricated with these pigments (Levinson *et al.*, 2004b,c).

We illustrate our characterization efforts by presenting results for four blue pigments (see Figure 1). Each pigment is described by a column of three solar spectral charts. The first chart shows the measured transmittance, measured reflectance, and calculated absorptance of a pigmented film; the second, its computed absorption coefficient  $K$  and backscattering coefficient  $S$ ; and the third, its measured and computed reflectances over black and white backgrounds, which serve as checks on the mathematical consistency of the results. The absorption coefficient  $K$  should be large in parts of the visible spectral range, to permit the attainment of desired colors, and should be small in the near infrared (NIR). The backscattering coefficient  $S$  should be small (or large) in the visible spectral range for formulating dark (or light) colors, and is preferably large in the NIR.

*Cobalt aluminate blue* ( $\text{CoAl}_2\text{O}_4$ ; U01) derives its appearance from modest scattering ( $S \sim 30 \text{ mm}^{-1}$ ) in the blue (400 - 500 nm) and strong absorption ( $K \sim 150 \text{ mm}^{-1}$ ) in the rest of the visible spectrum. It has very low absorption in the short NIR (700 - 1000 nm, containing 50% of the NIR energy), but exhibits an undesirable absorption band in the 1200 - 1600 nm range, which contains 17% of the NIR energy. A white background dramatically increases NIR reflectance but makes it lighter in color.

**Figure 1. Characterizations of Several Blue Pigments**



Each pigment is described by a column of three solar spectral charts. The first chart shows the transmittance, reflectance, and absorbance of a pigmented film; the second, its absorption coefficient  $K$  and backscattering coefficient  $S$ ; and the third, its measured and computed reflectances over black and white backgrounds, which serve as checks on the mathematical consistency of the results.

*Iron (a.k.a. Prussian or Milori) blue* (U10) is a weakly scattering pigment with strong absorption in the visible and short NIR, and weak absorption at longer wavelengths. It appears black and has little NIR reflectance over a black background, but looks blue and achieves a modest NIR reflectance (0.25) over a white background. It should be avoided in cool coatings.

*Ultramarine blue* (U11), a complex silicate of sodium and aluminum with sulfur, is a weakly scattering pigment with some absorption in the short NIR. If sparingly used, it can impart absorption in the yellow spectral region without introducing a great deal of NIR absorption. This is a durable inorganic pigment with some sensitivity to acid. While most colored inorganic pigments contain a transition metal such as Fe, Cr, Ni, Mn, and Co, ultramarine blue is unusual. It is a mixed oxide of Na, Si, and Al, with a small amount of sulfur. The metal oxide skeleton forms an open clathrate structure that stabilizes  $S_3$  ions in cages to form the chromophores. Thus isolated  $S_3$  molecules with an attached unpaired electron cause the light absorption in the 500-700 nm range, producing the blue color.

*Copper phthalocyanine blue* (“phthalo” blue) (U12) is a weakly scattering, dyelike pigment with strong absorption in the 500 - 800 nm range and weak absorption in the rest of the visible and NIR. Phthalo blue appears black and has minimal NIR reflectance over a black background, but looks blue and achieves a high NIR reflectance (0.63) over a white background. It is durable and lightfast, but as an organic pigment it is less chemically stable than (high temperature) calcined mixed metal oxides such as cobalt aluminate.

## **Pigment Property Database**

We have developed a preliminary database summarizing our characterizations of about 100 pigments. The database describes each pigment with a tab-delimited plaintext file that includes identification (name, color, and chemistry); mechanical properties (film thicknesses); spectral optical properties (measured reflectance, transmittance, and absorptance; derived absorption and backscattering coefficients; predicted reflectances over various backgrounds); and ancillary parameters generated in the derivation of absorption and backscattering coefficients. We have shared this database with our industrial partners to help them develop cool colored coatings and roofing products.

## **Cool-Color Formulation Software**

We are developing a model that estimates the spectral solar reflectance of coatings from (a) pigment properties (spectral absorption and backscattering coefficients); (b) coating composition (pigments, vehicle, and filler); and (c) coating geometry (thickness and roughness). This model will be implemented in software that suggests recipes to maximize the solar reflectance of a colored coating. The software will be available to pigment, coating, and roofing manufacturers.

## **Development of Cool Colored Roofing Prototypes**

We have surveyed methods of manufacturing various roofing materials, and are working with roofing manufacturers to design innovative techniques for producing cool-colored materials.

## **Survey of Manufacturing Methods**

We estimate that roofing shingles, tiles, and metal panels comprise over 80% (by roof area) of the western state residential roofing market. We contacted representative manufacturers of asphalt shingles, concrete and clay tiles, metal panels, and wood shakes to obtain information on the processes used to color their products. We also reviewed patent and other literature on the fabrication and coloration of roofing materials, with particular emphasis on asphalt roofing shingles.

**Shingles.** The solar reflectance of a new shingle is dominated by the solar reflectance of its granules, since by design, the surface of a shingle is well covered with granules. Hence, we focus on the production of cool granules.



Until recently, the way to produce granules with high solar reflectance has been to use titanium dioxide (TiO<sub>2</sub>) rutile, a white pigment. Since a thin layer of TiO<sub>2</sub> is reflective but not opaque, multiple layers are needed to obtain the desired solar reflectance. This technique has been used to produce “super-white” (meaning truly white, rather than gray) granulated shingles with solar reflectances exceeding 0.5. Manufacturers have also tried to produce colored granules with high solar reflectance by using nonwhite pigments with high NIR reflectance. However, like TiO<sub>2</sub>, cool-colored pigments are also partly transparent to NIR light; thus, any NIR light not reflected by the cool pigment is transmitted to the (typically dark) granule underneath, where it can be absorbed. To increase the solar reflectance of colored granules with cool pigments, multiple color layers, a reflective undercoating, and/or reflective aggregate should be used. Obviously, each additional coating increases the cost of production.

The application of pigmented coatings to roofing granules appears to be the critical process step. Several layers of silicate coatings can be involved, and may include not just one or more pigments, but the use of clay additives to control viscosity, biocides to prevent staining, and process chemistry controls to avoid unreacted dust on the product.

One way to reduce the cost is to produce cool-colored granules via a two-step, two-layer process. In the first step, the granule is pre-coated with an inexpensive pigment that is highly reflective to NIR light. In the second step, the cool-colored pigment is applied to the pre-coated granules.

**Tiles.** For colored tiles, there are three ways to improve the solar reflectance: (1) use of raw clay materials with low concentrations of iron oxides and elemental carbon; (2) use of cool pigments in the coating; and (3) application of the two-layered coating technique using pigmented materials with high solar reflectance as an underlayer. Although all these options are in principle easy to implement, they may require changes in the current production techniques that may add to cost of the finished products. Colorants can be included throughout the body of the tile, or used in a surface coating. Both methods need to be addressed.

**Metal panels.** Application of cool-colored pigments in metal roofing materials may require the fewest number of changes to the existing production processes. As in the cases of tile and asphalt shingle, cool pigments can be applied to metal via a single or a double-layered technique. If the raw metal is highly reflective, a single-layered technique may suffice. The coatings for metal shingles are thin, durable polymer materials. These thin layers use materials efficiently, but limit the maximum amount of pigment present. However, the metal substrate can provide some NIR reflectance if the coating is transparent in the NIR.

**Wood shakes.** We will survey methods of manufacturing wood shakes in the near future.

### **Innovative Methods for Application of Cool Coatings to Roofing Materials**

We have collaborated with 12 companies that manufacture roofing materials, including shingles, roofing granules, clay tiles, concrete tiles, tile coatings, metal panels, metal coatings, and pigments. To date, over 50 prototype cool shingles, 30 tiles or tile coatings, and 20 metal roofing prototypes have been developed and tested. The development work with our industrial partners has been iterative and has included selection of cool pigments, choice of base coats for the two-layer applications, and identification of pigments to avoid.

Figure 2 shows the iterative development of a cool black shingle. A conventional black roof shingle has a reflectance of about 0.04. On the first try to increase the solar reflectance of the shingle, we replaced the standard black pigment on the granules with one that is NIR reflective. That increased the reflectance of the granule to 0.12. On the second try, we used a two-layered technique where we first applied a layer of TiO<sub>2</sub> white base (increasing the solar reflectance of the base granule to 0.28) and then a layer of NIR-reflective black pigment. This increased the reflectance of the black granule to 0.16. On our third prototype, the base granule was coated in ultra-white (reflectance 0.44) and then with an NIR-reflective black pigment. This increased the solar reflectance to 0.18. Figure 2 also shows the performance limit (reflectance 0.25) where a 25- $\mu$ m thick layer of NIR-reflective black coating is applied on an opaque white background.

**Figure 2. Development of a Cool Black Shingle**

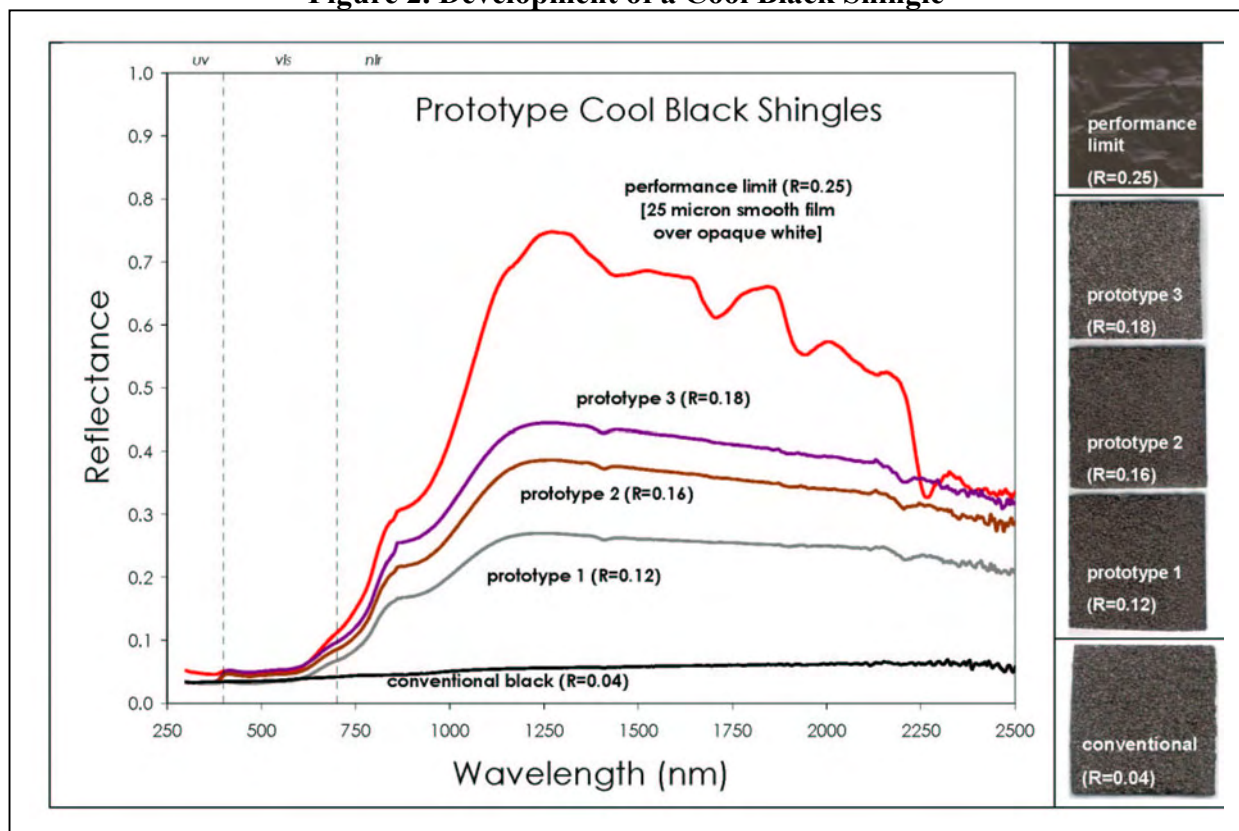


Figure 3 shows the results of similar efforts to develop coatings for concrete tile roofs, which yielded a palette of cool colors each with solar reflectance exceeding 0.4.

## Durability of Cool Colored Coatings

Natural, real-time weathering, such as outdoor exposure in Florida or Arizona, and accelerated tests using weatherometers are in progress to gauge the color-stability and integrity (warranty-related properties) of prototype roofing materials. Accelerated testing is essential because the cool pigment combinations must remain fade resistant or the product will not sell.

Pigment stability and discoloration resistance will be judged using a total color difference measure as specified by ASTM D 2244-93 (ASTM 1993).

**Figure 3. Solar Reflectance of Several Cool Coatings for Concrete Tile Roofs**

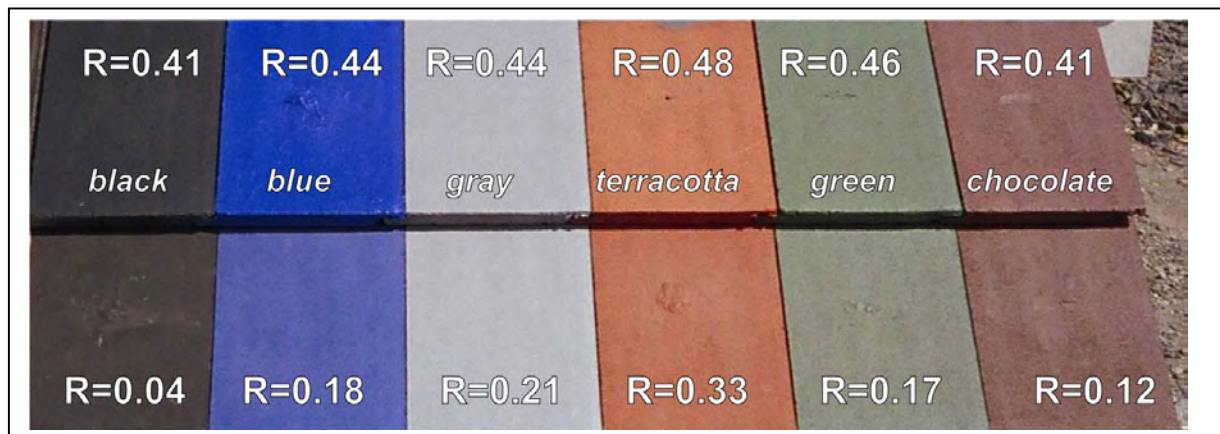


Image courtesy of American Rooftile Coatings (Fullerton, CA)

### **Natural Weathering**

Several different styles and colors of roof samples have been placed in seven of California's 16 climate zones for exposure studies. Reflectance and emittance data are recorded quarterly the first year and twice a year thereafter (weather data are available continuously). In addition, the solar spectral reflectance of each weathered sample is measured annually to gauge soiling and to document color changes too small to perceive.

We will also examine the roof samples for contaminants and determine the elemental composition and biomass on the surface of the roof products. The surface composition studies will identify the drivers affecting the soiling of the roof samples, which in turn will provide valuable information to manufacturers for improving the sustainability of their roof products. The data will be used to formulate an algorithm that correlates changes in reflectance with exposure.

### **Accelerated Weathering**

In collaboration with industrial partners, we are exposing samples to 5,000 hours of xenon-arc light in a weatherometer following ASTM G-155 (ASTM 2000).

### **Longevity of Cool Colored Roofing Materials**

We will soon begin to investigate the effect of reflectance on the useful life of roofing products. There have been claims that cool roofs will last longer, although no specific data have been offered. The research team will work with industry to design and implement a test method for this purpose and use laboratory and outdoor accelerated aging techniques to gather data on the effect.

Roofing materials fail mainly because of three processes: gradual changes to physical and chemical composition induced by the absorption of ultraviolet (UV) light; aging and weathering

(e.g., loss of plasticizers in polymers and low-molecular-weight components in asphalt), which may accelerate as temperature increases; and diurnal thermal cycling, which stresses the material by expansion and contraction. Our goal is to clarify the material degradation effects due to UV absorption and those due to heating. The results will be used to quantify the effect of solar reflectance on the useful life of roofs; provide data to manufacturers to develop better materials; and support development of appropriate ASTM standards.

## **Demonstration of Energy Savings**

Homeowners and utilities considering new rebate programs need proof that an aesthetically pleasing dark roof can be made to reflect like a white roof in the infrared spectrum, and save energy and money. Therefore, demonstrating the potential energy savings is paramount for fostering the market penetration of the cool pigment technology. Field experiments cover a range of conditions necessary to benchmark analytical tools and permit an accurate assessment of energy conservation potential over a range of climates. These experiments include measuring energy savings in pairs of homes at CA field sites, and thermal testing of tile roofs on a steep-slope attic assembly.

### **Building Energy Use Measurements at California Demonstration Sites**

We have set up a residential demonstration site in Fair Oaks, CA (near Sacramento) consisting of two pairs of single-family, detached houses roofed with metal and concrete tile. We are planning for another two pair of houses to demonstrate asphalt shingles and cedar shakes. The monitoring period will last at least through summer of 2005. The demonstration pairs each include one building roofed with a cool-pigmented product and a second building roofed with a conventionally (warmer) pigmented product of nearly the same color.

Solar reflectance and thermal emittance are measured twice a year. Temperatures at the roof surface, on the underside of the roof deck, in the mid-attic air, at the top of the insulation, on the interior ceiling's sheet rock surface, and inside the building are logged continuously by a data acquisition system. Relative humidity in the attic air and the residence are also measured. Heat flux transducers are embedded in the sloped roofs and the attic floor to measure the roof heat flows and the building heat leakage. We have instrumented the building to measure the total house and air-conditioning power demands. A fully instrumented meteorological weather station is set up to collect the ambient dry bulb temperature, the relative humidity, the solar irradiance, and the wind speed and wind direction.

### **Thermal Testing on Steep-slope Assembly at Oak Ridge National Laboratory**

The multiple hazard protection provided by concrete and clay tile from fire, wind and earthquake are making tile the preference of upper income residences in western and some southern states. The typical reflectance of tile is about 0.1; however, applying the cool pigments increases reflectance beyond 0.4 (Fig. 3). The thermal analysis of tile roofing is an interesting challenge because of the air gap formed between the tile and the roof deck. Yet that air gap poses significant energy savings as proved by Beal and Chandra (1999) who demonstrated a 45% daytime reduction in heat flux for a counter-batten tile roof (the reduction over a 24 hour cycle was much less due to differing rates of nocturnal cooling) as compared to a direct nailed shingle

roof. Quantifying the effect of the cool pigments on tile roofs requires testing and analysis to correctly model the heat flow across the air channel.

We are testing several concrete and clay tile on a steep-slope roof to further learn and document the effect of reflectance and emittance weathering on the thermal performance of the cool pigment roof systems. The Roof Tile Institute and its affiliate members are keenly interested in specifying tile roofs as cool roof products and they want to know the individual and combined effects of cool pigments and of venting the underside of concrete and clay roof tile. The data will help better formulate the simulation program, AtticSim, for predicting the thermal performance of the cool colored tile systems.

## **Market Introduction of Cool Colored Roofing Products**

Through close coordination with industry, utilities and code developers, this project is expected to have near-term success facilitating the deployment of cool colored roofing products, particularly in California. In addition to its ongoing close working relationship with coating manufacturers and roofing manufacturers, the team is working closely with California utilities and California codes-and-standards programs.

In April 2004, the research team and several roofing manufacturer representatives introduced emerging cool colored roofing products to the Emerging Technology Coordinating Council (ETCC). Members of the ETCC are responsible for emerging technology programs at each of the investor owned utilities. The emerging technology programs at the utilities are also a critical validation step that can lead to product incentives through the utilities' energy efficiency programs.

Many products developed as a result of this research will be able to meet the residential cool roof credit requirements contained in the 2005 Title 24 California Building Energy Efficiency Standards and the research team will work with the standards program staff to provide input on possible future code enhancements.

## **Conclusion**

The early results from this program indicate significant success in developing cool-colored materials for concrete tile, clay tile, and metal roofs. Since the inception of this program, the solar reflectance of commercially available products has increased to 0.30-0.45 from 0.05-0.25. To be cost effective, shingle manufacturers apply a very thin layer of pigments on the roofing granules. Use of a reflective undercoated (two-layered coating) is expected to soon yield several cost-effective cool-colored shingle products, with solar reflectances in excess of 0.25 (the EPA threshold for EnergyStar roofs). Our ongoing collaboration with granule and shingle manufacturers may yield shingles with solar reflectances exceeding 0.3.

## **Acknowledgements**

This work was supported by the California Energy Commission (CEC) through its Public Interest Energy Research Program (PIER), by the Laboratory Directed Research and Development (LDRD) program at Lawrence Berkeley National Laboratory (LBNL), and by the Assistant Secretary for Renewable Energy under Contract No. DE-AC03-76SF00098.

## References

- Akbari, H., S. Konopacki, and M. Pomerantz. 1999. "Cooling energy savings potential of reflective roofs for residential and commercial buildings in the United States," *Energy*, **24**, 391-407.
- Akbari, H., S. Bretz, H. Taha, D. Kurn, and J. Hanford. 1997. "Peak Power and Cooling Energy Savings of High-albedo Roofs," *Energy and Buildings* — Special Issue on Urban Heat Islands and Cool Communities, **25**(2);117–126.
- American Society for Testing and Materials (ASTM). 2000. Designation G155-00ae1: Standard Practice for Operating Xenon Arc Light Apparatus for Exposure of Non-Metallic Materials. West Conshohocken, Pa.: American Society for Testing and Materials.
- . 1993. Designation D2244-93: Standard Test Method for Calculation of Color Differences from Instrumentally Measured Color. West Conshohocken, Pa.: American Society for Testing and Materials.
- Beal, D. and S. Chandra. 1995. "The Measured Summer Performance of Tile Roof Systems and Attic Ventilation Strategies in Hot Humid Climates," Thermal Performance of the Exterior Envelopes of Buildings VI, U.S. DOE/ORNL/BETEC, December 4-8, 1995, Clearwater, FL.
- Konopacki, S., and H. Akbari. 2001. "Measured Energy Savings and Demand Reduction from a Reflective Roof Membrane on a Large Retail Store in Austin." Lawrence Berkeley National Laboratory Report No. LBNL-47149, Berkeley, CA.
- Konopacki, S., L. Gartland, H. Akbari, and L. Rainer. 1998. "Demonstration of Energy Savings of Cool Roofs." Lawrence Berkeley National Laboratory Report No. LBNL-40673, Berkeley, CA.
- Levinson, R., H. Akbari, S. Konopacki, and S. Bretz. 2004a. "Inclusion of cool roofs in nonresidential Title 24 prescriptive requirements," In Press. *Energy Policy*.
- Levinson, R., P. Berdahl, and H. Akbari. 2004b. "Spectral Solar Optical Properties of Pigments Part I: Model for Deriving Scattering and Absorption Coefficients from Transmittance and Reflectance Measurements." Draft
- . 2004c. "Spectral Solar Optical Properties of Pigments Part II: Survey of Common Colorants." Draft
- Miller, W.A., H. Akbari, R. Levinson, K.T. Loye, S. Kriner, R.G. Scichili, A.O. Desjarlais, S. Weil, and P. Berdahl. 2004. "Special Infrared Reflective Pigments Make a Dark Roof Reflect Almost Like a White Roof," to be published in Thermal Performance of the Exterior Envelopes of Buildings, IX, proceedings of ASHRAE THERM VIII, Clearwater, FL., Dec.

Parker, D.S., J.K. Sonne, and J.R. Sherwin. 2002. "Comparative Evaluation of the Impact of Roofing Systems on Residential Cooling Energy Demand in Florida," Proceedings of the 2002 ACEEE Summer Study on Energy Efficiency in Buildings, Vol. 1, p. 219, Pacific Grove, CA.

Petrie, T.W., T.K. Stovall, K.E. Wilkes, and A.O. Desjarlais. 2004. "Comparison of Cathedralized Attics to Conventional Attics: Where and When Do Cathedralized Attics Save Energy and Operating Costs?," to be published in Thermal Performance of the Exterior Envelopes of Buildings, IX, proceedings of ASHRAE THERM VIII, Clearwater, FL., Dec.

Rosenfeld, A. H., J. J. Romm, H. Akbari, and M. Pomerantz. 1998. "Cool Communities: Strategies for Heat Islands Mitigation and Smog Reduction," *Energy and Buildings*, **28**(1);51–62.

Western Roofing. 2004. Online at <http://WesternRoofing.net> .



# Cool Colored Roofs to Save Energy and Improve Air Quality\*

Hashem Akbari, Ronnen Levinson, William Miller<sup>†</sup>, and Paul Berdahl

Heat Island Group

Lawrence Berkeley National Laboratory

(510) 486-4287

[H\\_Akbari@lbl.gov](mailto:H_Akbari@lbl.gov)

<http://HeatIsland.LBL.gov/>

## ABSTRACT

Raising the solar reflectance of a roof from a typical value of 0.1–0.2 to an achievable 0.6 can reduce cooling-energy use in buildings by more than 20%. Cool roofs also reduce ambient outside air temperature, thus further decreasing the need for air conditioning and retarding smog formation.

We are collaborating with pigment manufacturers to characterize colorants, and with manufacturers of roofing materials to produce cool colored products, including asphalt shingles, concrete and clay tiles, metal roofing, wood shakes, and coatings. In this collaboration, we have identified and characterized pigments suitable for cool-colored coatings, and developed engineering methods for applying cool coatings to roofing materials. We are also measuring and documenting the laboratory and *in-situ* performances of roofing products. Demonstration of energy savings can accelerate the market penetration of cool-colored roofing materials. Early results from this effort have yielded colored concrete, clay, and metal roofing products with solar reflectances exceeding 0.4. Obtaining equally high reflectances for roofing shingles is more challenging, but some manufacturers have already developed several cost-effective colored shingles with solar reflectances of at least 0.25.

## Introduction

Coatings colored with conventional pigments tend to absorb the invisible “near-infrared” (NIR) radiation that bears more than half of the power in sunlight (Figure 1). Replacing conventional pigments with “cool” pigments that absorb less NIR radiation can yield similarly colored coatings with higher solar reflectance. These cool coatings lower roof surface temperature, reducing the need for cooling energy in conditioned buildings and making unconditioned buildings more comfortable.

Field studies in California and Florida have demonstrated cooling-energy savings in excess of 20% upon raising the solar reflectance of a roof to 0.6 from a prior value of 0.1–0.2 (Konopacki and Akbari, 2001; Konopacki *et al.*, 1998; Parker *et al.*, 2002). Energy savings are particularly pronounced in older houses that have little or no attic insulation, especially if the attic contains the air distribution ducts. At 8¢/kWh, the value of U.S. potential nationwide net commercial and residential energy savings (cooling savings minus heating penalties) exceeds \$750 million per year (Akbari *et al.*, 1999). Cool roofs also significantly reduce peak electric demand in summer (Akbari *et al.*, 1997; Levinson *et al.*, 2005a). The widespread installation of cool roofs can lower the ambient air temperature in a neighborhood or city, decreasing the need

---

\* Parts of this paper have been presented in an earlier conference publication (Akbari *et al.* 2004).

<sup>†</sup> Oak Ridge National Laboratory, Oak Ridge, Tennessee.

for air conditioning, retarding smog formation, and improving environmental comfort. These “indirect” benefits of reduced ambient air temperatures have roughly the same economic value as the direct energy savings (Rosenfeld *et al.*, 1998). Lower surface temperatures may also increase the lifetime of roofing products (particularly asphalt shingles), reducing replacement and disposal costs.

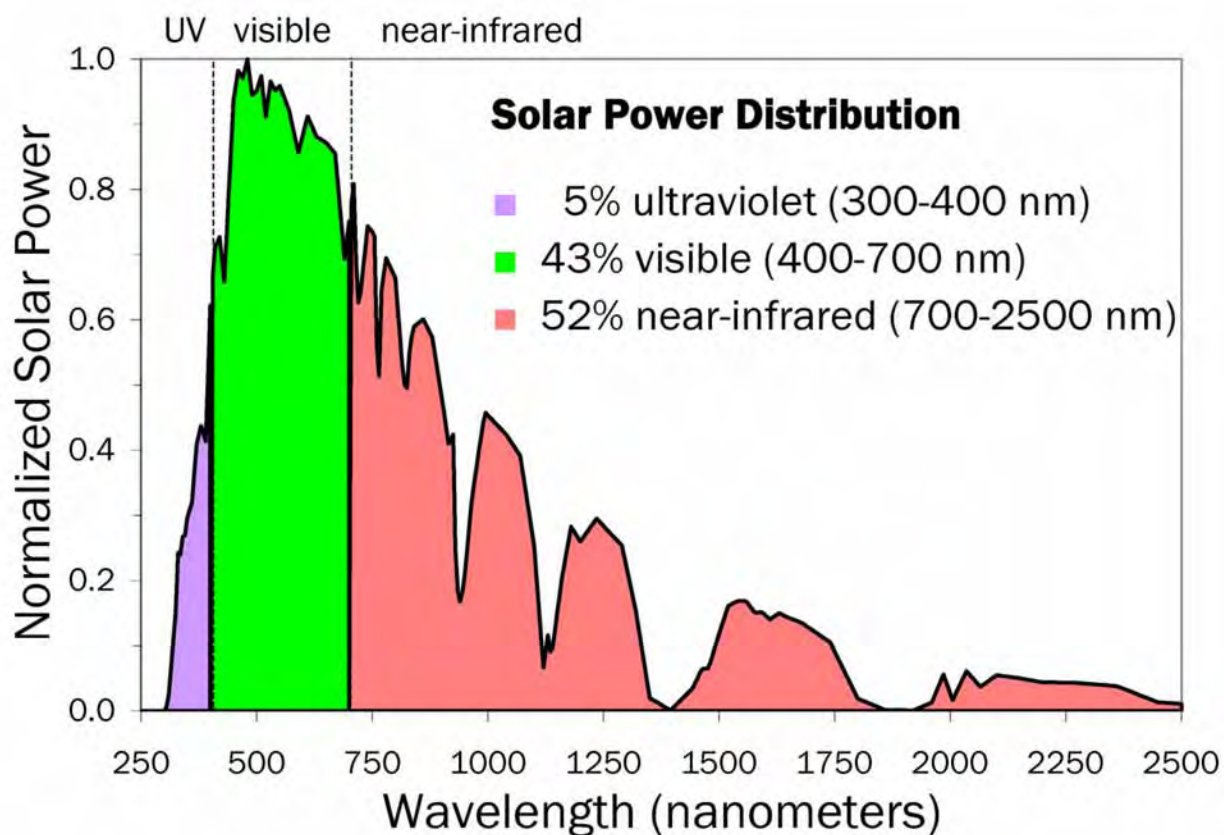


Figure 1. Peak-normalized solar spectral power; over half of all solar power arrives as invisible, “near-infrared” radiation

According to *Western Roofing Insulation and Siding* magazine (2002), the total value of the 2002 projected residential roofing market in 14 western U.S. states (AK, AZ, CA, CO, HI, ID, MT, NV, NM, OR, TX, UT, WA, and WY) was about \$3.6 billion (B). We estimate that 40% (\$1.4B) of that amount was spent in California. The lion’s share of residential roofing expenditure was for fiberglass shingle, which accounted for \$1.7B, or 47% of sales. Concrete and clay roof tiles made up \$0.95B (27%), while wood, metal, and slate roofing collectively represented another \$0.55B (15%). The value of all other roofing projects was about \$0.41B (11%). We estimate that the roofing market area distribution was 54–58% fiberglass shingle, 8–10% concrete tile, 8–10% clay tile, 7% metal, 3% wood shake, and 3% slate (Table 1).

Suitable cool *white* materials are available for most roofing products, with the notable exception (prior to March 2005<sup>\*</sup>) of asphalt shingles. Cool nonwhite materials are needed for all types of roofing. Industry researchers have developed complex inorganic color pigments that are dark in color but highly reflective in the near infrared (NIR) portion of the solar spectrum. The high near-infrared reflectance of coatings formulated with these and other “cool” pigments—e.g., chromium oxide green, cobalt blue, phthalocyanine blue, Hansa yellow—can be exploited to manufacture roofing materials that reflect more sunlight than conventionally pigmented roofing products.

Roofing Type	Market share by \$		Estimated market share by roofing area %
	\$B	%	
Fiberglass Shingle	1.70	47.2	53.6-57.5
Concrete Tile	0.50	13.8	8.4-10.4
Clay Tile	0.45	12.6	7.7-9.5
Wood Shingle/Shake	0.17	4.7	2.9-3.6
Metal/Architectural	0.21	5.9	6.7-7.2
Slate	0.17	4.7	2.9-3.6
Other	0.13	3.6	4.1-4.4
SBC Modified	0.08	2.1	2.4-2.6
APP Modified	0.07	1.9	2.2-2.3
Metal/Structural	0.07	1.9	2.2-2.3
Cementitious	0.04	1.1	1.2-1.3
Organic Shingles	0.02	0.5	0.6
<b>Total</b>	<b>3.60</b>	<b>100</b>	<b>100</b>

Table 1. Project residential roofing market in the U.S. western region surveyed by Western Roofing (2002). The 14 states included in the U.S. western region are AK, AZ, CA, CO, HI, ID, MT, NV, NM, OR, TX, UT, WA, and WY

Cool colored roofing materials are expected to penetrate the roofing market within the next few years. Preliminary analysis suggests that they may cost up to \$1/m<sup>2</sup> more than conventionally colored roofing materials. However, this would raise the total cost of a new roof (material plus labor) by only 2 to 5%.

We have collaborated with 12 companies that manufacture roofing materials, including shingles, roofing granules, clay tiles, concrete tiles, tile coatings, metal panels, metal coatings, and pigments. The development work with our industrial partners has been iterative and has included selection of cool pigments, choice of base coats for the two-layer applications (discussed later in this paper), and identification of pigments to avoid.

## Creating Cool Nonwhite Coatings

In order to determine how to optimize the solar reflectance of a pigmented coating matching a particular color, and how the performance of cool-colored roofing products compares to those of a standard materials, we (a) have identified and characterized the optical properties of

---

<sup>\*</sup> In March 2005, a major manufacturer of roofing shingles in California announced availability of cool colored shingles in four popular colors.

over 100 pigmented coatings; (b) have created a database of pigment characteristics; and (c) are developing a computer model to maximize the solar reflectance of roofing materials for a choice of visible color.

Pigment analysis begins with measurement of the reflectance  $r$  and transmittance  $t$  of a thin coating containing single pigment or binary mix of pigments (Levinson *et al.*, 2005b,c). These “spectral”, or wavelength-dependent, properties of the pigmented coating are measured at 441 evenly spaced wavelengths spanning the solar spectrum (300 – 2,500 nanometers). In addition, each sample is characterized by its computed spectral absorption coefficient  $K$  and backscattering coefficient  $S$ . A cool color is defined by a large absorption coefficient  $K$  in parts of the visible spectral range, to permit the attainment of desired colors, and a small absorption coefficient  $K$  in the near infrared (NIR). For cool colors, the backscattering coefficient  $S$  is small (or large) in the visible spectral range for formulating dark (or light) colors, and large in the NIR.

Inspection of the film’s spectral absorptance (calculated as  $1-r-t$ ) reveals whether a pigmented coating is cool (has low NIR absorptance) or hot (has high NIR absorptance). The spectral reflectance and transmittance measurements are also used to compute spectral rates of light absorption and backscattering (reflection) per unit depth of film. The spectral reflectance of a coating colored with a mixture of pigments can then be estimated from the spectral absorption and backscattering rates of its components.

We have produced a database detailing the optical properties of the characterized pigmented coatings (Figure 2). We are currently developing coating formulation software intended to minimize the NIR absorptance (and hence maximize the solar reflectance) of a color-matched pigmented coating.

## Creating Cool Nonwhite Roofing Products

We estimate that roofing shingles, tiles, and metal panels comprise more than 80% (by roof area) of the residential roofing market in the western United States. In this project, we have collaborated with manufacturers of many roofing materials in order to evaluate the best ways to increase the solar reflectance of these products. The results of our research have been utilized by the manufacturers to produce cool roofing materials. To date and as the direct result of this collaborative effort, manufactures of roofing materials have introduced cool shingles, clay tiles, concrete tiles, metal roofs, and concrete tile coatings.

In addition to using NIR reflective pigments in manufacturing of cool roofing materials, application of novel engineering techniques can further economically enhance the solar reflectance of colored roofing materials. Cool-colored pigments are partly transparent to NIR light; thus, any NIR light not reflected by the cool pigment is transmitted to the underneath layer, where it can be absorbed. To increase the solar reflectance of colored materials with cool pigments, multiple color layers, a reflective undercoating can be used. This method is referred as a two-layered technique.









Figure 3 demonstrates the application of the two-layered technique to manufacture cool colored materials. A thin layer of dioxazine purple (14–27  $\mu\text{m}$ ) is applied on four substrates: (a) aluminum foil ( $\sim 25 \mu\text{m}$ ), (b) opaque white paint ( $\sim 1000 \mu\text{m}$ ), (c) non-opaque white paint ( $\sim 25 \mu\text{m}$ ), and (d) opaque black paint ( $\sim 25 \mu\text{m}$ ). As it can be seen (and is confirmed by visible reflectance spectrum), the color of the material is black. However, the solar reflectance of the sample exceeds 0.4 when applied to an opaque white or aluminum foil substrate; while its solar reflectance over a black substrate is only 0.05.

## [R03] Red Iron Oxide (iii)

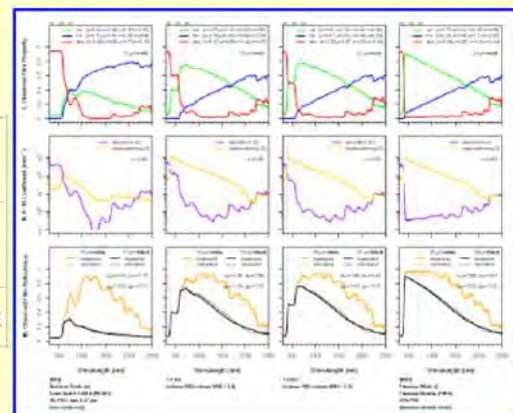
Paint Code	<b>R03</b>
Paint Name	Red Iron Oxide (iii)
Pigment Name	Ferro Red V-13810 (PR 101)
Color Family	Red/Orange
Color Subfamily	iron oxide red
Mean Particle Size (microns)	0.27
Dry Film PVC	3%
Pigment Datasheet	<a href="#">available</a>
Paint Datasheet	unavailable
LBNL Commentary	<a href="#">available</a>

## Masstone and Mixtures with White (Tints)

[\[R03\] Red Iron Oxide \(iii\)](#) +  
[\[W03\] Titanium White \(i\)](#)




image over white				
image over black				
spectral datafile	<a href="#">R03 masstone</a>	<a href="#">R03 tint 1:4</a>	<a href="#">R03 tint 1:9</a>	<a href="#">W03 masstone</a>

[guide to reading spectral datafiles](#)



## Mixtures with Nonwhite Colors

[\[R03\] Red Iron Oxide \(iii\)](#) +  
[\[B16\] Iron Titanium Brown Spinel \(i\)](#)

image over white			
image over black			
spectral datafile	<a href="#">R03 masstone</a>	<a href="#">R03+B16 mixture 1:1</a>	<a href="#">B16 masstone</a>

[guide to reading spectral datafiles](#)

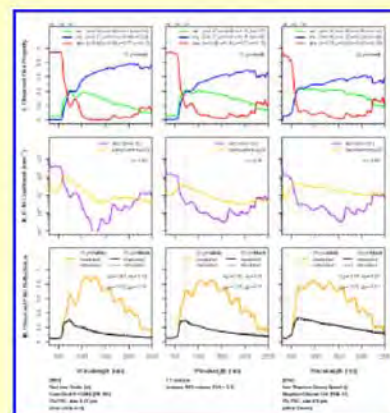


Figure 2. Description of an iron oxide red pigment in the Lawrence Berkeley National Lab pigment database



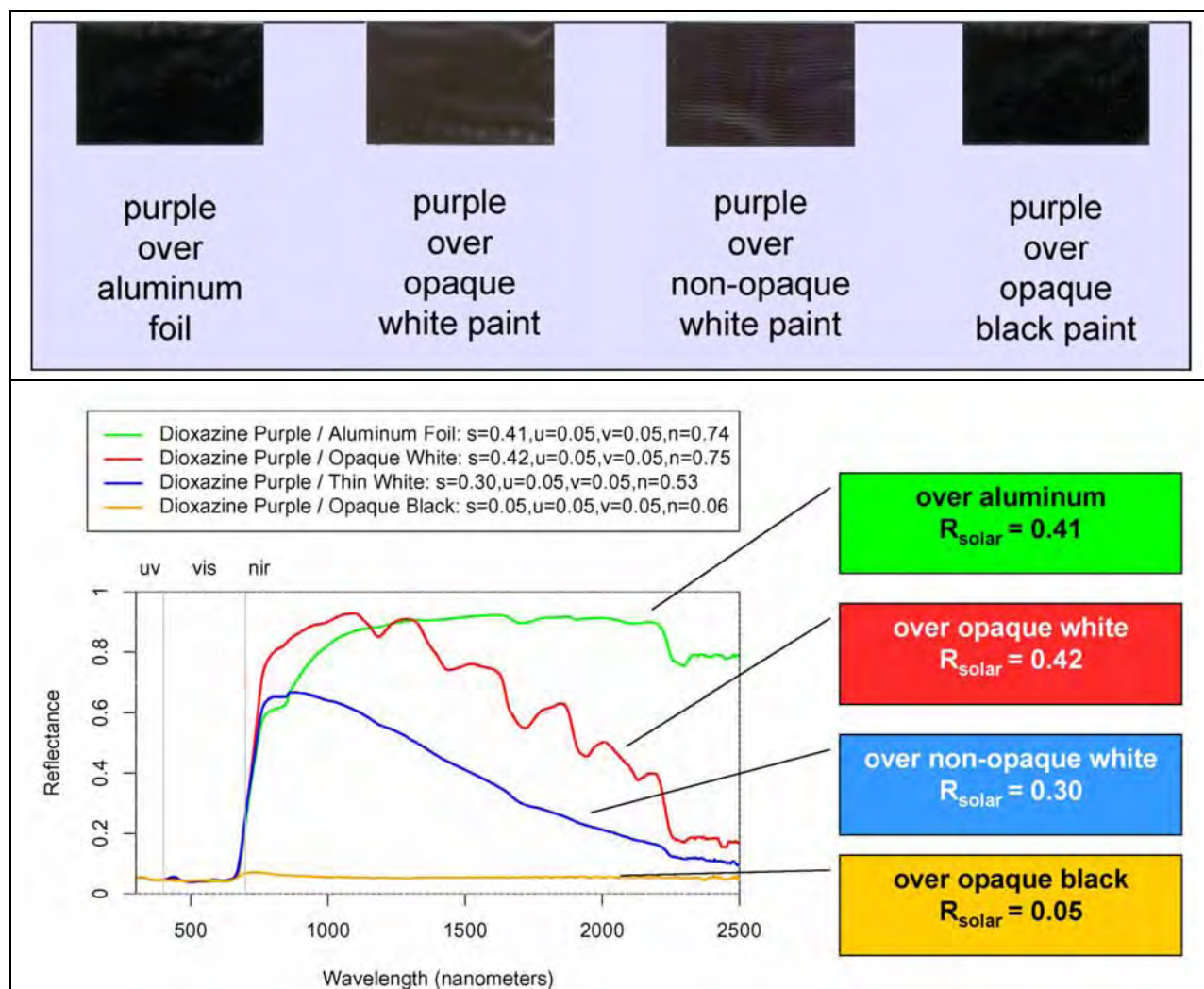


Figure 3. Application of the two-layered technique to manufacture cool colored materials

## Shingles

The solar reflectance of a new shingle, by design, is dominated by the solar reflectance of its granules, which cover over 97% of its surface. Until recently, the way to produce granules with high solar reflectance has been to use a coating pigmented with titanium dioxide ( $\text{TiO}_2$ ) rutile white. Because a thin  $\text{TiO}_2$ -pigmented coating is reflective but not opaque in the NIR, multiple layers are needed to obtain high solar reflectance. This technique has been used to produce “super-white” (meaning truly white, rather than gray) granulated shingles with solar reflectances exceeding 0.5 (see Figure 4).

Although white roofing materials are popular in some areas (e.g., Greece, Bermuda; see Figure 5), many consumers aesthetically prefer non-white roofs. Manufacturers have also tried to produce colored granules with high solar reflectance by using nonwhite pigments with high NIR reflectance. To increase the solar reflectance of colored granules with cool pigments, multiple color layers, a reflective undercoating, and/or reflective aggregate should be used. Obviously, each additional coating increases the cost of production.

Several cool shingles have been developed within the last year. Figure 6 shows examples of prototype cool shingles and compares their solar reflectances with those of the standard colors. Recently, a major manufacturer of roofing shingles in California announced availability of cool colored shingles in four popular colors. Figure 7 shows two houses with cool colored roofing shingles.

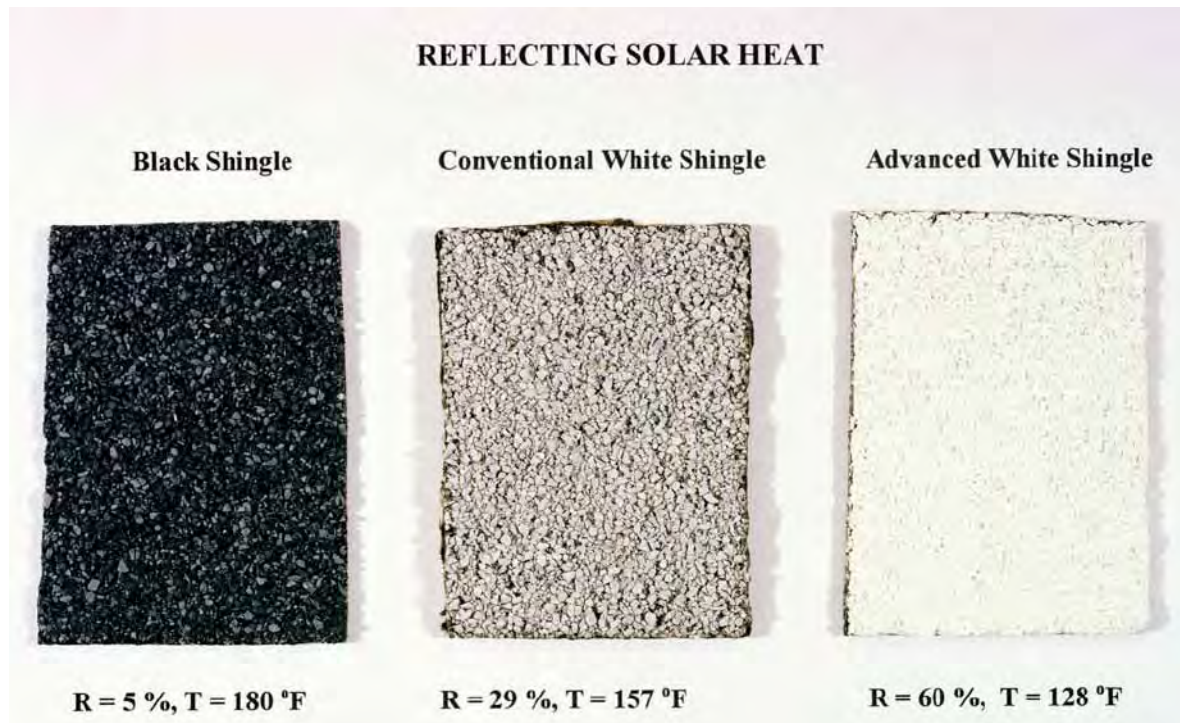


Figure 4. Development of super white shingles



Bermuda



Santorini (Greece)

Figure 5. White roofs and walls are used in Bermuda and Santorini (Greece)



### Standard Shingles



R=0.23



R=0.27



R=0.28

### Cool Shingles



R=0.28



R=0.36



R=0.37

Figure 6. Examples of prototype cool shingles



Figure 7. Test application of cool colored roofing shingles on two houses

## ***Tiles and Tile Coatings***

Clay and concrete tiles are used in many areas around the world. In the U.S., clay and concrete tiles are more popular in the hot climate regions. There are three ways to improve the solar reflectance of colored tiles: (1) use clay or concrete with low concentrations of light-absorbing impurities, such as iron oxides and elemental carbon; (2) color the tile with cool pigments contained in a surface coating or mixed integrally; and/or (3) include an NIR-reflective (e.g., white) sublayer beneath an NIR-transmitting colored topcoat. Although all these options

are in principle easy to implement, they may require changes in the current production techniques that may add to cost of the finished products. Colorants can be included throughout the body of the tile, or used in a surface coating. Both methods need to be addressed.

One of our industrial partners has developed a palette of cool nonwhite coatings for concrete tiles. Each of the cool colored coatings shown in Figure 8 has a solar reflectance better than 0.40. The solar reflectance of each cool coating exceeds that of a color-matched, conventionally pigmented coating by 0.15 (terracotta) to 0.37 (black). Another industrial partner also manufactures clay tiles in many colors (glazed and unglazed) with solar reflectance greater than 0.4 (See Table 1).

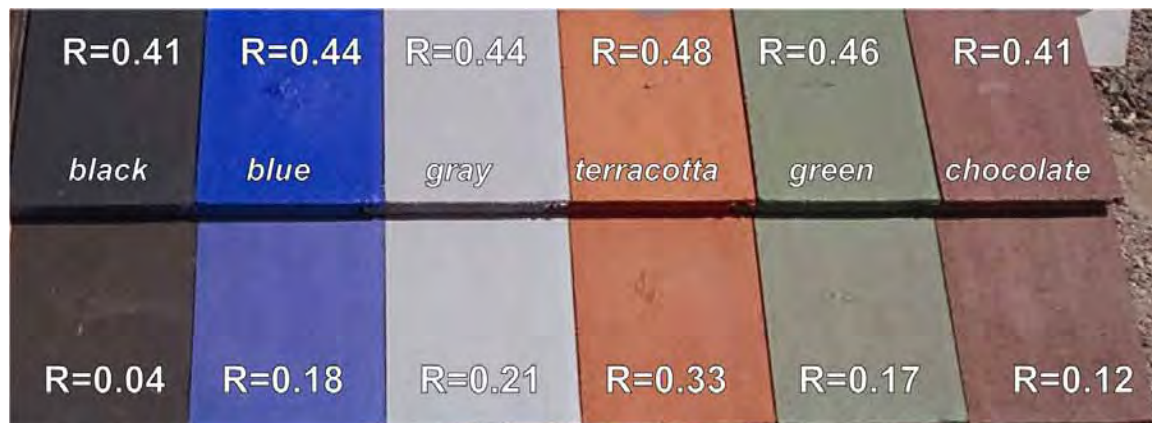


Figure 8. Palette of color-matched cool (top row) and conventional (bottom row) roof tile coatings developed by industrial partner American Roof tile Coatings. Shown on each coated tile is its solar reflectance R

## Metal Panels

Metal roofing materials are installed on a small (but growing) fraction of the U.S. residential roofs. Historically metal roofs have had only about 3% of the residential market. However, the architectural appeal, flexibility, and durability, due in part to the cool-colored pigments, has steadily increased the sales of painted metal roofing, and as of 2003 its sales volume has increased to 8% of the residential market, making it the fastest growing residential roofing product (F.W. Dodge 2003). Metal roofs are available in many colors and can simulate the shape and form of many other roofing materials (see Figure 9). Application of cool-colored pigments in metal roofing materials may require the fewest number of changes to the existing production processes. As in the cases of tile and asphalt shingle, cool pigments can be applied to metal via a single or two-layered technique. If the metal substrate is highly reflective, a single-layered technique may suffice. The coatings for metal shingles are thin, durable polymer materials. These thin layers use materials efficiently, but limit the maximum amount of pigment present. However, the metal substrate can provide some NIR reflectance if the coating is transparent in the NIR. Several manufactures develop cool colored metal roofs.









Model	Color	Initial solar reflectance	Solar reflectance after 3 years
<b>Weathered Green Blend</b>		0.43	0.49
<b>Natural Red</b>		0.43	0.38
<b>Brick Red</b>		0.42	0.40
<b>White Buff</b>		0.68	0.56
<b>Tobacco</b>		0.43	0.41
<b>Peach Buff</b>		0.61	0.48
<b>Regency Blue</b>		0.38	0.34
<b>Light Cactus Green</b>		0.51	0.52

Table 2. Sample cool colored clay tiles and their solar reflectances (Source: <http://www.MCA-Tile.com>)

### ***Durability of Cool Nonwhite Coatings***

Roofing materials fail mainly because of three processes: (1) gradual changes to physical and chemical composition induced by the absorption of ultraviolet (UV) light; (2) aging and weathering (e.g., loss of plasticizers in polymers and low-molecular-weight components in asphalt), which may accelerate as temperature increases; and (3) diurnal thermal cycling, which stresses the material by expansion and contraction. Our goal is to clarify the material degradation effects due to UV absorption and those due to heating. The results will be used to quantify the

effect of solar reflectance on the useful life of roofs, provide data to manufacturers to develop better materials, and support development of appropriate ASTM standards.

We are naturally weathering various types of conventionally- and cool-pigmented roofing products at seven California sites. Solar reflectance and thermal emittance are measured twice per year; weather data are available continuously. Solar spectral reflectance is measured annually to gauge soiling and to document imperceptible color changes.

We have also exposed roofing samples to 5,000 hours of xenon-arc light and to about 10,000 hours of fluorescent light in weatherometers, laboratory devices for accelerated aging. Figure 10 compares the total color change and reduction in gloss of cool roofing colored metals (CRCM) and standard colored metals exposed to accelerated fluorescent UV light. In almost all cases cool materials have performed better than standard materials.

## **Measurement of Energy Savings**

### ***Demonstration Homes***

We have set up a residential demonstration site in Fair Oaks, CA (near Sacramento) consisting of two pairs of single-family, detached houses roofed with metal and concrete tile. We are planning for another two pairs of houses to demonstrate asphalt shingles. The demonstration pairs each include one building roofed with a cool-pigmented product and a second building roofed with a conventionally (warmer) pigmented product of nearly the same color. The paired homes are adjacent, and share the same floor plan, roof orientation, and level of blown ceiling insulation of 3.37 m<sup>2</sup>K/W (R-19 insulation). Each home will be monitored through at least summer 2006.

Solar reflectance and thermal emittance are measured twice a year. Temperatures at the roof surface, on the underside of the roof deck, in the mid-attic air, at the top of the insulation, on the interior ceiling's sheet rock surface, and inside the building are logged continuously by a data acquisition system. Relative humidity in the attic air and the residence are also measured. Heat flux transducers are embedded in the sloped roofs and the attic floor to measure the roof heat flows and the building heat leakage. We have instrumented the building to measure the total house and air-conditioning power demands. A fully instrumented meteorological weather station is set up to collect the ambient dry bulb temperature, the relative humidity, the solar irradiance, and the wind speed and wind direction.

One of the Fair Oaks homes roofed with low-profile concrete tile was colored with a conventional chocolate brown coating (solar reflectance 0.10), while the other was colored with a matching cool chocolate brown with solar reflectance 0.41. The attic air temperature beneath the cool brown tile roof has been measured to be 3 to 5 K cooler than that below the conventional brown tile roof during a typical hot summer afternoon. The results for the pair of homes roofed with painted metal shakes are just as promising. There the attic air temperature beneath the cool brown metal shake roof (solar reflectance 0.31) was measured to be 5 to 7 K cooler than that below the conventional brown metal shake roof.

The application of cool colored coatings is solely responsible for these reductions in attic temperature. The use of these cool colored coatings also decreased the total daytime heat influx (solar hours 8AM – 5PM) through the south-facing metal shake roof by 31% (Figure 11).





(a)



(b)



(c)



(d)



(e)



(f)



(g)



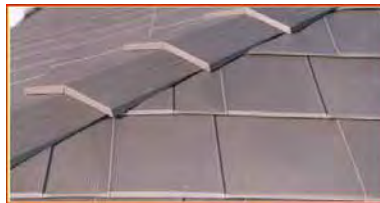
(h)



(i)



(j)



(k)



(l)

Figure 9. Simulated roofing products made from metal: (a) Advanta Shingles; (b) Bermuda Shakes; (c) Castle Top; (d) Dutch Seam Panel; (e) Granutiles; (f) Perma Shakes; (g) Scan Roof Tile; (h) Snap Seam Tile; (i) Techo Tile; (j) Verona Tile; (k) Oxford Shingles; and (l) Timbercreek Shakes. Products a-j are manufactured by ATAS International, Inc., while products k and l are manufactured by Classic Products, Inc. (Photos courtesy of ATAS International and Classic Products)

## ***Estimates of Energy and Peak Demand Savings***

To estimate the effect of cool-colored roofing materials, we calculated the annual cooling energy use of a prototypical house for most cooling dominant cities around the world. We used a simplified model that correlates the cool energy savings to annual cooling degree days (base

18°C) (CDD18<sup>\*</sup>). The model is developed by regression of simulated cooling energy use against CDD18. We performed parametric analysis and simulated the cooling- and heating-energy use of a prototypical house with varying level of roof insulation (R-0, R-1, R-3, R-5, R-7, R-11, R-19, R-30, R-38, and R-49) and roof reflectance (0.05, 0.1, 0.2, 0.4, 0.6, and 0.8) in more than 250 climate regions, using the DOE-2 building energy use simulation program. For each prototypical analysis, the parametric analysis led to 15,000 DOE-2 simulations. Then the resulting cooling- and heating-energy use was correlated to CDD18.

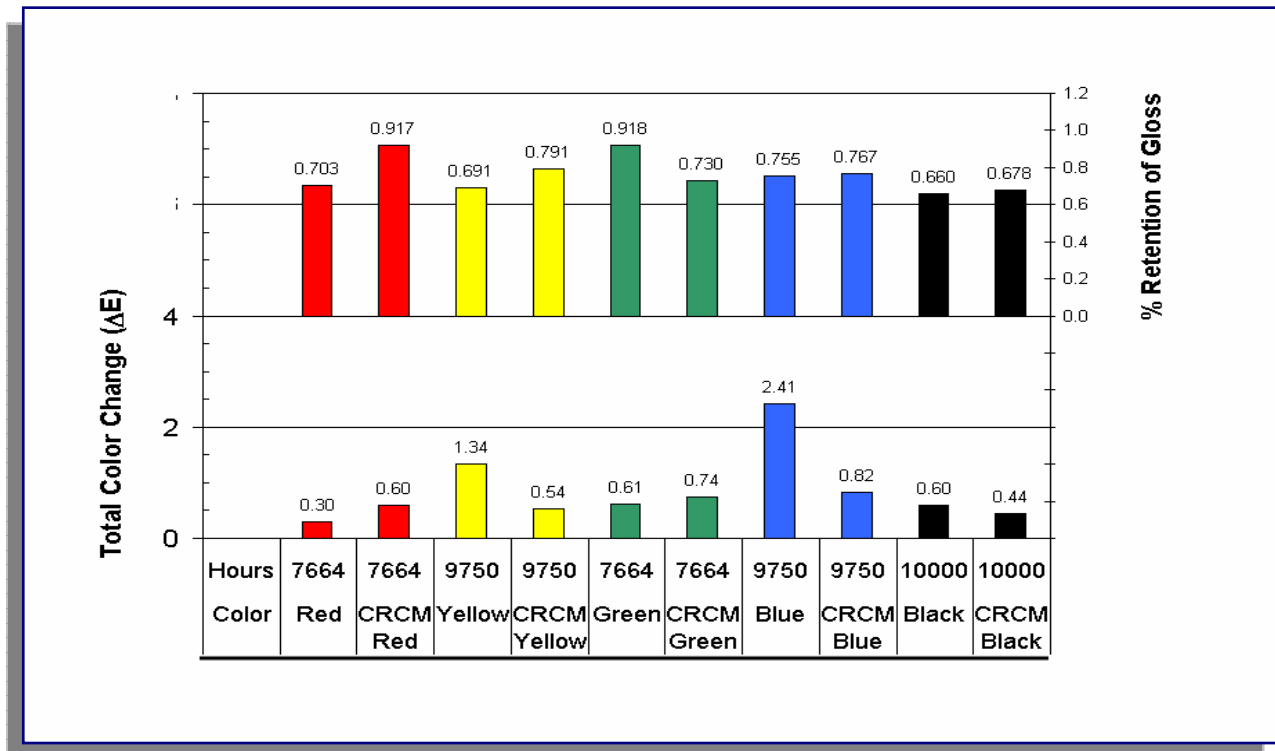


Figure 10. Fade resistance and gloss retention of painted metals (data courtesy of BASF)

The prototypical house used in this paper is assumed to have roofing insulation of 1.94 m<sup>2</sup>K/W (R-11 insulation). The coefficient of performance (COP) of the prototype house air conditioner is assumed to be 2.3. The estimates of savings are for an increase in roof solar reflectance from a typical dark roof of 0.1 to a cool-colored roof of 0.4. These calculations present the variation in energy savings in different climates around the world. The typical building may not necessarily be representative of the stock of house in all countries. Here, we only report of cooling energy savings; potential wintertime heating energy penalties are not accounted for in these results.

Table 3 shows CDD18 and potential cooling energy savings in kWh per year for a house with 100m<sup>2</sup> of roof area. The savings can be linearly adjusted for houses with larger or smaller roof areas. The savings range from approximately 250 kWh per year for mild climates to over

\* To calculate the cooling degree days for a particular day, find the day's average temperature by adding the day's high and low temperatures and dividing by two. If the number is below 18°C, there are no cooling degree days that day. If the number is more than 18°C, subtract 18°C from it to find the number of cooling degree days. The annual cooling degree days is simply the sum of all daily cooling degree days.

1000 kWh per year for very hot climates. For houses that are not air conditioned, cool-colored roofing materials offer comfort, typically at very reasonable costs.

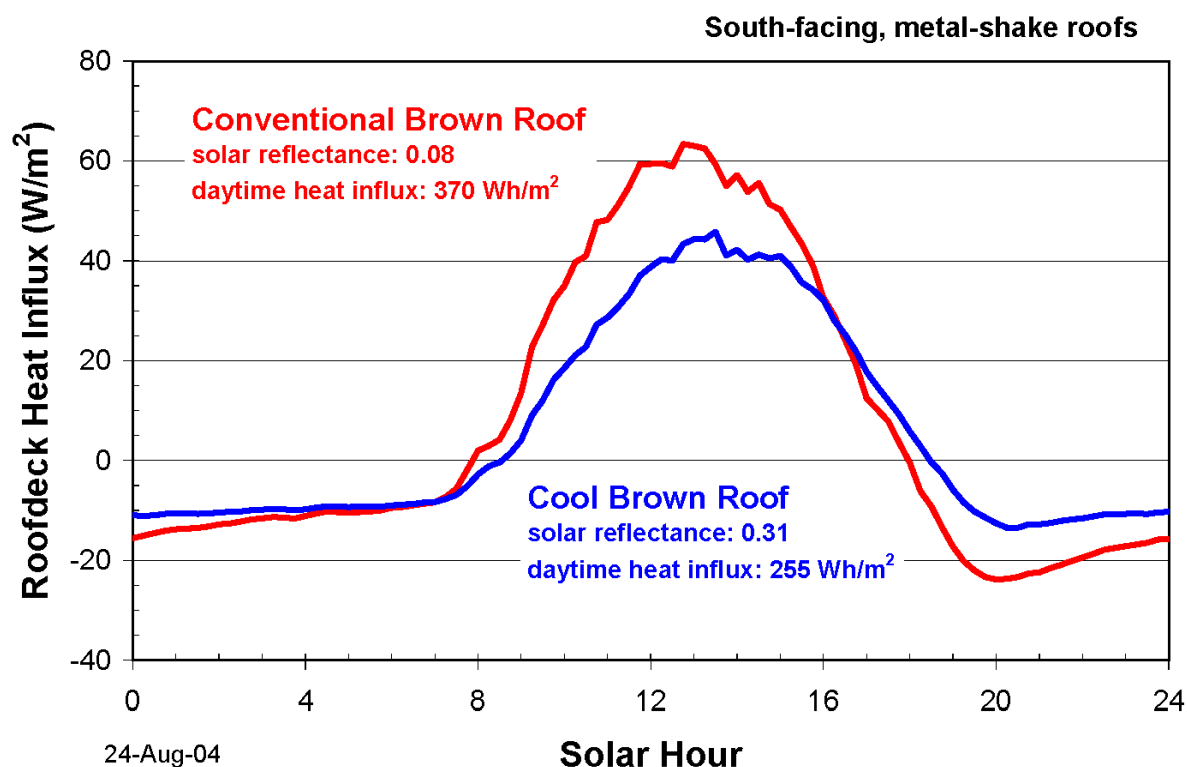


Figure 11. Heat flows through the roof decks of an adjacent pair of homes over the course of a hot summer day. The total daily heat influx through the cool brown metal shake roof (solar reflectance 0.31) between the solar hours of 8AM and 5PM is 31% lower than that through the conventional brown metal shake roof (solar reflectance 0.08).

## Conclusion

The results from this program indicate significant success in developing cool-colored materials for concrete tile, clay tile, metal roofs, and shingles. Since the inception of this program, the solar reflectance of commercially available colored roofing products has increased to 0.30–0.45 from 0.05–0.25 for all materials but shingles. To be cost effective, shingle manufacturers apply a very thin layer of pigments on the roofing granules. Use of a reflective undercoated (two-layered coating) has yielded several cost-effective cool-colored shingle products, with solar reflectances in excess of 0.25. Our ongoing collaboration with granule and shingle manufacturers may yield shingles with solar reflectances exceeding 0.3. The energy savings from the installation of cool roofs range from approximately 250 kWh per year for mild climates to over 1000 kWh per year for very hot climates. For houses that are not air conditioned, cool-colored roofing materials offer comfort, typically at very reasonable costs.

Country	City	CDD18	Savings	Country	City	CDD18	Savings
Albania	Tirana	715	312	Morocco	Rabat-Sale	606	280
Algeria	Alger/Dar-El-Beida	899	366	Mozambique	Maputo	2,085	715
Argentina	Buenos Aires/Ezeiza	693	305	Pakistan	Karachi Airport	3,136	1025
Australia	Sydney/K Smith	678	301	Panama	Howard AFB	3,638	1173
Bahamas	Nassau	2,511	841	Paraguay	Asuncion/Stroessner	2,218	755
Bermuda	St Georges/Kindley	1,802	632	Peru	Lima-Callao/Chavez	906	368
Bolivia	Trinidad	2,879	949	Philippines	Manila Airport	3,438	1114
Brazil	Belo Horizonte	1,702	603	Puerto Rico	San Juan/Isla Verde	3,369	1094
	Brasilia	1,353	500	Saudi Arabia	Dhahran	3,340	1085
	Rio de Janeiro	2,360	796		Medina	3,691	1189
	Sao Paulo	1,187	451		Riyadh	3,304	1075
Brunei	Brunei Airport	3,516	1137	Senegal	Dakar/Yoff	2,445	822
China	Beijing (Peking)	840	349	Singapore	Singapore/Changi	3,647	1176
	Shanghai/Hongqiao	1,129	434	Spain	Barcelona	533	258
Cuba	Havana/Casa Blanca	2,700	897		Madrid	886	362
Cyprus	Akrotiri	1,139	437	Syria	Damascus Airport	1,074	417
Egypt	Aswan	3,187	1040	Taiwan	Taipei	2,204	750
	Cairo	1,833	641	Tajikistan	Dusanbe	1,081	420
France	Nice	545	262	Tanzania	Dar es Salaam	2,922	962
Greece	Athenai/Hellenikon	1,030	405	Thailand	Bangkok	3,962	1269
Hong Kong	Royal Observatory	2,136	730		Chiang Mau	3,140	1026
India	Bombay/Santa Cruz	3,386	1099	Tunisia	Tunis/El Aouina	1,102	426
	Calcutta/Dum Dum	3,211	1047	Turkey	Istanbul/Yesilkoy	567	268
	New Delhi/Safdarjung	2,881	950	Turkmenistan	Ashkhabad	1,442	526
Indonesia	Djakarta/Halimperda	3,390	1100	United States	Phoenix	2,579	861
Italy	Palermo/Punta Raisi	1,058	413		Burbank/Hollywood	920	372
	Roma/Fiumicino	621	284		Sacramento	743	320
Jamaica	Kingston/Manley	3,656	1178		Washington/National	930	375
	Montego Bay/Sangster	3,112	1018		Miami	2,516	842
Japan	Kyoto	1,084	420		Atlanta	1,104	426
	Osaka	1,180	449		Honolulu, Oahu	2,651	882
	Tokyo	938	377		New Orleans/Moisant	1,627	580
Jordan	Amman	1,063	414		Memphis	1,324	491
Kenya	Nairobi Airport	566	268		Dallas-Ft Worth	1,519	549
Korea	Seoul	746	321	Uruguay	Montevideo/Carrasco	595	276
Libya	Tripoli/Idris	1,686	598	Venezuela	Caracas/Maiquetia	3,331	1083
Madagascar	Antananarivo/Ivato	701	308	Vietnam	Saigon (Ho Chi Minh)	3,745	1205
Malaysia	Kuala Lumpur	3,475	1125	Zimbabwe	Harare Airport	775	329
Mexico	Chihuahua	1,058	413				
	Mexico City	245	173				
	Acapulco/Alvarez	3,623	1169				

Table 3. Cooling degree days (base 18°C) and potential cooling energy savings (kWh per 100m<sup>2</sup> of roof area)

## Acknowledgement

This work was supported by the California Energy Commission (CEC) through its Public Interest Energy Research Program (PIER), and by the Assistant Secretary for Renewable Energy under Contract No. DE-AC03-76SF00098.



## References

- Akbari, H., P. Berdahl, R. Levinson, S. Wiel, A. Desjarlais, W. Miller, N. Jenkins, A. Rosenfeld, and C. Scruton. 2004. "Cool Colored Materials for Roofs." Proceedings of the 2004 ACEEE Summer Study on Energy Efficiency in Buildings, Vol. 1, p. 1, Pacific Grove, CA.
- Akbari, H., S. Konopacki, and M. Pomerantz. 1999. "Cooling energy savings potential of reflective roofs for residential and commercial buildings in the United States," *Energy*, **24**, 391-407.
- Akbari, H., S. Bretz, H. Taha, D. Kurn, and J. Hanford. 1997. "Peak Power and Cooling Energy Savings of High-albedo Roofs," *Energy and Buildings* — Special Issue on Urban Heat Islands and Cool Communities, **25**(2); 117–126.
- F.W. Dodge. 2003. Construction Outlook Forecast, F.W. Dodge Market Analysis Group, 24 Hartwell Avenue, Lexington, MA 02421. Telephone 800-591-4462.
- Konopacki, S. and H. Akbari. 2001. "Measured Energy Savings and Demand Reduction from a Reflective Roof Membrane on a Large Retail Store in Austin." Lawrence Berkeley National Laboratory Report No. LBNL-47149, Berkeley, CA.
- Konopacki, S., L. Gartland, H. Akbari, and L. Rainer. 1998. "Demonstration of Energy Savings of Cool Roofs." Lawrence Berkeley National Laboratory Report No. LBNL-40673, Berkeley, CA.
- Levinson, R., H. Akbari, S. Konopacki, and S. Bretz. 2005a. "Inclusion of cool roofs in nonresidential Title 24 prescriptive requirements," *Energy Policy*, **33** (2): 151-170.
- Levinson, R., P. Berdahl, and H. Akbari. 2005b. "Spectral Solar Optical Properties of Pigments Part I: Model for Deriving Scattering and Absorption Coefficients from Transmittance and Reflectance Measurements." *Solar Energy Materials & Solar Cells* (in press).
- . 2005c. "Spectral Solar Optical Properties of Pigments Part II: Survey of Common Colorants." *Solar Energy Materials & Solar Cells* (in press).
- Parker, D.S., J.K. Sonne, and J.R. Sherwin. 2002. "Comparative Evaluation of the Impact of Roofing Systems on Residential Cooling Energy Demand in Florida," Proceedings of the 2002 ACEEE Summer Study on Energy Efficiency in Buildings, Vol. 1, p. 219, Pacific Grove, CA.
- Rosenfeld, A.H., J.J. Romm, H. Akbari, and M. Pomerantz. 1998. "Cool Communities: Strategies for Heat Islands Mitigation and Smog Reduction," *Energy and Buildings*, **28**(1);51–62.
- Western Roofing. 2005. Online at <http://WesternRoofing.net> .

# COOL METAL ROOFING TESTED FOR ENERGY EFFICIENCY AND SUSTAINABILITY

William A. Miller, Ph.D., P.E.  
Oak Ridge National Laboratory

Andre Desjarlais  
Oak Ridge National Laboratory

Danny S. Parker  
Florida Solar Energy Center

Scott Kriner  
Metal Construction Association

## ABSTRACT

High solar reflectance and high infrared emittance roofs incur surface temperatures that are only about 5°F (3°C) warmer than the ambient air temperature, while a dark absorptive roof exceeds the ambient air temperature upwards of 75°F (40°C). In predominantly warm climates, the high solar reflectance and high infrared emittance roof drops the building's air conditioning load and reduces peak energy demands on the utility. In North American climates, being predominantly cold, a more moderate reflectance and a low (not high) emittance result in a warmer exterior roof temperature, which reduces heat loss from the building.

Temperature, heat flow, reflectance, and emittance field data have been catalogued for a full 3 years for 12 different painted and unpainted metal roofs exposed to weathering on an outdoor test facility at Oak Ridge National Laboratory (ORNL).

Habitat for Humanity homes were tested by the Florida Solar Energy Center (FSEC) for a full summer in Fort Myers, Florida. The houses were side-by-side, unoccupied and had different roofing systems designed to reduce the attic heat gain. Measurements showed that the white reflective roofs reduced cooling energy consumption by 18-26% and peak demand by 28-35%.

Results show that a judicious selection of the roof surface properties of reflectance and emittance represent the most significant energy and cost saving options available to homeowners and builders in predominantly hot climates.

## INTRODUCTION

Determining how weathering affects the solar reflectance and infrared emittance of metal roofs is of paramount importance for documenting the magnitude of the comfort cooling and heating energy load consumed by a building. The building's load, is directly related to the solar irradiance incident on the building; to the exterior temperature; to the level of roof, wall and foundation insulation; to the amount of fenestration; and to the building's tightness against unwanted air and moisture infiltration. The solar reflectance and infrared emittance and the airside convective currents strongly affect the envelope's exterior temperature. Our data show that in moderate to predominantly hot climates, an exterior roof surface with a high solar reflectance and high infrared emittance will reduce the exterior temperature and produce savings in comfort cooling. For predominantly heating-load climates, surfaces with moderate reflectance but low infrared emittance will save in comfort heating, although field data documenting the trade-off between reflectance and emittance are sparse.

Full building field tests in Florida and California using before-after experiments have examined the impact of reflective roofing on air conditioning (AC) energy use. In Florida tests measured air conditioning electrical savings averaged 19% (7.7 kWh/Day) (Parker et al., 1998). Even greater fractional savings have been reported for similar experiments in California (Akbari, et al., 1997).

---

### Author Note:

W. Miller, Specialist, Engineering Science and Technology Division, Oak Ridge National Laboratory, Oak Ridge, TN; A. Desjarlais, Program Leader, Building Envelope and Materials Research Program, Oak Ridge National Laboratory, Oak Ridge, TN; D. Parker, Principal Research Scientist, Florida Solar Energy Center, Cocoa, FL; S. Kriner, Technical Director, Metal Construction Association, Glenview, IL.

## Experimental Initiatives

The Buildings Technology Center (BTC) of ORNL has instrumented and field tested steep-slope- and low-slope-roof test sections of painted and unpainted metals for the past three years on a test building called the Envelope Systems Research Apparatus (ESRA). The low-slope assembly (Figure 1) consists of white-painted polyvinylidene fluoride (PVDF) galvanized steel<sup>1</sup>; off-white polyester; 55% Al-Zn coated steel<sup>2</sup> painted with a clear acrylic dichromate layer; unpainted galvanized steel; and unpainted 55% Al-Zn-coated steel. Five painted metal panels are being tested on the steep-slope assembly (Figure 1). Three panels of white-painted PVDF galvanized steel; three panels of 55% Al-Zn-coated steel painted with a clear acrylic dichromate layer; six panels of bronze-painted PVDF aluminum; and three panels of black-painted PVDF galvanized steel<sup>3</sup> were exposed to weather in east Tennessee. An asphalt-shingle roof section was included as the base of comparison. Salient features of the ESRA facility are fully discussed by Kriner and Miller (2001). Exposure sites were also setup to field test the identical painted and unpainted metal samples at Monroeville, PA, Fort Lauderdale, FL, Nova Scotia, Canada and Bethlehem, PA.

Florida Solar Energy Center (FSEC) instrumented seven side-by-side Habitat for Humanity (HFH) homes in Fort Myers, Florida with identical floor plans and orientation, but with different roofing systems designed to reduce attic heat gain (Figure 2). Six houses had R-19 ceiling insulation, and the seventh house had an unvented attic with insulation on the underside of the roof deck rather than the ceiling. All seven residences have a three bedroom, one bath floor plan and are of identical construction and exposure. Identical two-ton split system air conditioners with 5 kW strip heaters were installed in each of the seven homes. The houses underwent a series of tests in order to ensure that the construction and mechanical systems performed similarly. The following three-letter identification codes are used in the text, and the solar reflectance and infrared emittance of new material are also provided each roofing system :

Description of Test Roof on each HFH House	Label	Solar Reflectance	Infrared Emittance
• Dark gray fiberglass shingles	RGS	0.082	0.89
• White barrel-shaped tile	RWB	0.742	0.89
• White fiberglass shingle	RWS	0.240	0.91
• Flat white tile	RWF	0.773	0.89
• Terra cotta barrel-shaped tile	RTB	0.346	0.88
• White 5-vee metal	RWM	0.662	0.86
• Sealed attic with insulation on the roof plane	RSL	0.082	0.89

The salient features of the Habitat for Humanity homes and their respective roofs field tested in Fort Myers, Florida are fully described by Parker et al. (2001).

## DISCUSSION

### Reflectance and Emittance Surface Properties

The solar reflectance and the infrared emittance of a roof surface are important surface properties affecting the roof temperature, which in turn drives the heat flow through the roof. The reflectance and emittance are phenomenon occurring just a fraction of a micrometer within the irradiated surface. The solar reflectance gages the percentage of the sun's energy that a roof deflects off the building, and the infrared emittance is the percentage of infrared heat that a roof releases from the building. Reflectance and emittance are expressed as mathematical ratios. The reflectance ( $\rho$ ) determines the fraction of radiation incident from all directions that is diffusely reflected by the surface. The emittance ( $\epsilon$ ) describes how well the surface radiates energy away from itself as compared to a blackbody operating at the same roof temperature. The emittance of painted metal is about 0.90 while unpainted metal has values of about 0.10. The impact of emittance on roof temperature is just as important as that of reflectance.

Reflectivity measurements were made every 3 months on the ESRA's steep- and low-slope metal roofs; these measurements are shown in Figure 3. Each metal roof is described generically using an RxxEyy designation. Rxx states the solar reflectance of a new sample, 1.0 being a perfect reflector. Eyy defines the

---

<sup>1</sup> A zinc-coated steel sheet dipped in continuous coil form through a molten bath of zinc.

<sup>2</sup> This steel is exposed to a molten bath composed of 55% Al-43.5% Zn -1.5% Si at a temperature of 1100°F (593°C). The coating is solidified rapidly to enhance both the microstructure and the corrosion resistance.

<sup>3</sup> Black-painted polyvinylidene fluoride (PVDF) laminated with amorphous photovoltaic cells.

infrared emittance of the new sample, 1.0 being blackbody radiation. For example, the asphalt-shingle roof is labeled R09E91 in Figure 3. Its freshly manufactured surface properties are therefore 0.09-reflectance and 0.91-emittance. Kriner and Miller (2001) identify the RxxEyy designations for the different painted and unpainted test metals tested at ORNL.

After 3½ years of exposure, the white and bronze painted PVDF metal roofs, R64E83 and R07E87 respectively, have lost less than 5% of their original reflectance. The coated steel painted with a clear acrylic dichromate layer, R64E08, shows only a 12% loss in reflectance. In comparison the asphalt shingle roof, R09E91, increased a percentage point in reflectance after the 3½ years of exposure (Figure 3). The reflectance comparison is very important, because both R64E83 and R64E08 roofs reflected about 50% more solar energy away from these test roofs than did the asphalt shingle roof. Even more promising is the observed durability of the surface of the painted metals; reflectance remained fairly level. Less heat is therefore absorbed by the “cool” painted metal roofs and the building load and the peak utility load are reduced as compared to darker more absorptive roofs (i.e., R09E91).

Testing conducted at the roof slopes of 4-in of rise per 12-in of run (i.e., Steep Slope Roof [SSR] in Figure 3) and at ¼-in of rise per 12-in of run (i.e., Low Slope Roof [LSR] in Figure 3) further show that the slope of the roof has little effect on the loss of reflectance for the painted metal roofing having the PVDF finish. The painted metal appears to have excellent corrosion resistance. Their surface opacity have limited any photochemical degradation caused by ultraviolet light present in sunlight over the 3-years of testing. All painted metal roofs have maintained their original manufactured appearance. After 3½ years of exposure, rains with a measured pH of 4.3 in East Tennessee (National Atmospheric Deposition Program) have not etched the metal finish. ORNL scientists detected evidence of biological growth on some of the test roofs (Miller et al. 2002); however, the PVDF surface finish does not appear to allow the growth to attach itself and atmospheric pollution is washed off by rain.

Most dramatic are the trends observed in the solar reflectance and the infrared emittance of the painted metal roofs tested at different exposure sites across the country. Similar reflectance was measured in the hot, moist climate of Florida as compared to the predominantly cold climate of Nova Scotia (Figure 4). The Environmental Protection Agency’s Energy Star® Program requires field testing at three different building sites; however, the results for painted metal show the reflectance to be very similar whether exposed in Florida, Nova Scotia or Pennsylvania. Also solar reflectance and infrared emittance measures collected from the test fence exposure sites in Florida, Nova Scotia, Pennsylvania and also at Oak Ridge (Figure 4) are very similar to the reflectance and emittance measures recorded for the test roofs exposed on the ESRA in Oak Ridge (Figure 3). For this 3½ year time limited study, the changes in solar reflectance and infrared emittance of the painted PVDF metals is independent of climate! The results show that fence exposure data are a viable alternative for certifying the painted PVDF metal roofs as Energy Star compliant, because they yielded very similar trends as the identical roofs exposed on the ESRA.

The emittance of the painted metal roofs did not change much after 3½ years of weathering. In fact, the data in Figure 4 shows that the emittance increased slightly over time. The coated steel painted with a clear acrylic dichromate layer, R64E08, has a much lower emittance than the white PVDF (R64E83) roof. Note however that the emittance of several of the freshly manufactured coated steel samples painted with the clear acrylic dichromate layer varied from a low of 0.08 to a high of 0.20, probably because of the coating. Emittance trends of the low-slope coated and unpainted steel increased while those of the painted metal remained relatively flat, Kriner and Miller (2001).

### **Thermal Performance of Painted Metal Roofing at ORNL**

Increasing the solar reflectance or infrared emittance of a roof will reduce the exterior temperature, which in turn results in reduced building load. Solar reflectance effects naturally occur during the sunlight hours, while the effects of emittance occur continuously as long as there is a temperature difference between the metal and the radiant sky<sup>4</sup>.

Temperature data for metal roof surfaces on the steep-slope assembly of the ESRA are shown in Figure 5. These data are for a week of summer and winter weather having clear skies. Note that each label on the abscissa in Figure 5 is for midnight. The maximum daily ambient air temperature ranged from about 85°F to 95°F (29°C to 36°C) over the week in August. In February, the daily maximum air temperature ranged from 40°F to 60°F (4°C to 16°C). Peak air temperature usually occurs at about 4 P.M. with the peak roof temperature occurring slightly earlier at about 2 P.M.

The summer roof temperature for the R07E87, R26E90, and R09E91 (asphalt-shingle) sections all exceeded 160°F (71°C) and on some days reached a peak temperature of 165°F (74°C). The more reflective

---

<sup>4</sup> Measures of the global infrared irradiance made by the BTC’s field pyrgeometer used to calculate the radiant sky temperature from the equation for blackbody radiation:  $q_{IR} = \sigma T_{sky}^4$ .

R64E83 and R64E08 test sections had peak temperatures of about 115°F and 135°F (46°C to 57°C), respectively. The lower temperatures in turn imply less heat transmission into the building. On Aug 11, 2000, however, the R64E83 roof emittance was 0.826 as compared to 0.176 for the R64E08 test roof. Therefore, the 20°F (11°C) difference in roof temperature for the white PVDF versus the steel with clear acrylic layer is driven predominantly by the effect of emittance. The effect is even better depicted for the February data (Figure 5). During the evening hours, the lower emittance test roof (R64E08) maintains a temperature that exceeds the dew point temperature of the ambient air. Therefore, during the evening hours, less heat leaks to the outdoor ambient from the less emissive of the two metal roofs.

The temperature data of Figure 5 for the painted metals roofs were cast in terms of the average roof temperature averaged over the sunlight hours between 6 A.M. and 6 P.M. The averaged data were then fit using the solar reflectance and infrared emittance as independent variables, and the regression fits to these averaged roof temperature data are shown in Figure 6. Fixing the reflectance and decreasing the emittance causes the roof temperature to increase during August exposure. The hotter roof temperature in turn increases the heat entering the roof, which reveals why a low emittance is not thermally efficient on a hot summer day. For the August data one can see that a high solar reflectance and a high infrared emittance yields the coolest roof surface (Figure 6). The August data also reveals the interdependence of the infrared emittance and solar reflectance on roof heat flow. The lower the solar reflectance the greater is the effect of the infrared emittance on the roof temperature. Conversely the lower the infrared emittance the greater is the effect of the solar reflectance.

However, the effects of the infrared emittance observed in February are not as strong as those observed for the August data. Decreasing the infrared emittance caused less than a 5°F (3°C) increase in the average roof temperature; its effect is relatively flat in the winter. Decreasing the reflectance from 0.60 to 0.40 caused the average roof temperature to increase about 11°F (6°C). The results imply that the lowest heat loss from the roof occurs when the solar reflectance and the infrared emittance are low, and the effect of reflectance is more pronounced than is the effect of the emittance during this cold winter day.

Akbari and Konopacki (1998) performed DOE2.1e parametric simulations to estimate the impact of reflectance and emittance on the heating and cooling energy consumption for eleven metropolitan U.S. cities. Simulations were based on both old and new residential and commercial construction having respectively R-11 and R-19 levels of ceiling insulation. Nationwide, Akbari and Konopacki (1998) found that annually about \$0.75 billion can be saved by widespread implementation of light-colored roofs in cooling dominant climates.

Their simulations also showed that the infrared emittance effects both cooling and heating energy use. In cooling dominant climates, a low emittance roof yields a higher roof temperature and in turn increases the cooling load imposed on the building. Akbari and Konopacki (1998) simulations showed that changing the infrared emittance from 0.90 (typical emittance of most nonmetallic surfaces) to 0.25 (emittance of a shiny metallic surface) caused a 10% increase in the annual utility bill. However, in cold climates, a low emittance roof adds resistance to the passage of heat leaving the roof, which results in savings in heating energy. Akbari and Konopacki (1998) showed that in very cold climates with little or no summertime cooling, the heating energy savings resulting from decreasing the roof emittance almost reached 3% of the building's annual energy consumption.

Therefore, the design of a metal roof should focus on the both the solar reflectance and infrared emittance of the surface. High solar reflectance and high infrared emittance yield significant thermal benefits in predominantly cooling climates, while a modest solar reflectance and low infrared emittance produce modest thermal performance gains in predominantly heating load climates. During winter exposure, moisture problems with icings and ice dams may possibly be reduced by a low emittance roof because the lower emittance retains heat and has an exterior temperature during the evening hours that may exceed the dew point temperature of the outdoor air (see Figure 5 for R64E83 and R64E08 during the hours around midnight).

### **Thermal Performance of Painted Metal Roofing at FSEC**

While previous research efforts have investigated the thermal performance of various roofing systems, this particular study conducted by the FSEC and the Florida Power and Light Company represents the first time an attempt has been made to quantify roofing influence on cooling performance on identical, unoccupied, side-by-side residences. The project consisted of seven, single-family residential homes located in Fort Myers, Florida. The focus of the study was to investigate how various roofing systems impact air conditioning electrical demand. The houses underwent a series of tests in order to ensure that the construction and mechanical systems performed similarly. Details are not described here but can be found in the works by Parker, Sonne and Sherwin (2002).

The relative performance of the seven Habitat for Humanity (HFH) homes was evaluated for one month in the summer of 2000 under unoccupied and carefully controlled conditions. Table 1 summarizes the measured attic temperatures, cooling loads and savings for the seven homes over the unoccupied monitoring period; the data are ranked in descending order of total daily energy consumption. The average interior air temperature

near the thermostat in all homes was within 1°F of each other. However, because of the large influence of the thermostat temperature, we adjusted the monitored cooling results in Table 1 to account for set point differences among houses, (Parker et al. 2001).

Not surprisingly, the control home (RGS) has the highest consumption (17.0 kWh/day). The home with the terra cotta barrel tile (RTB) has a slightly lower use (16.0 kWh/day) for a 7.7% cooling energy reduction. Next is the home with the white shingles (15.3 kWh/day) – an 10.6% reduction. The sealed attic (RSL) comes in with a 7.8% cooling energy reduction (14.7 kWh/day). The true white roofing types (> 60% reflectance) had the lowest energy use. Both the white barrel (RWB) and white flat tile (RWF) roofs averaged a consumption of 13.3 kWh/day for respectively a 18.5% and 21.5% cooling energy reduction. The white metal roof (RWM) showed the largest impact with a 12.0 kWh/day July consumption, yielding a 24% reduction in cooling energy consumption.

**TABLE 1. Cooling Performance\* During Unoccupied Period: July 8<sup>th</sup> – 31<sup>st</sup>, 2000**

Site	Total kWh/day	Savings kWh/day	Thermo-stat (F)	Thermo-stat (C)	Mean Attic (F)	Mean Attic (C)	Max Attic (F)	Max Attic (C)	Temp. Adjust. %	Field EER	Final Saving %
RGS	17.0	0.00	77.2	25.11	90.8	32.7	135.6	57.5	0.0	8.30	0.0
RTB	16.0	1.01	77.0	25.0	87.2	30.7	110.5	43.6	-1.6	8.12	7.7
RWS	15.3	1.74	77.0	25.0	88.0	31.1	123.5	50.8	-1.2	9.06	10.6
RSL	14.7	2.30	77.7	25.4	79.0	26.1	87.5	30.8	5.4	8.52	7.8
RWB	13.3	3.71	77.4	25.2	82.7	28.2	95.6	35.3	2.8	8.49	18.5
RWF	13.2	3.83	77.4	25.2	82.2	27.9	93.3	34.1	2.1	7.92	21.5
RWM	12.0	5.00	77.6	25.3	82.9	28.3	100.7	38.2	4.9	8.42	24.0
* Final savings are corrected for differences in interior temperature and AC performance among houses.											

It is noteworthy that the average July outdoor ambient air temperature during the monitoring period (82.6°F [28.1°C]) was very similar to the 30-year average for Fort Myers (82°F [27.7°C]). Thus, the current data are representative of typical South Florida weather conditions. Relative to the standard control home, the data show two distinct groups in terms of performance:

- Terra Cotta tile, white shingle and sealed attic constructions produced approximately an 8-11% cooling energy reduction
- Reflective white roofing yielded a 19-24% reduction in the consumed cooling energy.

White flat tile performed slightly better than the white barrel due to its greater solar reflectance. The better performance of white metal is believed due to the effect of thermal mass. The metal roof incurred lower nighttime and early morning attic temperatures than did the tile or shingles, leading to lower nighttime cooling demand.

### Peak Day Performance

July 26<sup>th</sup> was one of the hottest and brightest days in the data collection period and was used to view the effects of maximum solar irradiance on the candidate roofing systems and to also evaluate peak influences on utility demand (Table 2). The average solar irradiance was 371 W/m<sup>2</sup> and the maximum outdoor ambient air temperature was 93.0°F (33.8°C).

The roof decking temperature (Figure 7) and subsequently the surface temperature were highest for the sealed attic construction (RSL) since the insulation under the decking forced much of the collected solar heat to migrate back out through the shingles. The sealed attic construction experienced measured deck temperatures that were 20°F (11.1°C) higher each sunny day than the control house. The white roofing systems (RWM, RWF and RWB) experienced peak deck temperatures approximately 40°F (22°C) cooler than the darker shingles on the control house (RGS in Figure 7). The terra cotta barrel tile was about 29°F (16°C) cooler on this July 26<sup>th</sup> day of peak solar irradiance.

The measured mid attic air temperatures above the ceiling insulation further revealed the impact of the white reflective roofs with max attic temperatures about 35 to 40 °F cooler than the control home (RGS). As expected, the home with the sealed attic had the lowest attic temperatures reaching a maximum of 87.5°F (30.8°C) compared with the 77°F (25°C) being maintained inside. However, the sealed attic case has no

insulation on the ceiling floor with only studs and sheet rock. Thus, from a cooling loads perspective, the low attic temperature with this construction is deceptive. Since ½ inch sheet rock has a thermal resistance  $R \leq 1$ , a significant level of heat transfer takes place across the uninsulated ceiling. While this construction method reduced attic air temperatures, it did not reduce ceiling heat transfer as well as other options. Ceiling heat fluxes are actually higher. In this case, the ceiling and duct system is unintentionally cooling the attic space, which can lead to the false impression that roof/attic loads are lower.

These data show that during periods of high solar irradiance the performance of the sealed attic case (RSL) suffers significantly. The tile and white shingle roofs did better at controlling demand than did the sealed attic on this very hot day. However, the white metal roof performed best showing peak savings of about 35% over the RGS control.

**TABLE 2.**  
**Summer Peak Day Cooling Performance: July 26<sup>th</sup>, 2000**

Site	Cooling Energy	Savings		Peak Period*		
		KWh	Percent	Demand (kW)	Savings (KW)	Percent
RGS	18.5 kWh		----	1.631	0.000	----
RTB	17.2 kWh	1.3	7%	1.570	0.061	3.7%
RSL	16.5 kWh	2.0	11%	1.626	0.005	0.3%
RWS	16.5 kWh	2.0	11%	1.439	0.192	11.8%
RWF	14.2 kWh	4.3	23%	1.019	0.612	37.5%
RWB	13.4 kWh	5.1	28%	1.073	0.558	34.2%
RWM	12.4 kWh	6.1	33%	0.984	0.647	39.7%
* Peak utility load occurred from 4 to 6 PM						

## CONCLUSIONS

The painted metal roofs have maintained their reflective surface; drops in reflectance are only about 5% after 3½ years of exposure. They appear to have an excellent corrosion-resistant surface whose opacity limits photochemical degradation caused by ultraviolet light present in sunlight. After 3½ years of exposure, rain has not etched the metal finish, and there is no evidence of any effects due to biological growth on the test roofs. Drops in solar reflectance are due more to airborne pollution than to any effect of the sun. Therefore, as roof slope increases, the washing action of precipitation increases, which helps to refresh the reflectance.

Exposure data for the more reflective painted metal roofs show the roofs qualify for the Energy Star® label for both steep-slope and low-slope roofing. In low-slope applications, the initial reflectance are borderline; however, the painted PVDF metal roofs maintain their reflectance above 0.5 after the required 3 years of exposure.

The design of a metal roof for predominantly heating-load application should focus first on the level of roof insulation, secondly on the surface reflectance and finally on the emittance of the surface. A moderate solar reflectance with a low infrared emittance showed the least heat leakage from the test roofs during the winter. In predominantly cooling-load climates, the high solar reflectance and high infrared emittance of white-painted metal roofs yielded the best thermal performance. Here, design should focus on increasing both the emittance and reflectance to decrease the exterior roof temperature, which in turn decreases the heat leakage into the building.

The FSEC field study demonstrated that the roof and attic exert a powerful influence on the cooling energy used in the seven side-by-side Habitat for Humanity homes tested in South Florida. Each of the examined alternative roofing systems were found to be thermally superior to standard dark shingles, both in providing lower attic temperatures and lower AC energy use. The sealed attic construction provided modest savings to cooling energy, but no real peak reduction due to its sensitivity to periods with high solar irradiance. The HFH field study points to the need for reflective roofing materials or lightcolored tile roofing for good energy performance with sealed attics.

The HFH project revealed essentially two classes of performance for the 1,144 square foot homes. Analysis showed the white highly reflective roofing systems (RWF, RWB and RWM) provide annual cooling energy reductions of 600 to 1,100 kWh in South Florida (18-26%). Savings of terra cotta tile roofs are modest at 3-9% (100-300 kWh), while shingles provide savings of 3-5% (110-210 kWh). Sealed attic construction produced savings of 6-11% (220-400 kWh). The highly reflective roofing systems showed peak demand impacts of 28-35% (0.8-1.0 kW). White metal had the best cooling related performance. Its high conductivity coupled with nocturnal radiation resulted in lower nighttime and early morning attic temperatures that lead to a reduced cooling demand during evening hours.

## REFERENCES

- Akbari, H., S., Bretz, H. Taha, D. Kurn, and J. Hanford. 1997. "Peak Power and Cooling Energy Savings of High-albedo Roofs," *Energy and Buildings — Special Issue on Urban Heat Islands and Cool Communities*, 25(2);117-126.
- Akbari, H., Konopacki, S.J. 1998. "The Impact of Reflectivity and Emissivity of Roofs on Building Cooling and Heating Energy Use," in Thermal Performance of the Exterior Envelopes of Buildings, VII, proceedings of ASHRAE THERM VIII, Clearwater, FL., Dec. 1998.
- Miller, W. A., and Kriner, S. 2001. "The Thermal Performance of Painted and Unpainted Structural Standing Seam Metal Roofing Systems Exposed to One Year of Weathering," in Thermal Performance of the Exterior Envelopes of Buildings, VIII, proceedings of ASHRAE THERM VIII, Clearwater, FL., Dec. 2001.
- Miller, W.A., Cheng, M-D., Pfiffner, S., and Byars, N. 2002. "The Field Performance of High-Reflectance Single-Ply Membranes Exposed to Three Years of Weathering in Various U.S. Climates," Final Report to SPRI, Inc., Aug., 2002.
- Parker, D. S., Sherwin, J. R. 1998. "Comparative summer attic thermal performance of six roof constructions." *ASHRAE Trans.*, Vol. 104, pt. 2, 1084–1092.
- Parker, D.S., Sonne, J. K., Sherwin, J. R. 2002. "Comparative Evaluation of the Impact of Roofing Systems on Residential Cooling Energy Demand in Florida," in ACEEE Summer Study on Energy Efficiency in Buildings, proceedings of American Council for an Energy Efficient Economy, Asilomar Conference Center in Pacific Grove, CA., Aug. 2002.
- Parker, D.S., Sonne, J.K., Sherwin, J.R. and Moyer N. 2001. "Comparative Evaluation of the Impact of Roofing Systems on Residential Cooling Energy Demand in Florida," Final Report FSEC-CR-1220-00, prepared for the Florida Power and Light Company, May 2001.



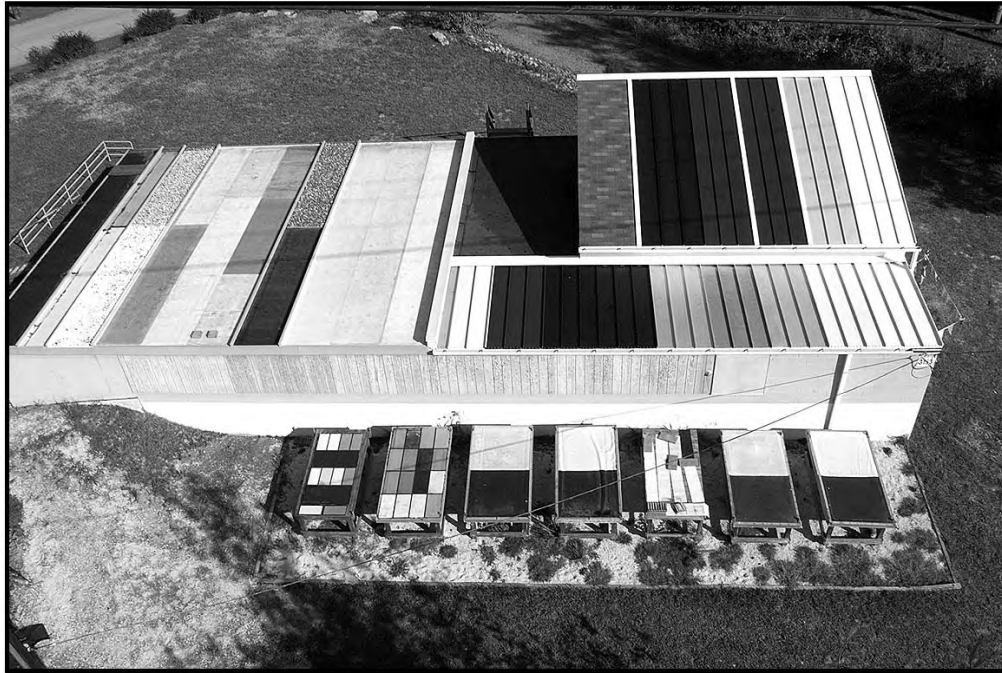


Figure 1. The Envelope Systems Research Apparatus used for testing painted and unpainted metal roofing.



Figure 2. Habitat for Humanity homes tested by the FSEC in Fort Myers, Florida.

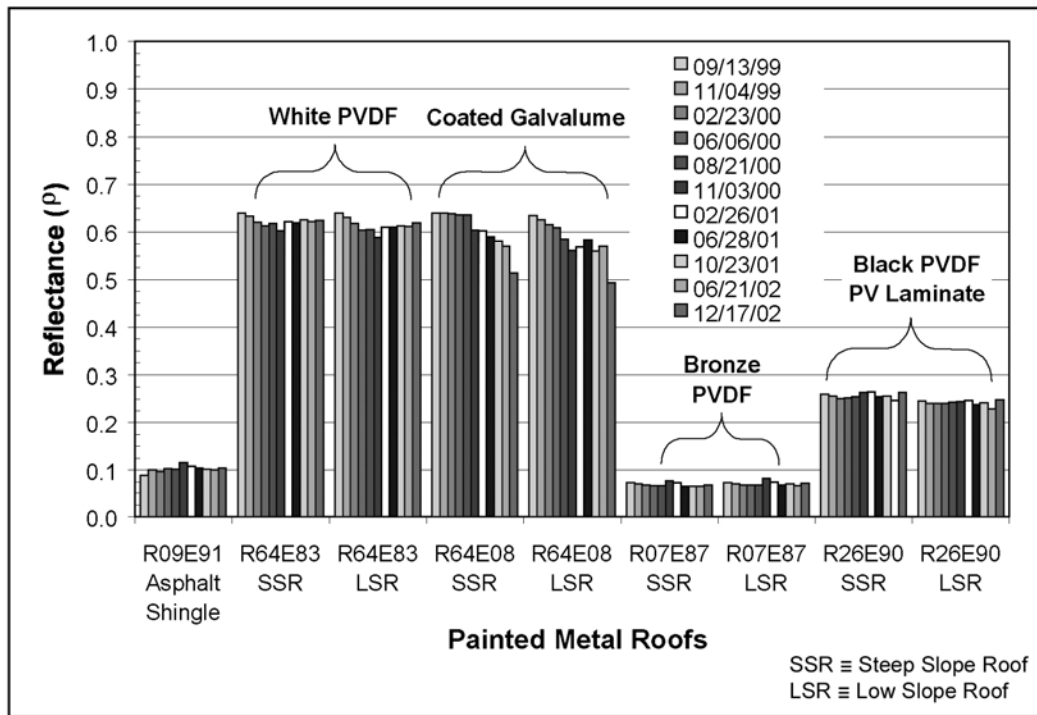


Figure 3. Solar reflectance of the painted metals exposed to weathering on the ESRA.

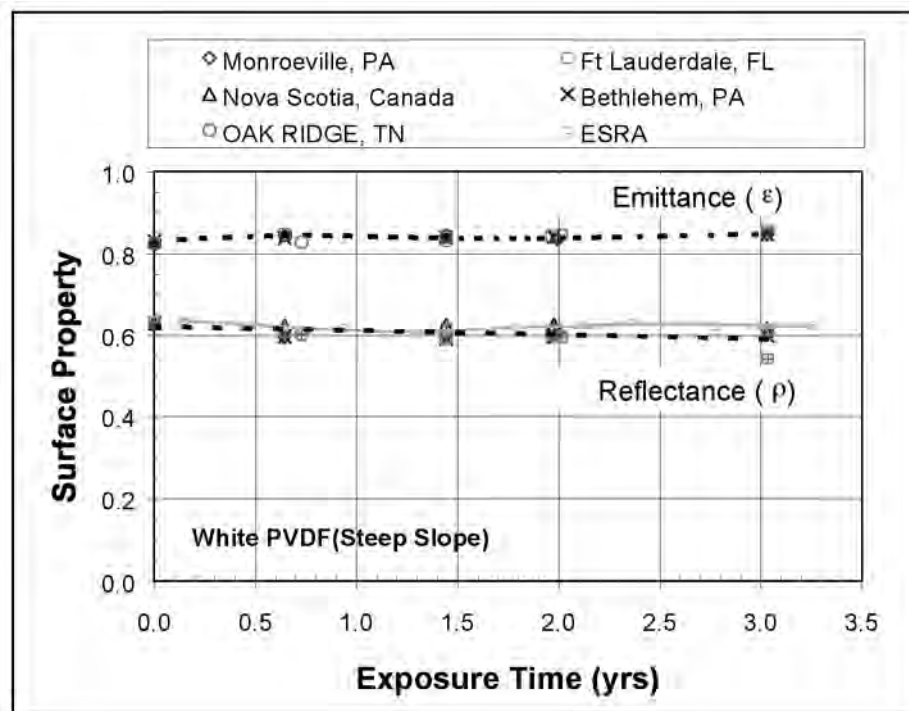


Figure 4. Solar reflectance and infrared emittance of white PVDF painted metal (R64E83).

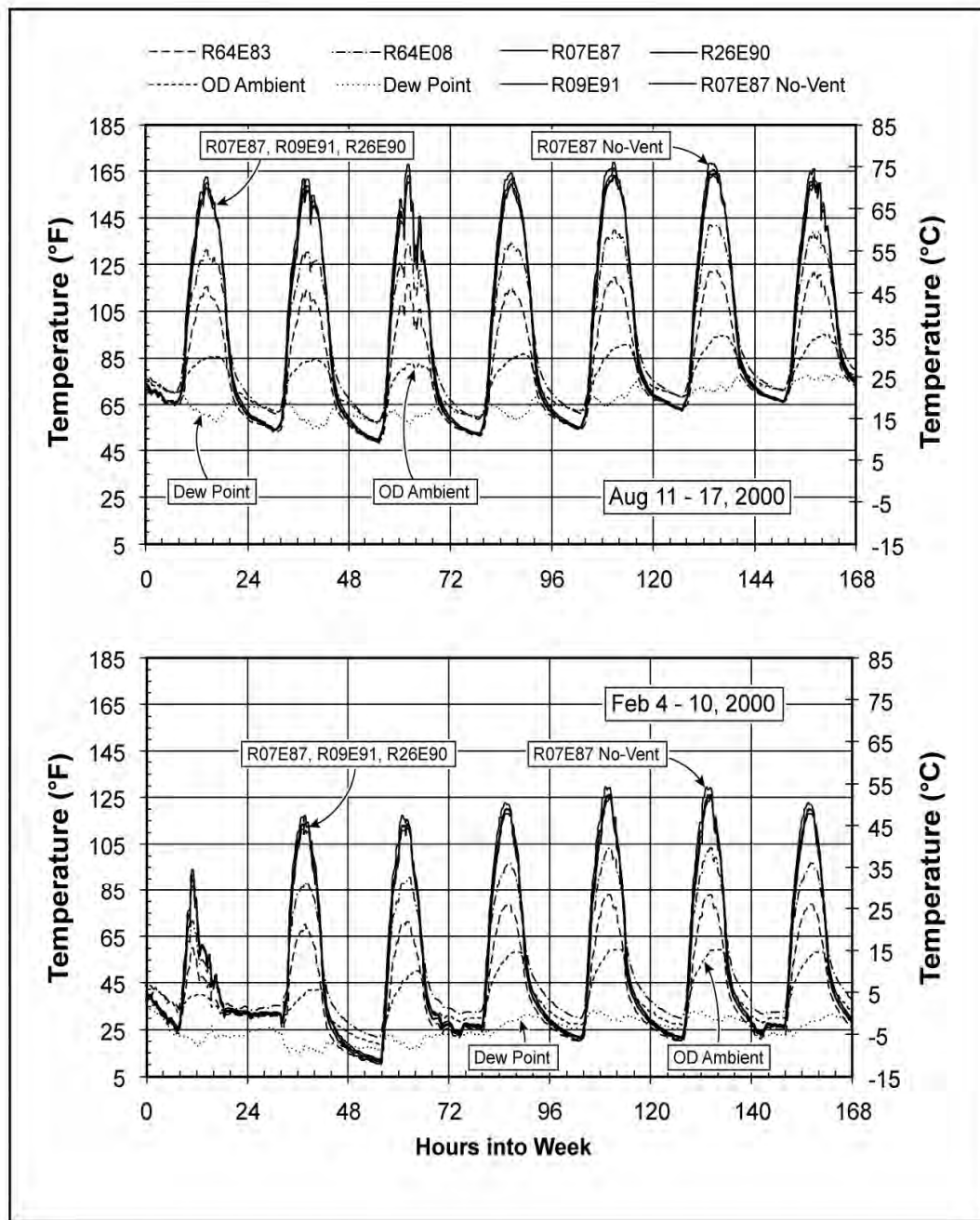


Figure 5. Field data collected for the steep-slope metal roof assembly for one week of summer and one week of winter data.

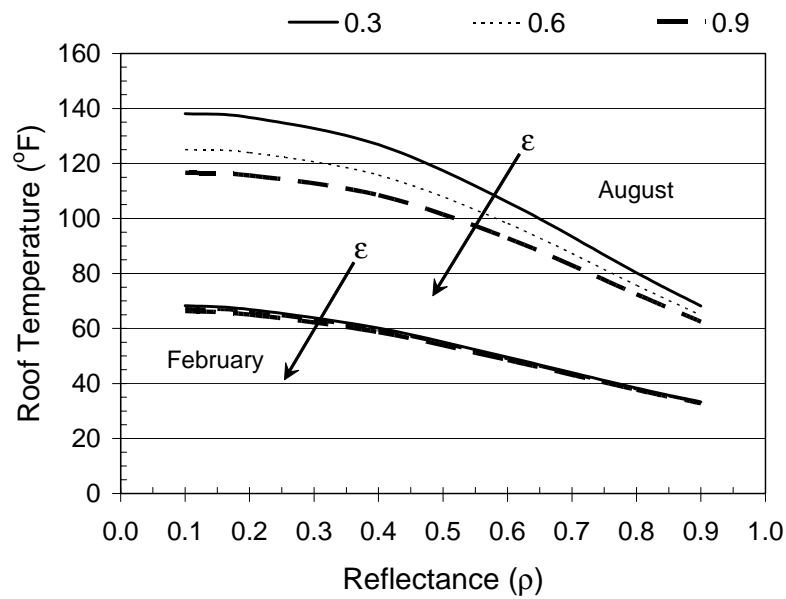


Figure 6. Roof temperature for painted metal roofs averaged over the sunlit hours.

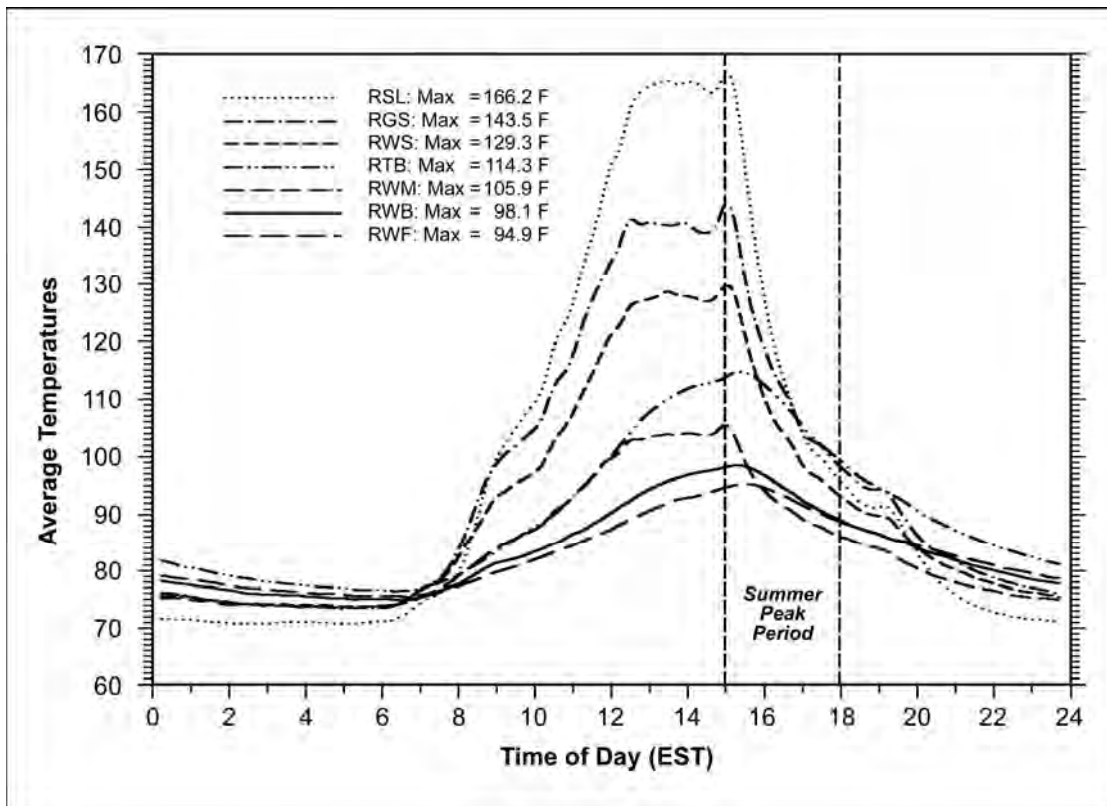


Figure 7. Deck temperatures measured on July 26, 2000.

# PVDF Coatings with Special IR Reflective Pigments

*William A. Miller,<sup>1</sup> Oak Ridge National Laboratory  
Kenneth T. Loye, FERRO Corporation  
André O. Desjarlais, Oak Ridge National Laboratory  
Robert P. Blonski, FERRO Corporation*

## ABSTRACT

Pigment colorant researchers have developed new complex inorganic color pigments (CICPs) that exhibit dark color in the visible spectrum and high reflectance in the near-infrared portion of the electromagnetic spectrum. CICPs can increase the infrared reflectance of building paints thereby dropping the surface temperatures of the roof and exterior walls. The lower temperatures in turn reduce the cooling-energy demand of the building. However, determining the effects of climate and solar exposure on the reflectance and the variability in color over time is of paramount importance for promoting the energy efficiency and for accelerating the market penetration of products using CICPs.

CICPs consisting of a mixture of infrared reflective pigments, chromic oxide ( $\text{Cr}_2\text{O}_3$ ) and ferric oxide ( $\text{Fe}_2\text{O}_3$ ) boosts the total hemispherical reflectance of a black polyvinylidene fluoride paint finish from 0.05 to 0.26. The increase in reflectance reduces the temperature of the painted surface, and as result xenon-arc exposure testing and two-years of field exposure testing show the CICPs have improved the fade resistance of polyvinylidene fluoride paints.

## Introduction

High-reflectance single-ply membranes, painted and unpainted metal, and spray-on roof coatings are reducing energy use in the commercial market as building contractors substitute these high-reflectance roofs for bitumen-based built-up roofing (BUR) and ethylene propylene diene monomer (EPDM). Since a high-reflectance low-slope roof cannot be seen from the ground, the roof's functionality is far more important than its looks. However, in steep-slope residential roofing the issues of appearance, cost, and then durability typically drive the selection of the roofing material because the homeowner wants the roof to complement the décor of the house while protecting the underlying residential structure for a long period of time at an affordable cost.

To homeowners, dark roofs simply look better than a highly reflective "white" roof. Yet the aesthetically pleasing dark roof can be made to reflect light like a "white" roof in the infrared portion of the solar energy spectrum. Researchers working with the Department of Defense developed new complex inorganic color pigments (CICPs) that exhibit dark color in the visible spectrum and high reflectance in the near-IR portion of the electromagnetic spectrum (Sliwinski, Pipoly & Blonski 2001).

---

<sup>1</sup>Dr. William A. Miller is a research engineer in the Buildings Technology Center of Oak Ridge National Laboratory (ORNL), Oak Ridge, Tennessee. Kenneth T. Loye is the Technical Manager of the Pigments Group at FERRO Corporation, Cleveland, Ohio. André O. Desjarlais is the manager of ORNL's Building Thermal Envelope Systems & Materials Program. Robert P. Blonski is a research chemist working in the Pigments Group at FERRO Corporation.

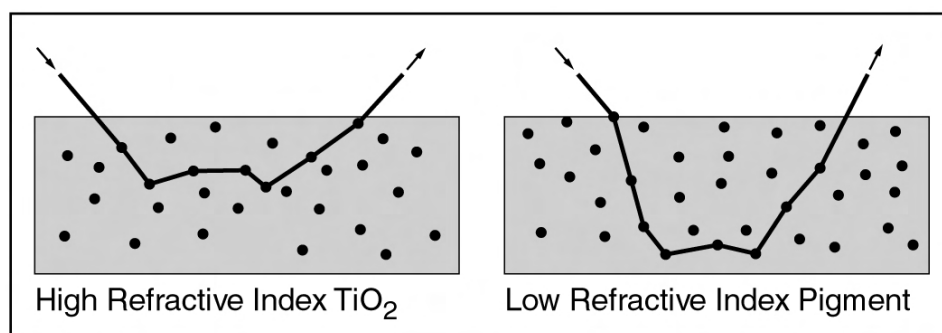
The opportunity exists for a significant impact on energy use in commercial buildings and residential housing, both in new construction and for re-roofing existing homes. The total sales volume for roofing and re-roofing is booming and nearly doubled between 1997 and 2000, from \$20 billion to \$36 billion (Good 2001). Of the sales volume in 2000, low-slope roofing accounted for 64% (\$21.7 billion), while steep-slope roofing comprised about 35.6% (\$12 billion) (Good 2001).

Our research estimates U.S. potential savings in excess of \$750 million per year in net annual energy bills (cooling-energy savings minus heating-energy penalties). These savings account for only the direct impact of cool roofs; savings would double once the indirect benefits (cooling of the ambient air) and smog reductions are included. The decrease in electric demand translates to a decrease of approximately 30.4 million tons in CO<sub>2</sub> emissions per year.

## Surface Properties Affecting Reflectance

Titanium dioxide (TiO<sub>2</sub>) is currently the most important white pigment used in the manufacture of paints and plastics. TiO<sub>2</sub> is chemically inert, insoluble, and very heat-resistant. It has been commercially processed from rutile since as early as 1941 (Du Pont Ti-Pure 1999). Rutile TiO<sub>2</sub> increases surface reflectance through refraction and diffraction of the light. As a light ray passes through a TiO<sub>2</sub> particle, the ray bends, or refracts, because light travels more slowly through the pigments than it does through the resin or binder. This occurs because TiO<sub>2</sub> has a much larger refractive index than the resin. This phenomenon is depicted in Figure 1 for two pigmented films. The film containing the pigment with higher refractive index bends the light more than does the film containing the lower refractive index pigment.

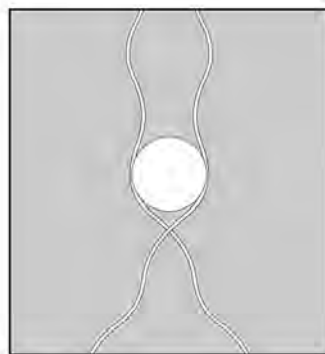
**Figure 1. Path of Light as It Penetrates Two Different Coatings, One Having Pigments with a Higher Refractive Index Than the Other**



The light travels a shorter path and does not penetrate as deeply into the film; therefore, less heat is absorbed. The reflectance of the surface increases because the surface opacity increases through refraction induced by the TiO<sub>2</sub> particles. In general, the greater the difference between the refractive index of the pigment and that of the resin or filler in which it is dispersed, the greater will be the light scattering and therefore the increase in surface reflectance, Martin and Pezzuto (1998).

Diffraction is another physical factor affecting a pigment's ability to scatter light. As a light ray passes by a TiO<sub>2</sub> particle, the ray bends, or diffracts, around the pigment (Fig. 2). Maximum diffraction occurs when the diameter of the pigment is slightly less than one-half the wavelength of the light to be scattered. Physical modifications of the size, the distribution, and the shape of pigment particles will therefore affect the light scattering. If particles are too large or too closely spaced, little diffraction occurs. Conversely, if the pigment particles are too small, the light will not "see" the particles. Commercially processed rutile TiO<sub>2</sub> has particle diameters ranging from about 200 to 300 nm and is highly reflective in the visible spectrum (yellow-green light at about 550 nm). However, as the wavelength of light increases, the reflectance of TiO<sub>2</sub> drops in the infrared spectrum especially for wavelengths beyond 1250 nm.

**Figure 2. Light Diffraction as a Light Ray Travels near a Pigment Particle**



## The “Optical” Properties of Pigments

Pigments are typically thought of in terms of their "color", that is, their reflectance spectrum in the 400 to 700 nm range. The performance of pigments, however, actually covers a much broader spectral region from the ultraviolet through the near infrared and beyond. A pigment interacts with electromagnetic radiation by either absorbing it, or scattering it as mathematically described by the Kubelka-Munk formalism. The equation relating the pigments absorption (K) and scattering (S) properties to the reflectance (ρ) of an infinitely thick sample is given by:

$$\frac{K}{S} = \frac{(1 - \rho)^2}{2\rho} \quad (1)$$

The pigment industry uses the Kubelka-Munk equation to parameterize the reflectance (ρ) of a pigment by the two wavelength dependent parameters, the pigments absorption coefficient (K) and its scattering coefficient (S), Billmeyer and Saltzman (2000). Laboratories and local paint and hardware stores custom match paints and coatings using Eq. 1 by color matching the mixture of pigments needed to match a target reflectance. The interaction of the absorption and scattering components of a pigment is of paramount importance to the response of the pigment to electromagnetic radiation, especially in wavelengths beyond the visible. And the engineering of pigment properties beyond the visible is well known to those involved with “radiation signature tailoring”, which is becoming increasingly important in both military and domestic applications.

## Scattering

The scattering characteristics of a pigment particle in a medium can be calculated using Mie Scattering Theory, Bohren and Huffman (1983). Figure 3

contains a curve of the scattering cross section of a  $\text{TiO}_2$  particle, index of refraction equal 2.7, versus particle size, in a medium of index of refraction of 1.5, calculated for a wavelength of 550 nm. The human eye sensitivity peaks at about 550 nm. According to this graph, the maximum scattering of a  $\text{TiO}_2$  particle for a wavelength of 550 nm occurs in a particle size range of about 200 to 300 nm, which is the particle size range of commercial white  $\text{TiO}_2$  pigments.  $\text{TiO}_2$  pigments in this size range scatter, that is, reflect, 550 nm electromagnetic radiation most efficiently and therefore yield optimum opacity at this wavelength. Particles of  $\text{TiO}_2$  below about 50 nm in size do not scatter 550 nm electromagnetic radiation at all; in fact, the particles are transparent.  $\text{TiO}_2$  pigment in the 50 nm particle size range is used in the topcoat of automobile finishes to increase the effective index of refraction of the topcoat making it look thicker.

**Figure 3. Mie Scattering Cross-section of  $\text{TiO}_2$ , having an index of refraction of 2.7, in a media of index 1.5 for wavelengths of a) 550 nm and b) 1500 nm. [1000 nm = 1  $\mu\text{m}$ ]**

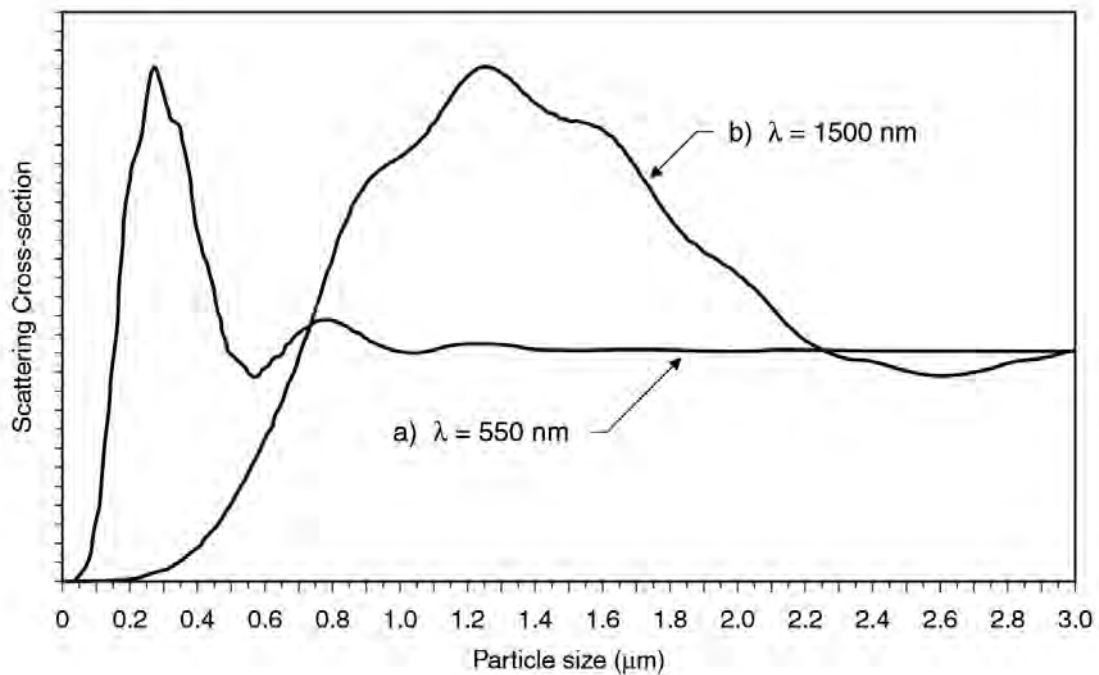


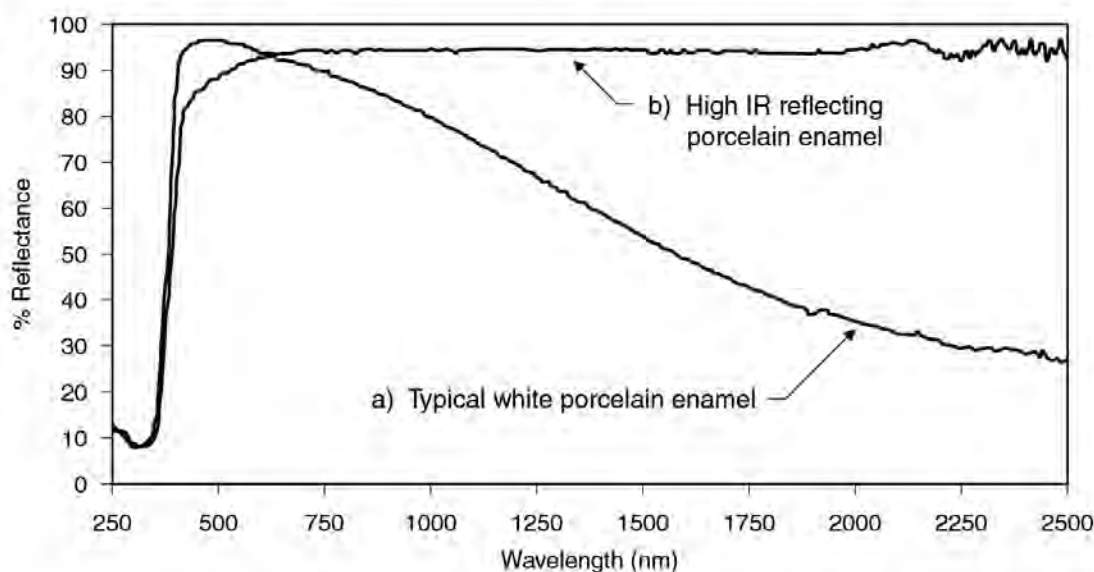
Figure 3 contains a second curve of the same scattering cross section calculation of a  $\text{TiO}_2$  particle at a wavelength of 1500 nm. For this wavelength the maximum scattering occurs at a particle size of about 1200 nm, and the particle becomes transparent at about 200 nm, that is, just about the size for maximum scattering of 550 nm electromagnetic radiation. The distribution of infrared radiation from a wood fire peaks at about 1500 nm, Berdahl (1998). If you wanted a coated surface that would reflect the infrared from a fire and protect the underlying surface, you would not use a standard white  $\text{TiO}_2$  pigment. Although this pigment is very white in the visible, it is effectively transparent to the infrared of a wood fire. Thus, whether a pigment particle scatters electromagnetic radiation at a given wavelength, or is transparent at that wavelength, depends primarily on its size.



## Absorption

The absorption of a pigment throughout the entire electromagnetic spectra is sensitive to the pigments chemical composition, to the valence state of its constituents, and to the arrangement of the atoms in the crystal structure of the pigment. Human eyes are sensitivity to electromagnetic radiation in the wavelength range from 400 to 700 nm, and the absorption of a pigment in this range gives it the “color” we see. As example, the “white color” property of  $\text{TiO}_2$ , used in porcelain enamel coatings for microwave ovens, is effectively “white” only in the visible spectrum (Fig. 4).

**Figure 4. Reflectance versus wavelength curves for a) a typical white porcelain enamel surface and b) a high infrared reflecting porcelain enamel surface.**



The first microwave ovens cooked food that was not as appealing as food cooked in a standard convection oven. A source of infrared radiation was needed to improve the browning of food and to quicken cooking time. The standard “white” porcelain enamel surface absorbs electromagnetic radiation for  $\lambda \geq 1000$  nm, that is, it will get hot (Fig. 4). Porcelain enamel is a glass coating that is manufactured by smelting titania and grinding the subsequent glass into a fine powder, known as a frit. Firing is done to melt the glass frit into a smooth layer. During the firing process, the  $\text{TiO}_2$  precipitates out of the enamel, giving the enamel its bright white color. The enamel contains iron contaminants, and if the valence charge of the iron ions is  $\text{Fe}^{2+}$  the enamel will strongly absorb infrared radiation (Fig. 4). To improve microwave cooking, researchers added an oxidizing agent to increase the valence of iron ions to  $\text{Fe}^{3+}$  or  $\text{Fe}^{4+}$ , which does not absorb infrared radiation, Faust and Evele (1999). Figure 4 contains the reflectance curve for an “infrared reflecting” porcelain enamel surface. The improved porcelain enamel coating is effectively “white” in the visible and also in the near infrared spectral regimes (Fig. 4). Therefore, chemistry can be used to alter the absorption and therefore the reflectance of a pigment. By blending metal oxides or oxide precursors and calcining them, the solids themselves become reactive.

Metal and oxygen ions in the solids rearrange to a form a new, more stable structure, termed a complex inorganic color pigment that is ideal for high-temperature coatings.

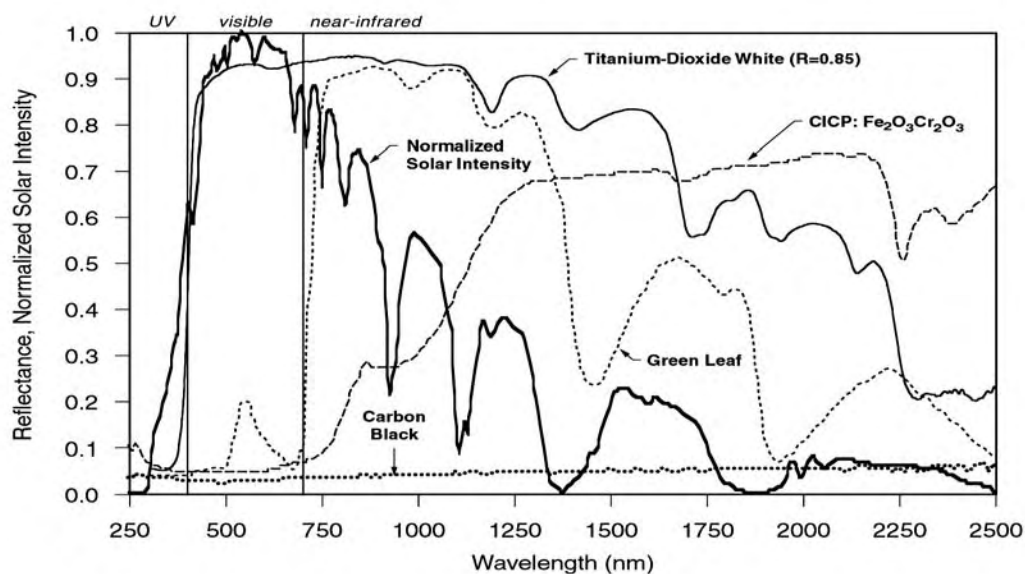
## Infrared Reflecting Complex Inorganic Color Pigments (CICPs)

The characteristics of CICPs being marketed as “infrared reflecting” are controlled over the range of wavelengths from 300 to 2500 nm. In order to control the optical properties of a pigment over this wide of a wavelength range requires great care in all aspects of the manufacturing process starting with the selection of raw materials and going all of the way through to the milling and finishing of the pigment, Sliwinski, Pipoly and Blonski (2001).

For years the vinyl siding industry has formulated different colors in the same polyvinyl chloride base by altering the content of  $\text{TiO}_2$  and black IR-reflective (IRR) paint pigments to produce “dark” siding that is “cool” in temperature (Ravinovitch and Summers 1984). Researchers discovered that a dark color is not necessarily dark in the infrared. Brady and Wake (1992) found that 1- $\mu\text{m}$  particles of  $\text{TiO}_2$  when combined with red iron, or ferric, oxide effectively scattered IR radiation at a wavelength of 2300 nm.

The new CICPs are used in paints for military camouflage to match the reflectance of background foliage in the visible and IR spectrum. At 750 nm the chlorophyll in foliage naturally boosts the reflectance of a plant leaf from 0.1 to about 0.9 (Fig. 5), which explains why a dark green leaf remains cool on a hot summer day.<sup>2</sup>

**Figure 5. Spectral Solar Reflectance of  $\text{TiO}_2$ , a Green Leaf, Standard Carbon Black and a Complex Inorganic Color Pigment Containing Infrared Reflective  $(\text{Fe,Cr})_2\text{O}_3$  Pigment (Normalized Solar Irradiance Shown for Reference)**



<sup>2</sup>Chlorophyll, the photosynthetic coloring material in plants, naturally reflects near-IR radiation.

CICPs, having been tailored for high IR reflectance similar to that of chlorophyll, are very suitable for roof applications where increased IR reflectance is desirable. CICPs consisting of a mixture of black IRR pigments, chromic oxide ( $\text{Cr}_2\text{O}_3$ ) and ferric oxide ( $\text{Fe}_2\text{O}_3$ ) boosts the total hemispherical reflectance of carbon black from 0.05 to 0.26 (see CIPC: $\text{Fe}_2\text{O}_3$ - $\text{Cr}_2\text{O}_3$  in Fig. 5). Typically, a black asphalt shingle or a black Kynar<sup>3</sup> metal roof has a reflectance of only about 0.05. The CICPs therefore boosts the reflectance by a factor of 5, and in the infrared spectrum CICPs boost the reflectance to almost 0.70 (Fig. 5).

CICPs are formed by calcinating blends of metal oxides or oxide precursors at temperatures over 1600°F (870°C). The calcination causes the metal and oxygen ions in the solids to rearrange in a new structure that is very heat-stable. The inherent heat stability of CICPs makes them ideal for high-temperature coatings in roofing applications. Because of their small particle size and high index of refraction, CICPs will effectively backscatter a significant amount of ultraviolet (UV) and IR light away from a surface.

## Thermal Performance of CICPs

CICPs offer excellent opportunities for improving the thermal performance of roofs. About 44% of the sun's total energy is visible to the eye (Fig. 5). Absorbing this 44% is what makes a black appear black. The absorbed light energy is however converted to heat energy and the temperature of the surface rises. Sunlight also emits another 51% of its energy in the invisible IR spectrum. Adding CICPs to roof materials will make the black roof absorb less light by reflecting near IR energy, which in turn results in a lower roof surface temperature.

Temperature measurements taken on a highly reflective roof show the surface as only about 5°F (3°C) warmer than the ambient air temperature, while a dark absorptive roof exceeds the ambient air temperature by more than 75°F (40°C). Lowering the exterior roof temperature will reduce the heat leakage into the building, which in turn, reduces the air conditioning load.

## Light-Color CICPs

The authors tested several IRR pigments against standard pigments using the ASTM D4803 test procedure (ASTM 1997a). This procedure has long been used by the vinyl siding industry to quantify the heat buildup properties of vinyl siding, even though it overstates the sample's properties in the near IR at the expense of visible portion of the spectrum (Ravinovitch and Summers 1984). Table 1 shows the temperatures for both CICPs and standard light-gray, mid-tone bronze, and dark-tone bronze colors when exposed to a flux of 484 Btu/(hr·ft<sup>2</sup>) [550 J/(hr·cm<sup>2</sup>)] emitted from an infrared heat lamp. These colors are very popular for low-slope roofing in commercial and academic applications where bronze Kynar<sup>®</sup> metal roofing is commonly used.

The colors containing CICPs show a significant drop in temperature as compared to the temperatures of standard light-gray, mid-tone bronze, and dark bronze colors. The temperature is 55°F (30.5°C) cooler for the light gray color if

---

<sup>3</sup>Kynar, the registered trademark for polyvinylidene fluoride (PVDF) paint finish, has excellent corrosion and abrasion resistance.

CICPs are contained in the pigment mixture. Similarly, a mid-tone bronze showed a 63°F (35°C) reduction in surface temperature. Even the dark-tone bronze had a measured 54°F (30°C) drop in temperature because the IRR pigments absorb less electromagnetic energy near the cutoff between the visible and infrared wavelengths. They have a more selective absorption band and reflect much of the infrared.

**Table 1. CICI Color Matches vs. Standard Pigmentation Exposed to ASTM D4803 Heat Lamp Protocol <sup>a</sup>**

Pigment	Pigment Constituents	Maximum Temperature	Temperature Difference (ΔT)
<b>Light gray</b>			
Standard	Carbon black 1.5% TiO <sub>2</sub> 96.8% Fe <sub>2</sub> O <sub>3</sub> 1.7%	202°F (94.4°C)	
CICP	IRR black 10% TiO <sub>2</sub> 90%	147°F (63.9°C)	55°F (30.5°C)
<b>Mid-tone bronze</b>			
Standard	Carbon black 11.8% TiO <sub>2</sub> 75.0% Fe <sub>2</sub> O <sub>3</sub> 13.2%	225°F (107.2°C)	
CICP	IRR black 50% TiO <sub>2</sub> 50%	162°F (72.2°C)	63°F (35°C)
<b>Dark-tone bronze</b>			
Standard	Carbon black 33% TiO <sub>2</sub> 29% Fe <sub>2</sub> O <sub>3</sub> 38%	220°F (104.4°C)	
CICP	IRR black 90% TiO <sub>2</sub> 10%	166°F (74.4°C)	54°F (30°C)

<sup>a</sup> A flux of 484 Btu/(hr·ft<sup>2</sup>) [550 J/(hr·cm<sup>2</sup>)] emitted from an infrared heat lamp.

## Dark-Color CICIPs

We also exposed dark colors containing the IRR pigments to the infrared heat lamp. Again, the increased reflectance in the near-IR spectrum (Fig. 6) significantly reduced the surface temperature as compared to carbon black. An IRR green was a measured 54°F (30°C) cooler than carbon black, an IRR dark brown was ~48.6°F (27°C) cooler, and an IRR black was a measured 46.8°F (26°C) cooler.

For our test site at Oak Ridge National Laboratory (ORNL), Oak Ridge, Tennessee, the maximum irradiance from the sun, at solar noon, is about 308 Btu/(hr·ft<sup>2</sup>) [350 J/(hr·cm<sup>2</sup>)]. ASTM procedure D4803 (ASTM 1997a) relates the intensity of solar irradiance to the intensity derived from the infrared lamp via a ratio of the temperature rises above the ambient air temperature (i.e., the ΔT for IRR black to the ΔT for standard carbon black, see the right side of Eq. 2) to predict the specimen's solar temperature rise by:

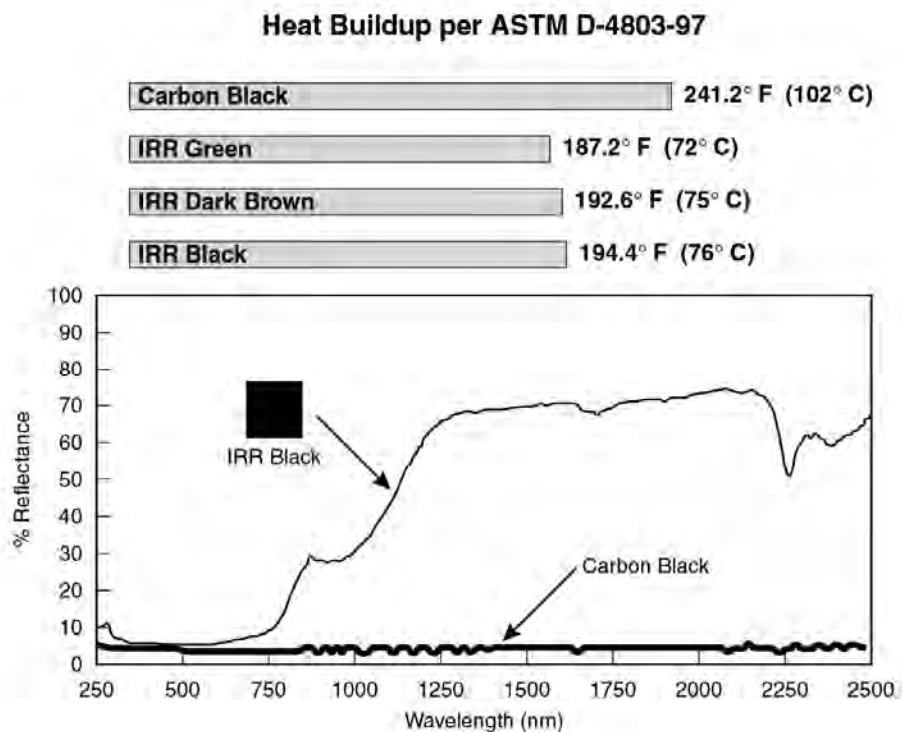
$$\left[ \frac{\Delta T_{\text{IRR Black}}}{\Delta T_{\text{black Kynar}}} \right]_{\text{solar}} = \left[ \frac{\Delta T_{\text{IRR Black}}}{\Delta T_{\text{black Kynar}}} \right]_{\text{ASTM D4803}} \quad (2)$$

where

$\Delta T_{\text{IRR Black}}$  = “predicted” temperature rise above the ambient air temperature for IRR black when exposed to solar irradiance

$\Delta T_{\text{black Kynar}}$  = “experimentally measured” temperature rise above the air temperature for a black Kynar® (~40°C above ambient as field-tested at ORNL)

**Figure 6. Heat Buildup of High-IRR Pigments vs. Standard Carbon Black and Reflectance of IRR Black vs. Standard Carbon Black**



Based on Equation (2) and summertime field data for a black Kynar® metal roof tested by Miller and Kriner (2001), the IRR black sample would be about 25°F (14°C) cooler at solar noon than a conventional dark roof.

## Durability and Weathering of CICPs

Testing protocols to determine the resistance to weathering of paints and coating systems designed for outdoor use include both natural, real-time weathering, such as outdoor exposure in Florida or Arizona, and accelerated tests using a weatherometer equipped with carbon-arc, fluorescent UV, and xenon-arc light sources. To evaluate color changes in roof samples with CICPs as compared to samples with standard colors, we used a two-year exposure test to natural sunlight in Florida and also a 5000-hour xenon-arc accelerated exposure test, following ASTM G-155 (ASTM 2000). Test data showed excellent light fastness for all the CICPs. Pigment stability and discoloration resistance were judged using a total color difference measure ( $\Delta E$ ) as specified by ASTM D 2244-

93 (ASTM 1993). The  $\Delta E$  value for all the colors tested was a color change of approximately 1.0 or less (Figs. 7 and 8).

The total color difference value,  $\Delta E$ , is a method adopted by the paint industry to numerically identify variability in color over periods of time. This value shows the difference in color between a standard and a batch and includes the three following values computed in the formula:

- lightness ( $L$ ), where a  $+L$  value is lighter and a  $-L$  value is darker;
- redness/greenness ( $a$ ), where a  $+a$  value is redder and a  $-a$  value is greener; and
- yellowness/blueness ( $b$ ) where a  $+b$  value is yellower and a  $-b$  value is bluer.

$$\Delta E = \left[ (\Delta L)^2 + (\Delta a)^2 + (\Delta b)^2 \right]^{1/2}, \quad (3)$$

where

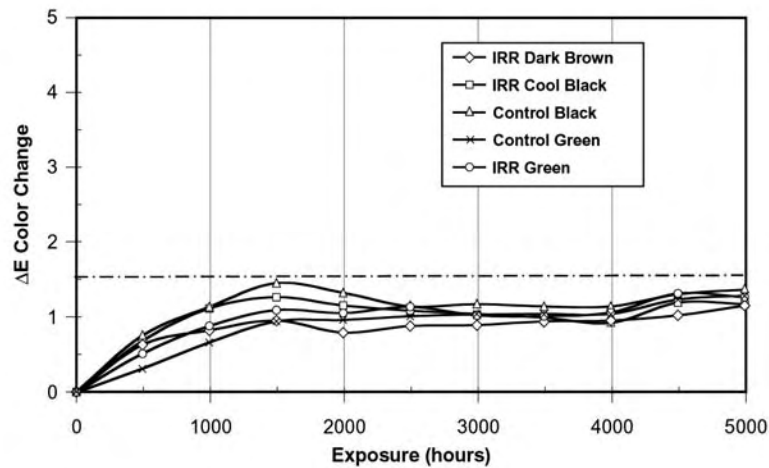
$$\Delta L = L_{\text{batch}} - L_{\text{standard}}$$

$$\Delta a = a_{\text{batch}} - a_{\text{standard}}$$

$$\Delta b = b_{\text{batch}} - b_{\text{standard}}$$

Typically, coil-coated metal roofing panels are warranted for 20 years or more and specify a  $\Delta E$  of 5 units or less for that period.  $\Delta E$  color changes of 1 unit or less are almost indistinguishable from the original color, and depending on the hue of color,  $\Delta E$  of 5 or less is considered very good.

**Figure 7. Total Color Difference ( $\Delta E$ ) Values for Color Samples in Xenon-Arc Accelerated Weathering Test**

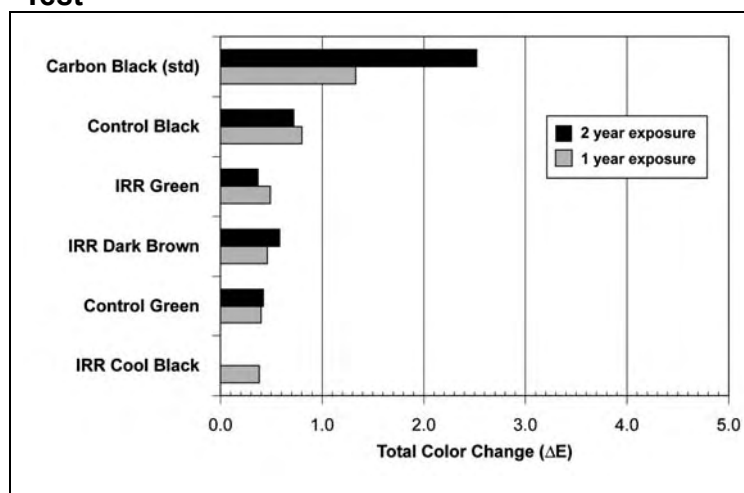


The xenon-arc accelerated weathering initially saw most of the colors rise in  $\Delta E$  up to about 1500 hours of exposure and then level off; at the end of 5000 hours all are clustered together at less than 1.5  $\Delta E$ , which is considered excellent results (Fig. 7). Control products with known performance characteristics were included in the testing to compare results with the new products.

The Florida exposure data in Figure 8 are just as promising, indicating that over the two-year test period the CICPs do not fade in the presence of ozone,

acid rain, SO<sub>x</sub>, NO<sub>x</sub>, or other airborne pollutants. Tests have shown that CICIPs remain colorfast in the presence of strong acids, bases, and oxidizing or reducing agents. They are non-migratory and showed no dissolving or bleeding in contact with airborne solvents. Most important, CICIPs retain their color when mixed with TiO<sub>2</sub> to produce light pastel shades which possess improved lightfast characteristics as compared to previously tried and proven standard colors.

**Figure 8. Total Color Difference ( $\Delta E$ ) Values for Color Samples in One-Year Florida Weathering Test**



## Conclusions

Accelerated weather testing using natural sunlight and xenon-arc weatherometer exposure proved that CICIPs retain their color. After two years of natural sunlight exposure in south Florida the CICIPs show excellent fade-resistance and remain colorfast. CICIPs are very stable pigments and have excellent discoloration resistance, as also proven by the 5000 hours of xenon-arc exposure; their measure of total color difference was a  $\Delta E$  value less than 1.5. Therefore, color changes in the CICIPs were indistinguishable from their original color.

CICIPs have a selective light absorption band in the infrared spectrum. They reflect much of the near-IR heat and therefore reduce the surface temperature upwards of 50°F (28°C) as compared to carbon black pigments when exposed to irradiance from an infrared lamp. For a steep-slope roof in the field, an IRR black would be about 25°F (14°C) cooler at solar noon than would a conventional dark roof. The lower exterior temperature leads to energy savings and provides an ancillary benefit in older existing houses with little or no attic insulation and poorly insulated ducts in the attic because the cooler attic temperature in turn leads to reduced heat gains to the air-conditioning ductwork.

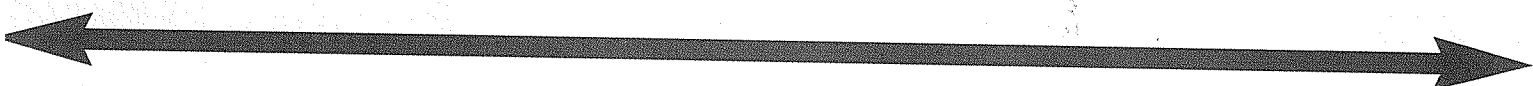
## References

American Society for Testing and Materials (ASTM). 1993. *Designation D2244-93: Standard Test Method for Calculation of Color Differences from*

- Instrumentally Measured Color*. West Conshohocken, Pa.: American Society for Testing and Materials.
- . 1997a. *Designation D4803-97: Heat Build-Up Apparatus Standard Test Procedure*. West Conshohocken, Pa.: American Society for Testing and Materials.
- . 2000. *Designation G155-00a: Standard Practice for Arc Operating Xenon Arc Light Apparatus for Exposure on Non-metallic Materials*. West Conshohocken, Pa.: American Society for Testing and Materials.
- Brady, R. F., and L. V. Wake. 1992. "Principles and Formulations for Organic Coatings with Tailored Infrared Properties." *Progress in Organic Coatings* 20:1–25.
- Du Pont Ti-Pure. 1999. *Titanium Dioxide for Plastics*. Wilmington, Del.: Du Pont Corporation.
- Good, C. 2001. "Eyeing the Industry: NRCA's Annual Market Survey Provides Interesting Industry Analyses." In *NRCA 2000–2001 Annual Market Survey*, 116–20. Rosemont, Ill.: National Roofing Contractors Association.
- Martin, P., and H. L. Pezzuto. 1998. "Pigments Which Reflect Infrared Radiation from Fire." U.S. Patent 5,811,180, September 22.
- Miller, W. A., and S. Kriner. 2001. "The Thermal Performance of Painted and Unpainted Structural Standing Seam Metal Roofing Systems Exposed to One Year of Weathering." In *Thermal Performance of the Exterior Envelopes of Buildings, VIII: Proceedings of ASHRAE THERM VIII*. Clearwater, Fla.: American Society of Heating, Refrigerating, and Air-Conditioning Engineers, Dec. 2–7.
- Ravinovitch, E. B., and J. W. Summers. 1984. "Infrared Reflecting Vinyl Polymer Compositions." U.S. Patent 4,424,292. January 3.
- Sliwinski, T. R., R. A. Pipoly, and R. P. Blonski. 2001. "Infrared Reflective Color Pigment." U.S. Patent 6,174,360, January 16.
- Billmeyer and Saltzman's Principles of Color Technology, 3rd Edition, R.S. Berns, John Wiley, New York, 2000
- Absorption and Scattering of Light by Small Particles, C.F. Bohren, D.R. Huffman, John Wiley, New York, 1983
- "Pigments Which Reflect Infrared Radiation from Fire", P.H. Berdahl, US Patent 5,811,180, issued September 22, 1998
- "Reflective Porcelain Enamel Coating Compositions", W.D. Faust, H.F. Evele, US Patent 6,004,894, issued December 21, 1999
- "Infrared Reflecting Colored Pigment", T.R. Sliwinski, R.A. Pipoly, R.P. Blonski, US Patents 6,174,360, issued 1/16/2001 and 6,454,848, issued 9/24/2002



# Cool Colors



## A Roofing Study is Developing Cool Products for Residential Roofs

By Hashem Akbari, Paul Berdahl, Andre Desjarlais, Nancy Jenkins, Ronnen Levinson, William Miller, Arthur Rosenfeld, Chris Scruton and Stephen Wiel

Raising the solar reflectance of a residential roof from a typical value of 0.1 or 0.2 to an achievable 0.5 can reduce cooling-energy use in buildings by more than 15 percent. Energy savings are particularly pronounced in older houses with minimal attic insulation, especially if the attic contains air distribution ducts.

Research conducted by Lawrence Berkeley National Laboratory (LBNL), Berkeley, Calif., estimates U.S. potential energy savings in excess of 750 million per year in net annual residential and commercial energy bills (cooling-energy savings minus heating-energy penalties) simply by installing "cool roofs"—that is, roofs that reflect a large fraction of incident sunlight. Cool roofs also significantly reduce peak electric demand in summer. Although preliminary analysis suggests there may be a surcharge of up to \$1 per square meter for cool roofing materials, this represents only 2 percent to 5 percent of the cost of installing a new residential roof.

The widespread installation of cool roofs can lower the ambient air temperature in a neighborhood or city, further decreasing the need for air conditioning. Lower ambient air temperatures reduce smog formation, increase environmental comfort and improve human health. Lower surface temperatures also may increase the lifetime of

roofing products (particularly asphalt shingles), reducing replacement and disposal costs. The collective benefits resulting from reduced ambient air temperature have roughly the same economic value as that of the energy savings achieved by reducing building heat gain through the roof.

The California Energy Commission, Sacramento, Calif., has engaged LBNL and Oak Ridge National Laboratory (ORNL), Oak Ridge, Tenn., in a three-year project to work with the roofing industry to develop and produce colored roofing products with high solar reflectance and encourage the home-building industry to use these products. LBNL and ORNL's goal is to make nonwhite cool roofing materials commercially available within three to five years. About two years into the study, researchers already have interesting findings to report.

### Nonwhite Cool Roofing Materials

Cool white materials are available for most roofing products with the notable exception of asphalt shingles. Cool nonwhite materials are needed for all types of roofing. Industry researchers have developed durable complex inorganic color pigments that are highly reflective to "near-infrared"

(NIR) solar radiation. This invisible spectrum contains more than 50 percent of the power in sunlight. The high NIR reflectance of coatings formulated with complex inorganic and other "cool" pigments—chromium oxide green, cobalt blue, phthalocyanine blue, Hansa yellow—can be exploited to manufacture colored roofing materials that reflect more sunlight than do conventionally pigmented roofing products.

Specifically, LBNL and ORNL aim to produce nonwhite shingles with solar reflectances not less than 0.3 and other types of nonwhite roofing products (tiles) with solar reflectances not less than 0.45. The reflectance goal for shingles is lower than that for other products because the roughness of a shingle's surface reduces its reflectance and because manufacturing constraints typically limit the reflectance of coatings applied to granules.

Research activities are designed to address the following five topics:

*Formulation of Cool-colored Coatings:* How can the total solar reflectance of a pigmented coating be maximized while matching a desired color?

*Development of Cool-colored Roofing Prototypes:* What is the relationship between the optical properties of a simple pigmented coating and those of a pigmented coating applied to roofing materials (granules, tiles)?

*Durability of Cool-colored Coatings:* How do cool-colored coatings weather and age?

*Longevity of Cool-colored Roofing Materials:* Does higher solar reflectance increase the lifetime of cool-colored roofing materials?

*Demonstration of Energy Savings:* What is the building-energy savings yielded by use of cool-colored roofing materials?

## Formulation of Cool-colored Coatings

To maximize the solar reflectance of a pigmented coating matching a particular color, LBNL has characterized the optical properties of more than 100 common and specialty pigments and is developing a computer model for design of color-matched cool pigmented coatings.

Each pigment initially is characterized by the solar spectral reflectance and transmittance of a pigmented coating (a free film of paint), measured at 5-nanometer (nm) intervals across the solar spectrum (300 to 2,500 nm). Solar spectral absorptance (1-reflectance-transmittance) is an excellent indicator of whether a pigment is cool (has low NIR absorptance) or hot (has high NIR absorptance). (See Figure 1a.)

The measured reflectance and transmittance are used to compute solar spectral absorption and backscattering coefficients, which indicate in the solar "Kubelka-Munk" (K-M) light-flux theory the rates at which pigment particles absorb and backscatter light in a pigmented coating. (See Figure 1b.) Finally, the film reflectances over black and white backgrounds predicted by the K-M theory are compared with measured reflectances to check the validity of the computed absorption and backscattering coefficients. (See Figure 1c.)

Cool nonwhite pigments must have absorption coefficients that are large in parts of the visible spectrum (to produce the desired color) and small in the NIR spectrum (to minimize absorption of visible solar radiation). The backscattering coefficient of a cool pigment ideally should be large in NIR to maximize reflectance in that spectrum, though weak NIR backscattering is acceptable if coating has an NIR-reflective background.

LBNL has developed a preliminary database summarizing characterizations of about 100 pigments and have shared this database with industrial partners to help them develop cool-

## Characterization of a Near-infrared-reflecting Cool Black Pigment

(About 25-micron- [1-mil-] thick film of chromium green-black hematite modified in clear binder of refractive index 1.5; 7 percent pigment volume concentration)

### Observed Film Property

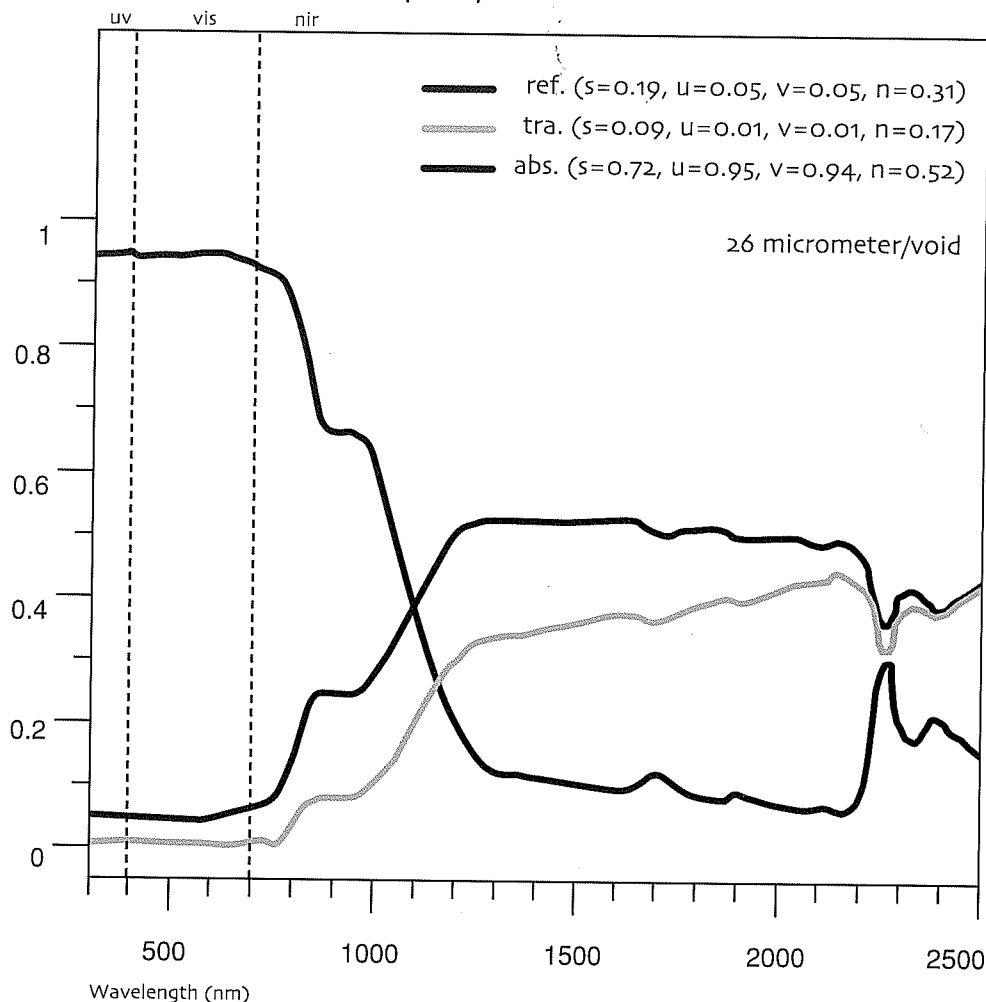


Figure 1a: Measured reflectance, measured transmittance and computed absorptance of a free film. Parenthetical values are irradiance-weighted averages over the solar (s), ultraviolet (u), visible (v) and near-infrared (n) spectra.

colored coatings and roofing products.

The researchers also are developing a model that estimates the solar spectral reflectance of coatings from pigment properties, including absorption and backscattering coefficients; coating composition, such as pigments, vehicle and filler; and coating geometry, including thickness, roughness and background. This model will be implemented in software that suggests recipes to

maximize the solar reflectance of a colored coating. The software will be available to pigment, coating and roofing manufacturers.

## Development of Cool-colored Roofing Prototypes

Researchers at LBNL and ORNL estimate that roofing shingles, tiles and metal panels comprise more

## K-M Coefficient (mm<sup>-1</sup>)

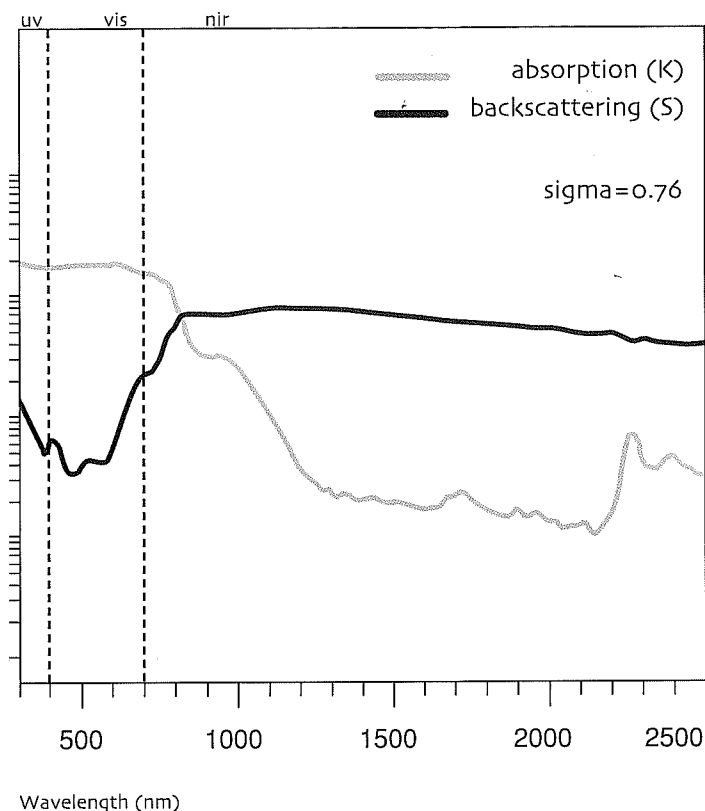


Figure 1b: "Kubelka-Munk" (K-M) absorption coefficient K and backscattering coefficient S

## Observed Film Reflectance

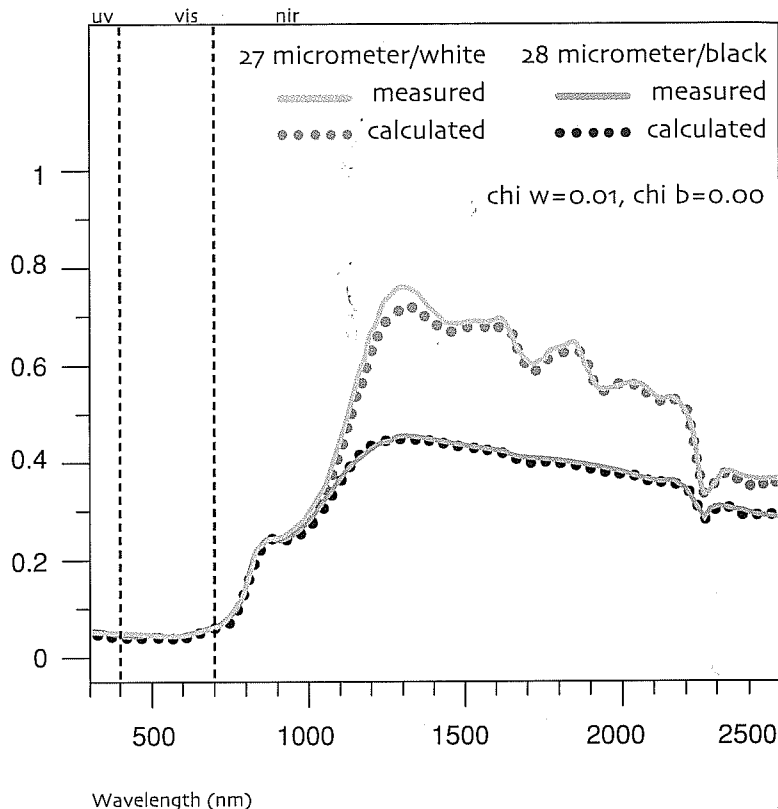


Figure 1c: Comparison of measured reflectances of the film over opaque white and opaque black backgrounds with values calculated from computed absorption and backscattering coefficients

80 percent (by roof area) of the residential roofing market in the western United States. The architects interviewed manufacturers of asphalt shingles, concrete and clay tiles, and metal panels to obtain information about the processes used to produce their products. Patent and other literature about the fabrication and coloration of roofing materials, especially asphalt roofing shingles, also have been reviewed.

## Shingles

The solar reflectance of a new shingle is dominated by the solar reflectance of its granules because—by design—the shingle's surface is well covered by granules. Until recently, the way to produce granules with high solar reflectance has been to use titanium dioxide (TiO<sub>2</sub>) rutile, a white pigment. The use of a thin layer of TiO<sub>2</sub> is reflective but not

opaque, multiple layers are needed to attain the desired solar reflectance. This technique has been used to produce "super-white" (meaning truly white, rather than gray) granulated shingles with solar reflectances exceeding 0.5.

Manufacturers also have tried to produce colored granules with high solar reflectance by using nonwhite pigments with high NIR reflectance. However, similar to TiO<sub>2</sub>, cool-colored pigments are partly transparent to NIR light. Thus, any NIR light not reflected by the cool pigment is transmitted to the (typically dark) granule underneath, where it can be absorbed. To increase the solar reflectance of granules colored with cool pigments, multiple color layers, a reflective undercoating and/or reflective aggregate should be used. Obviously, each additional coating increases production cost.

The application of pigmented coatings to roofing granules appears to be the critical process step.

Several layers of silicate coatings can be involved and may include not just one or more pigments but the use of clay additives to control viscosity, biocides to prevent staining and process chemistry controls to avoid residual dust on the product.

One way to reduce the cost is to produce cool-colored granules via a two-step, two-layer process. In the first step, the granule is precoated with an inexpensive pigment, such as TiO<sub>2</sub>, that is highly reflective to NIR light. In the second step, the cool-colored pigment is applied to the precoated granules.

## Tiles

There are three ways to improve the solar reflectance of colored tiles: use clay or concrete with low concentrations of light-absorbing impurities, such as iron oxides and elemental carbon;



Figure 3: Cool coatings developed for concrete roof tiles. The upper row shows six cool-colored coatings, each with solar reflectance  $R$  exceeding 0.4, which match conventionally pigmented coatings in the lower row.

Photo courtesy of American Rooftile Coatings, Fullerton, Calif.

R=0.41	R=0.44	R=0.44	R=0.48	R=0.46	R=0.41
BLACK	BLUE	GRAY	TERRACOTTA	GREEN	CHOCOLATE
R=0.04	R=0.18	R=0.21	R=0.33	R=0.17	R=0.12

Color the tile with cool pigments contained in a surface coating or mixed integrally; and/or include an NIR-reflective underlayer, such as white, beneath an NIR-transmitting colored topcoat. Although these options are in principle easy to implement, they may require changes in current production techniques that could add to the cost of finished products.

## Metal Panels

Incorporation of cool-colored pigments in metal roofing products may require the fewest number of changes to existing production processes. Cool pigments can be applied to metal via a single- or double-layered technique; if the raw metal is highly reflective, a single-layered technique may suffice. The coatings for metal shingles are thin, durable polymer materials. These thin layers use materials efficiently but limit the maximum amount of pigment present. The metal substrate can provide significant NIR reflectance if the coating is transparent in the NIR.

## Wood Shakes

In the near future, LBNL and ORNL will survey methods of manufacturing wood shakes.

## Sample Prototypes

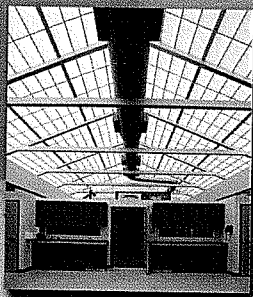
LBNL and ORNL have collaborated with 14 companies that manufacture roofing materials, including shingles, roofing granules, clay tiles, concrete tiles, tile coatings, metal panels, metal coatings and pigments. The development work has been iterative and included selection of cool pigments, choice of base coats for the two-layer applications and identification of pigments void.

## Color Black Shingle

Figure 2 shows the iterative development of a cool



## Energy-Efficient Daylighting



Guardian 275® Translucent Daylighting saves money by reducing the damaging effects of direct sunlight. Guardian 275® systems offer long-term benefits while providing cost-effective daylighting. Energy-saving insulation can be added to Guardian 275® translucent glazing systems to control heat loss and heat gain.

- **Energy-Efficient**
- **Reduces HVAC Loads**
- **Reduces Need for Artificial Lighting**
- **Reduces Student/Employee Absenteeism**
- **Virtually Eliminates UV Damage**
- **Glare-Free Natural Light**



Major Industries, Inc.  
P.O. Box 306  
Wausau, WI 54402-0306  
(715) 842-4616 voice  
(715) 848-3336 fax

Toll Free

**888 SkyCost**

[www.majorskylights.com](http://www.majorskylights.com)

CIRCLE NO. 20

## Prototype Cool Black Shingles

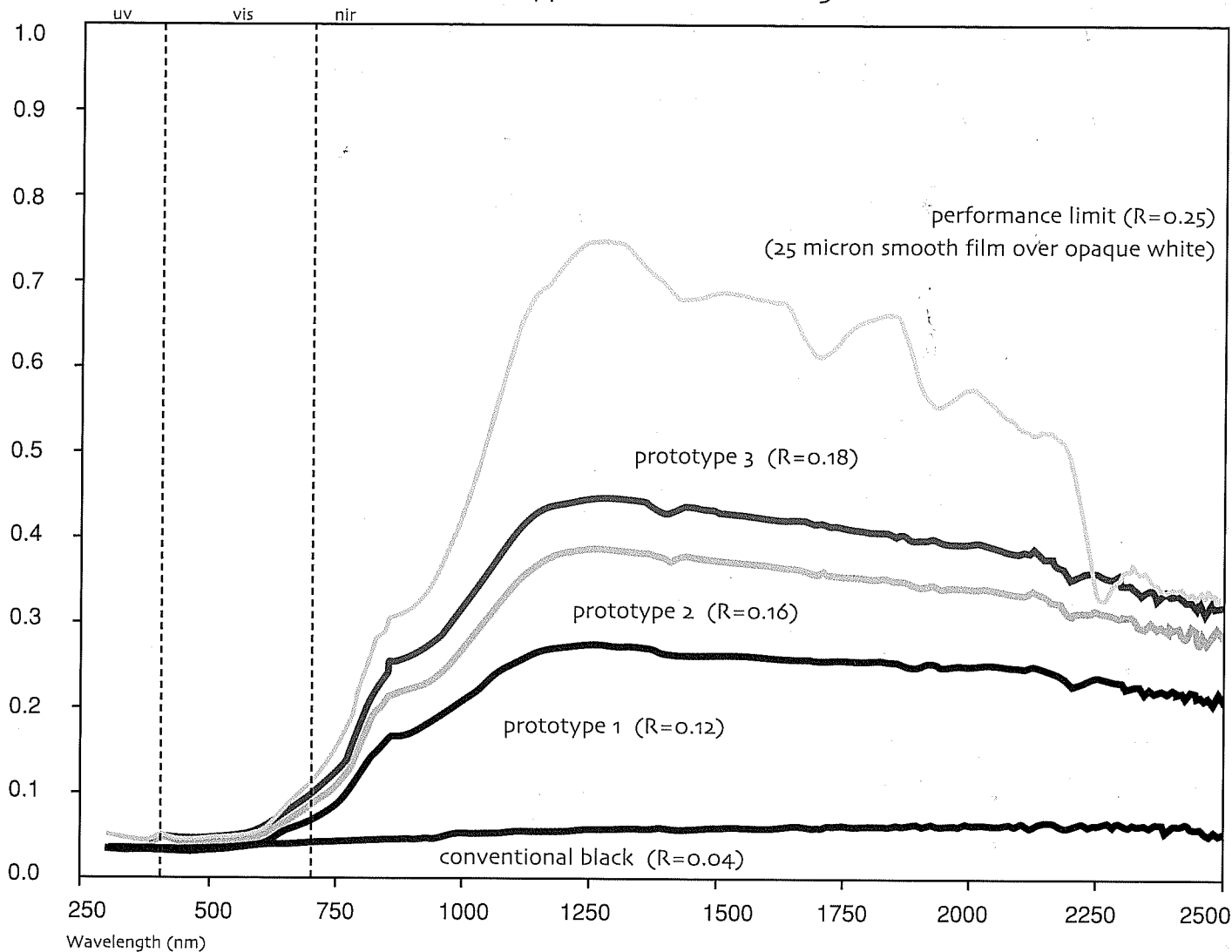


Figure 2: Development of a cool black shingle, showing effects of incorporating cool pigments and adding near-infrared reflecting underlayers

black shingle. A conventional black roof shingle has a reflectance of about 0.04. The researchers initially replaced the granule's standard black pigment with an NIR-reflecting black, increasing the solar reflectance of the shingle to 0.12. Next, an NIR-transmitting black was applied over a thin  $\text{TiO}_2$  white underlayer, increasing the shingle's solar reflectance to 0.16. Finally, the thickness of the white underlayer was increased, raising the shingle's reflectance to 0.18. Figure 2 also shows an approximate performance limit (reflectance 0.25), which was obtained when a 25-micron- (about 1-mil-) thick NIR-reflective black topcoat is applied over an opaque white background.

### Cool Concrete Tiles

Figure 3 shows the results of similar efforts to

develop coatings for concrete tile roofs, which yielded a palette of cool colors each with solar reflectance exceeding 0.4.

### Durability of Cool-colored Coatings

Samples of several roofing product styles and colors have been placed in seven of California's 16 climate zones for exposure studies. Solar reflectance and thermal emittance are measured twice per year, and weather data are available continuously. Solar spectral reflectance is measured annually to gauge soiling and document color changes too small to perceive.

IBNL and ORNL also will examine the roof samples for contaminants and biomass. The surface composition studies will identify the drivers affecting

the soiling of the roof samples, which will provide valuable information to manufacturers for improving the sustainability of their roofing products. The data will be used to formulate an algorithm correlating changes in reflectance with exposure.

In collaboration with industrial partners, the researchers are exposing samples to 5,000 hours of xenon-arc light in a weatherometer following ASTM Standard G155-00a1, "Standard Practice for Operating Xenon Arc Light Apparatus for Exposure of Non-Metallic Materials."

### Longevity of Cool-colored Roofing Materials

Roofing materials fail mainly because of three processes: gradual changes to physical and chemical composition induced by the absorption of

plet (UV) light; aging and weathering (loss of plasticizers in polymers and low-molecular-weight components in asphalt), which may increase as temperature increases; and diurnal thermal cycling, which stresses the material by expansion and contraction. The researchers soon begin to investigate reflectance effects on the useful life of roofing products to evaluate claims that cool roofs will last longer.

LBL and ORNL's goal is to clarify the material degradation effects caused by UV absorption and aging. The results will be used to quantify the effect of solar reflectance on the useful life of roofs, provide data to manufacturers to develop better materials and support development of appropriate standards.

## Demonstration of Energy Savings

The researchers have established a residential demonstration site in Fair Oaks, Calif., that includes two pairs of single-family, detached houses outfitted with metal and concrete tile. Two more pairs of houses will be added to demonstrate asphalt shingles and cedar shakes. The monitoring period will last at least through summer 2005. The demonstration pairs include one building roofed with a cool-pigmented product and a second building roofed with a conventionally (warmer) pigmented product of nearly the same color.

Solar reflectance and thermal emittance are measured twice per year. Temperatures at the roof surface, on the underside of the roof deck, in the attic air, at the top of the insulation, on the interior ceiling's Sheetrock surface and inside the building are logged continuously by a data acquisition system. Relative humidity in the attic and temperature also are measured. Heat-flux transducers are embedded in the sloped roof and attic floor to measure roof heat flow and building heat leakage. Researchers have instrumented the building to measure the total house and air-conditioning energy demands. A weather station collects the ambient dry bulb temperature, relative humidity, solar irradiance, and wind speed and direction.

ORNL is testing several varieties of concrete and tile on a steep-slope roof to further investigate the effect of weathering-induced changes to solar reflectance and thermal emittance on the thermal performance of a cool roof system. The Roof Tile

Institute and its affiliate members are keenly interested in specifying tile roofs as cool roof products and want to know the individual and combined effects of cool pigments and subtile ventilation. The data will help better formulate the institute's simulation program, AtticSim, to predict the thermal performance of the cool-colored tile systems.

## Early Results

The early results from this program indicate significant success in developing cool-colored materials for concrete tile, clay tile and metal roofs.

Since the inception of this program, the solar reflectance of commercially available products has increased from 0.05 - 0.25 to 0.30 - 0.45. Use of a reflective undercoated (two-layered) coating is expected to soon yield several cost-effective cool-colored shingle products with solar reflectances in excess of the ENERGY-STAR threshold for roofs of 0.25. LBNL and ORNL's ongoing collaboration with granule and shingle manufacturers may yield shingles with solar reflectances exceeding 0.3. For more information about the study, visit the project Web site, <http://coolcolors.lbl.gov>, or contact Hashem Akbari at (510) 486-4287 or [h\\_akbari@lbl.gov](mailto:h_akbari@lbl.gov).

Hashem Akbari is a group leader, staff scientist and principal investigator in the Environmental Energy Technologies Division of Lawrence Berkeley National Laboratory (LBNL), Berkeley, Calif. Paul Berdahl is an applied solid-state physicist whose interests include optical properties of semiconductors and complex materials, such as practical roofing materials. Andre Desjarlais is group leader of the Building Envelope Group of the Engineering Science and Technology Division at Oak Ridge National Laboratory (ORNL), Oak Ridge, Tenn. Nancy Jenkins is the PIER buildings program manager at the California Energy Commission (CEC), Sacramento, Calif. Ronnen Levinson is a scientist in the Heat Island Group at LBNL whose recent research has focused on the development of cool materials for roofs and pavements with emphasis on the optical characterization of pigments. William Miller is a research engineer in the Engineering Science and Technology Division of ORNL. Arthur Rosenfeld currently serves as commissioner of CEC. Chris Scruton is a program manager at CEC and oversees scientific research and development of projects focused on technologies applied to commercial and residential buildings. Stephen Wiel leads the Collaborative Labeling and Appliance Standards Program at LBNL, a program that stimulates the use of energy-efficiency standards and labels worldwide.

## Manufacturing Partners

3M Industrial Minerals, Pittsboro, N.C.  
[www.scotchgard.com/roofinggranules](http://www.scotchgard.com/roofinggranules)

American Rooftile Coatings, Fullerton, Calif.  
[www.americanrooftilecoatings.com](http://www.americanrooftilecoatings.com)

BASF, Mount Olive, N.J.  
[www.basf.com](http://www.basf.com)

CertainTeed Corp., Valley Forge, Pa.  
[www.certainteed.com](http://www.certainteed.com)

Custom-Bilt Metals, South El Monte, Calif.  
[www.custombiltmetals.com](http://www.custombiltmetals.com)

Elk Corp., Dallas  
[www.elkcorp.com](http://www.elkcorp.com)

Ferro Corp., Cleveland  
[www.ferro.com](http://www.ferro.com)

GAF Materials Corp., Wayne, N.J.  
[www.gaf.com](http://www.gaf.com)

Hanson Roof Tile, Fontana, Calif.  
[www.hansonrooftile.com](http://www.hansonrooftile.com)

ISP Minerals Inc., Hagerstown, Md.  
(301) 733-4000

MCA Tile, Corona, Calif.  
[www.mca-tile.com](http://www.mca-tile.com)

MonierLifetile LLC, Irvine, Calif.  
[www.monierlifetile.com](http://www.monierlifetile.com)

Shepherd Color Co., Cincinnati  
[www.shepherdcolor.com](http://www.shepherdcolor.com)

Steelscape Inc., Kalama, Wash.  
[www.steelscape-inc.com](http://www.steelscape-inc.com)

# Cool Color Roofs with Complex Inorganic Color Pigments

*William A. Miller,<sup>1</sup> Oak Ridge National Laboratory*

*Kenneth T. Loye, FERRO Corporation*

*André O. Desjarlais, Oak Ridge National Laboratory*

*Robert P. Blonski, FERRO Corporation*

## ABSTRACT

Temperature measurements taken on a highly reflective roof show the surface as only about 5°F (3°C) warmer than the ambient air temperature, while a dark absorptive roof exceeds the ambient air temperature by more than 75°F (40°C). Lowering the exterior roof temperature reduces the heat leakage into the building, which in turn, reduces the air conditioning load. In the residential market, however, the issues of aesthetics and durability are more important to the homeowner than are the potentials for reduced air-conditioning loads and reduced utility bills. Dark roofs simply look better than highly reflective “white” roofs. Yet the aesthetically pleasing dark roof can be made to reflect light like a “white” roof in the infrared portion of the solar energy spectrum. Researchers have formulated new complex inorganic color pigments (CICPs) that exhibit high reflectance in the near-infrared portion of the electromagnetic spectrum and boost the total hemispherical reflectance by a factor of 5 over that of conventional dark roofing.

## Introduction

A building’s required comfort cooling and heating energy, termed *load*, is directly related to several factors: the solar insolation absorbed by the building; the level of roof, wall, and foundation insulation; the amount of fenestration; and the building’s tightness against unwanted air and moisture infiltration. The solar reflectance and long-wave infrared (IR) emittance and the airside convective currents strongly affect the envelope’s exterior roof temperature, which in turn drives the load.

In the summer, the higher the roof temperature, the greater the potential for heat leakage into the building, and the greater the burden on the comfort cooling system. In winter, the lower the temperature, the greater the potential for heat leakage from the building, and the greater the energy consumed for comfort heating. In moderate to predominantly hot climates, an exterior roof surface with a high reflectance and high IR emittance will reduce the exterior temperature and produce savings in comfort cooling (Miller and Kriner 2001). For climates predominated by heating loads, surfaces with moderate reflectance and low IR emittance will save in comfort heating.

Field measurements of ten homes by Parker and Barkaszi (1997) showed that reflective white roofing reduced space-cooling energy use an average of 19% as compared to dark asphalt shingles. Measurements made during the summer by Parker and Sherwin (1998)

---

<sup>1</sup>Dr. William A. Miller is a research engineer in the Buildings Technology Center of Oak Ridge National Laboratory (ORNL), Oak Ridge, Tennessee. Kenneth T. Loye is the Technical Manager of the Pigments Group at FERRO Corporation, Cleveland, Ohio. André O. Desjarlais is the manager of ORNL’s Building Thermal Envelope Systems & Materials Program. Robert P. Blonski is a research chemist working in the Pigments Group at FERRO Corporation.



showed that white tile roofing caused a 76% reduction in the ceiling heat flux into the house relative to a black shingle roof; the second-best performer in this study, a white-painted metal surface, showed a 61% reduction. Field studies conducted by Parker et al. (1998) on several homes in Fort Myers, Florida, showed that the roof, attic, and air-conditioning ductwork accounted for about 25% of the total cooling load in residences. Highly reflective roofs yielded cooling energy savings upwards of 23% of the annual load.

Each field study documented energy savings by simply raising the reflectance of the roof from a value of about 5% to about 60%. The opportunity therefore exists for a significant impact on energy use in commercial buildings and residential housing, both in new construction and reroofing work. The total sales volume for roofing and reroofing is booming and nearly doubled between 1997 and 2000, from \$20 billion to \$36 billion (Good 2001). Of the sales volume in 2000, low-slope roofing accounted for 64% (\$21.7 billion), while steep-slope roofing comprised about 35.6% (\$12 billion) (Good 2001).

High-reflectance single-ply membranes, painted and unpainted metal, and spray-on roof coatings are reducing energy use in the commercial market as building contractors substitute these high-reflectance roofs for bitumen-based built-up roofing (BUR) and ethylene propylene diene monomer (EPDM). Since a high-reflectance low-slope roof cannot be seen from the ground, the roof's functionality is far more important than its looks. However, in steep-slope roofing the issues of appearance, cost, and then durability typically drive the selection of the roofing material because the homeowner wants the roof to complement the décor of the house while protecting the underlying residential structure for a long period of time at an affordable cost. To homeowners, dark roofs simply look better than a highly reflective "white" roof. With the new CICPs, however, an aesthetically pleasing dark roof can be made to reflect like a "white" roof in the infrared portion of the solar spectrum and save energy for both homeowners and utilities.

## **Surface Properties Affecting Reflectance**

Titanium dioxide ( $\text{TiO}_2$ ) is currently the most important white pigment used in the manufacture of paints and plastics.  $\text{TiO}_2$  is chemically inert, insoluble, and very heat-resistant. It has been commercially processed from rutile since as early as 1941 (Du Pont Ti-Pure 1999). Rutile  $\text{TiO}_2$  increases surface reflectance through refraction and diffraction of the light. As a light ray passes through a  $\text{TiO}_2$  particle, the ray bends, or refracts, because light travels more slowly through the pigments than it does through the resin or binder. This occurs because  $\text{TiO}_2$  has a much larger refractive index than the resin. This phenomenon is depicted in Figure 1 for two pigmented films. The film containing the pigment with higher refractive index bends the light more than does the film containing the lower refractive index pigment. The light travels a shorter path and does not penetrate as deeply into the film; therefore, less heat is absorbed. The reflectance of the surface increases because the surface opacity increases through refraction induced by the  $\text{TiO}_2$  particles. In general, the greater the difference between the refractive index of the pigment and that of the resin or filler in which it is dispersed, the greater will be the light scattering and therefore the increase in surface reflectance.

Diffraction is another physical factor affecting a pigment's ability to scatter light. As a light ray passes by a  $\text{TiO}_2$  particle, the ray bends, or diffracts, around the pigment (Fig. 2). Maximum diffraction occurs when the diameter of the pigment is slightly less than one-half



**Figure 1. Path of Light as It Penetrates Two Different Coatings, One Having Pigments with a Higher Refractive Index Than the Other**

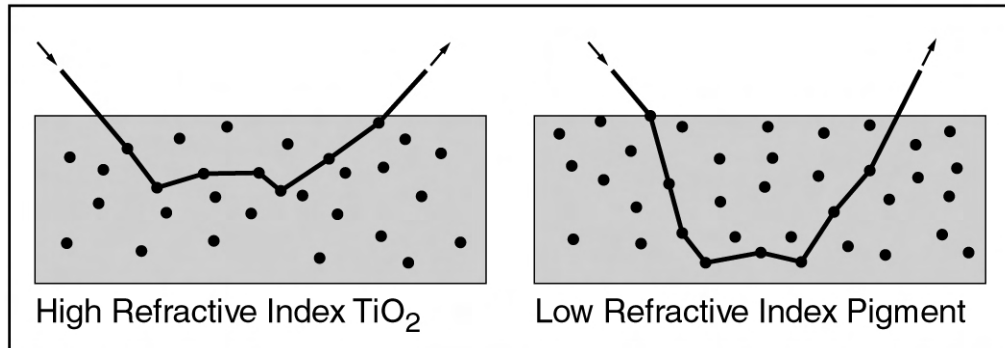
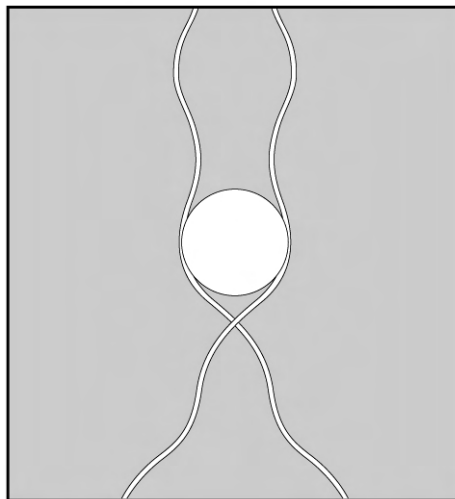


**Figure 2. Light Diffraction as a Light Ray Travels near a Pigment Particle**

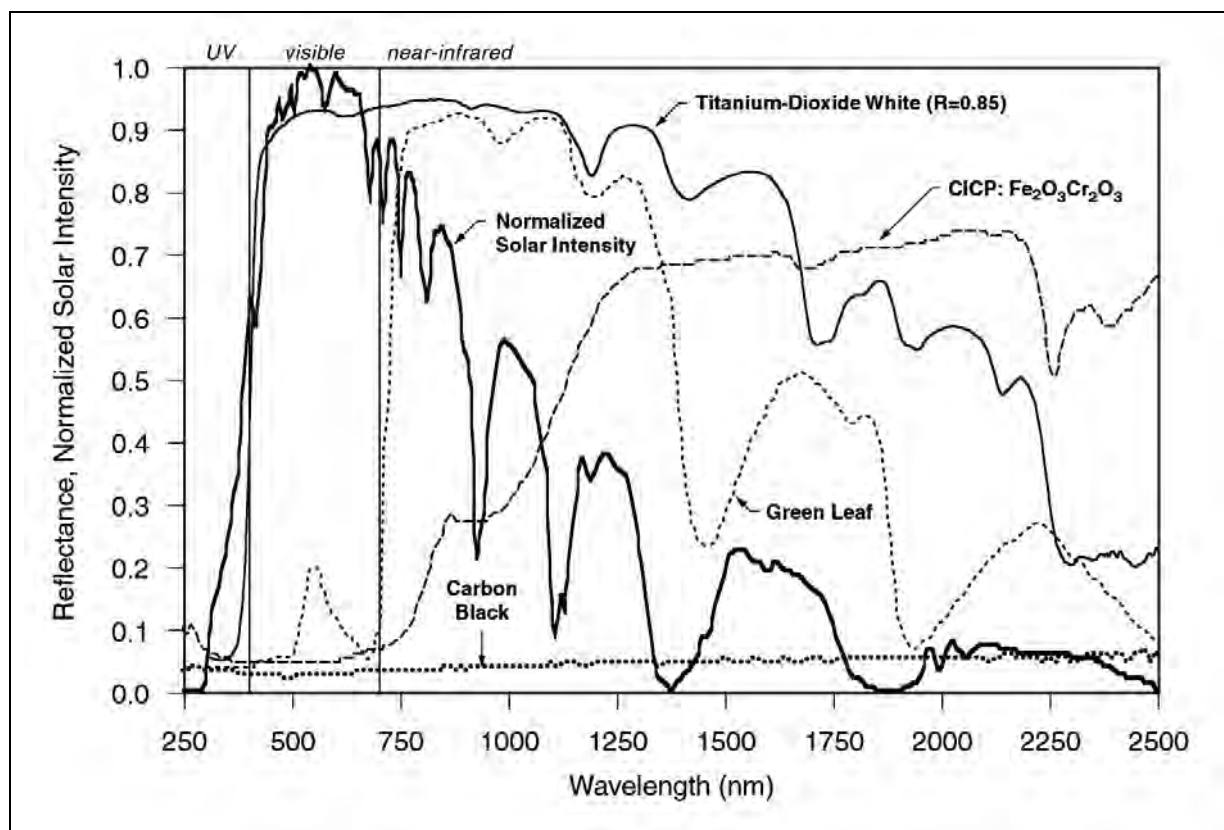


the wavelength of the light to be scattered. Physical modifications of the size, the distribution, and the shape of pigment particles will therefore affect the light scattering. If particles are too large or too closely spaced, little diffraction occurs. Conversely, if the pigment particles are too small, the light will not “see” the particles. Commercially processed rutile  $\text{TiO}_2$  has particle diameters ranging from about 200 to 300 nm and is highly reflective in the visible spectrum (yellow-green light at about 550 nm; see Fig. 3). However, as the wavelength of light increases, the reflectance of  $\text{TiO}_2$  drops in the infrared spectrum, especially for wavelengths exceeding 1250 nm (Fig. 3).

### **Complex Inorganic Color Pigments (CICPs)**

Aesthetically pleasing dark roofing can be formulated to reflect like a highly reflective “white” roof in the IR portion of the solar spectrum. For years the vinyl siding

**Figure 3. Spectral Solar Reflectance of  $\text{TiO}_2$ , a Green Leaf, Standard Carbon Black and a Complex Inorganic Color Pigment Containing Infrared Reflective  $(\text{Fe,Cr})_2\text{O}_3$  Pigment (Normalized Solar Irradiance Shown for Reference)**



industry has formulated different colors in the same polyvinyl chloride base by altering the content of  $\text{TiO}_2$  and black IR-reflective (IRR) paint pigments to produce “dark” siding that is “cool” in temperature (Ravinovitch and Summers 1984). Researchers discovered that a dark color is not necessarily dark in the infrared. Brady and Wake (1992) found that 1- $\mu\text{m}$  particles of  $\text{TiO}_2$  when combined with red iron, or ferric, oxide effectively scattered IR radiation at a wavelength of 2300 nm. Researchers working with the Department of Defense developed new complex inorganic color pigments (CICPs) that exhibit dark color in the visible spectrum and high reflectance in the near-IR portion of the electromagnetic spectrum (Sliwinski, Pipoly & Blonski 2001). The new CICPs are used in paints for military camouflage to match the reflectance of background foliage in the visible and IR spectrum. At 750 nm the chlorophyll in foliage naturally boosts the reflectance of a plant leaf from 0.1 to about 0.9 (Fig. 3), which explains why a dark green leaf remains cool on a hot summer day.<sup>2</sup>

CICPs, having been tailored for high IR reflectance similar to that of chlorophyll, are very suitable for roof applications where increased IR reflectance is desirable. A CICP consisting of a mixture of black IRR pigments, chromic oxide ( $\text{Cr}_2\text{O}_3$ ) and ferric oxide ( $\text{Fe}_2\text{O}_3$ ) boosts the total hemispherical reflectance of carbon black from 0.05 to 0.26 (see

<sup>2</sup>Chlorophyll, the photosynthetic coloring material in plants, naturally reflects near-IR radiation.

CICP:Fe<sub>2</sub>O<sub>3</sub>-Cr<sub>2</sub>O<sub>3</sub> in Fig. 3). Typically, a black asphalt shingle or a black Kynar®<sup>3</sup> metal roof has a reflectance of only about 0.05. The CICP therefore boosts the reflectance by a factor of 5, and in the infrared spectrum CICPs boost the reflectance to almost 0.70 (Fig. 3).

CICPs are formed by calcinating blends of metal oxides or oxide precursors at temperatures over 1600°F (870°C). The calcination causes the metal and oxygen ions in the solids to rearrange in a new structure that is very heat-stable. The inherent heat stability of CICPs makes them ideal for high-temperature coatings in roofing applications. Because of their small particle size and high index of refraction, CICPs will effectively backscatter a significant amount of ultraviolet (UV) and IR light away from a surface. Martin and Pezzuto (1998) observed that pigments that are transparent in the required spectral range and that have a refractive index substantially different from that of the binder work well as IRR pigments.

## Thermal Performance of CICPs

CICPs offer excellent opportunities for improving the thermal performance of roofs. About 44% of the sun's total energy is visible to the eye (Fig. 3). Absorbing this 44% is what makes a black appear black. Sunlight emits another 51% of its energy in the invisible IR spectrum. Adding CICPs to roof material can make a black roof reflect near IR energy and therefore maintain a lower roof surface temperature. Using a heat buildup test procedure described by Hardcastle (1979), Ravinovitch and Summers (1984) measured a 23.4°F (13°C) lowering of temperature when a mixture of Cr<sub>2</sub>O<sub>3</sub> and Fe<sub>2</sub>O<sub>3</sub> was used in place of carbon black.

## Light-Color CICPs

The authors tested several IRR pigments against standard pigments using the ASTM D4803 test procedure (ASTM 1997a). This procedure has long been used by the vinyl siding industry to quantify the heat buildup properties of vinyl siding, even though it overstates the sample's properties in the near IR at the expense of visible portion of the spectrum (Ravinovitch and Summers 1984). Table 1 shows the temperatures for both CICPs and standard light-gray, mid-tone bronze, and dark-tone bronze colors when exposed to a flux of 484 Btu/(hr·ft<sup>2</sup>) [550 J/(hr·cm<sup>2</sup>)] emitted from an infrared heat lamp. These colors are very popular for low-slope roofing in commercial and academic applications where bronze Kynar metal roofing is commonly used.

The colors containing CICPs show a significant drop in temperature as compared to the temperatures of standard light-gray, mid-tone bronze, and dark bronze colors. The temperature is 55°F (30.5°C) cooler for the light gray color if CICPs are contained in the pigment mixture. Similarly, a mid-tone bronze showed a 63°F (35°C) reduction in surface temperature. Even the dark-tone bronze had a measured 54°F (30°C) drop in temperature because the IRR pigments absorb less electromagnetic energy near the cutoff between the visible and infrared wavelengths. They have a more selective absorption band and reflect much of the infrared.

---

<sup>3</sup>Kynar, the registered trademark for polyvinylidene fluoride (PVDF) paint finish, has excellent corrosion and abrasion resistance.

**Table 1. CICP Color Matches vs. Standard Pigmentation  
Exposed to ASTM D4803 Heat Lamp Protocol <sup>a</sup>**

Pigment	Pigment Constituents		Maximum Temperature	Temperature Difference ( $\Delta T$ )
Light gray				
Standard	Carbon black	1.5%	202°F (94.4°C)	
	TiO <sub>2</sub>	96.8%		
	Fe <sub>2</sub> O <sub>3</sub>	1.7%		
CICP	IRR black	10%	147°F (63.9°C)	55°F (30.5°C)
	TiO <sub>2</sub>	90%		
Mid-tone bronze				
Standard	Carbon black	11.8%	225°F (107.2°C)	
	TiO <sub>2</sub>	75.0%		
	Fe <sub>2</sub> O <sub>3</sub>	13.2%		
CICP	IRR black	50%	162°F (72.2°C)	63°F (35°C)
	TiO <sub>2</sub>	50%		
Dark-tone bronze				
Standard	Carbon black	33%	220°F (104.4°C)	
	TiO <sub>2</sub>	29%		
	Fe <sub>2</sub> O <sub>3</sub>	38%		
CICP	IRR black	90%	166°F (74.4°C)	54°F (30°C)
	TiO <sub>2</sub>	10%		

<sup>a</sup> A flux of 484 Btu/(hr·ft<sup>2</sup>) [550 J/(hr·cm<sup>2</sup>)] emitted from an infrared heat lamp.

## Dark-Color CICPs

We also exposed dark colors containing the IRR pigments to the infrared heat lamp. Again, the increased reflectance in the near-IR spectrum (Fig. 4) significantly reduced the surface temperature as compared to carbon black. An IRR green was a measured 54°F (30°C) cooler than carbon black, an IRR dark brown was ~48.6°F (27°C) cooler, and an IRR black was a measured 46.8°F (26°C) cooler.

For our test site at Oak Ridge National Laboratory (ORNL), Oak Ridge, Tennessee, the maximum irradiance from the sun, at solar noon, is about 308 Btu/(hr·ft<sup>2</sup>) [350 J/(hr·cm<sup>2</sup>)]. ASTM procedure D4803 (ASTM 1997a) relates the intensity of solar irradiance to the intensity derived from the infrared lamp via a ratio of the temperature rises above the ambient air temperature (i.e., the  $\Delta T$  for IRR black to the  $\Delta T$  for standard carbon black, see the right side of Eq. 1) to predict the specimen's solar temperature rise by:

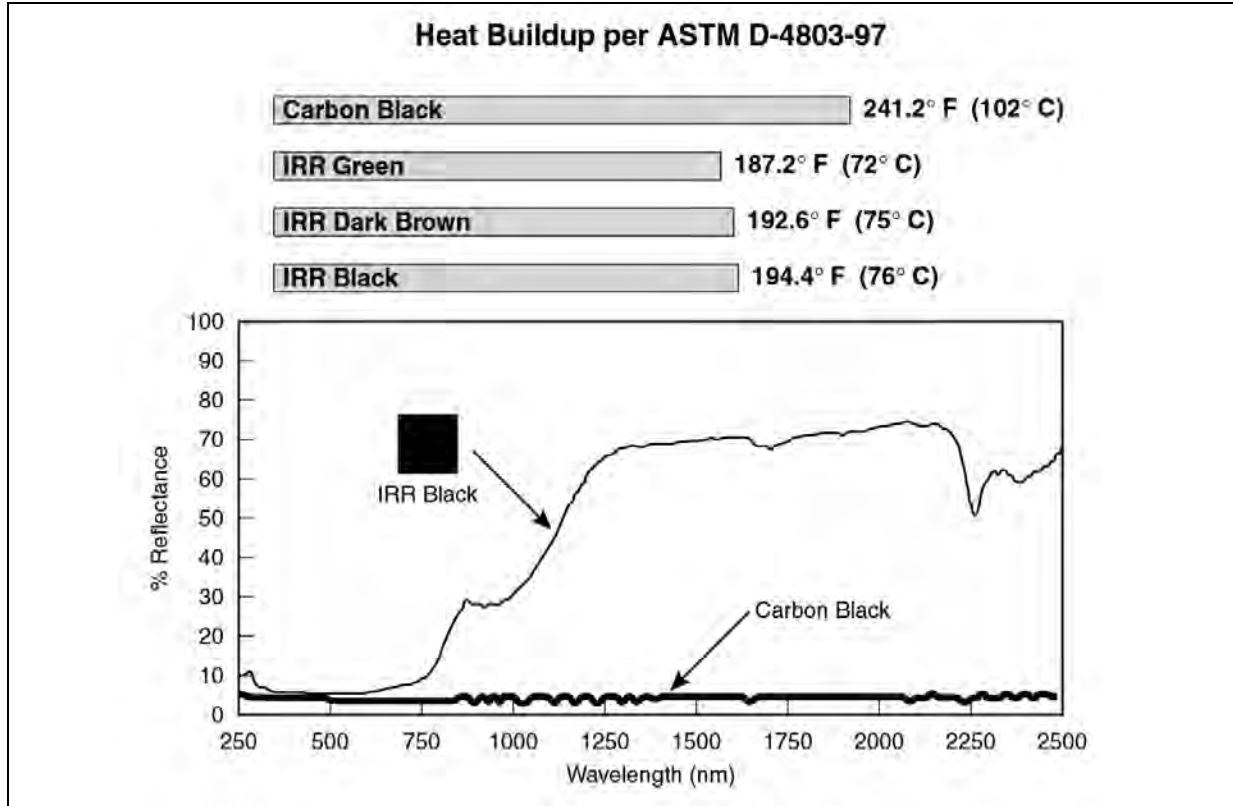
$$\left[ \frac{\Delta T_{\text{IRR Black}}}{\Delta T_{\text{black Kynar}}} \right]_{\text{solar}} = \left[ \frac{\Delta T_{\text{IRR Black}}}{\Delta T_{\text{carbon black}}} \right]_{\text{ASTM D4803}} \quad (1)$$

where

$\Delta T_{\text{IRR Black}}$  = “predicted” temperature rise above ambient air temperature for IRR black when exposed to solar irradiance

$\Delta T_{\text{black Kynar}}$  = “experimentally measured” temperature rise above ambient temperature for a black Kynar roof (~40°C above ambient as field-tested at ORNL)

**Figure 4. Heat Buildup of High-IRR Pigments vs. Standard Carbon Black and Reflectance of IRR Black vs. Standard Carbon Black**



Based on Equation (1) and summertime field data for a black Kynar metal roof tested at ORNL, the IRR black sample would be about 25°F (14°C) cooler at solar noon than a conventional dark roof.

## **Durability and Weathering of CICPs**

Testing protocols to determine the resistance to weathering of paints and coating systems designed for outdoor use include both natural, real-time weathering, such as outdoor exposure in Florida or Arizona, and accelerated tests using a weatherometer equipped with carbon-arc, fluorescent UV, and xenon-arc light sources. To evaluate color changes in roof samples with CICPs as compared to samples with standard colors, we used a one-year exposure test to natural sunlight in Florida and also a 5000-hour xenon-arc accelerated exposure test, following ASTM G-155 (ASTM 2000). Test data showed excellent light fastness for all the CICPs. Pigment stability and discoloration resistance were judged using a total color difference measure ( $\Delta E$ ) as specified by ASTM D 2244-93 (ASTM 1993). The  $\Delta E$  value for all the colors tested was a color change of approximately 1.0 or less (Figs. 5 and 6).

The total color difference value,  $\Delta E$ , is a method adopted by the paint industry to numerically identify variability in color over periods of time. This value shows the difference in color between a standard and a batch and includes the three following values computed in the formula:

- lightness ( $L$ ), where a  $+L$  value is lighter and a  $-L$  value is darker;
- redness/greenness ( $a$ ), where a  $+a$  value is redder and a  $-a$  value is greener; and
- yellowness/blueness ( $b$ ) where a  $+b$  value is yellower and a  $-b$  value is bluer.

$$\Delta E = \left[ (\Delta L)^2 + (\Delta a)^2 + (\Delta b)^2 \right]^{\frac{1}{2}}, \quad (2)$$

where

$$\Delta L = L_{\text{batch}} - L_{\text{standard}}$$

$$\Delta a = a_{\text{batch}} - a_{\text{standard}}$$

$$\Delta b = b_{\text{batch}} - b_{\text{standard}}$$

Typically, coil-coated metal roofing panels are warranted for 20 years or more and specify  $\Delta E$  of 5 units or less for that period.  $\Delta E$  color changes of 1 unit or less are almost indistinguishable from the original color, and depending on the hue of color,  $\Delta E$  of 5 or less is considered very good.

The xenon-arc accelerated weathering initially saw most of the colors rise in  $\Delta E$  up to about 1500 hours of exposure and then level off; at the end of 5000 hours all are clustered together at less than 1.5  $\Delta E$ , which is considered a very good result (Fig. 5). Control products with known performance characteristics were included in the testing to compare results with the new products. The Florida exposure data in Figure 6 is just as promising, indicating that over the one-year test period the CICPs do not fade in the presence of ozone, acid rain,  $\text{SO}_x$ ,  $\text{NO}_x$ , or other airborne pollutants. Tests have shown that CICPs remain colorfast in the presence of strong acids, bases, and oxidizing or reducing agents. They are non-migratory and showed no dissolving or bleeding in contact with airborne solvents.

## Conclusions

Accelerated weather testing using natural sunlight and xenon-arc weatherometer exposure proved that CICPs retain their color. After one year of natural sunlight exposure in south Florida the CICPs show excellent fade-resistance and remain colorfast. CICPs are very stable pigments and have excellent discoloration resistance, as proven by the 5000 hours of xenon-arc exposure; their measure of total color difference was a  $\Delta E$  value less than 1.5. Therefore, color changes in the CICPs were indistinguishable from their original color.

CICPs have a selective light absorption band in the infrared spectrum. They reflect much of the near-IR heat and therefore reduce the surface temperature upwards of 50°F (28°C) as compared to carbon black pigments when exposed to irradiance from an infrared lamp. For a steep-slope roof in the field, an IRR black would be about 25°F (14°C) cooler at solar noon than would a conventional dark roof. The lower exterior temperature leads to energy savings and provides an ancillary benefit in older existing houses with little or no attic

**Figure 5. Total Color Difference ( $\Delta E$ ) Values for Color Samples in Xenon-Arc Accelerated Weathering Test**

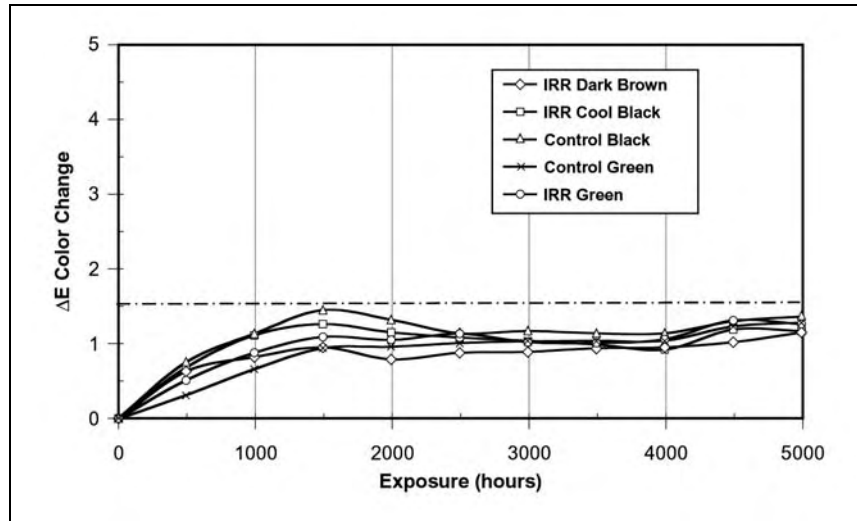
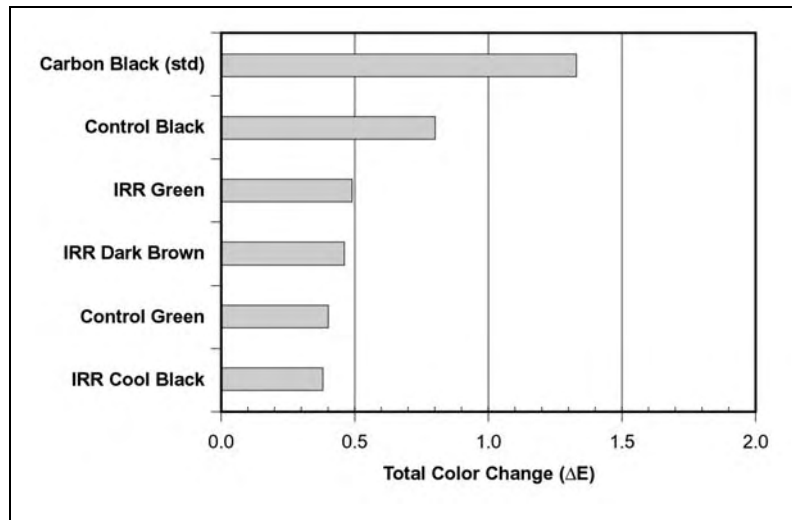


**Figure 6. Total Color Difference ( $\Delta E$ ) Values for Color Samples in One-Year Florida Weathering Test**



insulation and poorly insulated ducts in the attic because the cooler attic temperature in turn leads to reduced heat gains to the air-conditioning ductwork.

## Recommendations

The United States has about 102 million residential homes, with more than 1 million new homes being added each year (Kelso and Kinzey 2000). The space conditioning of these homes accounts for 5.78 quadrillion BTUs (quads) of site energy use per year (EIA 1995); of this amount of energy use, heat leakage through roofs contributes about 14% (Huang, Hanford & Yang 1999). The net national residential cooling load is about 1 quad, and

electrically driven air-conditioning is used in about 66 million U.S. residences (Census Bureau 1987).

Improving energy savings in residential housing for both new housing and existing homes can reduce utility loading significantly. The adoption of CICPs in roof manufacturers' products has the potential to save the nation about 0.1 quad per year. This decrease in electric demand would translate to a decrease of approximately 30.4 million tons in CO<sub>2</sub> emissions per year from utilities powered by coal. Hence, both air quality and quality of life would be improved if measures were enacted to implement the use of CICPs in tile, metal, wood shake, and asphalt shingle roofing products.

Therefore, Lawrence Berkeley National Laboratory (LBNL) and ORNL have initiated a collaborative research and development project in conjunction with pigment (colorant) manufacturers. LBNL and ORNL will work with roofing materials manufacturers to reduce the sunlit temperatures of asphalt shingles, roofing tiles, metal roofing, wood shakes, roofing membranes, and roof coatings.

The addition of CICPs to roofing products will reduce the exterior roof temperature and produce energy savings in space cooling. Moreover, in the case of asphalt shingles, durability and life expectancy should improve, helping to reduce the replacement and disposal costs of solid asphalt shingle roofing (asphalt shingles are typically replaced every 15 years).

The cost to the homeowner to achieve this efficiency improvement when replacing an asphalt roof is estimated to be an incremental cost of about 10¢ per square foot for the CICI reflective roof (Akbari, Berdahl & Levinson 2002). However, only prototypes have been developed in asphalt roofing. In coil-applied metal roofing, which is already painted, the cost could be anywhere from no additional cost to approximately 2¢ per square foot.

## References

- Akbari, H., P. Berdahl, and R. Levinson (Lawrence Berkeley National Laboratory). 2002. Personal communications.
- American Society for Testing and Materials (ASTM). 1993. *Designation D2244-93: Standard Test Method for Calculation of Color Differences from Instrumentally Measured Color*. West Conshohocken, Pa.: American Society for Testing and Materials.
- . 1997a. *Designation D4803-97: Heat Build-Up Apparatus Standard Test Procedure*. West Conshohocken, Pa.: American Society for Testing and Materials.
- . 1997b. *Designation G7-97: Standard Practice for Atmospheric Environmental Exposure Testing of Nonmetallic Materials*. West Conshohocken, Pa.: American Society for Testing and Materials.
- . 2000. *Designation G155-00a: Standard Practice for Arc Operating Xenon Arc Light Apparatus for Exposure on Non-metallic Materials*. West Conshohocken, Pa.: American Society for Testing and Materials.
- Brady, R. F., and L. V. Wake. 1992. "Principles and Formulations for Organic Coatings with Tailored Infrared Properties." *Progress in Organic Coatings* 20:1–25.



- Du Pont Ti-Pure. 1999. *Titanium Dioxide for Plastics*. Wilmington, Del.: Du Pont Corporation.
- Energy Information Administration (EIA). 1995. *1993 Residential Energy Consumption Survey (RECS)*. Washington, D.C.: U.S. Department of Energy.
- Good, C. 2001. "Eyeing the Industry: NRCA's Annual Market Survey Provides Interesting Industry Analyses." In *NRCA 2000–2001 Annual Market Survey*, 116–20. Rosemont, Ill.: National Roofing Contractors Association.
- Hardcastle, H. K. 1979. "The Cooling and Sizing Requirements of Vinyl House Siding." In *Coloring Technology for Plastics*. Ed. Ronald M. Harris. Norwich, N.Y.: William Andrew Publishing.
- Huang, J., J. Hanford, and F. Yang. 1999. *Residential Heating and Cooling Loads Component Analysis*. LBNL-44636. Berkeley, Calif.: Lawrence Berkeley National Laboratory.
- Kelso, J., and B. Kinzey. 2000. *BTS Core Data Book*. Silver Spring, Md: D&R International, and Richland, Wash.: Pacific Northwest National Laboratory.
- Martin, P., and H. L. Pezzuto. 1998. "Pigments Which Reflect Infrared Radiation from Fire." U.S. Patent 5,811,180, September 22.
- Miller, W. A., and S. Kriner. 2001. "The Thermal Performance of Painted and Unpainted Structural Standing Seam Metal Roofing Systems Exposed to One Year of Weathering." In *Thermal Performance of the Exterior Envelopes of Buildings, VIII: Proceedings of ASHRAE THERM VIII*. Clearwater, Fla.: American Society of Heating, Refrigerating, and Air-Conditioning Engineers, Dec. 2–7.
- Parker, D. S., and S. F. Barkaszi. 1997. "Roof Solar Reflectance and Cooling Energy Use: Field Research Results for Florida." *Energy and Buildings* 25 (2): 105–15.
- Parker, D. S., Y. J. Huang, S. J. Konopacki, L. M. Gartland, J. R. Sherwin, and L. Gu. 1998. "Measured and Simulated Performance of Reflective Roofing Systems in Residential Buildings." *ASHRAE Transactions* 104 (pt. 1B): 963–75.
- Parker, D. S., and J. R. Sherwin. 1998. "Comparative Summer Attic Thermal Performance of Six Roof Constructions." *ASHRAE Transactions* 104 (pt. 2): 1084–92.
- Ravinovitch, E. B., and J. W. Summers. 1984. "Infrared Reflecting Vinyl Polymer Compositions." U.S. Patent 4,424,292. January 3.
- Sliwinski, T. R., R. A. Pipoly, and R. P. Blonski. 2001. "Infrared Reflective Color Pigment." U.S. Patent 6,174,360, January 16.
- U.S. Bureau of the Census. 1987. *American Housing Survey: National Core and Supplement 1985–1987*. Washington, D.C.: Government Printing Office.

# Potentials of Urban Heat Island Mitigation\*

Hashem Akbari  
Heat Island Group  
Lawrence Berkeley National Laboratory  
(510) 486-4287  
[H\\_Akbari@lbl.gov](mailto:H_Akbari@lbl.gov)  
<http://HeatIsland.LBL.gov/>

## ABSTRACT

Urban areas tend to have higher air temperatures than their rural surroundings as a result of gradual surface modifications that include replacing the natural vegetation with buildings and roads. The term “Urban Heat Island” describes this phenomenon. The surfaces of buildings and pavements absorb solar radiation and become extremely hot, which in turn warm the surrounding air. Cities that have been “paved over” do not receive the benefit of the natural cooling effect of vegetation. As the air temperature rises, so does the demand for air-conditioning (a/c). This leads to higher emissions from power plants, as well as increased smog formation as a result of warmer temperatures. In the United States, we have found that this increase in air temperature is responsible for 5–10% of urban peak electric demand for *a/c* use, and as much as 20% of population-weighted smog concentrations in urban areas.

Simple ways to cool the cities are the use of reflective surfaces (rooftops and pavements) and planting of urban vegetation. On a large scale, the evapotranspiration from vegetation and increased reflection of incoming solar radiation by reflective surfaces will cool a community a few degrees in the summer. As an example, computer simulations for Los Angeles, CA show that resurfacing about two-third of the pavements and rooftops with reflective surfaces and planting three trees per house can cool down LA by an average of 2–3K. This reduction in air temperature will reduce urban smog exposure in the LA basin by roughly the same amount as removing the basin entire on-road vehicle exhaust. Heat island mitigation is an effective air pollution control strategy, more than paying for itself in cooling energy cost savings. We estimate that the cooling energy savings in U.S. from cool surfaces and shade trees, when fully implemented, is about \$5 billion per year (about \$100 per air-conditioned house).

## Introduction

Across the world, urban temperatures have increased faster than temperatures in rural areas. For example, from 1930 to 1990, downtown Los Angeles recorded a growth of 0.5 degrees C per decade (Akbari *et al.* 2001). Every degree increase adds about 500 megawatts (MW) to the air conditioning load in the Los Angeles Basin (Akbari *et al.* 2001). Similar increases are taxing the ability of developing countries to meet urban electricity demand, while increasing global GHG emissions. Local air pollution (e.g., particulates, volatile organics, and nitrogen oxides, which are precursors to ozone formation) are already a problem in most cities in developing countries. Higher temperatures mean increased ozone formation, with accompanying health impacts. LBNL has conducted research on both the electricity and air pollution effects of higher temperatures, and devised methods to reduce both effects. We have tested reflective coatings on building roofs and pavements, and tree-planting schemes, to demonstrate potential cost-effective reductions of

---

\* This paper is an abridged and updated version of an earlier paper published in *Solar Energy* (Akbari et al 2001).

energy use—between 10 and 40 percent. Among energy-efficiency solutions, cool roofs and cool pavements are ideally suited to hot climates that prevail in much of the developing world. Cool (light-colored) pavements also increase nighttime visibility and pavement durability.

Urban areas have typically darker surfaces and less vegetation than their surroundings (HIG 2005). These differences affect climate, energy use, and habitability of cities. At the building scale, dark roofs heat up more and thus raise the summertime cooling demands of buildings. Collectively, dark surfaces and reduced vegetation warm the air over urban areas, leading to the creation of urban "heat islands." On a clear summer afternoon, the air temperature in a typical city is as much as 2.5K higher than in the surrounding rural areas. Research shows that peak urban electric demand rises by 2–4% for each 1K rise in daily maximum temperature above a threshold of 15–20°C. Thus, the additional air-conditioning use caused by this urban air temperature increase is responsible for 5–10% of urban peak electric demand.

In California, Goodridge (1987, 1989) shows that, before 1940, the average urban-rural temperature differences for 31 urban and 31 rural stations in California were always negative, i.e., cities were cooler than their surroundings. After 1940, when built-up areas began to replace vegetation, the urban centers became as warm or warmer than the suburbs. From 1965 to 1989, urban temperatures increased by about 1K.

Regardless of whether there is an urban-rural temperature difference, data suggest that temperatures in cities are increasing. For example, the maximum temperatures in downtown Los Angeles are now about 2.5K higher than they were in 1930. The minimum temperatures are about 4K higher than they were in 1880 (Akbari *et al.* 2001). In Washington, DC, temperatures increased by about 2K between 1871 and 1987. The data indicate that this recent warming trend is typical of most U.S. metropolitan areas, and exacerbates demand for energy. Limited available data also show this increasing trend in urban temperatures in major cities of other countries (Figure 1.)

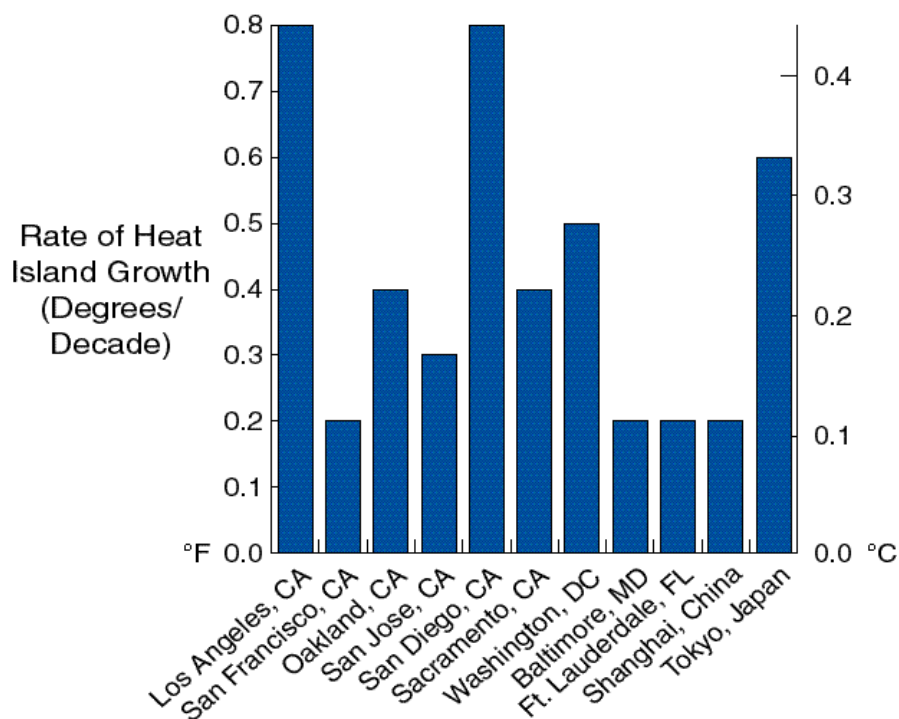
Not only do summer heat islands increase system-wide cooling loads, they also increase smog production because of higher urban air temperatures (Taha *et al.* 1994). Smog is created by photochemical reactions of pollutants in the air; and these reactions are more likely to intensify at higher temperatures. For example, in Los Angeles, for every 1°C the temperature rise above 22°C, incident of smog increases by 5%.

## Heat Islands Mitigation Technologies

Use of high-albedo<sup>†</sup> urban surfaces and planting of urban trees are inexpensive measures that can reduce summertime temperatures. The effects of modifying the urban environment by planting trees and increasing albedo are best quantified in terms of "direct" and "indirect" contributions. The direct effect of planting trees around a building or using reflective materials on roofs or walls is to alter the energy balance and cooling requirements of that particular building. However, when trees are planted and albedo is modified throughout an entire city, the energy balance of the whole city is modified, producing city-wide changes in climate. Phenomena associated with city-wide changes in climate are referred to as indirect effects, because they indirectly affect the energy use in an individual building. Direct effects give immediate benefits to the building that applies them. Indirect effects achieve benefits only with widespread deployment.

---

<sup>†</sup> When sunlight hits an opaque surface, some of the sunlight is reflected (this fraction is called the albedo =  $a$ ), and the rest is absorbed (the absorbed fraction is  $1-a$ ). Low- $a$  surfaces of course become much hotter than high- $a$  surfaces.

**Figure 1.** Increasing urban temperature trends over the last 3–8 decades in selected cities

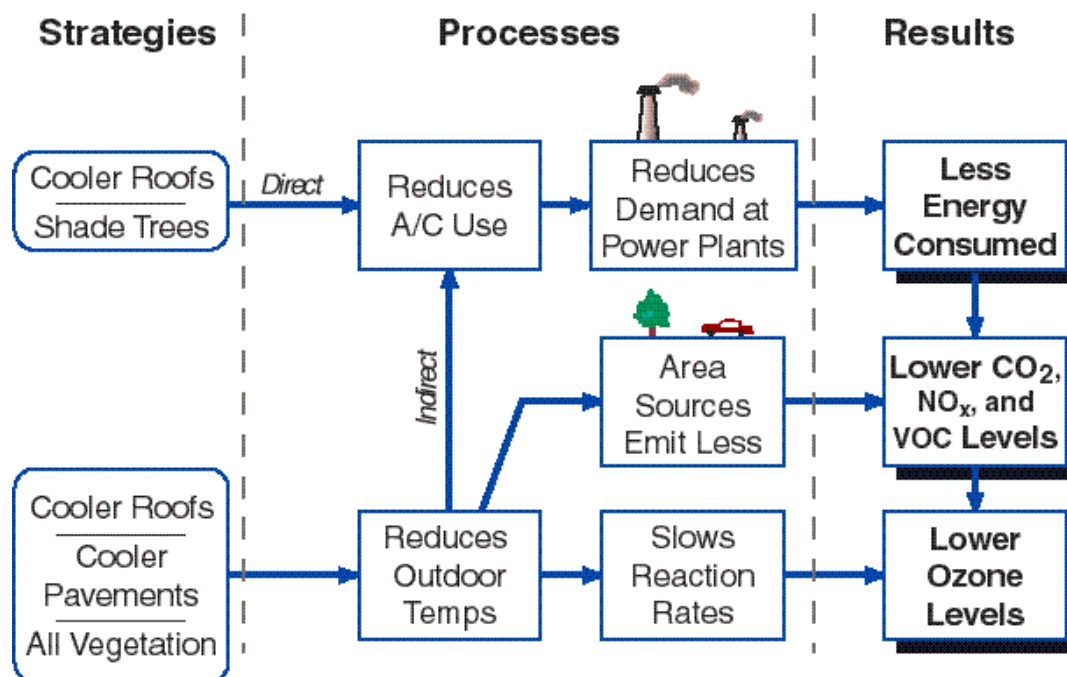
The issue of direct and indirect effects also enters into our discussion of atmospheric pollutants. Planting trees has the direct effect of reducing atmospheric CO<sub>2</sub> because each individual tree directly sequesters carbon from the atmosphere through photosynthesis. However, planting trees in cities also has an indirect effect on CO<sub>2</sub>. By reducing the demand for cooling energy, urban trees indirectly reduce emission of CO<sub>2</sub> from power plants. Akbari *et al.* (1990) showed that the amount of CO<sub>2</sub> avoided via the indirect effect is considerably greater than the amount sequestered directly. Similarly, trees directly trap ozone precursors (by dry-deposition, a process in which ozone is directly absorbed by tree leaves), and indirectly reduce the emission of these precursors from power plants (by reducing combustion of fossil fuels and hence reducing NO<sub>x</sub> emissions from power plants) (Taha 1996).

Over the past two decades, LBNL has been studying the energy savings and air-quality benefits of heat-island mitigation measures. The approaches used for analysis included direct measurements of the energy savings for cool roofs and shade trees, simulations of direct and indirect energy savings of the mitigation measures (cool roofs, cool pavements, and vegetation), and meteorological and air-quality simulations of the mitigation measures. **Figure 2** depicts the overall methodology used in analyzing the impact of heat-island mitigation measures on energy use and urban air pollution.

To understand the impacts of large-scale increases in albedo and vegetation on urban climate and ozone air quality, mesoscale meteorological and photochemical models are used (Taha *et al.* 1997). For example, Taha *et al.* (1995) and Taha (1996, 1997) used the Colorado State University Mesoscale Model (CSUMM) to simulate the Los Angeles Basin's meteorology and its sensitivity to changes in surface properties. More recently, we have utilized the PSU/NCAR mesoscale model (known as MM5) to simulate the meteorology. The Urban Airshed Model (UAM) was used to simulate the impact of the changes in meteorology and emissions on ozone

air quality. The CSUMM, MM5, and the UAM essentially solve a set of coupled governing conservation equations representing the conservation of mass (continuity), potential temperature (heat), momentum, water vapor, and chemical species continuity to obtain prognostic meteorological fields and pollutant species concentrations.

**Figure 2:** Methodology for energy and air-quality



## Cool Roofs

At the building scale, a dark roof is heated by the sun and thus directly raises the summertime cooling demand of the building beneath it. For highly absorptive (low-albedo) roofs, the difference between the surface and ambient air temperatures may be as high as 50K, while for less absorptive (high-albedo) surfaces with similar insulative properties, such as roofs covered with a white coating, the difference is only about 10K (Berdahl and Bretz 1997). For this reason, "cool" surfaces (which absorb little "insolation") can be effective in reducing cooling-energy use. Highly absorptive surfaces contribute to the heating of the air, and thus indirectly increase the cooling demand of (in principle) all buildings. In most applications, cool roofs incur no additional cost if color changes are incorporated into routine re-roofing and resurfacing schedules (Bretz *et al.* 1997 and Rosenfeld *et al.* 1992).

Most high-albedo roofing materials are light colored, although selective surfaces that reflect a large portion of the infrared solar radiation but absorb some visible light can be dark colored and yet have relatively high albedos (Levinson *et al.* 2005a,b, Berdahl and Bretz 1997).

### 1. Energy and Smog Benefits of Cool Roofs

#### Direct Energy Savings

Several field studies have documented measured energy savings that result from increasing roof solar reflectance (see **Table 1**). Akbari *et al.* (1997) reported monitored cooling-energy

savings of 46% and peak power savings of 20% achieved by increasing the roof reflectance of two identical portable classrooms in Sacramento, California. Konopacki *et al.* (1998) documented measured energy savings of 12–18% in two commercial buildings in California. Konopacki and Akbari (2001) documented measured energy savings of 12% in a large retail store in Austin, Texas. Akbari (2003) documented energy savings of 31–39 Wh/m<sup>2</sup>/day in two small commercial buildings with very high internal loads, by coating roofs with a white elastomer with a reflectivity of 0.70. Parker *et al.* (1998) measured an average of 19% energy savings in eleven Florida residences by applying reflective coatings on roofs. Parker *et al.* (1997) also monitored seven retail stores in a strip mall in Florida before and after applying a high-albedo coating to the roof and measured a 25% drop in seasonal cooling energy use. Hildebrandt *et al.* (1998) observed daily energy savings of 17%, 26%, and 39% in an office, a museum and a hospice, respectively, retrofitted with high-albedo roofs in Sacramento. Akridge (1998) reported energy savings of 28% for a school building in Georgia which had an unpainted galvanized roof that was coated with white acrylic. Boutwell and Salinas (1986) showed that an office building in southern Mississippi saved 22% after the application of a high-reflectance coating. Simpson and McPherson (1997) measured energy savings in the range of 5–28% in several quarter-scale models in Tucson AZ.

In addition to these building monitoring studies, computer simulations of cooling energy savings from increased roof albedo have been documented in residential and commercial buildings by many studies, including Konopacki and Akbari (1998), Akbari *et al.* (1998a), Parker *et al.* (1998), and Gartland *et al.* (1996). Konopacki *et al.* (1997) estimated the direct energy savings potential from high-albedo roofs in eleven U.S. metropolitan areas. The results showed that four major building types account for over 90% of the annual electricity and monetary savings: pre-1980 residences (55%), post-1980 residences (15%), and office buildings and retail stores together (25%). Furthermore, these four building types account for 93% of the total air-conditioned roof area. Regional savings were found to be a function of three factors: energy savings in the air-conditioned residential and commercial building stock; the percentage of buildings that were air-conditioned; and the aggregate regional roof area. Metropolitan-wide annual savings from the application of cool roofs on residential and commercial buildings were as much as \$37M for Phoenix and \$35M in Los Angeles and as low as \$3M in the heating-dominated climate of Philadelphia. Analysis of the scale of urban energy savings potential was further refined for five cities: Baton Rouge, LA; Chicago, IL; Houston, TX; Sacramento, CA; and Salt Lake City, UT by Konopacki and Akbari (2002, 2000).

The results for the 11 Metropolitan Statistical Areas (MSAs) were extrapolated to estimate the savings in the entire United States. The study estimates that nationally light-colored roofing could produce savings of about 10 TWh/yr (about 3.0% of the national cooling-electricity use in residential and commercial buildings), an increase in natural gas use by 26 GBtu/yr (1.6%), a decrease in peak electrical demand of 7 GW (2.5%) (equivalent to 14 power plants each with a capacity of 0.5 GW), and a decrease in net annual energy bills for the rate-payers of \$750M.

### Indirect Energy and Smog Benefits

Using the Los Angeles Basin as a case study, Taha (1996, 1997) examined the impacts of using cool surfaces (cool roofs and pavements) on urban air temperature and thus on cooling-energy use and smog. In these simulations, Taha estimates that about 50% of the urbanized area in the L.A. Basin is covered by roofs and roads, the albedos of which can realistically be raised by 0.30 when they undergo normal repairs. This results in a 2K cooling at 3 p.m. during an

August episode. This summertime temperature reduction has a significant effect on further reducing building cooling-energy use. The annual savings in Los Angeles are estimated at \$21M (Rosenfeld *et al.* 1998).

We have also simulated the impact of urban-wide cooling in Los Angeles on smog; the results show a significant reduction in ozone concentration. The simulations predict a reduction of 10–20% in population-weighted smog (ozone). In L.A., where smog is especially serious, the potential savings were valued at \$104M/year (Rosenfeld *et al.* 1998).

**Table 1.** Comparison of measured summertime air-conditioning daily energy savings from application of reflective roofs.  $\Delta\rho$  is change in roof reflectivity, RB is radiant barrier, duct is the location of air-conditioning ducts, and R-val is roof insulation in  $\text{Km}^2/\text{W}$ .

Location	Building type	Roof area [m <sup>2</sup> ]	Roof system			Savings
			R-val	duct	Δρ	[Wh/m <sup>2</sup> /day]
<b>California</b>						
Davis	Medical Office	2,945	1.4	Interior	0.36	68
Gilroy	Medical Office	2,211	3.3	Plenum	0.35	39
San Jose	Retail Store	3,056	RB	Plenum	0.44	4.3
Sacramento	School Bungalow	89	3.3	Ceiling	0.60	47
Sacramento	Office	2,285	3.3	Plenum	0.40	14
Sacramento	Museum	455	0	Interior	0.40	20
Sacramento	Hospice	557	1.9	Attic	0.40	11
Sacramento	Retail Store	1600	RB	None	0.61	72
San Marcus	Elementary School	570	5.3	None	0.54	45
Reedley	Cold Storage Facility					
	Cold storage	4900	5.1	None	0.61	69
	Fruit conditioning	1300	4.4	None	0.33	
	Packing area	3400	1.7	None	0.33	Nil (open to outdoor)
<b>Florida</b>						
Cocoa Beach	Strip Mall	1,161	1.9	Plenum	0.46	7.5
Cocoa Beach	School	929	3.3	Plenum	0.46	43
<b>Georgia</b>						
Atlanta	Education	1,115	1.9	Plenum	N/A	75
<b>Nevada</b>						
Battle Mountain	Regeneration	14.9	3.2	None	0.45	31
Carlin	Regeneration	14.9	3.2	None	0.45	39
<b>Texas</b>						
Austin	Retail Store	9,300	2.1	Plenum	0.70	39

## 2. Other Benefits of Cool Roofs

Another benefit of a light-colored roof is a potential increase in its useful life. The diurnal temperature fluctuation and concomitant expansion and contraction of a light-colored roof is smaller than that of a dark one. Also, the degradation of materials resulting from the absorption of ultra-violet light is a temperature-dependent process. For these reasons, cooler roofs may last longer than hot roofs of the same material.

## 3. Potential Problems with Cool Roofs

Several possible problems may arise from the use of reflective roofing materials (Bretz and Akbari 1994, 1997). A drastic increase in the overall albedo of the many roofs in a city has the potential to create glare and visual discomfort if not kept to a reasonable level. Fortunately, the glare for flat roofs is not a major problem for those who are at street level. For sloped roofs, the problem of glare should be studied in detail before proceeding with a full-scale implementation of this measure.

In addition, many types of building materials, such as tar roofing, are not well adapted to painting. Although such materials could be specially designed to have a higher albedo, this would entail a greater expense than painting. Additionally, to maintain a high albedo, roofs may need to be recoated or rewashed on a regular basis. The cost of a regular maintenance program could be significant.

A possible conflict of great concern is the fact that building owners and architects like to have the choice as to what color to select for their rooftops. This is particularly a concern for sloped roofs.

#### *4. Cost of Cool Roofs*

To change the albedo, the rooftops of buildings may be painted or covered with a new material. Since most roofs have regular maintenance schedules or need to be re-roofed or recoated periodically, the change in albedo should be done then to minimize the costs.

High-albedo alternatives to conventional roofing materials are usually available, often at little or no additional cost. For example, a built-up roof typically has a coating or a protective layer of mineral granules or gravel. In such conditions, it is expected that choosing a reflective material at the time of installation should not add to the cost of the roof. Also, roofing shingles are available in a variety of colors, including white, at the same price. The incremental price premium for choosing a white rather than a black single-ply membrane roofing material is less than 10%. Cool roofing materials that require an initial investment may turn out to be more attractive in terms of life-cycle cost than conventional dark alternatives. Usually, the lower life-cycle cost results from longer roof life and/or energy savings.

### **Cool Pavements**

The practice of widespread paving of city streets with asphalt began only within the past century. The advantages of this smooth and all-weather surface for the movement of bicycles and automobiles are obvious, but some of the associated problems are perhaps not so well appreciated. One consequence of covering streets with dark asphalt surfaces is the increased heating of the city by sunlight. The pavements in turn heat the air. LBNL has conducted studies to measure the effect of albedo on pavement temperature. The data clearly indicate that significant modification of the pavement surface temperature can be achieved: a 10K decrease in temperature for a 0.25 increase in albedo. If urban surfaces were lighter in color, more of the incoming light would be reflected back into space and the surfaces and the air would be cooler. This tends to reduce the need for air conditioning. Pomerantz *et al.* (1997) present an overview of cool paving materials for urban heat island mitigation.

#### *1. Energy and Smog Benefits of Cool Pavements*

Cool pavements provide only indirect effects through lowered ambient temperatures. Lower temperature has two effects: 1) reduced demand for electricity for air conditioning and 2) decreased production of smog (ozone). Rosenfeld *et al.* (1998) estimated the cost savings of



reduced demand for electricity and of the externalities of lower ozone concentrations in the Los Angeles Basin.

Simulations for Los Angeles (L.A.) basin indicate that a reasonable change in the albedo of the city could cause a noticeable decrease in temperature. Taha (1997) predicted a 1.5K decrease in temperature of the downtown area. The lower temperatures in the city are calculated based on the assumption that all roads and roofs are improved. From the meteorological simulations of three days in each season, the temperature changes for every day in a typical year were estimated for Burbank, typical of the hottest 1/3 of L.A. basin. The energy consumptions of typical buildings were then simulated for the original weather and also for the modified weather. The differences are the annual energy changes due to the decrease in ambient temperature. The result is a city-wide annual saving of about \$71M, due to combined albedo and vegetation changes. The kWh savings attributable to the pavement are \$15M/yr, or \$0.012/m<sup>2</sup>-yr. Analysis of the hourly demand indicates that cooler pavements could save an estimated 100 MW of peak power in L.A.

The simulations of the effects of higher albedo on smog formation indicate that an albedo change of 0.3 throughout the developed 25% of the city would yield a 12% decrease in the population-weighted ozone exceedance of the California air-quality standard (Taha 1997). It has been estimated (Hall *et al.* 1992) that residents of L.A. would be willing to pay about \$10 billion per year to avoid the medical costs and lost work time due to air pollution. The greater part of pollution is particulates, but the ozone contribution averages about \$3 billion/yr. Assuming a proportional relationship of the cost with the amount of smog exceedance, the cooler-surfaced city would save 12% of \$3 billion/yr, or \$360M/yr. As above, we attribute about 21% of the saving to pavements. Rosenfeld *et al.* (1998) value the benefits from smog improvement by altering the albedo of all 1250km<sup>2</sup> of pavements by 0.25 saves about \$76M/year (about \$0.06/m<sup>2</sup> per year).

## 2. Other Benefits of Cool Pavements

It has long been known that the temperature of a pavement affects its performance (Yoder & Witzak 1975). This has been emphasized by the new system of binder specification advocated by the Strategic Highway Research Program (SHRP). Beginning in 1987, this program led pavement experts to carry out the task of researching and then recommending the best methods of making asphalt concrete pavements. A result of this study was the issuance of specifications for the asphalt binder. The temperature range which the pavement will endure is a primary consideration (Cominsky *et al.* 1994). The performance grade (PG) is specified by two temperatures: (1) the average 7-day maximum temperature that the pavement will likely encounter, and (2) the minimum temperature the pavement will likely attain.

Reflectivity of pavements is also a safety factor in visibility at night and in wet weather, affecting the demand for electric street lighting. Street lighting is more effective if pavements are more reflective, which can lead to greater safety; or, alternatively, less lighting could be used to obtain the same visibility. These benefits have not yet been monetized.

## 3. Potential Problems with Cool Pavements

A practical drawback of high reflectivity is glare, but this does not appear to be a problem. We suggest a change in resurfacing using not black asphalt, with an albedo of about 0.05–0.12, but the application of a product with an albedo of about 0.35, similar to that of cement concrete. The experiment to test whether this will be a problem has already been performed: every day

millions of people drive on cement concrete roads, and we rarely hear of accidents caused by glare, or of people even complaining about the glare on such roads.

There is also a concern that, after some time, light-colored pavement will darken because of dirt. This tends to be true, but again, experience with cement concrete roads suggests that the light color of the pavement persists after long usage. Most drivers can see the difference in reflection between an asphalt and a cement concrete road when they drive over them, even when the roads are old.

#### *4. Cost of Cool Pavements*

It is clear that cooler pavements will have energy, environmental, and engineering benefits. The issue is then whether there are ways to construct pavements that are feasible, economical, and cooler. The economic question is whether the savings generated by a cool pavement over its lifetime are greater than its extra cost. Properly, one should distinguish between initial cost and lifetime costs (including maintenance, repair time, and length of service of the road). Often the initial cost is decisive.

A typical asphalt concrete contains about 7% of asphalt by weight, or about 17% by volume; the remainder is rock aggregate, except for a few percent of voids. In one ton of mixed asphalt concrete the cost of materials only is about \$28/ton, of which about \$9 is in the binder and \$19 is in the aggregate. For a pavement about 10 cm thick (4 inches), with a density of 2.1 ton/m<sup>3</sup>, the cost of the binder is about \$2 per m<sup>2</sup> and aggregate costs about \$4.2 per m<sup>2</sup>.

Using the assumptions for Los Angeles, a cooler pavement would generate a stream of savings of \$0.07/m<sup>2</sup> per year for the lifetime of the road—about 20 years. The present value of potential savings at a real discount rate of 3% is \$1.1/m<sup>2</sup>. This saving would allow for purchase of a binder costing \$3/m<sup>2</sup>, instead of \$2/m<sup>2</sup>—or 50% more. Alternatively, one could buy aggregate; instead of spending \$4.2/m<sup>2</sup>, one can now afford \$5.2/m<sup>2</sup> (a 20% more expensive, whiter aggregate). It is doubtful that such modest increases in costs can buy much whiter pavements.

At some times in its life, a pavement needs to be maintained, i.e., resurfaced. This offers an opportunity to get cooler pavements economically. Good maintenance practice calls for resurfacing a new road after about 10 years (Dunn 1996) and the lifetime of resurfacing is only about 5 years. Hence, within 10 years, all the asphalt concrete surfaces in a city can be made light colored. As part of this regular maintenance, any additional cost of the whiter material will be minimized.

For pavements, the energy and smog savings may not pay for whiter roads. However, if the lighter-colored road leads to substantially longer lifetime, the initial higher cost may be offset by lifetime savings.

### ***Shade trees and urban vegetation***

Akbari 2002 provides an overview of benefits and cost associated with planting urban trees. Shade trees intercept sunlight before it warms a building. The urban forest cools the air by evapotranspiration. Trees also decrease the wind speed under their canopy and shield buildings from cold winter breezes. Urban shade trees offer significant benefits by both reducing building air conditioning and lowering air temperature, and thus improving urban air quality by reducing smog. Over the life of a tree, the savings associated with these benefits vary by climate region and can be up to \$200 per tree. The cost of planting trees and maintaining them can vary from \$10 to \$500 per tree. Tree planting programs can be designed to be low cost, so they can offer

savings to communities that plant trees.

### *1. Energy and Smog Benefits of Shade Trees*

#### Direct Energy Savings

Data on measured energy savings from urban trees are scarce. In one experiment, Parker (1981) measured the cooling-energy consumption of a temporary building in Florida before and after adding trees and shrubs and found cooling-electricity savings of up to 50%. In the summer of 1992, Akbari *et al.* (1997) monitored peak-power and cooling-energy savings from shade trees in two houses in Sacramento, California. The collected data included air-conditioning electricity use, indoor and outdoor dry-bulb temperatures and humidities, roof and ceiling surface temperatures, inside and outside wall temperatures, insolation, and wind speed and direction. The shading and microclimate effects of the trees at the two monitored houses yielded seasonal cooling-energy savings of 30%, corresponding to average savings of 3.6 and 4.8 kWh/day. Peak-demand savings for the same houses were 0.6 and 0.8 kW (about 27% savings in one house and 42% in the other).

DeWalle *et al.* (1983), Heisler (1989), and Huang *et al.* (1990) have focused on measuring and simulating the wind-shielding effects of tree on heating- and cooling-energy use. Their analysis indicated that a reduction in infiltration because of trees would save heating-energy use. However, in climates with cooling-energy demand, the impact of windbreak on cooling is fairly small compared to the shading effects of trees and, depending on climate, it could decrease or increase cooling-energy use. In cold climates, the wind-shielding effect of trees can reduce heat-energy use in buildings. However, using strategically placed deciduous trees can decrease winter heating penalties. Akbari and Taha (1992) simulated the wind-shielding impact of trees on heating-energy use in four Canadian cities. For several prototypical residential buildings, they estimated heating-energy savings in the range of 10–15%.

Taha *et al.* (1996) simulated the meteorological impact of large-scale tree-planting programs in 10 U.S. metropolitan areas: Atlanta GA, Chicago IL, Dallas TX, Houston TX, Los Angeles CA, Miami FL, New York NY, Philadelphia PA, Phoenix AZ, and Washington, DC. The DOE-2 building simulation program was then used to estimate the direct and indirect impacts of trees on saving cooling-energy use for two building prototypes: a single-family residence and an office. The calculations accounted for a potential increase in winter heating-energy use, and showed that in most hot cities, shading a building can save annually \$5 to \$25 per 100m<sup>2</sup> of roof area of residential and commercial buildings.

#### Indirect Energy and Smog Benefits

Taha *et al.* (1996) estimated the impact on ambient temperature resulting from a large-scale tree-planting program in the selected 10 cities. They used a three-dimensional meteorological model to simulate the potential impact of trees on ambient temperature for each region. The mesoscale simulations showed that, on average, trees can cool down cities by about 0.3K to 1K at 2 pm.; in some simulation cells the temperature was decreased by up to 3K. The corresponding air-conditioning savings resulting from ambient cooling by trees in hot climates ranges from \$5 to \$10 per year per 100m<sup>2</sup> of roof area of residential and commercial buildings. Indirect effects are smaller than the direct effects of shading, and, moreover, require that the entire city be planted.

Rosenfeld *et al.* (1998) studied the potential benefits of planting 11M trees in the Los Angeles Basin. They estimate an annual total savings of \$270 million from direct and indirect

energy savings and smog benefit; about 2/3 of the savings resulted from the reduction in smog concentration resulting from meteorological changes due to the evapotranspiration of trees. It also has been suggested that trees improve air quality by dry-depositing NO<sub>x</sub>, O<sub>3</sub>, and PM10 particulates. Rosenfeld *et al.* (1998) estimate that 11M trees in LA will reduce PM10 by less than 0.1%, worth only \$7M, which is disappointingly smaller than the benefits of \$180M from smog reduction.

The present value (PV) of savings is calculated to find out how much a homeowner can afford to pay for shade trees. Rosenfeld *et al.* (1998) estimate that, on this basis, the direct savings to a homeowner who plants three shade trees would have a present value of about \$200 per home (\$68/tree). The present value of indirect savings was smaller, about \$72/home (\$24/tree). The PV of smog savings was about \$120/tree. Total PV of all benefits from trees was thus \$210/tree.

## 2. Other Benefits of Shade Trees

There are other benefits associated with urban trees. Some of these include improvement in the quality of life, increased value of properties, decreased rain run-off water and hence a protection against floods (McPherson *et al.* 1994). Trees also directly sequester atmospheric carbon dioxide, but Rosenfeld *et al.* (1998) estimate that the direct sequestration of CO<sub>2</sub> is less than one-fourth of the emission reduction resulting from savings in cooling-energy use. These other benefits of trees are not considered in the cost benefit analysis shown in this paper.

## 3. Potential Problems with Shade Trees

There are some potential problems associated with trees. Some trees emit volatile organic compounds (VOCs) that exacerbate the smog problem. Obviously, selection of low-emitting trees should be considered in a large-scale tree-planting program. Benjamin *et al.* (1996) have prepared a list of several hundred tree species with their average emission rate.

In dry climates and areas with a serious water shortage, drought-resistant trees are recommended. Some trees need significant maintenance that may entail high costs over the life of the trees. Tree roots can damage underground pipes, pavements and foundations. Proper design is needed to minimize these effects. Also, trees are a fuel source for fire; selection of appropriate tree species and planting them strategically to minimize the fire hazard should be an integral component of a tree-planting program.

## 4. Cost of Trees

The cost of a citywide tree-planting program depends on the type of program offered and the types of trees recommended. At the low end, a promotional planting of trees 5–10 feet high costs about \$10 per tree, whereas a professional tree-planting program using fairly large trees could amount to \$150–470 a tree (McPherson 1994). McPherson has collected data on the cost of tree planting and maintenance from several cities. The cost elements include planting, pruning, removal of dead trees, stump removal, waste disposal, infrastructure repair, litigation and liability, inspection, and program administration. The data provide details of the cost for trees located in parks, in yards, and along streets, highways, and houses. The present value of all these life-cycle costs (including planting) is \$300–500 per tree. Over 90% of the cost is associated with professional planting, pruning, tree and stump removal. On the other hand, a program administered by the Sacramento Municipal Utility District (SMUD) and Sacramento Tree Foundation in 1992–1996 planted 20-foot tall trees at an average cost of \$45 per tree. This only

includes the cost of a tree and its planting; it does not include pruning, removal of dead trees, and removal of stumps. With this wide range of costs associated with trees, in our opinion, tree costs should be justified by other amenities they provide beyond air-conditioning and smog benefits. The best programs are probably the information programs that provide data on energy and smog savings of trees to the communities and homeowners that are considering planting trees for other reasons.

## 5. Conclusions

Cool surfaces (cool roofs and cool pavements) and urban trees can have a substantial effect on urban air temperature and hence can reduce cooling-energy use and smog. We estimate that about 20% of the national cooling demand can be avoided through a large-scale implementation of heat-island mitigation measures. This amounts to 40 TWh/year savings, worth over \$4B per year by 2015 in cooling-electricity savings alone. Once the benefits of smog reduction are accounted for, the total savings could add up to over \$10B per year.

Achieving these potential savings is conditional on receiving the necessary federal, state, and local community support. Scattered programs for planting trees and increasing surface albedo already exist, but to start an effective and comprehensive campaign would require an aggressive agenda. We are collaborating with the American Society for Testing of Materials (ASTM), the Cool Roof Rating Council (CRRC), and the industry, to create test procedures, ratings, and labels for cool materials. The cool roofs criteria and standards are incorporated into the Building Energy Performance Standards of ASHRAE (American Society of Heating Refrigeration, and Airconditioning Engineers), California Title 24, and the California South Coast's Air Quality Management Plans. Many field projects have demonstrated the energy benefits of cool roofs and shade trees. The South Coast Air Quality Management District and the United States Environmental Protection Agency (EPA) now recognize that air temperature is as much a cause of smog as NO<sub>x</sub> or volatile organic compounds. In 1992, the EPA published a milestone guideline for tree planting and light-colored surfacing (Akbari *et al.* 1992). Many countries have joined efforts in developing heat-island-reduction programs to improve urban air quality. The efforts in Japan are of notable interest.

## 6. Acknowledgement

This work was supported by the Assistant Secretary for Conservation and Renewable Energy, Office of Building Technologies of the U. S. Department of Energy and the California Energy Commission under contract No. DE-AC0376SF00098.

## 7. References

- Akbari, H. 2003. "Measured energy savings from the application of reflective roofs in 2 small non-residential buildings," *Energy*, **28**:953-967.
- Akbari, H., 2002. "Shade trees reduce building energy use and CO<sub>2</sub> emissions from power plants," *Environmental Pollution*, **116**:S119-S126.
- Akbari, H., M. Pomerantz, and H. Taha. 2001. "Cool surfaces and shade trees to reduce energy use and improve air quality in urban areas," *Solar Energy*, **70**(3):295-310.
- Akbari, H., S. Konopacki, C. Eley, B. Wilcox, M. Van Geem and D. Parker. 1998a. "Calculations for Reflective Roofs in Support of Standard 90.1," *ASHRAE Transactions*

104(1):984-995.

- Akbari, H., L. Gartland, and S. Konopacki. 1998b. "Measured Energy Savings of Light-colored Roofs: Results from Three California Demonstration Sites," *Proceedings of the 1998 ACEEE Summer Study on Energy Efficiency in Buildings*, Vol. 3, p. 1.
- Akbari, H., S. Bretz, D. Kurn, and J. Hanford. 1997. "Peak Power and Cooling Energy Savings of High-Albedo Roofs," *Energy and Buildings* **25**:117-126.
- Akbari, H., S. Bretz, H. Taha, D. Kurn, and J. Hanford. 1997. "Peak Power and Cooling Energy Savings of High-albedo Roofs," *Energy and Buildings - Special Issue on Urban Heat Islands and Cool Communities*, **25**(2):117-126.
- Akbari, H., S. Davis, S. Dorsano, J. Huang, and S. Winnett (editors). 1992. *Cooling Our Communities: A Guidebook on Tree Planting and Light-Colored Surfacing*, U. S. Environmental Protection Agency, Office of Policy Analysis, Climate Change Division.
- Akbari, H., A. Rosenfeld, and H. Taha. 1990. "Summer Heat Islands, Urban Trees, and White Surfaces," *ASHRAE Transactions*, **96**(1), American Society for Heating, Refrigeration, and Air Conditioning Engineers, Atlanta, Georgia.
- Akbari, H. and H. Taha. 1992. "The Impact of Trees and White Surfaces on Residential Heating and Cooling Energy Use in Four Canadian Cities," *Energy, the International Journal*, **17**(2):141-149.
- Akridge, J. 1998. "High-Albedo Roof Coatings - Impact on Energy Consumption," *ASHRAE Technical Data Bulletin* **14**(2).
- Benjamin, M.T., M. Sudol, L. Bloch, and A.M. Winer. 1996. "Low-emitting urban forests: A taxonomic methodology for assigning isoprene and monoterpene emission rates," *Atmospheric Environment*, **30**(9):1437-1452.
- Berdahl, P. and S. Bretz. 1997. "Preliminary Survey of the Solar Reflectance of Cool Roofing Materials," *Energy and Buildings - Special Issue on Urban Heat Islands and Cool Communities*, **25**(2):149-158.
- Boutwell, C. and Y. Salinas. 1986. "Building for the Future—Phase I: An Energy Saving Materials Research Project," Oxford: Mississippi Power Co., Rohm and Haas Co. and the University of Mississippi.
- Bretz, S., H. Akbari, and A. Rosenfeld. 1997. "Practical Issues for Using High-Albedo Materials to Mitigate Urban Heat Islands," *Atmospheric Environment*, **32**(1):95-101.
- Bretz, S. and H. Akbari. 1997. "Long-term Performance of High-Albedo Roof Coatings," *Energy and Buildings - Special Issue on Urban Heat Islands and Cool Communities*, **25**(2):159-167.
- Bretz, S. and H. Akbari. 1994. "Durability of High-Albedo Roof Coatings," *Proceedings of the ACEEE 1994 Summer Study on Energy Efficiency in Buildings*, Vol. 9, p. 65.
- Cominsky, R.J., G.A. Huber, T.W. Kennedy, and M. Anderson. 1994. The Superpave Mix Design Manual for New Construction and Overlays. SHRP-A-407. Washington, DC: National Research Council.
- DeWalle D.R., G.M. Heisler, R.E. Jacobs. 1983. "Forest home sites influence heating and cooling energy," *Journal of Forestry*, **81**(2):84-87.

- Dunn, B.H. 1996. "What you need to know about slurry seal," *Better Roads* March 1996: 21-25.
- Gartland, L., S. Konopacki, and H. Akbari. 1996. "Modeling the Effects of Reflective Roofing," *Proceedings of the ACEEE 1996 Summer Study on Energy Efficiency in Buildings* 4:117-124. Pacific Grove, CA.
- Goodridge, J. 1989. "Air temperature trends in California, 1916 to 1987," J. Goodridge, 31 Rondo Ct., Chico CA 95928.
- Goodridge, J. 1987. "Population and temperature trends in California," *Proceedings of the Pacific Climate Workshop*, Pacific Grove CA, March 22-26.
- Hall, J.V., A.M. Winer, M.T. Kleinman, F.M. Lurmann, V. Brajer and S.D. Colome. 1992. "Valuing the Health Benefits of Clean Air," *Science*, **255**: 812-817.
- HIG. 2005. Heat Island Group world-wide web: <http://HeatIsland.LBL.gov> . Lawrence Berkeley National Laboratory, Berkeley, CA.
- Heisler, G.M. 1989. "Effects of trees on wind and solar radiation in residential neighborhoods," Final report on site design and microclimate research, ANL No. 058719, Argonne National Laboratory, Argonne, IL.
- Hildebrandt, E., W. Bos and R. Moore. 1998. "Assessing the Impacts of White Roofs on Building Energy Loads," *ASHRAE Technical Data Bulletin* **14**(2).
- Huang, Y.J., H. Akbari, H. Taha. 1990. "The wind-shielding and shading effects of trees on residential heating and cooling requirements," *ASHRAE Transactions*, **96**(1), American Society of Heating, Refrigeration, and Air conditioning Engineers, Atlanta, Georgia, (February).
- Konopacki, S. and H. Akbari. 2002 "Energy savings of heat-island-reduction strategies in Chicago and Houston (including updates for Baton Rouge, Sacramento, and Salt Lake City," Lawrence Berkeley National Laboratory Report LBL-49638, Berkeley, CA.
- Konopacki, S. and H. Akbari. 2001. "Measured Energy Savings and Demand Reduction from a Reflective Roof Membrane on a Large Retail Store in Austin," Report number LBNL-47149. Berkeley, CA: Lawrence Berkeley National Laboratory, 2001.
- Konopacki, S. and H. Akbari. 2000. "Energy Savings Calculations for Heat Island Reduction Strategies in Baton Rouge, Sacramento and Salt Lake City," Lawrence Berkeley National Laboratory Report LBNL-42890. Berkeley, CA.
- Konopacki, S. and H. Akbari. 1998. "Simulated Impact of Roof Surface Solar Absorptance, Attic, and Duct Insulation on Cooling and Heating Energy Use in Single-Family New Residential Buildings," Lawrence Berkeley National Laboratory Report LBNL-41834. Berkeley, CA.
- Konopacki, S., H. Akbari, L. Gartland, and L. Rainer. 1998. "Demonstration of Energy Savings of Cool Roofs," Lawrence Berkeley National Laboratory Report LBNL-40673. Berkeley, CA.
- Konopacki, S., H. Akbari, S. Gabersek, M. Pomerantz, and L. Gartland. 1997. "Cooling Energy Saving Potentials of Light-Colored Roofs for Residential and Commercial Buildings in 11 U.S. Metropolitan Areas," Lawrence Berkeley National Laboratory Report LBNL-39433,

Berkeley, CA.

- Levinson, R., P. Berdahl, and H. Akbari. 2005a. "Solar spectral optical properties of pigments, part I: Model for deriving scattering and absorption coefficients from transmittance and reflectance measurements," *Solar Energy Materials & Solar Cells* (in press).
- , 2005b. "Solar spectral optical properties of pigments, part II: Survey of common colorants," *Solar Energy Materials & Solar Cells* (in press).
- McPherson, E.G., D.J. Nowak, and R.A. Rowntree. 1994. "Chicago's urban forest ecosystem: results of the Chicago Urban Forest Climate Project," Forest Service, U. S. Dept. of Agriculture. NE-186.
- Milford, J.B., G.R. Armistead, and G.J. McRae. 1989. "A New Approach to Photochemical Pollution Control: Implications of Spatial Patterns in Pollutant Responses to Reduction in Nitrogen Oxides and Reactive Organic Emissions," *Environmental Science and Technology*, **23**, pp. 1290-1301.
- Parker, D., J. Huang, S. Konopacki, L. Gartland, J. Sherwin, and L. Gu. 1998. "Measured and Simulated Performance of Reflective Roofing Systems in Residential Buildings," *ASHRAE Transactions* **104**(1):963-975.
- Parker, D., J. Sonne, and J. Sherwin. 1997. "Demonstration of Cooling Savings of Light Colored Roof Surfacing in Florida Commercial Buildings: Retail Strip Mall," Florida Solar Energy Center Report FSEC-CR-964-97. Cocoa, FL.
- Parker, J. H. 1981. "Use of landscaping for energy conservation," Department of Physical Sciences, Florida International University, Miami, Florida.
- Pomerantz, M., H. Akbari, A. Chen, H. Taha, and A.H. Rosenfeld. 1997. "Paving Materials for Heat Island Mitigation," Lawrence Berkeley National Laboratory Report LBNL-38074. Berkeley, CA
- Rosenfeld, A.H., J.J. Romm, H. Akbari, and M. Pomerantz. 1998. "Cool Communities: Strategies for Heat Islands Mitigation and Smog Reduction," *Energy and Buildings*, **28**, pp. 51-62.
- Rosenfeld A., H. Akbari, H. Taha, and S. Bretz. 1992. "Implementation of Light-Colored Surfaces: Profits for Utilities and Labels for Paints," *Proceedings of the ACEEE 1992 Summer Study on Energy Efficiency in Buildings*, Vol. 9, p. 141.
- Simpson J.R. and E.G. McPherson. 1997. "The Effect of Roof Albedo Modification on Cooling Loads of Scale Residences in Tucson, Arizona," *Energy and Buildings*; **25**:127-137.
- Taha, H. 1997. "Modeling the impacts of large-scale albedo changes on ozone air quality in the South Coast Air Basin," *Atmospheric Environment*, **31**(11):1667-1676.
- Taha, H. 1996. "Modeling the Impacts of Increased Urban Vegetation on the Ozone Air Quality in the South Coast Air Basin," *Atmospheric Environment*, **30**(20):3423-3430.
- Taha, H., S. Douglas, and J. Haney. 1994. "The UAM Sensitivity Analysis: The August 26-28 1987 Oxidant Episode," Chapter 1 in "Analysis of Energy Efficiency and Air Quality in the South Coast Air Basin - Phase II", by H. Taha *et al.*, Lawrence Berkeley Laboratory Report LBL-35728, Berkeley, CA.



- Taha, H., S. Douglas, J. Haney, A. Winer, M. Benjamin, D. Hall, J. Hall, X. Liu, and B. Fishman. 1995. "Modeling the ozone air quality impacts of increased albedo and urban forest in the South Coast Air Basin," Lawrence Berkeley Laboratory Report LBL-37316, Berkeley, CA.
- Taha, H., S. Konopacki, and S. Gabersek. 1996. "Modeling the Meteorological and Energy Effects of Urban Heat Islands and their Mitigation: A 10-Region Study," Lawrence Berkeley Laboratory Report LBL-38667, Berkeley, CA.
- Taha, H., S. Douglas, and J. Haney. 1997. "Mesoscale meteorological and air quality impacts of increased urban albedo and vegetation," *Energy and Buildings - Special Issue on Urban Heat Islands and Cool Communities*, **25**(2):169-177.
- Yoder, E.J. and M.W. Witzak. 1975. *Principles of Pavement Design*, New York, NY: Wiley and Sons.

# **Solar Spectral Optical Properties of Pigments**

Ronnen Levinson, Ph.D.

Paul Berdahl, Ph.D.

Hashem Akbari, Ph.D.

Owners of homes with pitched roofs visible from ground level often prefer non-white roofing products for aesthetic considerations. This paper reports on a collaborative research between a U.S. national laboratory and the industry for developing cool colored materials for sloped roofs. The suitability of a pigment for inclusion in “cool” colored coatings with high solar reflectance can be determined from its solar spectral backscattering and absorption coefficients. Pigment characterization is performed by dispersing the pigment into a transparent film and then measuring spectral transmittance and reflectance. Measurements of the reflectance of film samples on black and white substrates are also used. Various pigments are characterized by determination of absorption and backscattering coefficients as functions of wavelength in the solar spectral range of 300 to 2500 nanometers. Pigments in widespread use are examined, with particular emphasis on those that may be useful for formulating non-white materials that can reflect the near-infrared (NIR) portion of sunlight, such as the complex inorganic color pigments (mixed metal oxides). These materials remain cooler in sunlight than comparable colors. NIR-absorptive pigments are to be avoided. High NIR reflectance can be produced by a reflective metal substrate, an NIR-reflective underlayer, or directly by using of a pigment that scatters strongly in the NIR.

# Solar Spectral Optical Properties of Pigments<sup>1</sup>

Owners of homes with pitched roofs visible from ground level often prefer non-white roofing products for aesthetic considerations. This paper reports on a collaborative research between a U.S. national laboratory and the industry for developing cool colored materials for sloped roofs. The suitability of a pigment for inclusion in “cool” colored coatings with high solar reflectance can be determined from its solar spectral backscattering and absorption coefficients. Pigment characterization is performed by dispersing the pigment into a transparent film and then measuring spectral transmittance and reflectance. Measurements of the reflectance of film samples on black and white substrates are also used. Various pigments are characterized by determination of absorption and backscattering coefficients as functions of wavelength in the solar spectral range of 300 to 2500 nanometers. Pigments in widespread use are examined, with particular emphasis on those that may be useful for formulating non-white materials that can reflect the near-infrared (NIR) portion of sunlight, such as the complex inorganic color pigments (mixed metal oxides). These materials remain cooler in sunlight than comparable colors. NIR-absorptive pigments are to be avoided. High NIR reflectance can be produced by a reflective metal substrate, an NIR-reflective underlayer, or directly by using of a pigment that scatters strongly in the NIR.

## INTRODUCTION

Nonwhite pigments with high near-infrared (NIR) reflectance historically have been used to camouflage military surfaces (by mimicking foliage) and to minimize solar heating of dark exterior architectural surfaces, such as colored vinyl siding and gray battleship hulls (Brade and Wake, 1992; Burkhart et al., 2001; Sliwinski et al., 2001). In recent years roofing manufacturers have incorporated NIR-reflecting pigments in coatings applied to a variety of nonwhite roofing products, such as metal panels and clay tiles (Nixon, 2003; Ferro, 2004; Shepherd, 2004; BASF, 2004; Custom-Bilt, 2004; MCA, 2004). In this paper we compute the solar spectral absorption and backscattering coefficients of a wide variety of pigments that may be used in architectural coatings.

Visible light (400 to 700 nanometers) accounts for only 43% of the energy in the air-mass 1.5 global solar irradiance spectrum (300 to 2500 nm) typical of North-American insolation (ASTM, 2003); the remainder arrives as near-infrared (700 to 2500 nm, 52%) or ultraviolet (300 to 400 nm, 5%) radiation (Figure). Hence, replacing NIR-absorbing (“conventional”) roofing with visually similar, infrared-reflecting (“cool”) roofing can significantly reduce building heat gain.

A cool coating must have low visible transmittance to hide its background and low NIR absorptance to minimize NIR heat gain. Cool films may be subclassified as either “NIR-reflecting” or “NIR-transmitting.” An NIR-reflecting film is always cool, while an NIR-transmitting film requires an NIR-reflecting background (e.g., a shiny metal or a white coating) to form a colored NIR-reflecting composite (Brady and Wake, 1992; Genjima and Mockizuki, 2003).

A paint is a dispersion of pigment particles (e.g., titania) in a clear binder, such as acrylic. The propagation of light through pigmented coatings is of natural interest to the coating and colorant industries and has been extensively studied over the past century. One of the simplest and most popular continuum models is the two-flux theory introduced by Schuster in 1905 and popularized by Kubelka and Munk (Kubelka, 1948; Kortum, 1969; Bohren, 1987; Judd, 1952; Johnson, 1988). The Kubelka-Munk (K-M)

---

<sup>1</sup> Ronnen Levinson, Ph.D. is scientist, Environmental Energy Technologies Division, Lawrence Berkeley National Laboratory. Paul Berdahl, Ph.D. is applied solid-state physicist, Environmental Energy Technologies Division, Lawrence Berkeley National Laboratory. Hashem Akbari, Ph.D. is staff scientist and Heat Island Group leader, Environmental Energy Technologies Division, Lawrence Berkeley National Laboratory.

model describes the one-dimensional, bidirectional propagation of diffuse light through a film by parameterizing the rates at which the film absorbs and/or backscatters light.

We compute absorption and backscattering coefficients from spectrometer measurements of film reflectance and transmittance. We examine 87 pigmented coatings, identifying both cool pigments — i.e., those that can be used to make NIR-reflecting or NIR-transmitting cool coatings — and pigments that should be excluded from cool coatings. Our goal is to provide complete solar spectral absorption and backscattering coefficients describing a large palette of pigments potentially usable for architectural coatings.

This summary paper highlights major results of our pigment characterization research. The theory, experimental procedure, and the measured and computed spectral properties of the pigments are fully detailed in Levinson et al. (2005a,b).

We note that our study concerns only the solar radiative properties of roof coatings. Thermal radiative properties, mechanical durability, and lightfastness are generally outside its scope.

## THEORY

The purpose of our measurements and model of radiant transfer in single-pigment coatings is to obtain backscattering and absorption coefficients  $S$  and  $K$  that approximately characterize the pigment. High precision is not the goal, but a reliable general characterization of each individual pigment is. We cover the solar spectral region from 300 to 2500 nm at 5-nm intervals. Each wavelength is treated independently of all others except for the use of the forward scattering ratio. Since the K-M model applies to diffuse illumination, whereas we are using collimated radiation, the treatment may be expected to be more accurate in strongly scattering films in which a fully diffuse radiation field quickly develops. However, we have used a formulation in which a non-scattering pigment (e.g., a dye) is assigned a  $K$  value approximating Beer's law for diffuse radiation traversing a slab. In summary, we are not expecting precise characterization, but expect to extract consistent, reliable and practical information for each pigment.

The one-dimensional propagation of light through a coating is approximated by the two-flux Kubelka-Munk (K-M) theory, in which downward and upward beams can be absorbed and/or backscattered as they traverse the film. All light in the film is assumed to be diffuse (subscript  $d$ ), either because the film is diffusely illuminated, or because the film is strongly scattering. The downward diffuse flux  $i_d(z)$  and upward diffuse flux  $j_d(z)$  within the film are modelled by

$$-\frac{di_d}{dz} = -(K + S)i_d + S j_d \quad (1)$$

$$-\frac{dj_d}{dz} = -(K + S)j_d + S i_d \quad (2)$$

where  $K$  and  $S$  are coefficients of absorption and backscattering, respectively. The fluxes and coefficients are wavelength specific.

Our theory and algorithm for computing the coefficients  $K$  and  $S$  from measurements of the reflectance and transmittance of pigmented coatings in contact with air (i.e., paint films in a spectrometer) are detailed in Levinson et al. (2005a).

## EXPERIMENT

The optical properties of 87 pigment films — 4 white, 21 black or brown, 14 blue or purple, 11 green, 9 red or orange, 14 yellow and 14 pearlescent — were characterized by computing spectral K-M coefficients and non-spectral forward scattering ratios from spectral measurements of film reflectance and transmittance. Our methodology is detailed in Levinson et al. (2005a).

## PIGMENT CLASSIFICATION

For convenience in presentation, the pigments were grouped by color “family” (e.g., green) and then categorized by chemistry (e.g., chromium oxide green). Some families span two colors (e.g., black/brown) because it is difficult to consistently identify color based on pigment name and color index (convention for identifying colorants (Society of Dyers and Colorists and American Association of Textile Chemists and Colorists, 2004). For example, a dark pigment may be marketed as “black,” but carry a “pigment brown” color index designation and exhibit red tones more characteristic of brown than of black. Pigment categories are presented in the order of simpler inorganics, more complex inorganics and then finally organics. Each member of a color family is assigned an identification code  $Xnn$ , where  $X$  is the color family abbreviation and  $nn$  is a serial number. For example, the 11 members of the green color family (“G”) have identification codes G01 through G11.

The same pigment may be present in more than one pigmented film. For example, our survey includes four titanium dioxide white films (W01-W04). However, the concentration of pigment, pigment particle size and/or source of the pigment (manufacturer) may vary from film to film.

## PIGMENT PROPERTIES BY COLOR AND CATEGORY

Table 1 summarizes some relevant bulk properties of the pigmented films in each category, such as NIR reflectances over black and white backgrounds. The measured and computed spectral properties of each pigmented film (reflectance, transmittance, absorptance, absorption coefficient and scattering coefficient) are charted in Levinson et al. (2005b). Space limitations preclude the presentation of spectral charts in the current paper.

When examining spectral optical properties, it is worth noting that most of the NIR radiation in sunlight arrives at the shorter NIR wavelengths. Of the 52% of solar energy delivered in the NIR spectrum (700 - 2500 nm), 50% lies within 700 - 1000 nm; 30% lies within 1000 - 1500 nm; and 20% lies within 1500 - 2500 nm (Figure 1). We refer to the 700 - 1000 nm region containing half the NIR solar energy (and a quarter of the total solar energy) as the “short” NIR.

In the discussions below, black and white *backgrounds* are assumed to be opaque, with observed NIR reflectances of 0.04 and 0.87, respectively. Note that in the absence of the air-film interface, the continuous refractive index (CRI) NIR reflectances of the black and white backgrounds are 0.00 and 0.94, respectively.

Note that the descriptions of pigments as “hot” or “cool” in the following are only qualitative, in the sense that a pigmented coating with a high NIR absorptance (approaching 1) is hot, and a pigmented coating with a low NIR absorptance (approaching 0) is cool. We are not aware of any official standards by which pigments can be designed cool or hot.

The NIR absorptances of the various pigmented coatings are quantitatively compared at the end of this section.

## White

All four whites were titanium dioxide ( $\text{TiO}_2$ ) rutile. Other white pigments (not characterized in this study) include zinc oxide, zinc sulfide, antimony oxide, zirconium oxide, zirconium silicate (zircon) and the anatase phase of  $\text{TiO}_2$ .

$\text{TiO}_2$  rutile is a strongly scattering, weakly absorbing, stable, inert, nontoxic, inexpensive and hence extremely popular white pigment (Lewis, 1998).  $\text{TiO}_2$  whites W01 - W04 exhibit similar curves of strong backscattering and weak absorption in the visible and NIR, except for drops in backscattering around 1500-2000 nm seen for W03 and W04. These last two samples are undiluted and 12:1 diluted versions of the same artist color.

Physically, the light scattering is due to the difference between the refractive index of the rutile particles (2.7) and that of the surrounding transparent medium (1.5). At high pigment volume concentrations, the presence of numerous nearby rutile particles raises the effective refractive index of the surrounding medium and thereby reduces the efficiency of scattering. This fall in scattering efficiency is termed pigment crowding (Blakey and Hall, 1998).

Rutile is a direct bandgap semiconductor and therefore has a very abrupt transition from low absorption to high absorption that occurs at 400 nm, the boundary between the visible and ultraviolet regions. For wavelengths below 400 nm (photon energies above 3.1 eV), the absorption is so strong that our data saturate, except in the case of the highly dilute (2% PVC) sample W04. At wavelengths above 400 nm, absorption is weak; most of the spectral features may be attributed to the binders used. One of the four white pigments (W01) has a slightly less abrupt transition at 400 nm — there is an absorption “tail” near the band edge. This type of behavior is likely due to impurities in the  $\text{TiO}_2$ .

The sharp rise in absorbance near 300 nm shown for some films, such as W04, is an artifact due to the use of a polyester substrate.

## Black/Brown

### Carbon Black, Other Non-Selective Black.

Carbon black, bone black (10% carbon black + 84% calcium phosphate), copper chromite black ( $\text{CuCr}_2\text{O}_4$ ) and synthetic iron oxide black ( $\text{Fe}_3\text{O}_4$  magnetite) (B01 - B04) are weakly scattering pigments with strong absorption across the entire solar spectrum. Carbon black B01 is the most strongly absorbing, but all four are “hot” pigments.

Most non-selective blacks are metallic in nature, with free electrons permitting many different allowed electronic transitions and therefore broad absorption spectra. Carbon black is a semi-metal that has many free electrons, but not as many as present in highly conductive metals. Both the iron oxide (magnetite) and copper chromite blacks are (electrically conducting) metals.

### Chromium Iron Oxide Selective Black.

Chromium iron oxide selective blacks (B05 - B11) are mixed metal oxides (chromium green-black hematite, chromium green-black hematite modified, chromium iron oxide, or chromium iron nickel black spinel) formulated to have NIR reflectance significantly higher than carbon and other non-selective blacks. Some, such as chromium green-black hematite B06, appear more brown than black. While these pigments have good scattering in the NIR, with a backscattering coefficient at 1000 nm about half that of  $\text{TiO}_2$  white, they are also quite absorbing ( $K \sim 50 \text{ mm}^{-1}$ ) in the short NIR. These pigments are visibly hiding (opaque to visible radiation) and NIR transmitting, so use of a white background improves their NIR reflectances without significantly changing their appearances.

Pure chromium oxide green ( $\text{Cr}_2\text{O}_3$ ), pigment green 17, has the hematite crystal structure and will be discussed further together with other green pigments. When some of the chromium atoms are replaced by iron, a dark brownish black with the same crystal structure is obtained — i.e., a traditional cool black pigment (e.g., B06-B11; B05 differs because it contains nickel and has a spinel structure). It is sometimes designated as Cr-Fe hematite (Swiler, 2002) or chromium green-black hematite (DCMA, 1991) and has been used to formulate infrared-reflective vinyl siding since about 1984 (Rabonovitch and Summers, 1984). A number of modern recipes for modified versions of this basic cool black incorporate minor amounts of a variety of other metal oxides. One example is the use of a mixture of 93.5 g of chromium oxide, 0.94 g of iron oxide, 2.38 g of aluminum oxide and 1.88 g of titanium oxide (Sliwinski et al., 2001). The mixture is calcined at about 1100°C to form hematite-structure crystallites of the resulting mixed metal oxide.

### **Organic Selective Black.**

Perylene black (B12) is a weakly scattering, dyelike organic pigment that absorbs strongly in the visible and very weakly in the NIR. Its sharp absorption decrease at 700 nm gives this pigment a jet black appearance and an exceptionally high NIR reflectance (0.85) when applied over white. Perylene pigments exhibit excellent lightfastness and weatherfastness, but their basic compound (dianhydride of tetracarboxylic acid) may or may not be fast to alkali; Herbst and Hunger (1993) and Lewis (1988) disagree on the latter point.

### **Iron Oxide Brown.**

Iron oxide browns (B13 - B15) such as burnt sienna, raw sienna and raw umber exhibit strong absorption in part of the visible spectrum and low absorption in the NIR. These can provide effective cool brown coatings if given a white background, though this will make some (e.g., burnt sienna B13) appear reddish. These browns are “natural” and can be expected to contain various impurities.

### **Other Brown.**

Other browns characterized (B16 - B21) include iron titanium (Fe-Ti) brown spinel, manganese antimony titanium buff rutile and zinc iron chromite brown spinel. These mixed-metal oxides have strong absorption in most or all of the visible spectrum, plus weak absorption and modest scattering in the NIR. A white undercoating improves the NIR reflectance of all browns, but brings out red tones in iron titanium brown spinels B16 and B17.

The cool Fe-Ti browns (B16 - B18) have spinel crystal structure and basic formula  $\text{Fe}_2\text{TiO}_4$  (DCMA, 1991; Brabers, 1995). Despite the presence of  $\text{Fe}^{2+}$  ions, the infrared absorption of this material is weak. (In many materials, the  $\text{Fe}^{2+}$  ion is associated with infrared absorption (Glebov and Boulos, 1998; Clark, 1999); see also our data for  $\text{Fe}_3\text{O}_4$  in Levinson et al. (2005b). The current data demonstrate that the absorption spectra also depend on the environment of the  $\text{Fe}^{2+}$  ion.) We also note that while B17 and B18 are nominally the same material, the details of the absorption are different.

We have not yet characterized a synthetic iron oxide hydrate brown (e.g.,  $\text{FeOOH}$ ).

## **Blue/Purple**

### **Cobalt Aluminate Blue, Cobalt Chromite Blue.**

Cobalt aluminate blue (nominally  $\text{CoAl}_2\text{O}_4$ , but usually deficient in Co (Buxbaum, 1998) U01 - U05) and cobalt chromite blue ( $\text{Co}[\text{Al,Cr}]_2\text{O}_4$ ; U06 - U09) derive their appearances from modest scattering ( $S \sim 30 \text{ mm}^{-1}$ ) in the blue (400 - 500 nm) and strong absorption ( $K \sim 150 \text{ mm}^{-1}$ ) in the rest of the visible spectrum. They have very low absorption in the short NIR, but exhibit an undesirable absorption band in

the 1200 - 1600 nm range, which contains 17% of the NIR energy. A white background dramatically increases NIR reflectance but makes some (e.g., cobalt aluminum blue spinel U02) much lighter in color.

### **Iron Blue.**

Iron (a.k.a. Prussian or Milori) blue (U10) is a weakly scattering pigment with strong absorption in the visible and short NIR and weak absorption at longer wavelengths. It appears black and has little NIR reflectance over a black background, but looks blue and achieves a modest NIR reflectance (0.25) over a white background. It is not ideal for cool coating formulation.

### **Ultramarine Blue.**

Ultramarine blue (U11), a complex silicate of sodium and aluminum with sulfur, is a weakly scattering pigment with some absorption in the short NIR. If sparingly used, it can impart absorption in the yellow spectral region without introducing a great deal of NIR absorption. This is a durable inorganic pigment with some sensitivity to acid (Lewis, 1988).

While most colored inorganic pigments contain a transition metal such as Fe, Cr, Ni, Mn, or Co, ultramarine blue is unusual. It is a mixed oxide of Na, Si and Al, with a small amount of sulfur ( $\text{Na}_{\{7.5\}}\text{Si}_6\text{Al}_6\text{O}_{\{24\}}\text{S}_{\{4.5\}}$ ). The metal oxide skeleton forms an open clathrate sodalite structure that stabilizes  $\text{S}_3^{2-}$  ions in cages to form the chromophores (Buxbaum, 1998: s. 3.5; Clark and Cobbold, 1978). Thus isolated  $\text{S}_3$  molecules with an attached unpaired electron cause the light absorption in the 500-700 nm range, producing the blue color. The refractive index of ultramarine blue is not very different from the typical matrix value of 1.5 (Buxbaum, 1998: s. 3.5), so the pigment causes little scattering.

### **Phthalocyanine Blue.**

Copper phthalocyanine blue (U12 - U13) is a weakly scattering, dyelike pigment with strong absorption in the 500 - 800 nm range and weak absorption in the rest of the visible and NIR. Phthalo blue appears black and has minimal NIR reflectance over a black background, but looks blue and achieves a high NIR reflectance (0.63) over a white background (U12). It is durable and lightfast, but as an organic pigment it is less chemically stable than (high temperature) calcined mixed metal oxides such as the cobalt aluminates and chromites.

General information on the structure and properties of phthalocyanines is available in Mckeown (1998). The refractive index varies with wavelength and exceeds 2 in the short wavelength part of the infrared spectrum (Wilbrandt et al., 1996). Therefore the weak scattering we observe in our samples indicates that the particle size is quite small. The pigment handbook indicates a typical particle diameter of 120 nm (Lewis, 1988), which is consistent with our data.

### **Dioxazine Purple.**

Dioxazine purple (U14) is an organic optically similar to phthalo blue, but even more absorbing in the visible and less absorbing in the NIR. It is nearly ideal for formulation of dark NIR-transparent layers, but is subject to the chemical stability considerations noted above for phthalo blue.

## **Green**

### **Chromium Oxide Green, Modified Chromium Oxide Green.**

Chromium oxide green  $\text{Cr}_2\text{O}_3$  (G01 - G02) exhibits strong scattering alternating with strong absorption across the visible spectrum and strong scattering and mild absorption in the NIR. Since the pigment is almost opaque in the visible, a thin layer of chromium oxide green over a white background yields a medium-green coating with good NIR reflectance (0.57 for 13- $\mu\text{m}$  thick film G02). The modified chromium



oxide green (G03) is mostly chromium oxide, with small amounts of iron oxide, titanium dioxide and aluminum oxide (Sliwinski et al., 2001). A layer of the modified chromium oxide green over a white background produces a medium green with excellent NIR reflectance (0.71).

Cr<sub>2</sub>O<sub>3</sub> green is often mentioned as an infrared-reflective pigment that is useful for simulating the high infrared reflectance of plant leaves. Indeed, a high NIR reflectance is observed. However, our data for sample films G01 and G02 do show that there is a broadband absorption of about 10 mm<sup>-1</sup> in the near-infrared. While our measurements of absorptance coefficient are not precise for low absorptances (Levinson et al., 2005a), this value is clearly distinct from zero. Pure Cr<sub>2</sub>O<sub>3</sub>, fired in air, tends to become slightly rich in oxygen, which results in p-type semiconducting behavior (de Cogan and Lonergan, 1974; Goodenough, 1984). Thus it is possible that the broadband IR absorption of Cr<sub>2</sub>O<sub>3</sub> is due to free carrier absorption by mobile holes. de Cogan and Lonergan (1974) also report that doping with Al can reduce the p-type conductivity in Cr<sub>2</sub>O<sub>3</sub>, so it seems likely that doping with Al and/or certain other metals can also reduce the IR absorption.

The modified chromium oxide green G03 is similar to G01 and G02 Cr<sub>2</sub>O<sub>3</sub>. However its green reflectance peak at 550 nm is somewhat smaller and its infrared absorption is clearly much smaller than those of samples G01 and G02.

### **Cobalt Chromite Green.**

Cobalt chromite green (G04 - G06) is similar to cobalt chromite blue and is commonly used for military camouflage.

### **Cobalt Titanate Green.**

Cobalt titanate green (G07 - G09) is similar to cobalt chromite green, but scatters more strongly across the entire solar spectrum and has a pronounced absorption trough around 500 nm. A white background makes cobalt teal G07 very NIR reflective (0.73) but also appear light blue (hence, the name teal). The other two cobalt titanate greens (G08, G09) have respectable NIR reflectances (0.47, 0.37) over white and appear medium green.

### **Phthalocyanine Green.**

Phthalocyanine green (G10 - G11) is similar to phthalocyanine blue, but absorbs more strongly in the short NIR. Hence, the NIR reflectance of a thin phthalo green film over white, while respectable, is only 70% of that achieved by a thin layer of phthalo blue over white (0.45 for G10 vs. 0.63 for U12).

## **Red/Orange**

### **Iron Oxide Red.**

Iron oxide red (R01 - R04) derives its appearance from weak scattering and very strong absorption in the 400 - 600 nm band. One of the iron oxide reds (R01) exhibits moderate absorption across the NIR that may be due to doping of the Fe<sub>2</sub>O<sub>3</sub> hematite crystals with impurities or result from broadband absorbing impurity phases such as Fe<sub>3</sub>O<sub>4</sub>; it is not a cool pigment. However, the remaining three iron oxide reds weakly absorb in the NIR and present both a dark red appearance and good NIR reflectance (0.53 - 0.67) over a white background. R02 also has a respectable NIR reflectance (0.38) over a black background and has backscattering S comparable with TiO<sub>2</sub> white in the NIR.

### **Cadmium Orange.**

Cadmium orange (R05) has weak scattering and very strong absorption in the 400 - 600 nm band, followed by strong scattering and virtually no absorption at longer wavelengths. Applied over a white

background, it appears bright orange and has very high NIR reflectance (0.87) — essentially the same as that of the white background. Cadmium orange (and cadmium yellow, below) are Cd(S,Se) direct bandgap semiconductors. They exhibit sharp transitions between absorbing and non-absorbing regions and have high refractive indices (e.g., 2.5 for CdS) that lead to large scattering coefficients. However, sensitivity to acid and the toxicity of cadmium limit their applications.

### **Organic Red.**

Organic red pigments (R06 - R09) such as acra burnt orange, acra red, monastral red and naphthol red light have weak scattering and strong (sometimes very strong) absorption up to 600 nm, followed by very weak absorption and moderate-to-weak scattering at longer wavelengths. As a result they yield a medium-red color and a very high NIR reflectance (0.83 - 0.87) when applied over a white background. Masstones of acra burnt orange, acra red and naphthol red light are all lightfast; their tints are slightly less so (Lewis, 1988).

## **Yellow**

### **Iron Oxide Yellow.**

Iron oxide yellow FeOOH (Y01) is a brownish yellow similar to iron oxide red. It appears tan and has a high NIR reflectance (0.70) when applied over a white background.

### **Cadmium Yellow.**

Cadmium yellow (Y02) is similar to cadmium orange. It appears bright yellow and has very high NIR reflectance (0.87) over white.

### **Chrome Yellow.**

Chrome yellow PbCrO<sub>4</sub> (Y03) is optically similar to cadmium yellow but exhibits a more gradual reduction in absorptance. It appears bright yellow and achieves a high NIR reflectance (0.83) over white. In some applications, the presence of lead and/or the Cr(VI) ion impose limitations.

### **Chrome Titanate Yellow.**

Chrome titanate yellow (Y04 - Y07) is similar to chrome yellow, but scatters more strongly in the NIR. Its scattering coefficient can exceed 100 mm<sup>-1</sup> in the short NIR, suggesting that this pigment might be used in place of titanium dioxide white to provide a background of high NIR reflectance. Over a black background, chrome titanate yellow appears brown to green and has moderate to high NIR reflectance (0.26 - 0.62). Over white, it appears orange to yellow and has very high NIR reflectance (0.80 - 0.86). Y07 over black produces a medium brown with NIR reflectance 0.62.

The curves for Y04 and Y05 illustrate how the backscattering coefficient *S* varies with particle size (manufacturer data). For smaller particles, the decrease in *S* with increasing wavelength is more dramatic.

### **Nickel Titanate Yellow.**

Nickel titanate yellow (Y08 - Y11) is similar to chrome titanate yellow. Note that these compounds usually also contain antimony in their formulation. Over white, it appears a muted yellow and yields very high NIR reflectance (0.77-0.87); over black, it appears yellowish green and achieves moderate to high NIR reflectance (0.22 - 0.64). Y11 is a particularly good candidate to use over black.

### **Strontium Chromate Yellow + Titanium Dioxide.**

Strontium chromate yellow (solids mass fraction 11%) mixed with titanium dioxide (solids mass fraction 9%) in a paint primer (Y12) appears greenish brown over a black background and pale yellow over a white background. It has very low absorption (order  $1 \text{ mm}^{-1}$ ) and strong scattering (order  $100 \text{ mm}^{-1}$ ) at 1000 nm, giving it a good NIR reflectance over black (0.38) and a very high NIR reflectance over white (0.86).

### **Hansa Yellow, Diarylide Yellow.**

Hansa yellow (Y13) and diarylide yellow (Y14) are weakly scattering, dyelike organic pigments with high absorption below 500 nm and very weak absorption elsewhere. Over white, they appear bright yellow and orange-yellow, respectively and yield very high NIR reflectance (0.87).

## **Pearlescents**

### **Mica + Titanium Dioxide.**

Mica flakes coated with titanium dioxide (P01 - P09) exhibit strong scattering and weak absorption, producing their colors (e.g., gold, blue, green, orange, red, violet, or bright white) via thin-film interference. Some have scattering coefficients exceeding  $100 \text{ mm}^{-1}$  in the near infrared. Over white, they appear white and have very high NIR reflectance (0.88 - 0.90); over black, they achieve their named colors and have high NIR reflectance (0.35 - 0.54). The NIR reflectance of a pearlescent film over an opaque white background can exceed that of the background.

### **Mica + Titanium Dioxide + Iron Oxide.**

Mica flakes coated with titanium dioxide and iron oxide (P10 - P14) are in most cases similar to mica flakes coated with only titanium dioxide, but are more absorbing, less scattering, darker and somewhat less reflecting in the NIR. The exception is rich bronze P13, which has very high absorption and would not make a suitable cool pigment.

## **Aluminum + Iron Oxide + Silicon Oxide**

While not characterized in the current study, the solar spectral reflectances of single-layer (iron oxide  $\text{Fe}_2\text{O}_3$ ) or double layer ( $\text{Fe}_2\text{O}_3$  on silicon dioxide  $\text{SiO}_2$ ) interference coatings on aluminum flakes are presented in Smith et al. (2003a,b).

## **Cool and Hot Pigments**

A simple way to evaluate the utility of a pigmented coating for “cool” applications is to consider its NIR absorptance and NIR transmittance. If the NIR absorptance is low, the pigment is cool. However, a cool pigment that has high NIR transmittance will require an NIR-reflective background (typically white or metallic) to produce an NIR-reflecting coating. Charts of the NIR absorptance and transmittance of the members of each color family are shown in Figure 2. An ideal cool pigment would appear near the lower left corner of the chart, indicating that it is weakly absorbing, weakly transmitting and thus strongly reflecting in the NIR. Pigments appearing higher on the left side of the chart will form a cool coating if given an NIR-reflective background. Use of pigments appearing toward the right side of the chart (i.e., those with strong NIR absorption) should be avoided in cool applications. It should be noted that these charts do not provide perfect comparisons of “cool” performance because they show the NIR properties of films of varying thickness ( $10 - 37 \text{ }\mu\text{m}$ ) and visible hiding (visible transmittance 0 - 0.43 for non-pearlescents and 0.02 - 0.54 for the pearlescents). Black-filled circles indicate visible transmittance less than 0.1; gray-filled circles, between 0.1 and 0.3; and white-filled circles, above 0.3.

There are cool films in the white, yellow, brown/black, red/orange, blue/purple and pearlescent families with NIR absorptance less than 0.1. These films have moderate to high NIR transmittances (0.25 - 0.85), indicating that they would require an NIR-reflective background to perform well. There are also other slightly less cool black/brown, blue/purple, green, red/orange, yellow and pearlescent films with NIR absorptance less than 0.2. These have somewhat lower NIR transmittances (0.20 - 0.70), but are still far from NIR-opaque. A handful of pearlescent, blue/purple and red/orange films, along with half a dozen brown/black films, have NIR absorptances exceeding 0.5 and may be considered warm. A few nonselective blacks with NIR absorptance approaching unity may be considered hot.

Other useful metrics for “coolness” are NIR reflectances over white and black backgrounds (Table 1). Over a white background, the coolest pigments — i.e., those with NIR reflectances of at least 0.7 — include members of the pearlescent, white, yellow, black/brown, red/orange and blue/purple color families: mica coated w/titanium dioxide (0.88-0.90), titanium dioxide white (0.87-0.88), cadmium yellow (0.87), cadmium orange (0.87), Hansa yellow (0.87), diarylide yellow (0.87), organic selective black (0.85), organic red (0.83-0.87), dioxazine purple (0.82), chrome titanate yellow (0.80-0.86), nickel titanate yellow (0.77-0.87), modified chromium oxide green (0.71) and iron oxide yellow (0.70). Other pigments with NIR reflectances of at least 0.5 include members of the blue/purple, black/brown and green color families: cobalt aluminum blue (0.62-0.70), cobalt chromite blue (0.55-0.70), phthalo blue (0.55-0.63), cobalt chromite green (0.58-0.64), ultramarine blue (0.52), chromium oxide green (0.50-0.57) and other brown (0.50-0.74). Over a black background, the coolest pigments — in this case, those with NIR reflectances of at least 0.3 — include members of the white, yellow, black/brown, red/orange, pearlescent and green color families: titanium dioxide white (0.24-0.65), nickel titanate yellow (0.22-0.64), chrome titanate yellow (0.26 - 0.62), mica coated w/titanium dioxide (0.35-0.54), mica + titanium dioxide + iron oxide, chromium oxide green (0.33-0.40), other brown (0.22-0.40), strontium chromate yellow + titanium dioxide (0.38), iron oxide red (0.19-0.38), chromium iron oxide selective black (0.11-0.35) and cobalt titanate green (0.21-0.30).

## CONCLUSIONS

Our characterizations of the solar spectral optical properties of 87 predominately single-pigment paint films with thicknesses ranging from 10 to 37  $\mu\text{m}$  have identified cool pigments in the white, yellow, brown/black, red/orange, blue/purple and pearlescent color groupings with NIR absorptances less than 0.1, as well as other pigments in the black/brown, blue/purple, green, red/orange, yellow and pearlescent groupings with NIR absorptances less than 0.2. Most are NIR transmitting and require an NIR-reflecting background to form a cool coating. Over an opaque white background, some pigments in the pearlescent, white, yellow, red/orange, green and blue/purple families offer NIR reflectances of at least 0.7, while other pigments in the blue/purple, black/brown and green color families have NIR reflectances of at least 0.5. A few members of the white, yellow, pearlescent and green color families have NIR scattering sufficiently strong to yield NIR reflectances of at least 0.3 (and up to 0.64) over a black background.

Use of pigments with NIR absorptances approaching unity (e.g., nonselective blacks) should be minimized in cool coatings, as might be the use of certain pearlescent, blue/purple, green and red/orange and brown/black pigments with NIR absorptances exceeding 0.5.

## ACKNOWLEDGEMENTS

This work was supported by the California Energy Commission (CEC) through its Public Interest Energy Research Program (PIER), by the Laboratory Directed Research and Development (LDRD) program at Lawrence Berkeley National Laboratory (LBNL), and by the Assistant Secretary for Renewable Energy under Contract No. DE-AC03-76SF00098. The authors wish to thank CEC Commissioner Arthur Rosenfeld and PIER program managers Nancy Jenkins and Chris Scruton for their support and advice. Special thanks go also to Mark Levine, director of the Environmental Energy Technologies Division at LBNL, and Stephen Wiel, head of the Energy Analysis Department at LBNL, for their encouragement and support in the initiation of this project. We also wish to thank the following people for their assistance: Kevin Stone and Melvin Pomerantz, LBNL; Michelle Vondran, John Buchko, and Robert Scichili, BASF

Corporation; Richard Abrams, Robert Blonski, Ivan Joyce, Ken Loye, and Ray Wing, Ferro Corporation; Tom Steger and Jeffrey Nixon, Shepherd Color Company; and Robert Anderson, Liquitex Artist Materials.

## REFERENCES

ASTM (American Society for Testing and Materials). 2003. "ASTM G 173-03: Standard Tables for Reference Solar Spectral Irradiance at Air Mass 1.5: Direct Normal and Hemispherical on 37° Tilted Surface." Technical report, American Society for Testing and Materials.

BASF Industrial Coatings. 2004. "Ultra-Cool<sup>TM</sup>: The New Heat Reflective Coatings from BASF." <<http://www.ultra-cool.basf.com>>.

Blakey, R.R. and J.E. Hall. 1988. "Titanium Dioxide." Chapter A in *Pigment Handbook, Volume I*. John Wiley and Sons, pp.1-42.

Bohren, Craig F. 1987. "Multiple Scattering of Light and Some of Its Observable Consequences." *American Journal of Physics*, vol 55, no. 6 (June): 524-533.

Brabers, V.A.M. 1995. "The Electrical Conduction of Titanomagnetites." *Physica B*, vol. 205: 143–152.

Brady, R.F. and L.V. Wake. 1992. "Principles and Formulations for Organic Coatings with Tailored Infrared Properties." *Progress in Organic Coatings*, vol. 20, no. 1: 1-25.

Burkhart, Gil, Terry Detrie, and Dan Swiler. 2001. "When Black Is White." *Paint and Coatings Industry Magazine*. (January).

Buxbaun, Gunter. 1998. *Industrial Inorganic Pigments*. Wiley-VCH, 2nd edition.

Clark, R.J.H. and D.G. Cobbold. 1978. "Characterization of Sulfur Radical Anions in Solutions of Alkali Polysulfides in Dimethylformamide and Hexamethylphosphoramide and in the Solid State in Ultramarine Blue, Green, and Red." *Inorganic Chemistry*, vol. 17: 3169–3174.

Clark, R.N. 1999. "Spectroscopy of Rocks and Minerals, and Principles of Spectroscopy." Chapter 1 in *Manual of Remote Sensing, volume 3: Remote Sensing for the Earth Sciences*, pp. 3-58. John Wiley and Sons, <<http://speclab.cr.usgs.gov>>, Fig. 5.

Custom-Bilt Metals. 2004. "Ultra-Cool<sup>TM</sup> Coating Saves Energy and Money on Custom-Bilt Metals Roofing Systems." <<http://www.custombiltmetals.com>>.

DCMA (Dry Color Manufacturer's Association). 1991. *Classification and Chemical Description of the Complex Inorganic Color Pigments*. Dry Color Manufacturer's Association, P.O. Box 20839, Alexandria, VA 22320.

de Cogan, D. and G.A. Lonergan. 1974. "Electrical conduction in Fe<sub>2</sub>O<sub>3</sub> and Cr<sub>2</sub>O<sub>3</sub>." *Solid State Communications*, vol. 15: 1517-1519.

Ferro Corporation. 2004. "Cool Colors<sup>TM</sup> and Eclipse<sup>TM</sup> Pigments." <<http://ferro.com>>.

Genjima, Yasuhiro and Haruhiko Mochizuki. 2002. "Infrared Radiation Reflector and Infrared Radiation Transmitting Composition." U.S. Patent 6,366,397 B1, April 16.

Glebov, L.B. and E.N. Boulos. 1998. "Absorption of Iron and Water in the Na<sub>2</sub>O-CaO-MgO-SiO<sub>2</sub> Glasses, II. Selection of Intrinsic, Ferric, and Ferrous Spectra in the Visible and UV Regions." *J. Non-Crystalline Solids*, vol. 242: 49-62.

Goodenough, Hamnett. 1984. "Oxides of Chromium." Chapter 9.15.2.5.1 in *Landolt-Bornstein Numerical Data and Functional Relationships in Science and Technology, New Series, Group III: Crystal and Solid-State Physics, Volume 17g (Semiconductors: Physics of Non-Tetrahedrally Bonded Binary Compounds III)*. Berlin: Springer-Verlag.

Herbst, Willy and Klaus Hunger. 1993. *Industrial Organic Pigments*. VCH.

Johnston, Ruth M. 1988. "Color Theory." Chapter D-b in *Pigment Handbook, Volume III*. John Wiley and Sons.

Judd, Deane B. 1952. *Color in Business, Science, and Industry*. John Wiley and Sons.

Kortum, Gustav. 1969. *Reflectance Spectroscopy: Principles, Methods, Applications*. Springer.

Kubelka, P. 1948. "New Contributions to the Optics of Intensely Light-Scattering Materials, Part I." *Journal of the Optical Society of America*, vol. 38: 448.

Levinson, Ronnen, Paul Berdahl, and Hashem Akbari. 2005a. "Solar Spectral Optical Properties of Pigments, Part I: Model for Deriving Scattering and Absorption Coefficients from Transmittance and Reflectance Measurements." *Solar Energy Materials & Solar Cells* (in press).

———. 2005b. "Solar Spectral Optical Properties of Pigments, Part II: Survey of Common Colorants." *Solar Energy Materials & Solar Cells* (in press).

Lewis, Peter A. 1988. *Pigment Handbook, Volume I*. John Wiley and Sons.

MCA Tile. 2004. "MCA Tile ENERGY STAR Roof Products." <<http://www.mcatile.com>>.

McKeown, N.B. 1998. *Phthalocyanine Materials: Synthesis, Structure and Function*. Cambridge: Cambridge University Press.

Nixon, Jeffrey D. 2003. "The Chemistry Behind 'Cool Roofs'." *eco-structure*, vol. 1, no. 1: 63–65.

Rabinovitch, E. B. and J. W. Summers. 1984. "Infrared Reflecting Vinyl Polymer Compositions." U.S. Patent 4,424,292.

Schuster, A. 1905. "Radiation through a Foggy Atmosphere." *Astrophys. J.*, vol. 21, no. 1.

Shepherd Color Company. 2004. "Arctic Infrared-Reflecting Pigments." <<http://shepherdcolor.com>>.

Sliwinski, Terrence R., Richard A. Pipoly, and Robert P. Blonski. 2001. "Infrared Reflective Color Pigment." U.S. Patent 6,174,360 B1, January 16.

Smith, G.B., A. Gentle, P. Swift, A. Earp, and N. Mronga. 2003a. "Coloured Paints Based on Coated Flakes of Metal as the Pigment, for Enhanced Solar Reflectance and Cooler Interiors: Description and Theory." *Solar Energy Materials & Solar Cells*, vol. 79, no. 2: 163-177.

———. 2003b. "Coloured Paints Based on Iron Oxide and Silicon Oxide Coated Flakes of Aluminium as the Pigment, for Energy Efficient Paint: Optical and Thermal Experiments." *Solar Energy Materials & Solar Cells*, vol. 79, no. 2: 179-197.

Society of Dyers and Colourists and American Association of Textile Chemists and Colorists. 2004. *Colour Index International: Fourth Online Edition*. <<http://www.colour-index.org>>.

Swiler, Daniel Russell. 2002. "Manganese Vanadium Oxide Pigments." U.S. Patent 6,485,557 B1, November 26.

Wilbrandt, S., O. Stenzel, A. Stendal, U. Beckers, and C. von Borczyskowski. 1996. "The Linear Optical Constants of Thin Phthalocyanine and Fullerite Films from the Near Infrared to the UV Spectral Regions: Estimation of Electronic Oscillator Strength Values." *J. Phys. B*, vol. 29: 2589-2595.

Table 1. Ranges of NIR Reflectance Over White ( $ROW_{NIR}$ ), NIR reflectance over black ( $ROB_{NIR}$ ), Visible Transmittance ( $T_{vis}$ ) and Thickness ( $\delta$ ) Measured for Pigmented Films in Each Pigment Category.

Category	$ROW_{NIR}$	$ROB_{NIR}$	$T_{vis}$	$\delta$ ( $\mu m$ )	Film Codes
titanium dioxide white	0.87-0.88	0.24-0.65	0.10-0.42	17-29	W01-W04
carbon black	0.05-0.06	0.04-0.04	0.03-0.07	16-19	B01-B02
other non-selective black	0.04-0.05	0.04-0.05	0.00-0.07	20-24	B03-B04
chromium iron oxide selective black	0.23-0.48	0.11-0.35	0.00-0.15	19-26	B05-B11
organic selective black	0.85	0.10	0.01	23	B12
iron oxide brown	0.47-0.61	0.06-0.27	0.03-0.24	14-26	B13-B15
other brown	0.50-0.74	0.22-0.40	0.01-0.24	17-28	B16-B21
cobalt aluminate blue	0.62-0.71	0.09-0.20	0.16-0.28	16-23	U01-U05
cobalt chromite blue	0.55-0.70	0.10-0.25	0.05-0.28	16-26	U06-U09
iron blue	0.25	0.05	0.27	12	U10
ultramarine blue	0.52	0.05	0.20	23	U11
phthalocyanine blue	0.55-0.63	0.06-0.08	0.21-0.22	14-26	U12-U13
dioxazine purple	0.82	0.05	0.21	10	U14
chromium oxide green	0.50-0.57	0.33-0.40	0.00-0.01	12-26	G01-G02
modified chromium oxide green	0.71	0.22	0.22	23	G03
cobalt chromite green	0.58-0.64	0.14-0.18	0.17-0.28	13-23	G04-G06
cobalt titanate green	0.37-0.73	0.21-0.30	0.04-0.22	10-24	G07-G09
phthalocyanine green	0.42-0.45	0.06-0.07	0.10-0.20	13-25	G10-G11
iron oxide red	0.31-0.67	0.19-0.38	0.00-0.08	13-26	R01-R04
cadmium orange	0.87	0.26	0.18	10	R05
organic red	0.83-0.87	0.06-0.14	0.15-0.32	11-27	R06-R09
iron oxide yellow	0.70	0.21	0.16	19	Y01
cadmium yellow	0.87	0.29	0.25	11	Y02
chrome yellow	0.83	0.34	0.18	24	Y03
chrome titanate yellow	0.80-0.86	0.26-0.62	0.05-0.23	17-26	Y04-Y07
nickel titanate yellow	0.77-0.87	0.22-0.64	0.09-0.51	17-27	Y08-Y11
strontium chromate yellow + titanium dioxide	0.86	0.38	0.21	19	Y12
Hansa yellow	0.87	0.06	0.43	11	Y13
diarylide yellow	0.87	0.08	0.35	12	Y14
mica + titanium dioxide	0.88-0.90	0.35-0.54	0.31-0.54	17-37	P01-P09
mica + titanium dioxide + iron oxide	0.27-0.85	0.25-0.44	0.02-0.42	20-24	P10-P14



Figure 1. Air Mass 1.5 Hemispherical Solar Spectral Irradiance Typical of North American Insolation (5% Ultraviolet, 43% Visible, 52% Near-Infrared) (ASTM, 2003).}

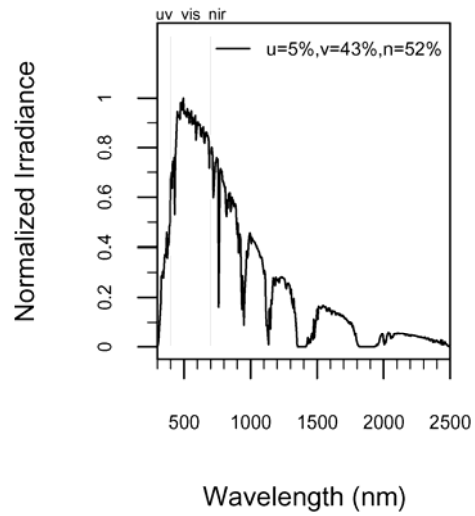
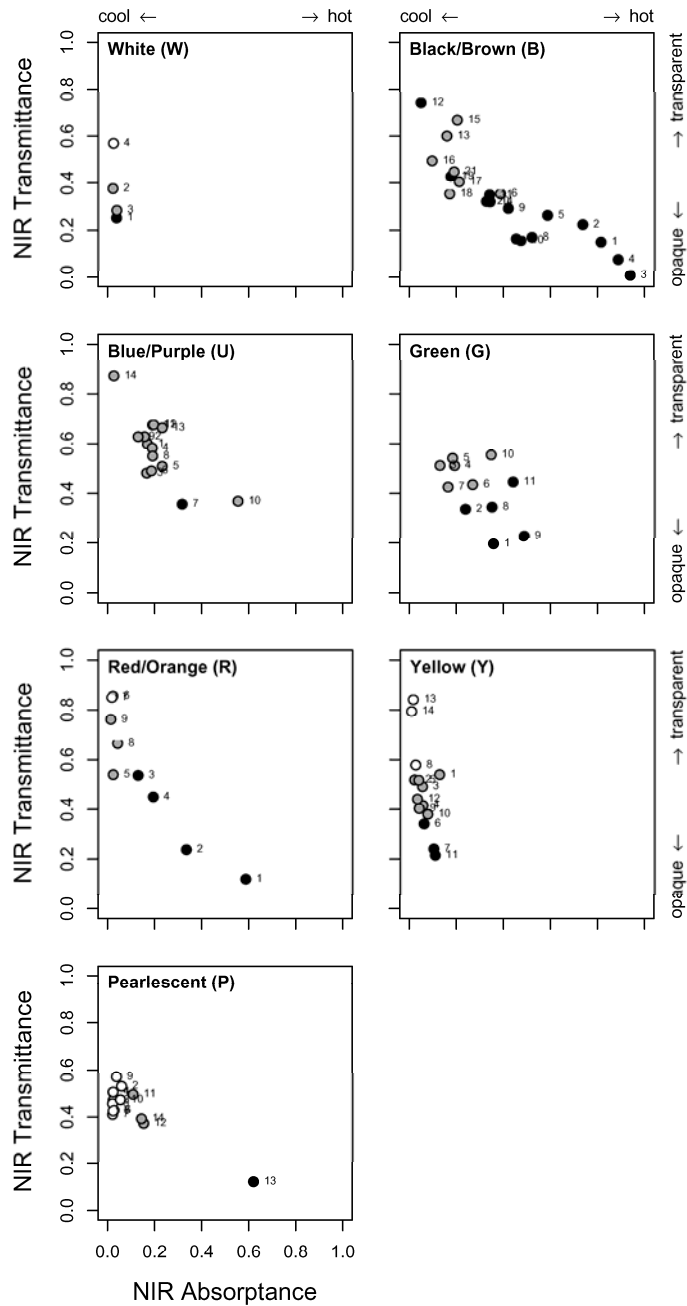


Figure 2. NIR Absorptances and Transmittances of 87 Pigmented Films.

A pigment with low NIR-absorptance is cool, but a cool pigment with high NIR transmittance requires an NIR-reflecting background. The color of each circle's interior indicates visible transmittance: black, less than 0.1; gray, between 0.1 and 0.3; white, over 0.3.



## **Aging and Weathering of Cool Roofing Membranes**

*Hashem Akbari, Asmeret A. Berhe, and Ronnen Levinson, Heat Island Group, Lawrence  
Berkeley National Laboratory (LBNL)*

*Stanley Graveline and Kevin Foley, Sarnafil*

*Ana H. Delgado and Ralph M. Paroli, Institute for Research in Construction, National  
Research Council (NRC), Canada*

### **ABSTRACT**

Aging and weathering can reduce the solar reflectance of cool roofing materials. This paper summarizes laboratory measurements of the solar spectral reflectance of unweathered, weathered, and cleaned samples collected from single-ply roofing membranes at various sites across the United States. Fifteen samples were examined in each of the following six conditions: unweathered; weathered; weathered and brushed; weathered, brushed and then rinsed with water; weathered, brushed, rinsed with water, and then washed with soap and water; and weathered, brushed, rinsed with water, washed with soap and water, and then washed with an algaecide. Another 25 samples from 25 roofs across the United States and Canada were measured in their unweathered state, weathered, and weathered and wiped.

We document reduction in reflectivity resulted from various soiling mechanisms and provide data on the effectiveness of various cleaning approaches. Results indicate that although the majority of samples after being washed with detergent could be brought to within 90% of their unweathered reflectivity, in some instances an algaecide was required to restore this level of reflectivity.

# Aging and Weathering of Cool Roofing Membranes<sup>\*</sup>

## ABSTRACT

Aging and weathering can reduce the solar reflectance of cool roofing materials. This paper summarizes laboratory measurements of the solar spectral reflectance of unweathered, weathered, and cleaned samples collected from single-ply roofing membranes at various sites across the United States. Fifteen samples were examined in each of the following six conditions: unweathered; weathered; weathered and brushed; weathered, brushed and then rinsed with water; weathered, brushed, rinsed with water, and then washed with soap and water; and weathered, brushed, rinsed with water, washed with soap and water, and then washed with an algaecide. Another 25 samples from 25 roofs across the United States and Canada were measured in their unweathered state, weathered, and weathered and wiped.

We document reduction in reflectivity resulted from various soiling mechanisms and provide data on the effectiveness of various cleaning approaches. Results indicate that although the majority of samples after being washed with detergent could be brought to within 90% of their unweathered reflectivity, in some instances an algaecide was required to restore this level of reflectivity.

## Introduction

The solar reflectance or albedo of a roof's surface affects roof temperature, air temperature above the roof, and the heating and cooling energy use in buildings (Akbari and Konopacki, 1998). Lighter colored roofing membranes, including those covered with high-albedo, low-absorptance, white coating materials, reflect incident solar energy, enabling them to stay cooler in the sun than low-albedo roofing materials. Young (1998) and Akbari and Konopacki (1998) found that cool roofing membranes can reduce building cooling energy use by 10% to 50%, that can result in savings of \$10 to \$100 per year per 100 m<sup>2</sup> roof surface. In cities, cool roofs can reduce summertime air temperature of their surroundings by 1-2 K (Akbari and Konopacki, 1998; Young, 1998; Pomerantz et al., 1999 and Akbari et al., 1999).

Cool materials for low-sloped roofs are characteristically white with smooth surfaces (Eilert, 2000). But the albedo of light-colored roofing materials changes, because of aging, weathering, and discoloration—which results from weathering. In this paper, we present data from two independent series of tests carried out at Lawrence Berkeley National Laboratory (LBNL) and National Research Council (NRC) in Canada. The LBNL study included measuring the spectral solar reflectance of 15 weathered roofing membranes from eight cities across the United States. The study also investigated the effect of four cleaning treatments in restoring the reflectance relative to its original levels. The NRC study also included measuring the solar reflectance of 25 weathered roofing membranes from 25 cities across the United States and Canada. But only the effects of two cumulative cleaning processes in restoring the solar reflectance were measured. All membranes were produced by the same manufacturer.

## Effects of Light Colored Roofs

Roof temperature strongly influences air temperature inside and outside of buildings. Solar absorptance, thermal emittance, convection coefficient, and heat conduction through a roofing membrane, all affect the roof surface temperature (Pomerantz et al., 1999). Consequently, lighter colored (reflective), cool roofs reduce the demand for indoor cooling by controlling the temperature from the outside and therefore heat flow into buildings.

The reduction in annual electricity use resulting from the application of cool roofs is greatest for buildings in areas with short cold seasons, because cool roofs have the potential to increase heating energy demand during extended cold periods (Levinson et al., 2005). However, significant annual net energy savings have been calculated for northern locations such as Chicago, Salt Lake City, and Toronto, through the implementation of heat island reduction strategies (Akbari and Konopacki, 2004; Konopacki and Akbari, 2002).

---

<sup>\*</sup> Hashem Akbari, Asmeret A. Berhe, and Ronnen Levinson, Heat Island Group, Lawrence Berkeley National Laboratory (LBNL); Stanley Graveline and Kevin Foley, Sarnafil; Ana H. Delgado and Ralph M. Paroli, Institute for Research in Construction, National Research Council (NRC), Canada

Recognizing the potential energy savings that could be achieved through the use of reflective roofing materials, the US Environmental Protection Agency (EPA) and the US Department of Energy (DOE) introduced the Energy Star Roof Products Program in 1999. Energy Star labeled membranes must meet defined minimum reflectivity levels according to their intended applications (low and high slope). Looking to curb energy demand, beginning in 2005, the State of California will prescribe the use of cool roofs on low-sloped non-residential buildings in their Title 24 Energy Code.

The reduced temperatures of reflective roofing surfaces, in turn, keeps air blowing over the roof and downwind from the buildings cooler (Taha, 1996). In large metropolitan areas, this contributes to a reduction in the urban heat island which reduces smog formation and the greenhouse effect (Akbari et al., 1990, 1999, 2001; Akbari and Konopacki, 1998; Pomerantz et al., 1999).

The United States Green Building Council's (USGBC) Leadership in Energy and Environmental Design (LEED) recognizes these benefits by awarding a point for the use of highly reflective and emissive roof materials in their green building rating system. The City of Chicago is looking to introduce an urban heat island ordinance that would call for the use of high reflectance roof materials beginning in 2008.

Typically, all non-metallic materials absorb the sun energy in the ultraviolet (UV) band (0.30-0.40  $\mu\text{m}$ ). Ultraviolet light is characterized as the major factor in aging and material degradation. Although the aging is primarily caused by UV absorption, the degradation process is highly temperature dependent. For the same UV absorption, the higher the temperature and temperature fluctuations through a day, the faster the material degrades. Reflective surfaces, by keeping the surface temperature low during the sunlit hours that result in less diurnal thermal expansion and contraction, may have a longer useful life.

Cooler roof surface temperatures have also been found to improve the performance of roof insulation. The thermal resistance of insulation materials installed immediately below a black membrane has been found to be up to 30% lower than advertised, when measured at peak summertime temperatures in Austin, Texas (Konopacki and Akbari, 2001).

## Effect of Aging and Weathering

The durability and solar reflectance of high albedo, cool roofs is affected by weathering (Paroli et al., 1993). Precipitation, dust and air pollutant depositions can degrade the solar reflectance of cool roof materials (Eilert, 2000). Over a period of several years, light colored roofing surfaces are typically expected to lose about 20% of their initial solar reflectance. Aged roofing membranes show a greater increase in absorptance on short wavelengths than long wavelengths (Berdahl et al., 2002).

Berdahl et al. (2002) indicated that the soil deposited on the surface of roofing membranes is made up of elemental carbon, hydrocarbons and other deposits that along with the soil further reduce the reflectivity of the membranes. Soiling and accumulation of carbonaceous particles is a serious problem in or around urban centers that are exposed to higher levels of fossil fuel combustion. Since carbonaceous aerosols can travel fast in the mixing atmosphere, they can spread to both urban and rural places to create a similar effect.

## Methodology

To investigate these and other related phenomena, this study was carried out on 15 membranes from eight locations that have been weathered for five to eight years and additional membranes from 25 other locations (Whelan et al., 2004), exposed 15 to 22 years. Solar (0.3 – 2.5  $\mu\text{m}$ ), UV (0.3 – 0.4  $\mu\text{m}$ ), visible (0.4 – 0.7  $\mu\text{m}$ ), and near-infrared (0.7 – 2.5  $\mu\text{m}$ ) reflectances were analyzed.

## Sample Description

The LBNL received weathered membranes (about 30-cm square) from 15 roofs while the NRC received membranes from 25 roofs. All samples contained at least one hot air welded seam. The bottom flap of material within the overlap was protected from weathering (but may still have been exposed to some elevated temperatures) and is thus labeled “unweathered.” The roofing membranes were made of about 1.2-mm to 1.5-mm thick polyvinyl chloride (PVC). The top half of most of the samples was white from the use of a rutile-phase titanium dioxide ( $\text{TiO}_2$ ) pigment, while a few were very light gray in color. The 15 LBNL roof membrane samples were collected from eight locations where they had been installed for five to eight years (see **Table 1**). The 25 NRC roof membrane samples were from various locations in the United States and Canada, and had a top surface which was light gray in color. Buildings selected for

sampling were chosen based on owner willingness to allow sample removal, and geographic and climate location.

**Table 1:** Location, Length of Time Since Installation, and Solar Reflectance of Weathered and Cleaned Samples, Studied at the LBNL

Sample			Solar Reflectance					
Sample No.	Location	Date of Installation	Uncleaned	Wiped	Rinsed	Detergent-Washed	Algae-Cleaner Washed	Unweathered
<b>Group A (white)</b>								
1	Springfield, MA	09/22/1995	0.54	0.68	0.70	0.77	0.82	0.80
2	Springfield, MA	05/31/1995	0.55	0.73	0.72	0.76	0.77	0.82
3	Lancaster, OH	03/28/1995	0.59	0.76	0.75	0.80	0.81	0.81
4	Heath, OH	04/01/1995	0.57	0.72	0.72	0.78	0.79	0.80
5	West Hampton, NJ	05/01/1995	0.71	0.71	0.71	0.73	0.77	0.79
6	West Hampton, NJ	02/04/1993	0.69	0.69	0.71	0.72	0.77	0.81
7	Plantation, FL	11/04/1994	0.35	0.43	0.64	0.65	0.79	0.82
8	Plantation, FL	11/04/1994	0.32	0.42	0.59	0.68	0.80	0.79
11	Solano Beach, CA	09/20/1992	0.38	0.47	0.71	0.78	0.82	0.81
12	Solano Beach, CA	09/20/1992	0.52	0.65	0.69	0.80	0.80	0.81
13	Alpharetta, GA	04/01/1995	0.45	0.59	0.66	0.69	0.79	0.80
<b>Group B (very light gray)</b>								
9	Gardena, CA	10/25/1995	0.50	0.58	0.60	0.62	0.63	0.63
10	Gardena, CA	10/25/1995	0.49	0.60	0.61	0.63	0.63	0.63
14	Bethesda, MD	04/28/1995	0.50	0.59	0.59	0.63	0.64	0.63
15	Fredericksburg, VA	11/06/1995	0.48	0.60	0.62	0.63	0.64	0.63

Note: The cleaning process was cumulative. All samples went through a cleaning process progression of dry wiping, rinsing with water, washing with detergent, and washing with algae cleaners.

## Measurement Protocols

Although some membranes received at LBNL were more soiled than others, all the samples appeared to be in good mechanical condition when the measurements were taken. For each sample, the most heavily soiled spot of each membrane was exposed to the different cleaning treatments.

The cleaning process was made to replicate natural and professional cleaning of the roofs, as given in **Table 2**. The unweathered samples refer to the part of the sample that was underneath the weathered part (i.e., in the overlap) and was assumed to have the optical properties of new membrane. The weathered samples were the soiled exposed samples. On each sample, we carried out a progression of four cleaning processes. First, each sample was dry wiped to simulate the effect of the dust removal by wind. After the measurements of the dry wiped samples, they were rinsed with running water to simulate the effect of rain. Samples were also washed with detergent and sodium hypochlorite (NaClO) and sodium hydroxide (NaOH) solution (algae cleaners) to simulate the effect of professional cleaning. The unweathered and uncleaned samples were handled in such a way so as not to alter the conditions under which they were collected. For each of the wet cleaning treatments, the sample was allowed to dry before the spectral reflectance measurements were taken.

For the samples received at the NRC, specimens taken from two different areas (1 and 2) of the “as received” top (weathered) sheet were analyzed before and after cleaning (see **Table 3**). Cleaning was

achieved by using water and a cloth to wipe off the dirt. No detergent or algicide was used. One to two specimens from the bottom sheet (underlap) without cleaning were analyzed. In some cases, two specimens were analyzed before and after cleaning. This was done to check for differences in the solar reflectivity values between the two areas or between the dirty and clean top surface of the bottom sheet.

**Table 2: Cleaning Processes**

Sample	Cleaning Process	To Replicate
Unexposed	None	Unweathered, aged condition
Uncleaned	None	Weathered, aged condition
Wiped	Wiped with dry cloth	Effect of wind and sweeping
Rinsed	Rinsed with running water	Effect of rain
Detergent-Washed	Phosphate-free household detergent with brush	Professional cleaning
Algae-Cleaner Washed	Sodium Hypochlorite (NaClO) and Sodium Hydroxide (NaOH) solution, with brush	Professional cleaning

**Table 3: Weighted Average Solar Reflectance of Samples Studied at the NRC**

Sample			Solar reflectance		
Sample ID	Location	Year Installed	Top: Uncleaned	Top: Washed and Wiped	Bottom: Unweathered
1D	Canton, MA	1979	0.48	0.50	0.52
2A	Wenham, MA	1984	0.32	0.41	0.55
2D	Wenham, MA	1984	0.39	0.44	0.51
3A	Woburn, MA	1983	0.39	0.41	0.48
4B	Dickson, TX	1984	0.40	0.45	0.49
5B	Tyler, TX	1981	0.41	0.46	0.50
6A	Eules, TX	1984	0.42	0.49	0.51
7A	City of Industry, CA	1979	0.44	0.50	0.53
8A	El Segundo, CA	1982	0.39	0.43	0.50
9B	Mountain View, CA	1983	0.40	0.45	0.52
10B	Lacey, WA	1982	0.40	0.43	0.51
11B	Ft. Steilacoom, WA	1983	0.45	0.47	0.52
12A	Atlanta, GA	1986	0.42	0.48	0.50
13A	Jacksonville, FL	1982	0.41	0.47	0.52
14A	Appleton, WI	1985	0.38	0.44	0.49
15B	Mt. Prospect, IL	1981	0.33	0.39	0.49
15D	Mt. Prospect, IL	1981	0.50	0.52	0.54
16A	Park Ridge, IL	1984	0.35	0.42	0.50
17B	Hackensack, NJ	1986	0.35	0.41	0.50
18A	Englewood, NJ	1985	0.39	0.43	0.48
18C	Englewood, NJ	1985	0.32	0.37	0.48
19A	Iowa, IA	1982	0.34	0.4	0.49
20B	Davis, CA	1981	0.47	0.49	0.52
21A	Haileybury, ON	1981	0.48	0.49	0.55
21C	Haileybury, ON	1981	0.44	0.47	0.51
22A	Hamilton, ON	1984	0.34	0.38	0.51
24A	Oakville, ON	1977	0.43	0.46	0.48
25A	Sarnia, ON	1984	0.37	0.43	0.50

All samples were analyzed using a Varian Cary-5 UV-Vis-NIR spectrophotometer equipped with a total integrating sphere (ASTM, 1996). Spectral reflectance measurements were weighted according to

the ASTM G 159-98 to obtain the overall solar reflectance (ASTM, 1998). This standard is a combination of an editorial revision of tables E 891 and E 892 to make the reference solar spectral energy standard harmonious with ISO 9845-11992. The ASTM G 159 states that the conditions chosen for these tables "are representative of average conditions in the 48 contiguous states of the United States. In real life, a large range of atmospheric conditions can be encountered, resulting in more or less important variations in the atmospheric extinction. Thus, considerable departure from the present reference spectra might be observed depending on time of the day, geographical location, and other fluctuating conditions in the atmosphere."

## Results

The results of the LBNL measurements are summarized in Table 1 and **Figures 1** and **2**. The samples can be divided in two groups: Group A with the unweathered solar reflectance of about 0.80 (see Figure 1) and Group B with unweathered solar reflectance of about 0.63 (see Figure 2).

The solar reflectance of the weathered samples in Group A ranged from 0.32 to 0.71 with a median of 0.55 (see **Figure 3**). With wiping, the solar reflectance improved to 0.42 to 0.75 with a median of 0.69. Rinsing with water improved the solar reflectance to 0.59 to 0.75 with a median of 0.71. Further washing with detergent improved the solar reflectance to 0.65 to 0.80 with a median of 0.77. And washing with an algae cleaner practically restored the solar reflectance of the samples to their unweathered values (the range was 0.77 to 0.82 with a median of 0.80). The solar reflectance of the unweathered samples ranged from 0.79 to 0.82 with a median of 0.80.

There were only four samples in Group B. The solar reflectance of these unweathered samples was 0.63 (see **Figure 4**). The solar reflectance of the weathered samples in Group B ranged from 0.48 to 0.50. Wiping and rinsing with water improved the solar reflectance to 0.59 to 0.62, practically approaching the solar reflectance of the unweathered samples.

The results of the NRC measurements are summarized in Table 3 (see also **Figure 5**). The weighted average solar reflectance for the unweathered (bottom) and weathered (top) surfaces of the gray colored samples ranges from 0.29 to 0.55. As should be expected, surfaces display a higher reflectance value after cleaning. The top side of the bottom (unweathered) sheet also showed higher solar reflectance than the weathered side of the top sheet. Only 10 surfaces (bottom and/or top) out of the 25 tested have slightly over 0.5 solar reflectance. Based on previous work done at the NRC, bottom flaps can be used as a reference material when no original material is available. In most cases, the bottom flap retains most, if not all, of the original properties. It was decided that this would also be done for the reflectivity data. However, in some cases, the bottom flap was found to be dirty and had to be cleaned. It is speculated that the bottom flap may have picked up dirt at the time of installation simply from the environment.

In summary, it is interesting to note that a simple cleaning with water and cloth allowed the samples to regain a substantial part of their original reflectivity. Furthermore, it appears that the roofing materials evaluated in this study did not lose *any* inherent reflectivity with aging, but rather, in-situ reflectivity diminishment was because of obfuscation by atmospheric deposition (primarily by soot) and other "local" environmental factors.

## Conclusion

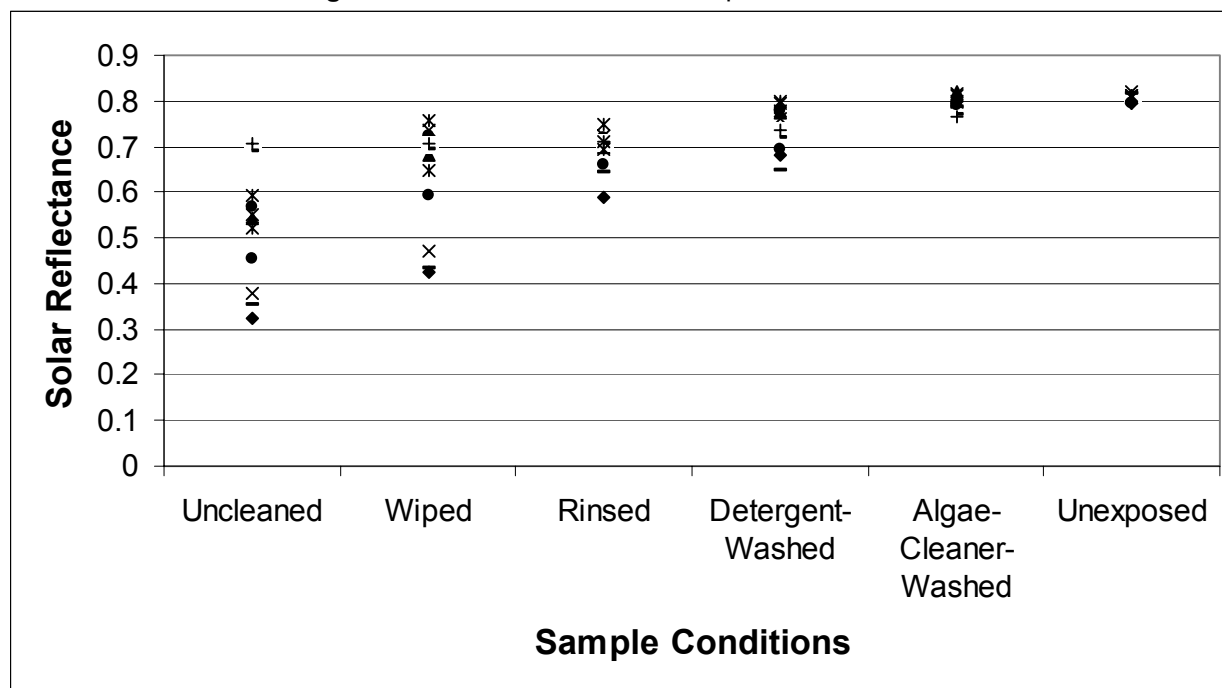
The experiments conducted at the LBNL suggest that for the PVC roofing materials studied that are not covered with algae, wiping and rinsing with water (simulating the annual cleaning by rain) have restored the solar reflectance of the sample to at least 80% of the solar reflectance of the unweathered samples. For samples with algae, washing with detergent and algae-cleaners has practically restored the solar reflectance of the weathered roofing membranes to the solar reflectance of the unweathered membranes.

The solar reflectance measurements from the NRC indicated that with a few exceptions, all roofs have a weighted averaged solar reflectance of less than 0.6. There was no unweathered material available at the time of the analysis. Hence, no final conclusions can be drawn about the effect of weathering on solar reflectance of the roof material analyzed. However, as in the case of the samples analyzed by the LBNL, at least 70%, and as much as 100%, of the initial reflectivity was regained by simply washing the PVC membranes with water (no cleaning detergent).



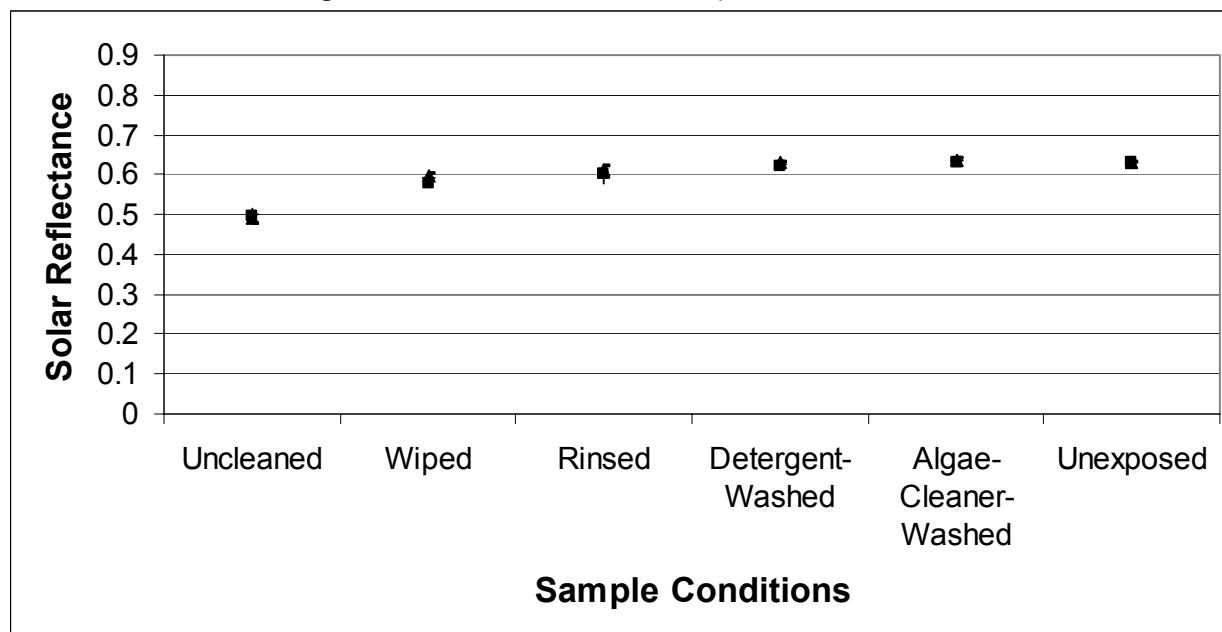
Thus, if high reflectivity is critical to the roof owner, then it would be recommended that the regular maintenance protocol include power washing the membrane (for cases with no significant potentials for algae growth) on a frequency to be determined according to the roof's requirements.

**Figure 1: Solar Reflectance of Samples 1-8 and 11-13**



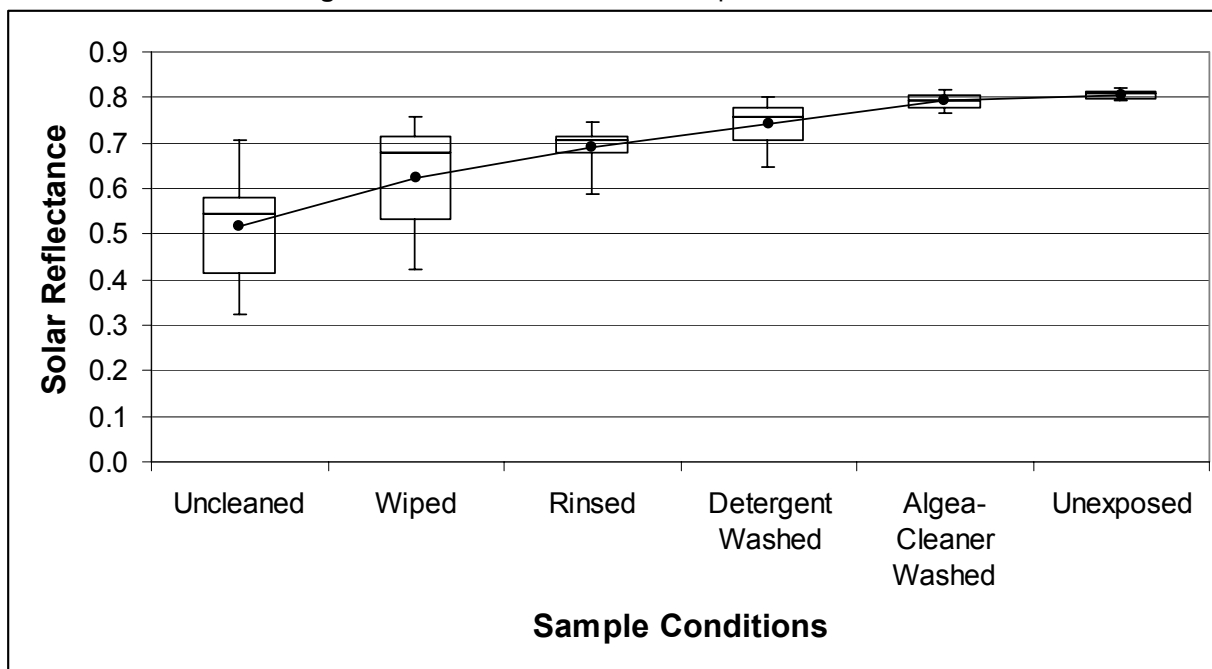
Note: Values are Hemispherical Solar reflectance calculated with air mass 1.5

**Figure 2: Solar Reflectance of Samples 9-10 and 14-15**



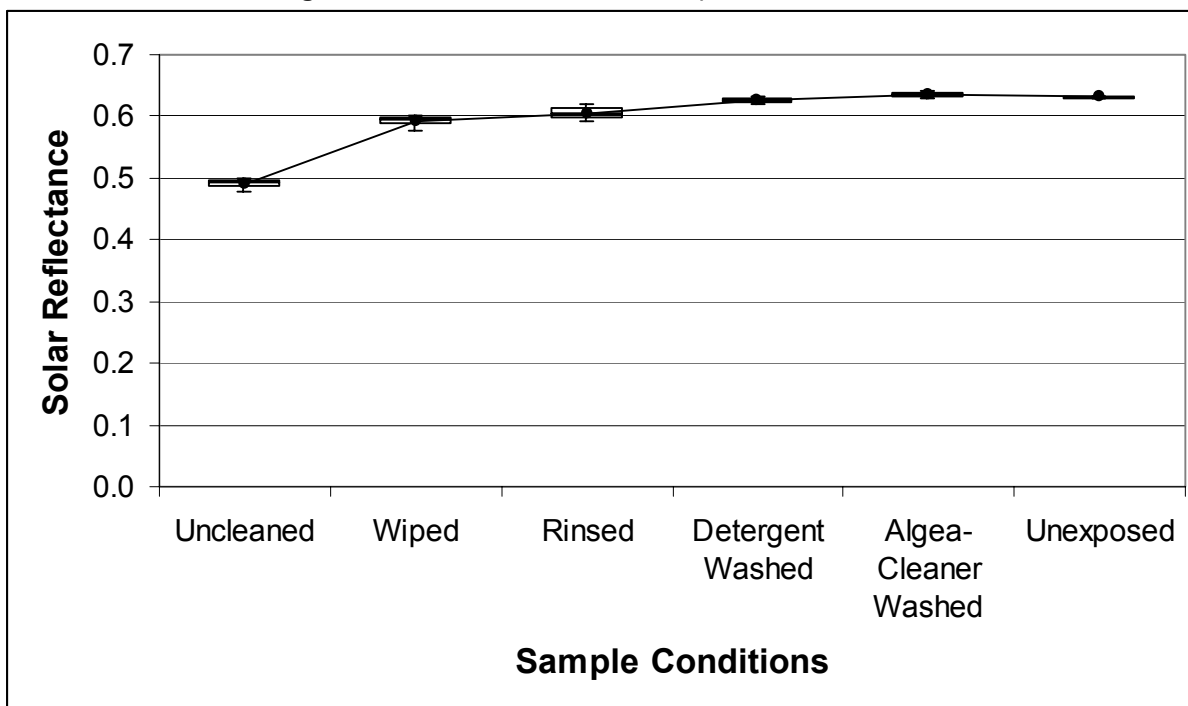
Note: Values are hemispherical solar reflectance calculated with an air mass of 1.5

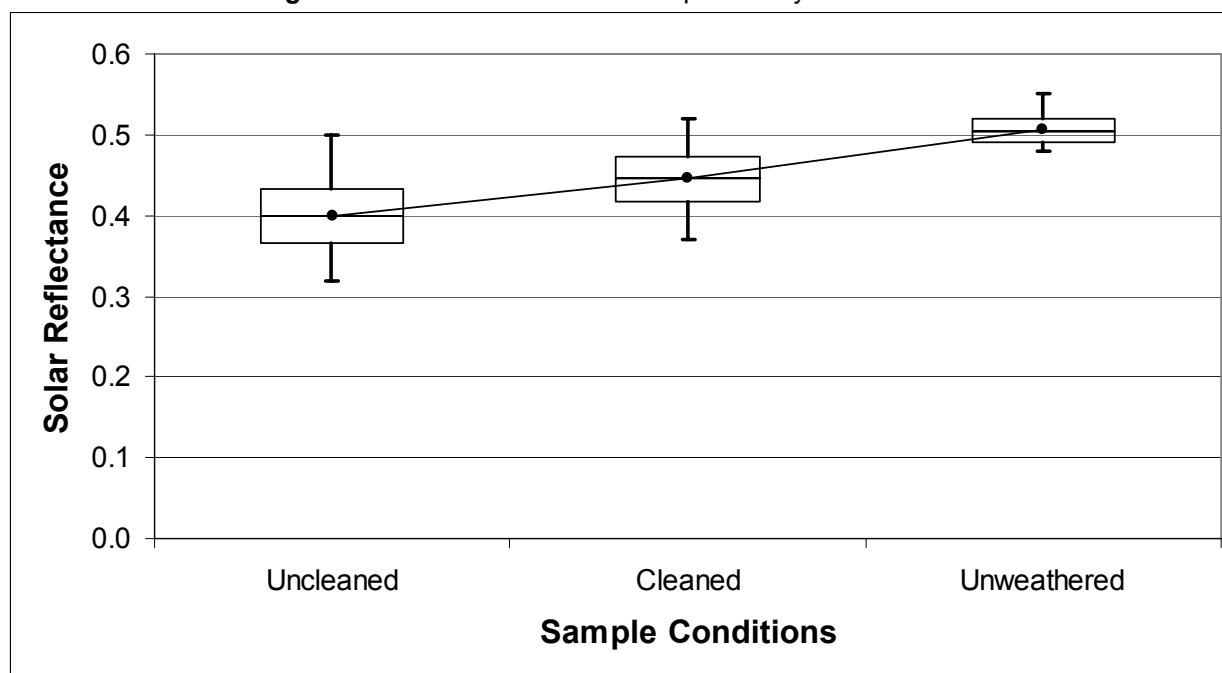
**Figure 3: Solar Reflectance of Samples 1-8 and 11-13**



Note: The data show the minimum, 25<sup>th</sup> quartile, 50<sup>th</sup> quartile (median), 75<sup>th</sup> quartile, and maximum solar reflectance of the samples. The solid line shows the average reflectance of all samples.

**Figure 4: Solar Reflectance of Samples 9-10 and 14-15**



**Figure 5:** Solar Reflectance of Samples Analyzed at the NRC

Note: The data show the minimum, 25<sup>th</sup> quartile, 50<sup>th</sup> quartile (median), 75<sup>th</sup> quartile, and maximum solar reflectance of the samples. The solid line shows the average reflectance of all samples.

## Acknowledgements

This work was supported by the U.S. Environmental Protection Agency under IAG DW89938442-01-2 and by the Assistant Secretary for Energy Efficiency and Renewable Energy, Building Technologies, of the U.S. Department of Energy, under Contract No. DE-AC03-76SF00098. We thank Sarnafil US Inc. for providing us with the samples and treatments for this study and also for supplying the necessary information.

## References

- Akbari, H. and S.J. Konopacki 1998. "The Impact of Reflectivity and Emissivity of Roofs on Building Cooling and Heating Energy Use." *Proceedings of the Thermal Performance of The Exterior Envelopes of Building VII*. December 6-10, 1998. Clearwater Beach, FL.
- . 2004. "Energy Impacts of Heat Island Reduction Strategies in Toronto, Canada." *Energy* 29: 191-210.
- Akbari, H., S. Konopacki and M. Pomerantz. 1999. "Cooling Energy Saving Potential for Reflective Roofs for Residential and Commercial Buildings in the United States." *Energy* 24: 391-407.
- Akbari, H., M. Pomerantz, and H. Taha. 2001. "Cool surfaces and shade trees to reduce energy use and improve air quality in urban areas." *Solar Energy* 70, no 3: 295-310.
- Akbari, H., A.H. Rosenfeld and H. Taha. 1990. "Summer Heat Islands, Urban Trees and White Surfaces." *ASHRAE Transactions* 96, no. 1.
- ASTM (American Society for Testing and Materials). 1996. Standard Test Method for Solar Absorptance, Reflectance, and Transmittance of Materials Using Integrating Spheres. Technical report, ASTM E 903-96.
- . 1998. Standard Tables for References Solar Spectral Irradiance at Air Mass 1.5: Direct Normal and Hemispherical for a 370 Tilted Surface. Technical report, G 159-98. (Hemispherical values were used.)

- Berdahl, P., H. Akbari, and L.S. Rose. 2002. "Aging of reflective roofs: soot deposition," *Applied Optics* 41, no. 12: 2355-2360.
- Eilert, P. 2000. High Albedo (Cool) Roofs: Codes and Standards Enhancement (CASE) Study. Pacific Gas and Electric Company.
- Konopacki, S.J., and H. Akbari. 2001. *Measured Energy Savings and Demand Reduction from a Reflective Roof Membrane on a Large Retail Store in Austin*. Lawrence Berkeley National Laboratory Report No. LBNL-47149, Berkeley, CA.
- . 2002. Energy Savings for Heat Island Reduction Strategies in Chicago and Houston (Including Updates for Baton Rouge, Sacramento, and Salt Lake City. Lawrence Berkeley National Laboratory Report No. LBNL-49638, Berkeley, CA.
- Levinson, R., H. Akbari, S.J. Konopacki, and S. Bretz. 2005. "Inclusion of cool roofs in nonresidential Title 24 prescriptive requirements," *Energy Policy* 33, no. 2: 151-170.
- Paroli, R.M., O. Dutt, A.H. Delgado and H.K. Stenman. 1993. "Ranking PVC Roofing Membranes Using Thermal Analysis." *Journal of Materials and Civil Engineering* 5, no. 1: 83-95.
- Pomerantz, M., H. Akbari, P. Berdahl, S.J. Konopacki, H. Taha and A.H. Rosenfeld. 1999. "Reflective Surfaces for Cooler Buildings and Cities." *Philosophical Magazine B* 79, no. 9: 1457-1476.
- Taha, H. 1996. "Modeling the Impacts of Large-Scale Albedo Changes on Ozone Air Quality in the South Coast Air Basin." *Atmospheric Environment* 31, no. 11: 1667-1676.
- Whelan, B.J., S.P. Graveline, A.H. Delgado, K. Liu, R.M. Paroli. 2004. "Field Investigation and Laboratory Testing of Exposed Poly (Vinyl Chloride) Roof Systems." CIB World Building Congress.
- Young, R. 1998. "Cool Roofs: light –colored coverings reflect energy savings and environmental benefits." *Building Design and Construction* 39, no. 2: 62-64.

# Cooler Tile-Roofed Buildings with Near-Infrared-Reflective Nonwhite Coatings

Ronnen Levinson, Lawrence Berkeley National Laboratory (contact)<sup>1</sup>

Hashem Akbari, Lawrence Berkeley National Laboratory<sup>2</sup>

Joe Reilly, American Rooftile Coatings<sup>3</sup>

## Abstract

Owners of homes with pitched roofs visible from ground level often prefer non-white roofing products for aesthetic considerations. Non-white, near-infrared-reflective architectural coatings can be applied in-situ to pitched concrete or clay tile roofs to reduce tile temperature, building heat gain, and cooling power demand, while simultaneously improving the roof's appearance. Scale model measurements of building temperatures and heat-flux were combined with solar and cooling energy use data to estimate the effects of such cool roof coatings in various California data. Under typical conditions—e.g.,  $1 \text{ kW m}^{-2}$  summer afternoon insolation, R-11 attic insulation, no radiant barrier, and a 0.3 reduction in solar absorptance—absolute reductions in roof surface temperature, attic air temperature, and ceiling heat flux are about 12 K, 6.2 K, and  $3.7 \text{ W m}^{-2}$ , respectively. For a typical  $1,500 \text{ ft}^2$  ( $139 \text{ m}^2$ ) house with R-11 attic insulation and no radiant barrier, reducing roof absorptance by 0.3 yields whole-house peak power savings of 230, 210, and 210 W in Fresno, San Bernardino, and San Diego, respectively. The corresponding absolute and fractional cooling energy savings are  $92 \text{ kWh yr}^{-1}$  (5%),  $67 \text{ kWh yr}^{-1}$  (6%), and  $8 \text{ kWh yr}^{-1}$  (1%), respectively. These savings are about half those previously reported for houses with non-tile roofs. With these assumptions, the statewide peak cooling power and annual cooling energy reductions would be 240 MW and  $63 \text{ GWh yr}^{-1}$ , respectively. These energy savings would reduce annual emissions from California power plants by 35 kilotonnes  $\text{CO}_2$ , 11 tonnes  $\text{NO}_x$ , and 0.86 tonnes  $\text{SO}_x$ . The economic value of cooling energy savings is well below the cost of coating a tile roof, but the simple payback times for using cool pigments in a roof tile coating are modest (5-7 years) in the hot climates of Fresno and San Bernardino.

---

<sup>1</sup> 1 Cyclotron Road, MS 90R2000, Berkeley, CA 94720; tel. 510/486-7494; RMLevinson@LBL.gov

<sup>2</sup> 1 Cyclotron Road, MS 90R2000, Berkeley, CA 94720; tel. 510/486-4287; H\_Akbari@LBL.gov

<sup>3</sup> 432 Cienaga Drive, Fullerton, CA 92835; tel. (714) 680-6436; jcreilly@adelphia.net

**Key Words:** tile roof, cool coating, near-infrared reflective, building simulation, cooling energy, cooling power, California, cool roof, [COOLTILE IR COATINGS™](#)

## Introduction

Owners of homes with pitched roofs visible from ground level often prefer non-white roofing products for aesthetic considerations. American Rooftile Coatings [ARC; Fullerton, CA] has developed non-white, near-infrared (NIR)-reflective architectural coatings that can be applied in-situ to pitched concrete or clay tile roofs. These coatings can reduce tile temperature, building heat gain, and cooling power demand, while simultaneously improving the roof's appearance. Such NIR-reflective roof coatings can cool tiles while allowing choice of color by reflecting a significant fraction of the 52% of solar energy that arrives as invisible, NIR radiation<sup>4</sup> (Levinson *et. al* 2004a, 2004b).

Previous studies have measured and/or simulated reductions in cooling energy use and/or peak cooling power demand achieved by retrofitting houses with *white* roofs. For example, Parker *et al.* (1998) measured energy savings averaging 19% for eleven Florida homes, while Akbari *et al.* (1997), measured cool-roof energy savings exceeding 80% at a house in Sacramento. (The Sacramento house was unusual in that its walls were well-shaded by trees, making its roof the primary source of solar heat gain.) Konopacki and Akbari (2000), Konopacki *et al.* (1997), and Akbari and Konopacki (2004) have simulated residential cooling energy and peak demand savings in many North American cities and estimate savings of about 10-20%, depending on the house construction and roof insulation. Cool-roof simulations have been used to develop the EPA EnergyStar Roofing Comparison Calculator (EPA 2004) and the DOE Cool Roof Calculator (DOE 2004), online tools that calculate cool-roof savings as a function of reflectance increase, building characteristics, cooling equipment, and climate.

Since cooling power and energy savings are proportional to increase in roof reflectance (Konopacki *et al.* 1997), white-roof savings can be scaled down to estimated savings achievable

---

<sup>4</sup> In the air-mass 1.5 hemispherical solar irradiance considered typical of North American ground-level insolation, 52% of the energy arrives as near-infrared radiation (0.7 – 2.5 microns). The remainder arrives in the ultraviolet (0.3 – 0.4 microns, 5%) and visible (0.4 – 0.7 microns, 43%) spectra.

by (typically less reflective) nonwhite cool roofs. However, these savings are not directly applicable to tile-roofed homes, because the flow of heat from roof to building can be significantly decreased by the well-ventilated gap between tile and roofdeck.

The current study uses measurements from scale models to quantify the reductions in roof surface temperature, attic air temperature, and ceiling heat flux that are achieved by finishing roof tiles with NIR-reflective coatings. This data is then used to predict the energy savings that would accrue in various climates to full-scale homes roofed with NIR-reflective tiles.

We have monitored the interior and exterior temperatures of four adjacent, 1:10 scale, air-conditioned model houses sited in the hot, inland Southern California city of Riverside. The four buildings were roofed with concrete tiles finished with black, white, cool color (NIR reflecting), and standard color (NIR absorbing) coatings, respectively. The thermal performances of the buildings with matching cool and standard color roofs were compared to each other and to those of the black- and white-roofed reference buildings. From this comparison we characterized the thermal performance of the cool roof tile coating, and extrapolated the results to estimate potential reductions in peak cooling power demand and annual cooling energy consumption by homes in various California climates.

## Theory

### Reductions in Roof Surface Temperature, Attic Air Temperature, and Ceiling Heat Flux

Neglecting thermal storage and linearizing the exchange of thermal radiation between the roof and its environment, reductions in roof surface temperature  $T_s$ , attic air temperature  $T_a$ , and ceiling heat flux  $q$  are proportional to the reduction  $\Delta\alpha$  in the solar absorptance of the roof. That is,

$$\Delta x = k_x \times I \Delta\alpha \quad (1)$$

where  $I$  is insolation [ $\text{W m}^{-2}$ ];  $x$  is a building property ( $T_s$ ,  $T_a$ , or  $q$ ); and the property-specific sensitivity (coefficient)  $k_x$  depends on the thermal resistances (hereafter, simply “resistances”;  $\text{m}^2 \text{K W}^{-1}$ ) to convection of heat from the roof to the outside air, radiation of heat from the roof to its radiative exchange surface, and transfer of heat from the roof to the air-conditioned interior

(Appendix). This simplified model of building heat transfer can be used to determine  $k_x$  by regressing measurements of building property reduction  $\Delta x$  to reduction in absorbed insolation,  $I \Delta \alpha$ .

## Cooling Power Savings

If a house is cooled by an air-conditioner with coefficient of performance COP, reducing ceiling heat flux by  $\Delta q$  [ $\text{W m}^{-2}$ ] decreases cooling power demand per unit ceiling area  $P$  [ $\text{W m}^{-2}$ ] by

$$\Delta P = \text{COP}^{-1} \Delta q = \text{COP}^{-1} k_q I \Delta \alpha \quad (2)$$

## Cooling Energy Savings

The annual cooling energy savings per unit ceiling area [ $\text{kWh m}^{-2}$ ] will be

$$\Delta E = \frac{1}{\text{COP}} \times \int_{\tau_{\text{load}}} \Delta q(\tau) d\tau = \frac{1}{\text{COP}} \times k_q \Delta \alpha \int_{\tau_{\text{load}}} I(\tau) d\tau \quad (3)$$

where COP is the air conditioner's coefficient of performance (output cooling power / input electrical power), assumed constant;  $\tau$  is time; and  $\int_{\tau_{\text{load}}} I(\tau) d\tau$  is the annual global horizontal insolation [ $\text{kWh m}^{-2}$ ] incident on the roof during those hours in which there is a positive ceiling heat flux into the interior of the house that is then removed by air conditioning. This insolation load may be estimated as  $\phi \times d_{\text{annual}} \times \bar{J}$ , where  $\bar{J}$  is the annual average daily insolation [ $\text{kWh day}^{-1}$ ] weighted according to monthly distribution of cooling degree days,  $d_{\text{annual}}$  is the number of days per year on which the building is air-conditioned, and  $\phi$  represents the fraction of daily insolation that generates a ceiling heat flux that must be removed by the air conditioner. The weighted daily insolation can be estimated from historical weather and solar data, while the number of operating days can be estimated from simulations of annual cooling energy consumption.

Since the fraction of daily insolation that generates a ceiling heat flux that must be removed by the air conditioner depends on both the thermal mass of the roof and on the operating schedule of a building's cooling equipment, a proper estimation of the fraction  $\phi$  requires modeling outside



the scope of the current study. Hence, we arbitrarily set  $\phi$  to its midrange value of 0.5, with the observation that our estimates of energy savings can be linearly rescaled to another value of  $\phi$ .

## Statewide Savings

### Cooling Power

If the reduction in cooling power demand per unit ceiling area per unit decrease in solar absorptance of a house in California climate  $i$  is  $(\Delta P / \Delta \alpha)_i$  [W m<sup>-2</sup>], the potential reduction in peak cooling power demand  $\Delta \tilde{P}_{CA}$  [W] for the state of California (assuming that building cooling demand peaks at the same time as overall power demand) may be estimated as

$$\Delta \tilde{P}_{CA} = \Delta \alpha_{\text{avg}} \sum_i (\Delta P / \Delta \alpha)_i A_i \quad (4)$$

where  $\Delta \alpha_{\text{avg}}$  is the average expected reduction in solar absorptance, and  $A_i$  is the aggregate ceiling area of air-conditioned, potentially coatable tile-roofed houses in regions of California whose weather we can characterize by that of climate  $i$  (Fresno, San Bernardino, or San Diego). We further assume that in each climate, some fraction  $f$  of houses are roofed with coatable tiles, and that the average ceiling area of a house is  $A_{\text{ceiling}}$ . If the number of air-conditioned houses in each climate is  $N_i$ , then  $A_i = f A_{\text{ceiling}} N_i$ , yielding statewide power savings

$$\Delta \tilde{P}_{CA} = f \Delta \alpha_{\text{avg}} A_{\text{ceiling}} \sum_i (\Delta P / \Delta \alpha)_i N_i \quad (5)$$

The California Energy Commission has published yearly estimates of the number of air-conditioned houses in each of its 16 demand forecasting climate zones<sup>5</sup> (Figure 9, p.32). We estimate  $N_i$  by assigning the houses located in each of the forecasting climate zones to one of the three simulation climates (Table 6, p.26).

### Cooling Energy

The statewide reduction in annual cooling energy consumption,  $\Delta \tilde{E}_{CA}$  [kWh yr<sup>-1</sup>] may be estimated from the analogous expression

---

<sup>5</sup> Note that the Forecasting Climate Zones are not the same as the California Thermal Zones used in building simulations.

$$\Delta \tilde{E}_{CA} = f \Delta \alpha_{\text{avg}} A_{\text{ceiling}} \sum_i (\Delta E / \Delta \alpha)_i N_i \quad (6)$$

## Emissions

Energy savings reduce emissions of carbon dioxide (CO<sub>2</sub>), nitrogen oxides (NO<sub>x</sub>), and sulfur oxides (SO<sub>x</sub>) from California power plants at the rates of 563 kg CO<sub>2</sub>, 17 g NO<sub>x</sub>, and 14 g SO<sub>x</sub> per MWh (ICF Consulting, 1999).

## Experiment

### Construction, Installation, and Instrumentation of the Scale Models

We tested four identical, 1:10 scale, single-room wooden houses modeled after desert homes. Each building had

- a concrete tile roof mounted on a pitched deck;
- a naturally ventilated attic;
- R-11 (1.9 m<sup>2</sup> K W<sup>-1</sup>) foam-board insulation constituting the room's ceiling and lining the inside of the room's floor and walls;
- an aluminum foil facing on the top of the ceiling;
- white exterior walls;
- a thermoelectric air conditioner with a cooling output of 120 W (400 BTU h<sup>-1</sup>), controlled by an electronic thermostat capable of regulating the air temperature inside the room to within 0.2K; and
- a resistive heating element in the center of the room available to supply a known heat load during calibration of the air conditioner.

The attic's natural ventilation was provided by two pairs of 5-cm diameter holes in its gable equipped with removable plugs. One pair of holes was closed, while each member of the other pair was half-closed (i.e., fitted with half-circle plugs).

The scale models (denoted *A*, *B*, *C*, and *D*) were installed in a courtyard on the grounds of the Riverside Public Utilities (RPU) facility in Riverside, CA (Figure 1, p.28). Each building was set

on temporary concrete footers, and oriented to align the ridge of its roof along an east-west line. The goal was to provide each building's roof with full southern solar exposure free from shading by local mountains, surrounding structures and neighboring scale models. The courtyard was modestly windy, with mid-afternoon peak windspeeds of 1.5 to 2 m s<sup>-1</sup> (3.4 – 4.5 mph).

Each building was instrumented with precision thermistors (accuracy  $\pm 0.2\text{K}$ , response time 15s) to measure the temperatures of the tile upper surface, tile lower surface, deck upper surface, deck lower surface, attic air, ceiling upper surface, ceiling lower surface, and room air. Heat fluxes ( $\text{W m}^{-2}$ ) through the tile, deck, and ceiling were determined by dividing the temperature difference across each structural element (K) by the element's thermal resistance ( $\text{m}^2 \text{K W}^{-1}$ ). The input power drawn by each air conditioner was determined from voltage and current transducers (power = voltage  $\times$  current).

An on-site weather station was erected to measure ambient air temperature, horizontal insolation, relative humidity, wind speed, and wind direction. A pair of dataloggers were programmed to record 1-minute averages of all measurements, and connected to a dedicated phone line. We periodically downloaded these results via modem. The one-minute measurements were averaged over 15-minute intervals to reduce noise and compact the data set.

Uniformity of building construction and orientation was increased by coating the roofs of all 4 buildings black, then rotating buildings and sealing leaks to reduce building-to-building variations in measured temperatures.

## **Coating Formulation, Tile Preparation, and Reflectance Measurement**

Six experimental NIR reflective coatings—terracotta (red), chocolate (brown), gray, green, blue, and black—were prepared, each similar in appearance to a conventional coating (Figure 2, p.29). These formulations provide a reasonably full color palette. The first four NIR-reflective coatings were single-layer systems (i.e., color on gray tile), while the blue and black NIR-reflective coatings were formed by applying a NIR-transmitting layer of color over an opaque, highly-reflective white undercoating.

The solar reflectances of 25-cm<sup>2</sup> tile chips finished with each standard and cool coating were measured in the lab according to ASTM Test Method C 1549 (Devices & Services Solar

Spectrum Reflectometer) (ASTM 2003a). All coatings had thermal emittance circa 0.9, and each cool coating had a solar reflectance  $\rho$  exceeding 0.4 (Table 1, p.24).

Standard and cool versions of each of the six color coatings were airlessly sprayed onto tiles and trim pieces, preparing 20 tiles per coating.

## **Trials**

The roof of building *C* was left black ( $\rho=0.04$ ), and building *B* reroofed with white tiles ( $\rho=0.85$ ). Over the course of a summer, building *D* was reroofed with a series of standard color tiles, while building *A* was reroofed with a series of matching cool colors tiles. Hence, at any given time building *C* had a black roof, building *B* had a white roof, building *D* had a standard color roof, and building *A* had a cool color roof matching that of building *D*.

Each color-pair trial included several days during which the air conditioners were turned off, and several more during which they were turned on (Table 1, p.24). Two days of clear-weather data were selected for each color-pair trial: one on which the buildings were air conditioned, and another on which they were not (Table 1, p.24).

On any given day, all thermostats were programmed to the same setpoint, which was typically about 5K below the expected daily peak outside air temperature. It would have been preferable to use a constant setpoint typical of real-house operation (e.g., 24°C), but the device in the black-roofed house tended to saturate (fail to meet cooling load) when the outside air temperature exceeded the setpoint by more than 5K. Our budget did not permit the installation of additional or higher-capacity cooling units.

## **Results**

### **Thermal Performance of Tile Coatings on the Scale Models**

#### **Measured Reductions in Temperature, Heat Flux**

The performance of each cool roof tile coating was gauged by measured reductions (standard color value – matching cool color value) in the daily peak values of roof surface temperature  $T_s$ , attic air temperature  $T_a$ , interior air temperature  $T_i$  of an unconditioned building, and heat flux  $q$

into the ceiling of an air-conditioned building (Table 2, p.24). The coatings reduced roof surface temperature by 5-10 K and ceiling heat flux by about 10 to 20%.

Note that the ceiling heat flux was computed assuming a ceiling undersurface temperature of 24°C to make the flux values relevant to real-house performance.<sup>6</sup> Also, noise originating from transient building-to-building differences in incident solar radiation was decreased by basing these peak reductions on full days of data from all four buildings (Appendix).

We note that the reductions in peak roof surface temperature, attic air temperature, unconditioned interior air temperature, and ceiling heat flux each decrease as the roof-level windspeed increases. Hence, reductions may be smaller for peak daily windspeeds greater than the  $1.5 - 2 \text{ m s}^{-1}$  observed at the experimental site.

#### **Regressed Sensitivities of Temperature, Heat Flux to Reduction in Absorbed Insolation**

Reductions in peak temperature ( $\Delta T_s$ ,  $\Delta T_a$ ,  $\Delta T_i$ ) and peak heat flux ( $\Delta q$ ) were linearly regressed to the reduction in absorbed insolation  $I \Delta \alpha$  to yield sensitivities  $k_x$ , where  $x = T_s, T_a, T_i$ , or  $q$  (Figure 3 - Figure 6, pp.29-31).

The top of the foam board insulation that comprised the ceiling was faced with aluminum foil (thermal emittance about 0.07). This foil acted as a radiant barrier, increasing the radiative resistance between ceiling and roofdeck from about R-1 (what would be observed if both ceiling and roofdeck had emittance of 0.9) to about R-14. The radiative resistance in a house without a radiant barrier would be much lower, and the heat flux through the ceiling much higher. Since the sensitivities determined from the measured data apply only to a building with (a) R-11 aggregate resistance of the ceiling plus attic insulation and (b) a radiant barrier, heat transfer theory (Appendix) was used to extrapolate sensitivities for a building that (a) does not have a radiant barrier; (b) has ceiling resistance R-2; and (c) has attic insulation varying from R-0 to R-30 (Table 3, p.25).

---

<sup>6</sup> Ceiling heat flux is the ratio of the temperature difference across the ceiling to the thermal resistance of the ceiling. Since the ceiling was formed by a slab of R-11 insulation, the temperature of the ceiling's upper surface was minimally affected by the temperature of its underside. Hence, the "standardized" ceiling heat flux was computed as  $(T_{\text{top of ceiling}} - 24^\circ\text{C}) / R_{\text{ceiling}}$ .

Typical sensitivities (reduction in temperature or flux per reduction in absorbed insolation) extrapolated for an air-conditioned house with R-11 attic insulation, an R-2 ceiling, and no radiant barrier are approximately 41 K / (kW m<sup>-2</sup>) for roof surface temperature, 21 K / (kW m<sup>-2</sup>) for attic temperature, and 12 W m<sup>-2</sup> / (kW m<sup>-2</sup>) for ceiling heat flux per unit ceiling area. Hence, under typical conditions—e.g., R-11 attic insulation, 1 kW m<sup>-2</sup> insolation, 0.3 reduction in solar absorptance—absolute reductions in roof surface temperature, attic air temperature, and ceiling heat flux would be about 12 K (21 °F), 6.2 K (8.0 °F), and 3.7 W m<sup>-2</sup>, respectively.

## Cooling Power and Energy Savings of the Scale Models

The instantaneous cooling power demand  $\tilde{P}$  [W] of each scale model was calculated as the total power drawn by its thermoelectric air conditioner minus the constant power demand of the device's always-on fans. Building cooling power demand can be used to determine the reduction (standard color building value – cool color building value) in each of four quantities:

- building cooling power demand per unit ceiling area,  $P$  [W m<sup>-2</sup>];
- building cooling load per unit ceiling area,  $\text{COP}^{-1} P$  [W m<sup>-2</sup>];
- daily building cooling energy use per unit ceiling area,  $E = \int_{\text{day}} P d\tau$  [kWh m<sup>-2</sup>], and
- daily building cooling load per unit ceiling area,  $\text{COP}^{-1} E$  [kWh m<sup>-2</sup>].

Here  $\tau$  is time, and COP is the coefficient of performance of each thermoelectric air conditioner, measured in nighttime's calibration trials as the ratio of cooling power demand [W] to known resistive heat flux [W].

After a great deal of analysis, it was determined that direct determination of scale-model cooling power and energy savings was impractical, because

- the cooling load of each building was dominated by heat gains through the walls, making the ceiling contribution difficult to measure;
- wall thermal resistance varied building to building, primarily because of infiltration around and/or conduction through the wall-mounted air conditioner; and

- the COP of each thermoelectric device was temperature dependent, meaning that COP values determined during nighttime calibrations of the devices were not necessarily applicable to operation at higher daytime temperatures.

Hence, we decided to base estimates of real-house cooling power savings on reduction in ceiling heat flux, which was easier to measure.

## Estimated Cooling Power Savings for Full-Scale Houses

Figure 7 (p.31) charts the peak cooling power savings per unit decrease in solar absorptance,  $\Delta P/\Delta\alpha$ , versus ceiling insulation, estimated via Eq. (2) for full-scale houses (without radiant barriers) in three California climates: Fresno (Central Valley), San Bernardino, and San Diego (coastal). Results for common levels of attic insulation are also presented in Table 4 (p.25). Whole-house peak cooling power savings  $\Delta\tilde{P}$  [W] may be computed by multiplying the tabulated value of  $\Delta P/\Delta\alpha$  (5.5, 5.1, and 5.0 W m<sup>-2</sup> for Fresno, San Bernardino, and San Diego, respectively, assuming R-11 ceiling insulation) by ceiling area (e.g.,  $A = 139$  m<sup>2</sup> [1,500 ft<sup>2</sup>]) and decrease in solar absorptance (e.g.,  $\Delta\alpha = 0.3$ ). Whole-house peak power savings are 230, 210, and 210 W in Fresno, San Bernardino, and San Diego, respectively.

## Estimated Cooling Energy Savings for Full-Scale Houses

Figure 8 (p.32) charts the annual cooling energy savings per unit decrease in solar absorptance,  $\Delta E/\Delta\alpha$ , versus ceiling insulation, for the same three climates—Fresno, San Bernardino, and San Diego. Results for common levels of attic insulation are also presented in Table 4 (p.25). Whole-house cooling energy savings  $\Delta\tilde{E}$  [kWh yr<sup>-1</sup>] may be computed by multiplying the tabulated value of  $\Delta E/\Delta\alpha$  (2.2, 1.6, and 0.2 kWh m<sup>-2</sup> yr<sup>-1</sup> for Fresno, San Bernardino, and San Diego, respectively, assuming R-11 attic insulation) by ceiling area and decrease in solar absorptance. The whole-house energy savings are 92, 67, and 8 kWh yr<sup>-1</sup> in Fresno, San Bernardino, and San Diego, respectively.

For a typical ceiling area of 1,500 ft<sup>2</sup> (139 m<sup>2</sup>) and a typical reduction in roof absorptance of 0.3, the whole-house peak power savings were 230, 210, and 210 W, respectively, while the whole-

house energy savings were 92, 67, and 8 kWh yr<sup>-1</sup>, respectively. At 0.12 \$/kWh, the values of energy savings in Fresno, San Bernardino, and San Diego are 11, 8, and 1 \$/yr.

If the area of the sloped tile roof is about 1.5 times the ceiling area, or 209 m<sup>2</sup>, the cost of coating the roof (at 15 \$/m<sup>2</sup>) about \$3100. Of this, the premium for using cool pigments in place of standard pigments (at 0.27 \$/m<sup>2</sup>) is about \$56. Hence, while the economic value of the energy savings derived from a cool colored roof tile coating is far below than cost of the coating, the simple payback times for the cost *premium* associated with using cool pigments in the coating are about 5 and 7 years in the hot climates of Fresno and San Bernardino, respectively.

These energy savings can be cast as fractions of cooling energy use by using California Energy Commission projections of average annual residential cooling energy use in each climate. Assuming a typical house flat roof area of 1,500 ft<sup>2</sup> (139 m<sup>2</sup>), average cooling energy uses in Fresno, San Bernardino, and San Diego in the year 2000 were 12.1, 8.2, and 4.3 kWh m<sup>-2</sup> yr<sup>-1</sup>, respectively (CEC 2000). Hence, fractional savings were 5%, 6%, and 1% in these three climates.

## Statewide Reductions in Power Demand, Energy Consumption, and Emissions

There are about 2.41, 1.01 and 3.01 million air-conditioned California homes in climates characterizable by those of Fresno, San Bernardino, and San Diego, respectively (Table 6). If  $f = 20\%$  of California houses were roofed with coatable tiles, and all had R-11 attic insulation and an average ceiling area of 139 m<sup>2</sup> (1,500 ft<sup>2</sup>), roof tile coatings that lower solar absorptance by 0.3 would yield statewide peak demand savings of

$$0.20 \times 0.3 \times 139 \times (5.5 \times 2,410,000 + 5.1 \times 1,010,000 + 5.0 \times 3,010,000) = 280 \text{ MW}$$

The aggregate cooling energy use reduction would be

$$0.20 \times 0.3 \times 139 \times (2.2 \times 2,410,000 + 1.6 \times 1,010,000 + 0.2 \times 3,010,000) = 63 \text{ GWh yr}^{-1}$$

which at \$0.12 kWh<sup>-1</sup> is worth about \$7.5 M yr<sup>-1</sup>.

These energy savings would reduce annual emissions from California power plants by 35 kilotonnes CO<sub>2</sub>, 11 tonnes NO<sub>x</sub>, and 0.86 tonnes SO<sub>x</sub>.



## Discussion

Power savings (per unit ceiling area) were about half those reported for Florida houses with R-11 attic insulation (Parker *et al.* 1998). This may result from

- the high thermal resistance between the roof tiles and roofdeck, which adds about R-2 to the roof-to-interior thermal resistance (Appendix);
- convective roofdeck cooling by air flowing between tile and deck; and/or
- natural attic ventilation in the model houses.

It should be also noted that there is additional uncertainty in the energy savings because of the arbitrary assumption that half of the daily insolation incident on a house results in ceiling heat flux that must be removed by air conditioning. However, our results can be linearly rescaled to another value of this fraction  $\phi$ . Similarly, our estimates of statewide savings are proportional to the fraction of California homes roofed with coatable tiles, assumed to be  $f = 0.2$ . These savings can be linearly rescaled to another value of the fraction  $f$ .

Peak power demand reductions in cooler climates (e.g., San Diego) may eliminate the need for air conditioning in some homes by keeping the interior air temperature of a house below the thermostatic setpoint. This would permit homeowners to avoid the purchase of air-conditioning equipment.

## Conclusions

Application of NIR-reflective roof tile coatings yielded measurable reductions in roof surface temperature, attic air temperature, unconditioned interior air temperature, and ceiling heat flux. The coatings reduced roof surface temperature by about 5 to 10 K and ceiling heat flux by about 10 to 20%.

The coatings are predicted to save about 230 W ( $1.7 \text{ W m}^{-2}$ ) in peak cooling power and 92 kWh  $\text{yr}^{-1}$  ( $0.7 \text{ kWh m}^{-2} \text{ yr}^{-1}$ ) in cooling energy for a 1,500  $\text{ft}^2$  ( $139 \text{ m}^2$ ) Fresno house with R-11 attic insulation. The economic value of annual energy savings is much less than the total cost of a tile coating, but in the hot Fresno climate, the simple payback time for the cost premium of using

cool pigments in a roof tile coating is only 5 years. Savings can be about 3 times higher for houses with minimal ceiling insulation. The peak power demand reductions in cooler climates (e.g., San Diego) may eliminate the need to purchase an air conditioner.

Statewide reductions in peak cooling power demand and annual cooling energy consumption would be 240 MW and 63 GWh yr<sup>-1</sup>, respectively. These energy savings would reduce annual emissions from California power plants by 35 kilotonnes CO<sub>2</sub>, 11 tonnes NO<sub>x</sub>, and 0.86 tonnes SO<sub>x</sub>.

A survey and analysis of the California new construction and retrofit markets for cool tile coatings should be conducted to better quantify the potential savings that these coatings may afford, as well as their market acceptability.

## Acknowledgements

This work was supported by the California Energy Commission (CEC) through its Public Interest Energy Research Program (PIER) / Energy Innovation Small Grant Program (EISG), and by the Assistant Secretary for Renewable Energy under Contract No. DE-AC03-76SF00098.

We would like to acknowledge the valuable assistance of David Wright, Atoya Mendez, Steven Lafund and especially Klaus Meister of Riverside Public Utilities; Dennis DeBartolomeo and Paul Berdahl of Lawrence Berkeley National Laboratory; and Glen Sharp of the Energy Commission. We thank Jerry Vandewater and Chris Dodge from Monier-Lifetile for supplying the tile. We also thank various other contributors who helped to make this project a success, including Phil Bremenstuhl of C. T. Consultants; Bob Sypowicz and John Wauchope of MCC, Inc.; Dave Getty, Steve Aprea, Bernie Cunningham, and Peter Croft for blueprint drawings, construction, installation and Visio drawings; Jim Dunn and Ken Loye of Ferro Company; Phil Avery and Craig Blockfelter of BASF; and Dana Harding and Mike Muldown of Consolidated Color Corporation.

## References

- Akbari, H., S. Bretz, D. Kurn and J. Hanford. 1997. Peak power and cooling energy savings of high-albedo roofs. *Energy and Buildings* **25**:117-126.
- Akbari, H. and S. Konopacki. 2004. Energy impacts of heat island reduction strategies in Toronto, Canada. *Energy*, **29**, 191-210. Also Lawrence Berkeley National Laboratory Report LBNL-49172, Berkeley, CA, November 2001.
- ASTM. 2003a. C1549-02: Standard test method for determination of solar reflectance near ambient temperature using a portable solar reflectometer. Annual Book of ASTM Standards 04.06. Philadelphia, PA: American Society for Testing and Materials.
- California Energy Commission (CEC). 2000. California energy demand, 2000-2010. P200-00—002. Sacramento, CA: California Energy Commission.

DOE. 2004. DOE Cool Roof Calculator. Online at <http://www.ornl.gov/sci/roofs+walls/facts/CoolCalcEnergy.htm> .

EPA. 2004. EnergyStar Roofing Comparison Calculator. Online at <http://roofcalc.com> .

ICF Consulting. 1999. Emissions factors, global warming potentials, unit conversions, emissions, and related facts. Online at <http://www.epa.gov/appdstar/pdf/brochure.pdf> .

Konopacki, S. and H. Akbari. 2000. Energy savings calculations for heat island reduction strategies in Baton Rouge, Sacramento and Salt Lake City. Lawrence Berkeley National Laboratory Report LBNL-42890. Berkeley, CA.

Konopacki, S. and H. Akbari. 2001. Measured energy savings and demand reduction from a reflective roof membrane on a large retail store in Austin. LBNL-47149. Berkeley, CA: Lawrence Berkeley National Laboratory.

Konopacki, S. and H. Akbari. 2002. Energy savings of heat-island-reduction strategies in Chicago and Houston (including updates for Baton Rouge, Sacramento, and Salt Lake City). Lawrence Berkeley National Laboratory Report LBL-49638, Berkeley, CA.

Konopacki, S., H. Akbari, M. Pomerantz, S. Gabersek and L. Gartland. 1997. Cooling energy savings potential of light-colored roofs for residential and commercial buildings in 11 U.S. metropolitan areas". Lawrence Berkeley National Laboratory Report LBNL-39433. Berkeley, CA.

Levinson, R., P. Berdahl, and H. Akbari. 2004a. Solar spectral optical properties of pigments, part I: model for deriving scattering and absorption coefficients from transmittance and reflectance measurements. Submitted to *Solar Energy Materials & Solar Cells*.

Levinson, R., P. Berdahl, and H. Akbari. 2004b. Solar spectral optical properties of pigments, part II: survey of common colorants. Submitted to *Solar Energy Materials & Solar Cells*.

Parker, D., J. Huang, S. Konopacki, L. Gartland, J. Sherwin and L. Gu. 1998. Measured and simulated performance of reflective roofing systems in residential buildings. *ASHRAE Transactions* **104**(1):963-975.

Schultz, Don. 1983. Measurement and evaluation of the energy conservation potential in California's residential sector. Publication 400-83-026. Sacramento, CA: California Energy Commission.

# Appendix

## Building Heat Transfer

### Roof Energy Balance

We can obtain approximate but highly useful relations for the thermal properties of a building by neglecting thermal storage and linearizing the exchange of thermal radiation. With these assumptions, the quasi-steady energy balance on the surface of a roof may be written

$$\alpha I = R_o^{-1} (T_s - T_o) + R_r^{-1} (T_s - T_r) + R_i^{-1} (T_s - T_i) \quad (\text{A1})$$

where  $\alpha$  is the roof's solar absorptance (1-solar reflectance);  $I$  is insolation [ $\text{W m}^{-2}$ ];  $T_s$ ,  $T_o$ ,  $T_r$ , and  $T_i$  are the temperatures [K] of the roof surface, outside air, radiative exchange surface seen by the roof (e.g., the sky), and the air inside the room, respectively; and  $R_o$ ,  $R_r$ , and  $R_i$  are the thermal resistances (hereafter, simply “resistances”;  $\text{m}^2 \text{K W}^{-1}$ ) to convection of heat from the roof to the outside air, radiation of heat from the roof to the its radiative exchange surface, and transfer of heat from the roof's surface to the air-conditioned interior, respectively.

### Absolute Roof Surface Temperature, Attic Air Temperature, and Ceiling Heat Flux

Eq. (A1) can be solved to find the roof's surface temperature,

$$T_s = \frac{\alpha I R_o R_r R_i + R_i R_r T_o + R_o R_r T_i + R_o R_i T_r}{R_o R_r + (R_o + R_r) R_i} \quad (\text{A2})$$

and the roof-to-interior, or “ceiling,” heat flux [ $\text{W m}^{-2}$ ]

$$q = R_i^{-1} (T_s - T_i) \quad (\text{A3})$$

If the resistance of the ceiling plus the attic insulation is  $R_c$ , and the resistance between the top of the roof and the bottom of the roofdeck is  $R_d$ , the temperatures of the insulation top and roofdeck bottom will be

$$T_{\text{insulation top}} = T_i + q R_c \quad (\text{A4})$$

and

$$T_{\text{roofdeck bottom}} = T_s - q R_d \quad (\text{A5})$$

respectively. The attic air temperature,  $T_a$ , will be approximately the average of these two surface temperatures:

$$T_a = \frac{T_{\text{insulation top}} + T_{\text{roofdeck bottom}}}{2} = \frac{(T_s + T_i) + q(R_c - R_d)}{2} \quad (\text{A6})$$

### Normalized Roof Surface Temperature, Attic Air Temperature, and Ceiling Heat Flux

Any thermal property  $x$  of a building with a colored roof can be compared to the corresponding properties of an otherwise-identical white-roofed building,  $x_w$ , and an otherwise-identical black-roofed building,  $x_b$ , using the normalization

$$\hat{x} \equiv \frac{x - x_w}{x_b - x_w} \quad (\text{A7})$$

If all roofs are good thermal emitters, and colored roofs have solar absorptances between those of the white and black roofs, the normalized thermal properties have expected values between 0 (white) and 1 (black). Inspection of Eqs. (A2) through (A6) shows that the normalized roof surface temperature, attic air temperature, and ceiling heat flux are all equal, constant, and dependent only on the solar absorptances of the roofs:

$$\hat{T}_s = \hat{T}_a = \hat{q} = \frac{\alpha - \alpha_w}{\alpha_b - \alpha_w} \quad (\text{A8})$$

### Averaging Normalized Properties to Eliminate Transients

In practice, the tendency of dark, thermally-massive surfaces to heat more rapidly than light, thermally-massive surfaces, combined with minor, solar-angle-related differences among buildings in incident insolation and radiative cooling, will make these normalized properties vary somewhat over the course of the day. One way to characterize the thermal performance of a colored-roof building is to use a daytime-averaged value of each normalized property,  $\hat{x}_{\text{avg}}$ , and invert the normalization definition [Eq. (A7)] to express the absolute colored-roof building property  $x$  in terms of the absolute white- and black-roofed building properties  $x_w$  and  $x_b$ :

$$x \approx x_w + (x_b - x_w) \hat{x}_{\text{avg}} \quad (\text{A9})$$

This characteristic is particularly useful when comparing the thermal properties of two colored-roof buildings (e.g., a cool red and a standard red) for which the difference in their absolute values might be comparable in magnitude to solar-angle-dependent noise. For example, this technique may be used to evaluate the absolute difference between the daily peak properties of a cool roof and a standard roof as

$$\Delta x_{\text{peak}} \approx (x_{b,\text{peak}} - x_{w,\text{peak}}) (\hat{x}_{\text{standard,avg}} - \hat{x}_{\text{cool,avg}}) \quad (\text{A10})$$

### **Absolute Reductions in Roof Surface Temperature, Attic Air Temperature, and Ceiling Heat Flux**

Further inspection of Eqs. (A2) through (A6) indicates that reducing roof solar absorptance by  $\Delta\alpha$  (say, by switching from a standard color coating to a cool color coating) will lower the roof surface temperature, attic air temperature, and ceiling heat flux by

$$\Delta T_s = \frac{R_o R_r R_i}{R_o R_r + (R_o + R_r) R_i} \times I \Delta\alpha \quad (\text{A11})$$

$$\Delta T_a = \frac{R_i + R_c - R_d}{2 R_i} \Delta T_s \quad (\text{A12})$$

and

$$\Delta q = R_i^{-1} \Delta T_s \quad (\text{A13})$$

respectively. Since the reductions in roof surface temperature, attic air temperature, and ceiling heat flux are all proportional to the decrease in absorbed solar radiation (or increase in reflected solar radiation),  $I \Delta\alpha$ , this suggests that measured reductions in each property  $x$  should be regressed to  $I \Delta\alpha$  to yield an empirical relation of the form

$$\Delta x = k_x \times I \Delta\alpha \quad (\text{A14})$$

where  $k_x$  is a fitted sensitivity.

### **Variation of Ceiling Heat Flux With Thermal Resistances**

The reduction in ceiling heat flux,  $\Delta q$ , and hence the sensitivity  $k_q$  measured in a scale model, depend on its various thermal resistances. The sensitivity  $k'_q$  applicable to another building whose resistances are denoted with primes may be extrapolated from the measured  $k_q$  via the relation

$$\frac{k'_q}{k_q} = \frac{\Delta q'}{\Delta q} = \frac{(R_o + R_r) R_i + R_o R_r}{(R_o + R_r) R'_i + R_o R_r} \quad (\text{A15})$$

The roof surface and attic air temperature sensitivities may similarly be extrapolated via the relations



$$\frac{k'_{T_s}}{k_{T_s}} = \frac{\Delta T'_s}{\Delta T_s} = \frac{R'_i}{R_i} \times \frac{\Delta q'}{\Delta q} \quad (\text{A16})$$

and

$$\frac{k'_{T_a}}{k_{T_a}} = \frac{\Delta T'_a}{\Delta T_a} = \frac{R'_i + R'_c - R'_d}{R_i + R_c - R_d} \times \frac{\Delta q'}{\Delta q} \quad (\text{A17})$$

respectively.

**Example.**  $\Delta q$  and  $k_q$  are measured using a model house whose concrete roof tiles are painted with a high-emittance coating [ $R_r \approx 0.17 \text{ m}^2 \text{ K W}^{-1}$ ] and situated in a moderate wind [ $R_o \approx 0.08 \text{ m}^2 \text{ K W}^{-1}$ ]. The ceiling of the model house is an R-11 rigid foam board [ $R_c = 1.9 \text{ m}^2 \text{ K W}^{-1}$ ] with an aluminum foil upper face (average thermal emittance 0.06). Assuming the only mode of heat transfer between the tile and deck and between the deck and ceiling is radiative, the thermal resistance from the roof to the ceiling is the sum of the conductive resistance of the tile [ $R \approx 0.03 \text{ m}^2 \text{ K W}^{-1}$ ], the radiative resistance between the tile and deck [ $R \approx 0.2 \text{ m}^2 \text{ K W}^{-1}$ ], the conductive resistance of the wooden deck [ $R \approx 0.08 \text{ m}^2 \text{ K W}^{-1}$ ], and the radiative resistance between the deck and ceiling [ $R \approx 2.8 \text{ m}^2 \text{ K W}^{-1}$ ].<sup>7</sup> That is,  $R_s \approx 3.1 \text{ m}^2 \text{ K W}^{-1}$ , and  $R_i = R_s + R_c \approx 4.7 \text{ m}^2 \text{ K W}^{-1}$ . We can use Eq. (A15) to estimate  $\Delta q'$  and  $k'_q$  for a similarly tiled and situated real house that has an R-2 ceiling ( $0.35 \text{ m}^2 \text{ K W}^{-1}$ ) topped with R-11 attic insulation ( $1.9 \text{ m}^2 \text{ K W}^{-1}$ ), but does not have a radiant barrier:

$$\frac{k'_q}{k_q} = \frac{\Delta q'}{\Delta q} = \frac{(0.08 + 0.17)(4.7) + (0.08)(0.17)}{(0.08 + 0.17)(2.8) + (0.08)(0.17)} = 1.7 \quad (\text{A18})$$

Hence, the absolute increase in ceiling heat flux for the real house would be 1.7 times greater than that measured for the model house. In the limiting case of a real house with no attic

---

<sup>7</sup> The high thermal resistance between the lower surface of the roofdeck and the upper surface of the scale-model house ceiling results from the low thermal emittance of the foil facing on the top of the insulation board that serves as the ceiling. The expression for radiative thermal resistance  $R$  between two parallel surfaces of emittances  $\varepsilon_1$  and  $\varepsilon_2$  is  $R = h_r^{-1} (\varepsilon_1^{-1} + \varepsilon_2^{-1} - 1)$ . The radiation coefficient  $h_r \approx 4 \sigma \bar{T}^3$ , where  $\sigma$  is the Stefan-Boltzmann constant and  $\bar{T}$  is a temperature characteristic of the surfaces.

insulation [ $R'_c = 0.35$  and  $R'_t = 0.85$ ], the absolute increase in ceiling heat flux would be about 3 times greater than that for a real house with R-11 attic insulation.

## Estimated Energy Savings for Full-Scale House

### Estimating Annual Energy Savings from Annual Load-Hour Insolation

Assume that reducing roof solar absorptance by  $\Delta\alpha$  decreases ceiling heat flux [ $\text{W m}^{-2}$ ] by  $\Delta q = k_q \times I \Delta\alpha$ , where  $I$  is global horizontal insolation [ $\text{kW m}^{-2}$ ] and  $k_q$  is an experimentally determined sensitivity. The annual cooling energy savings [ $\text{kWh}$ ] accrued to a house of ceiling area  $A$  will be

$$\Delta E = \frac{1}{\text{COP}} \times A \int_{\tau_{\text{load}}} \Delta q(\tau) d\tau = \frac{1}{\text{COP}} \times A k_q \Delta\alpha \int_{\tau_{\text{load}}} I(\tau) d\tau \quad (\text{A19})$$

where COP is the air conditioner's coefficient of performance (output cooling power / input electrical power),  $\tau$  is time, and  $\int_{\tau_{\text{load}}} I(\tau) d\tau$  is the annual global horizontal insolation [ $\text{kWh m}^{-2}$ ] incident on the roof during those hours in which there is a positive ceiling heat flux into the interior of the house that is then removed by air conditioning.

### Estimating Annual Load-Hour Insolation from Annual Operating Days and Monthly Cooling Degree Days

The number of operating days in month  $m$  can be estimated by apportioning the number of annual operating days  $d_{\text{annual}}$  according to the fraction of annual cooling degree days (say, CDD24C) contained in each month,  $f_m \equiv \frac{\text{CDD24C}_m}{\text{CDD24C}_{\text{annual}}}$ :

$$d_m = f_m \times d_{\text{annual}} \quad (\text{A20})$$

The average daily insolation [ $\text{kWh day}^{-1}$ ] in month  $m$  is

$$J_m = \frac{1}{\text{calendar days in month } m} \times \int_{\text{month } m} I(\tau) d\tau \quad (\text{A21})$$

A residential air conditioner is typically scheduled to activate in late afternoon; hence, it has to remove heat that has built up in the structure over the course of the day, as well as remove the flux coming through the ceiling during its hours of operation. We assume that some fraction  $\phi$  (say, half) of all insolation received during a day on which the air conditioner runs results in

ceiling heat flux that must ultimately be removed from the building interior by the air conditioner. This yields

$$\int_{\tau_{\text{load}}} I(\tau) d\tau = \phi \sum_m d_m J_m = \phi d_{\text{annual}} \sum_m f_m J_m = \phi d_{\text{annual}} \bar{J} \quad (\text{A22})$$

where  $\bar{J}$  is the CDD24C-weighted average of daily insolation [ $\text{kWh m}^{-2} \text{ day}^{-1}$ ] (Table 7, p.27).

### Estimating Annual Operating Days

Consider a typical 1,500  $\text{ft}^2$  ( $A = 139 \text{ m}^2$ ), single-family house cooled by a 3-ton (36  $\text{kBTU h}^{-1}$ ), EER-8 unit drawing 4.5 kW. If the air conditioner typically runs  $n$  hours/day (say,  $n = 6$ ) when the weather is warm enough to require operation, the annual number of operating days  $d_{\text{annual}}$  is

$$d_{\text{annual}} = \frac{\tilde{E}}{\tilde{P} \times n} \quad (\text{A23})$$

where  $\tilde{E} = A \times E$  is annual cooling energy consumption [ $\text{kWh}$ ] and  $\tilde{P} = A \times P$  is cooling power demand [ $\text{kW}$ ]. We obtain  $\tilde{E}$  from prior simulations of annual cooling energy consumption versus level of ceiling insulation  $R_c$  for houses in three California climates: hot Central-Valley city Fresno; temperate Inland-Empire city San Bernardino; and cool, coastal San Diego (Schultz 1983). Regression of the simulated data yields climate-specific functions of the form

$$\tilde{E} = \tilde{E}_0 + bU_i \quad (\text{A24})$$

where  $\tilde{E}_0$  is the annual cooling energy consumption due to heat sources other than the ceiling (e.g., wall and internal loads),  $U_i \equiv R_i^{-1}$  is the thermal conductance from roof to interior [ $\text{W m}^{-2} \text{ K}^{-1}$ ], and  $bU_i$  is the annual cooling energy consumption due to heat gain through the ceiling (Figure 10, p.33). The roof-to-interior resistance is the sum of the roof assembly resistance (R-1.8), attic insulation (R-0 to R-30), and ceiling resistance (R-1.8). The number of operating hours,  $\tilde{E}/\tilde{P}$ , versus ceiling resistance in each climate is shown in Table 8 (p.27).

## Tables

Table 1. Color-pair trial solar reflectances and schedule (summer 2003). Note that since the roof surface is opaque, solar reflectance increase  $\Delta\rho$  is equivalent to solar absorptance decrease  $\Delta\alpha$ .

Color	$\rho_{\text{standard}}$	$\rho_{\text{cool}}$	$\Delta\rho$	Trial Dates	Clear-Weather Day, A/C On	Clear-Weather Day, A/C Off
TERRACOTTA	0.33	0.48	0.15	Jun 6 – Jul 1	Jun 15	Jun 30
CHOCOLATE	0.12	0.41	0.29	Jul 6 – 15	Jul 6	Jul 10
GRAY	0.21	0.44	0.23	Jul 17 – Aug 6	Jul 27	Jul 31
GREEN	0.17	0.46	0.29	Aug 8 - 19	Aug 16	Aug 8
BLUE	0.19	0.44	0.25	Aug 21– Sep 3	Aug 22	Aug 31
BLACK	0.04	0.41	0.37	Sep 4- Oct 6	Sep 14	Sep 5

Table 2. Reductions in scale-model peak tile surface temperature, peak attic air temperature, peak ceiling heat flux (A/C on only), and peak interior air temperature (A/C off only) measured in each of six color-pair trials.

decrease in solar absorptance ( $\Delta\alpha = \Delta\rho$ )	terracotta 0.15	chocolate 0.29	gray 0.23	green 0.29	blue 0.25	black 0.37
<b>AC on</b>						
trial date	2003-6-15	2003-7-10	2003-7-27	2003-8-16	2003-8-22	2003-9-14
peak horizontal insolation ( $\text{kW m}^{-2}$ )	873	778	817	834	822	734
reduction of peak tile surface temperature (K)	4.6	8.6	6.7	9.6	8.2	13.8
reduction of peak attic air temperature (K)	1.9	3.7	2.8	3.9	2.3	5.5
reduction of peak ceiling heat flux ( $\text{W m}^{-2}$ )	1.0 (13%)	1.7 (17%)	1.4 (15%)	2.0 (17%)	1.1 (13%)	2.1 (21%)
<b>AC off</b>						
trial date	2003-6-30	2003-7-6	2003-7-31	2003-8-8	2003-8-31	2003-9-5
peak horizontal insolation ( $\text{W m}^{-2}$ )	863	847	848	856	794	766
reduction of peak tile surface temperature (K)	5.5	9.4	6.8	11.0	8.2	13.5
reduction of peak attic air temperature (K)	3.0	4.0	2.8	4.5	2.4	7.2
reduction of peak interior air temperature (K)	0.8	1.0	1.1	1.1	0.7	1.8

Table 3. Sensitivities of the peak roof surface temperature, attic air temperature, and ceiling heat flux in an air-conditioned house to peak decrease in absorbed insolation. Values are extrapolated from the scale-model results and assume a real house with an R-2 ceiling and no radiant barrier.

Attic Insulation (ft <sup>2</sup> h F BTU <sup>-1</sup> )	Roof Surface Temperature Sensitivity $k_{T_s} = \Delta T_s / I \Delta \alpha$ [K / (kW m <sup>-2</sup> )]	Attic Air Temperature Sensitivity $k_{T_a} = \Delta T_a / I \Delta \alpha$ [K / (kW m <sup>-2</sup> )]	Ceiling Heat Flux Sensitivity $k_q = \Delta q / I \Delta \alpha$ [(W m <sup>-2</sup> ) / (kW m <sup>-2</sup> )]
0	39.4	12.1	38.9
7	40.9	19.2	16.5
11	41.2	20.5	12.4
19	41.4	21.8	8.3
30	41.6	22.7	5.7

Table 4. Reductions in each of three climates in peak tile surface temperature, attic air temperature, ceiling heat flux, cooling power demand, and cooling energy use of an air-conditioned house per unit reduction in solar absorptance, tabulated versus ceiling insulation. Note that all figures must be multiplied by the reduction in solar absorptance (e.g.,  $\Delta \alpha = 0.3$ ).

Attic Insulation (ft <sup>2</sup> h F BTU <sup>-1</sup> )		0	7	11	19	30
Fresno	Tile Surface Temperature Reduction $\Delta T_s / \Delta \alpha$ (K)	40.9	42.4	42.7	43.0	43.2
	Attic Air Temperature Reduction $\Delta T_a / \Delta \alpha$ (K)	12.5	20.0	21.3	22.7	23.5
	Ceiling Heat Flux Reduction $\Delta q / \Delta \alpha$ (W m <sup>-2</sup> )	40.4	17.1	12.9	8.6	5.9
	Cooling Power Demand Reduction $\Delta P / \Delta \alpha$ (W m <sup>-2</sup> )	17.2	7.3	5.5	3.7	2.5
	Cooling Energy Use Reduction $\Delta E / \Delta \alpha$ (kWh m <sup>-2</sup> yr <sup>-1</sup> )	9.0	3.0	2.2	1.4	0.9
San Bernardino	Tile Surface Temperature Reduction $\Delta T_s / \Delta \alpha$ (K)	38.0	39.5	39.7	40.0	40.2
	Attic Air Temperature Reduction $\Delta T_a / \Delta \alpha$ (K)	11.6	18.6	19.8	21.1	21.9
	Ceiling Heat Flux Reduction $\Delta q / \Delta \alpha$ (W m <sup>-2</sup> )	37.6	15.9	12.0	8.0	5.5
	Cooling Power Demand Reduction $\Delta P / \Delta \alpha$ (W m <sup>-2</sup> )	16.0	6.8	5.1	3.4	2.3
	Cooling Energy Use Reduction $\Delta E / \Delta \alpha$ (kWh m <sup>-2</sup> yr <sup>-1</sup> )	6.8	2.2	1.6	1.0	0.7
San Diego	Tile Surface Temperature Reduction $\Delta T_s / \Delta \alpha$ (K)	37.0	38.4	38.7	38.9	39.1
	Attic Air Temperature Reduction $\Delta T_a / \Delta \alpha$ (K)	11.3	18.1	19.3	20.5	21.3
	Ceiling Heat Flux Reduction $\Delta q / \Delta \alpha$ (W m <sup>-2</sup> )	36.6	15.5	11.7	7.8	5.4
	Cooling Power Demand Reduction $\Delta P / \Delta \alpha$ (W m <sup>-2</sup> )	15.6	6.6	5.0	3.3	2.3
	Cooling Energy Use Reduction $\Delta E / \Delta \alpha$ (kWh m <sup>-2</sup> yr <sup>-1</sup> )	0.7	0.2	0.2	0.1	0.1

Table 5. Annual cooling energy savings per unit decrease in roof solar absorptance vs. ceiling insulation. Shown in each three climates are absolute savings, savings as a fraction of cooling energy required to dissipate the roof heat load, and savings as a fraction of whole-house cooling energy. Note that all figures must be multiplied by the reduction in solar absorptance (e.g.,  $\Delta\alpha = 0.3$ ).

Attic Insulation (ft <sup>2</sup> h F BTU <sup>-1</sup> )	FRESNO			SAN BERNARDINO			SAN DIEGO		
	absolute (kWh m <sup>-2</sup> yr <sup>-1</sup> )	roof fraction	house fraction	absolute (kWh m <sup>-2</sup> yr <sup>-1</sup> )	roof fraction	house fraction	absolute (kWh m <sup>-2</sup> yr <sup>-1</sup> )	roof fraction	house fraction
0	9.0	97%	33%	6.8	74%	29%	0.7	64%	26%
7	3.0	80%	14%	2.2	60%	12%	0.2	51%	11%
11	2.2	77%	11%	1.6	57%	9%	0.2	48%	8%
19	1.4	74%	7%	1.0	54%	6%	0.1	46%	6%
30	0.9	72%	5%	0.7	53%	4%	0.1	44%	4%

Table 6. Year-2003 number of air-conditioned houses in each Energy Commission demand forecasting climate zone (FCZ), and the fraction assigned to each simulation climate (Fresno, San Bernardino, or San Diego).

Forecasting Climate Zone	Houses (thousands)	Fresno	San Bernardino	San Diego
FCZ01	147			100%
FCZ02	314	100%		
FCZ03	907	100%		
FCZ04	660			100%
FCZ05	70			100%
FCZ06	435	100%		
FCZ07	176	100%		
FCZ08	820			100%
FCZ09	616	50%		50%
FCZ10	1007		100%	
FCZ11	279			100%
FCZ12	394	50%		50%
FCZ13	460			100%
FCZ14	0		100%	
FCZ15	0		100%	
FCZ16	145	50%		50%
<b>Total Houses (thousands)</b>	<b>6,430</b>	<b>2,410</b>	<b>1,010</b>	<b>3,010</b>

Table 7. Monthly cooling degree days at 24°C (CDD24C), average daily insolation (energy/area), and average peak insolation (power/area) in three climates. Shown also is each climate's CDD24C-weighted annual average daily insolation,  $\bar{J}$ .

month	FRESNO				SAN BERNARDINO				SAN DIEGO			
	CDD24C (days)	CDD24C fraction	average daily sun (kWh m <sup>-2</sup> )	average peak sun (W m <sup>-2</sup> )	CDD24C (days)	CDD24C fraction	average daily sun (kWh m <sup>-2</sup> )	average peak sun (W m <sup>-2</sup> )	CDD24C (days)	CDD24C fraction	average daily sun (kWh m <sup>-2</sup> )	average peak sun (W m <sup>-2</sup> )
January	0	0.00	2.33	419	0	0%	3.03	532	0	0%	2.33	428
February	0	0.00	3.60	599	0	0%	3.77	624	0	0%	3.18	543
March	0	0.00	4.95	746	0	0%	4.51	738	0	0%	4.45	700
April	0	0.00	6.47	900	0	0%	5.52	816	0	0%	5.44	786
May	20	0.04	7.55	967	0	0%	6.96	956	0	0%	6.28	841
June	92	0.18	8.66	1038	38	10%	7.37	946	0	0%	7.42	939
July	180	0.35	8.22	994	127	34%	7.50	965	0	0%	7.22	928
August	150	0.29	7.28	934	130	35%	6.22	891	10	67%	6.21	861
September	72	0.14	6.05	851	75	20%	5.76	831	5	33%	5.74	817
October	0	0.00	4.58	712	3	1%	4.52	713	0	0%	4.35	682
November	0	0.00	3.18	543	0	0%	3.59	600	0	0%	2.88	491
December	0	0.00	2.35	438	0	0%	2.89	516	0	0%	2.41	435
$\bar{J}$			<b>7.70</b>				<b>6.67</b>				<b>6.05</b>	

Table 8. Annual hours of residential air-conditioner operation versus attic insulation, simulated in each of 3 climates.

Attic Insulation (ft <sup>2</sup> h F BTU <sup>-1</sup> )	Fresno (h yr <sup>-1</sup> )	San Bernardino (h yr <sup>-1</sup> )	San Diego (h yr <sup>-1</sup> )
0	841	735	84
7	671	568	64
11	642	539	60
19	612	510	57
30	594	492	55

## Figures



Figure 1. Four identical 1:10-scale model houses sited in a courtyard at the Riverside Public Utilities facility in Riverside, CA. Counterclockwise from left (east), the four buildings are shown with (A) cool chocolate, (B) white, (C) black, and (D) standard chocolate roof tile coatings. An instrument shed lies in the center, while a weather tower stands in the foreground.



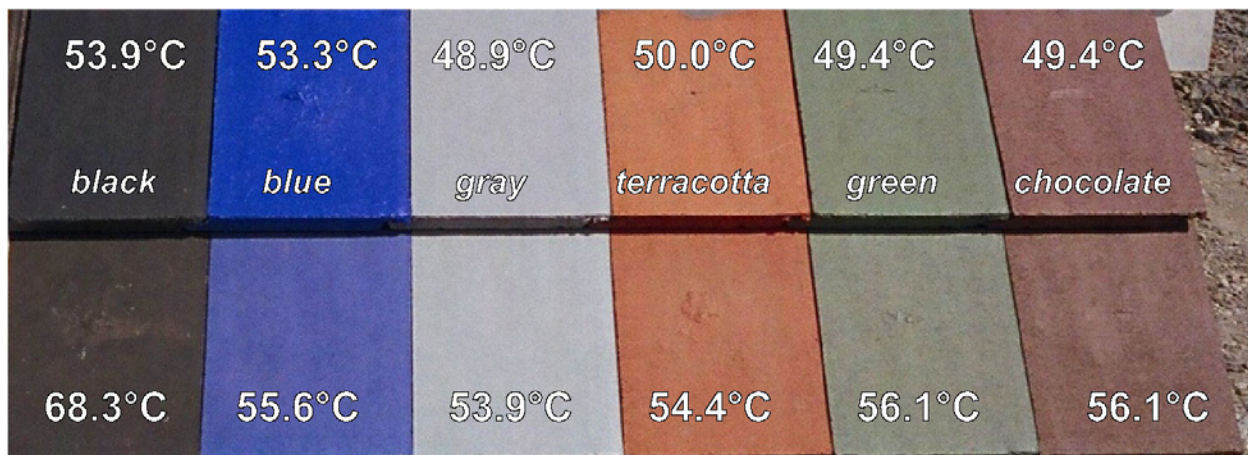


Figure 2. Appearance and surface temperatures of cool tile coatings (top row) formulated to match standard color coatings (bottom row). Surface temperatures were measured from 11:20 – 11:30AM solar on 17 September 2003 (outside air temperature 27°C, horizontal global insolation 820 W m<sup>-2</sup>).

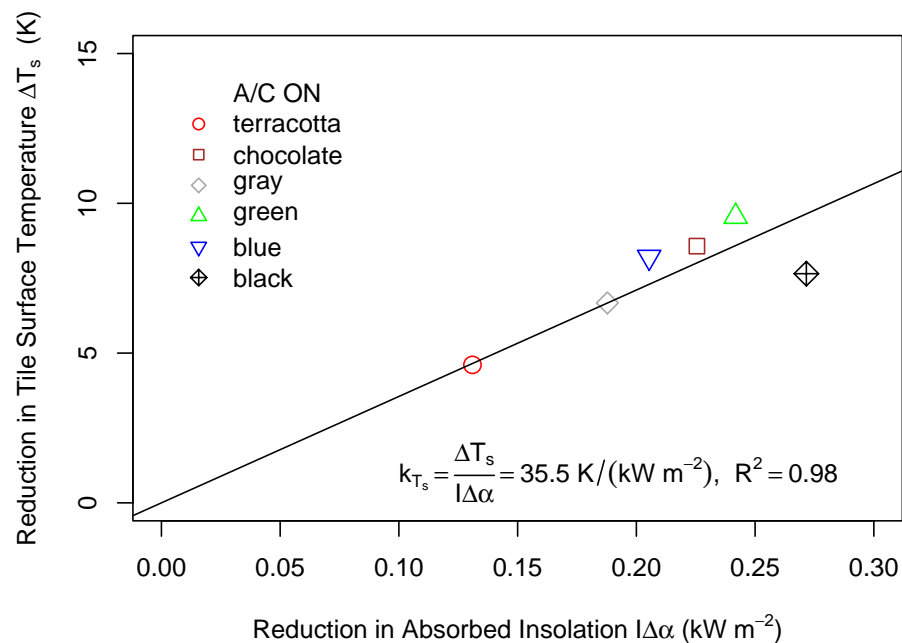


Figure 3. Measured reduction in peak roof tile surface temperature of an air-conditioned scale model vs. reduction in peak absorbed insolation achieved by switching from a standard color coating to a cool color coating.

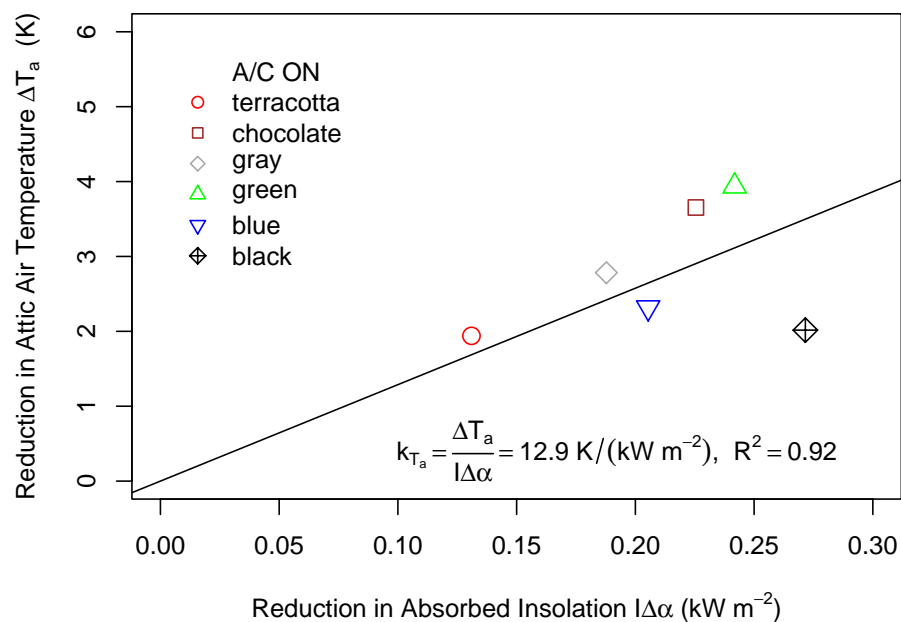


Figure 4. Measured reduction in peak attic air temperature of an air-conditioned scale model vs. reduction in peak absorbed insolation achieved by switching from a standard color coating to a cool color coating.

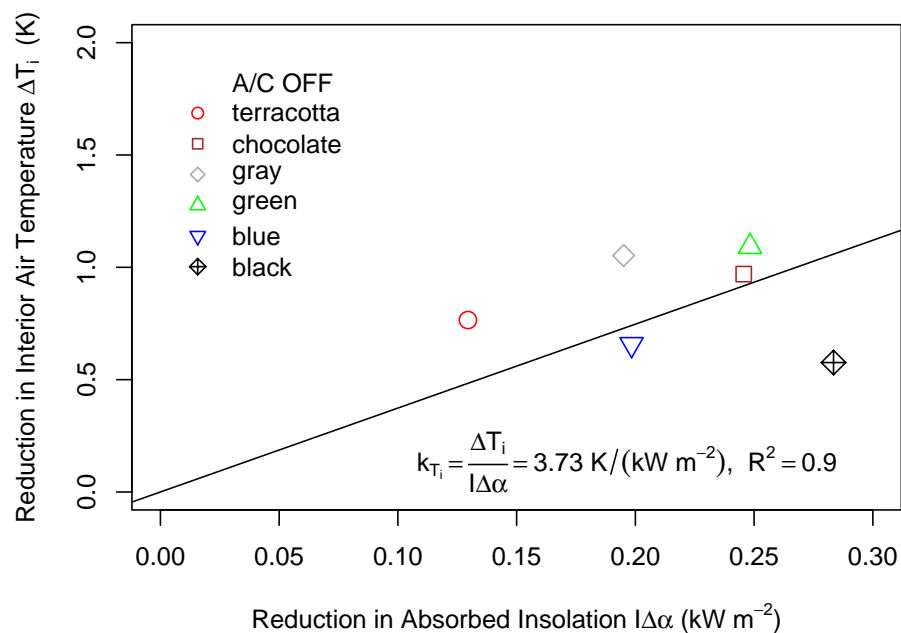


Figure 5. Measured reduction in peak interior air temperature of an unconditioned scale model vs. reduction in peak absorbed insolation achieved by switching from a standard color coating to a cool color coating.

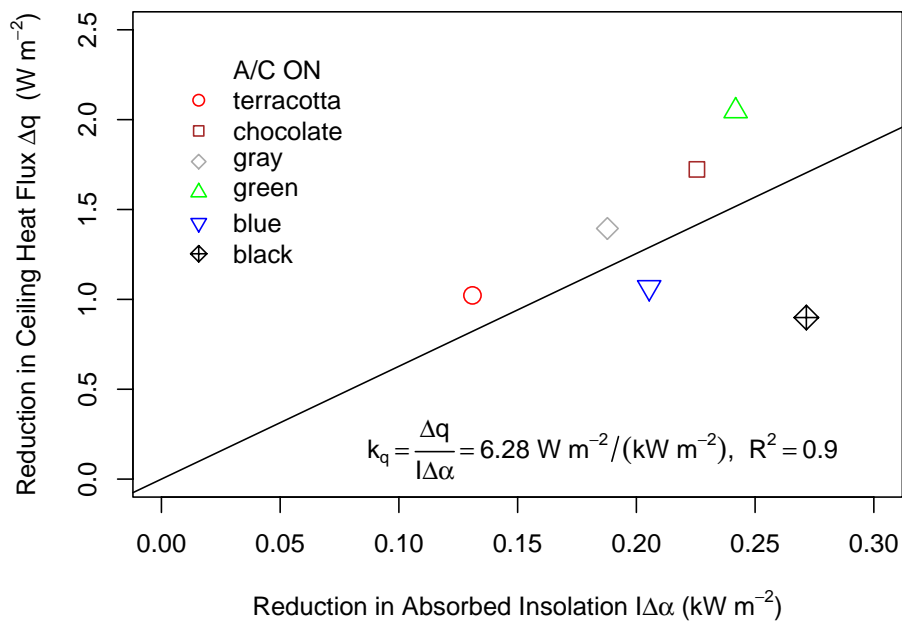


Figure 6. Measured reduction in peak ceiling heat flux into an air-conditioned scale model vs. reduction in peak absorbed insolation achieved by switching from a standard color coating to a cool color coating. Note that heat flux values have been adjusted to assume a common interior air temperature of 24°C.

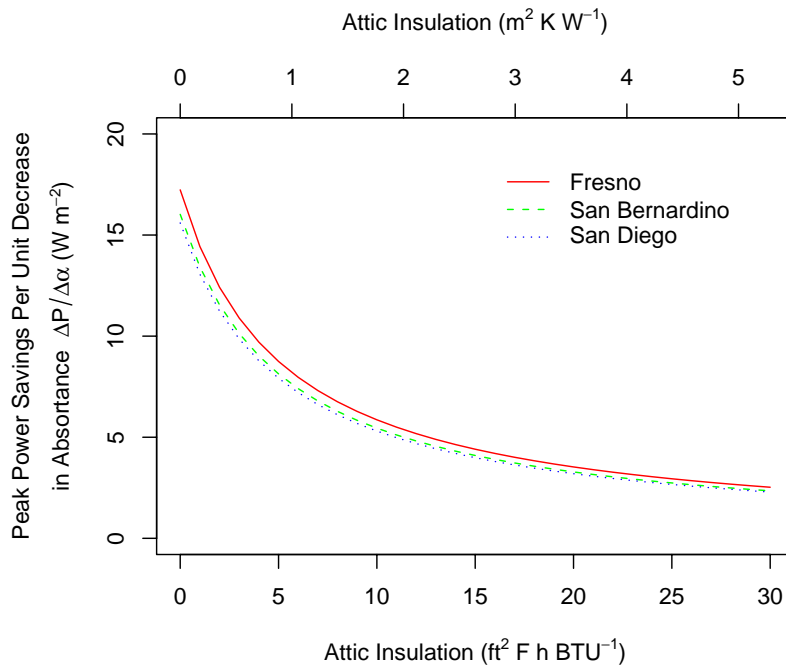


Figure 7. Estimated savings in real-house peak cooling power demand ( per unit ceiling area) per unit decrease in solar absorbance versus ceiling insulation. Note that this curve must be multiplied by reduction in roof solar absorbance (e.g.,  $\Delta\alpha = 0.3$ ) to obtain actual savings.

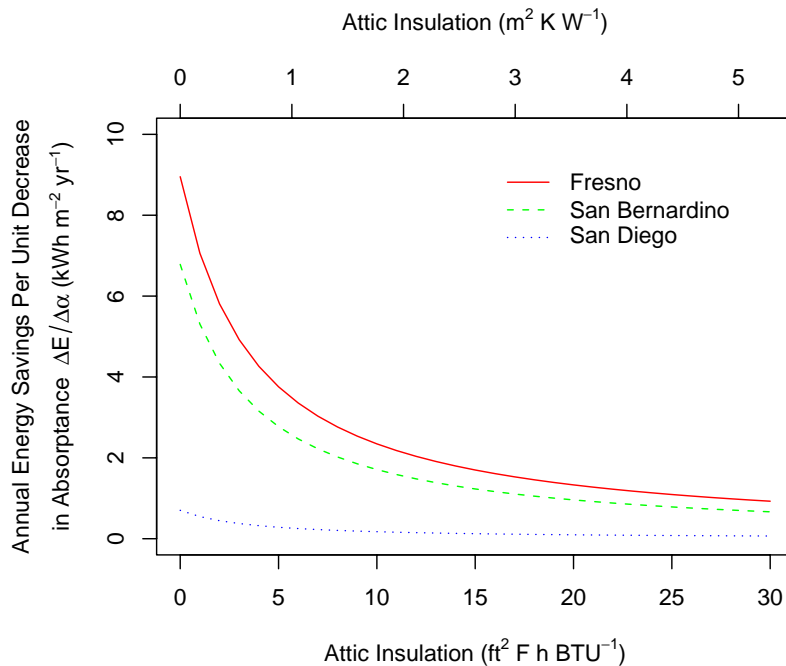


Figure 8. Estimated savings in real-house annual cooling energy consumption (per unit ceiling area) per unit decrease in solar absorptance versus ceiling insulation. Note that this curve must be multiplied by reduction in roof solar absorptance (e.g.,  $\Delta\alpha = 0.3$ ) to obtain actual savings.



Figure 9. The Energy Commission's 16 demand forecasting climate zones in California. Note that these differ from the California Thermal Zones commonly used in building simulations.

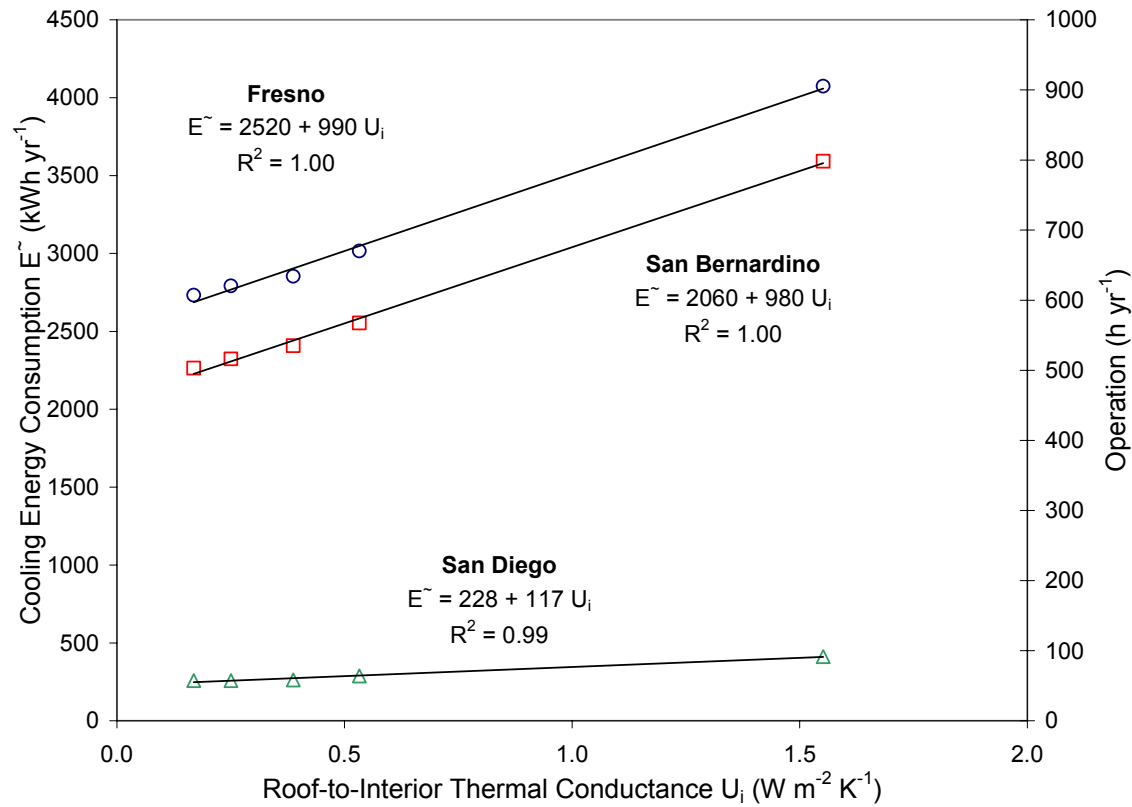


Figure 10. Annual cooling energy consumed by a 1,500 ft<sup>2</sup> (139 m<sup>2</sup>) single-family house versus roof-to-interior thermal conductance, simulated in each of three climates. Annual hours of operation assume a 3-ton, EER-8 air conditioner (power demand 4.5 kW).

# PROFESSIONAL ROOFING

## Cooling down the house

### Residential roofing products soon will boast "cool" surfaces

by **Hashem Akbari and André Desjarlais**

Energy-efficient roofing materials are becoming more popular, but most commercially available products are geared toward the low-slope sector. However, research and development are taking place to produce "cool" residential roofing materials.

In 2002, the California Energy Commission asked Lawrence Berkeley National Laboratories (LBNL), Berkeley, Calif., and Oak Ridge National Laboratories (ORNL), Oak Ridge, Tenn., to collaborate with a consortium of 16 manufacturing partners and develop "cool" non-white roofing products that could revolutionize the residential roofing industry.

The commission's goal is to create dark shingles with solar reflectances of at least 0.25 and other nonwhite roofing products—including tile and painted metal—with solar reflectances not less than 0.45. The manufacturing partners have raised the maximum solar reflectance of commercially available dark products to 0.25-0.45 from 0.05-0.25 by reformulating their pigmented coatings. (For a list of the manufacturers, see "[Manufacturing partners](#)," page 36.)

Because coatings colored with conventional pigments tend to absorb invisible "near-infrared" (NIR) radiation that bears more than half the power of sunlight (see Figure 1), replacing conventional pigments with "cool" pigments that absorb less NIR radiation can yield similarly colored coatings with higher solar reflectances. These cool coatings lower roof surface temperatures, reducing the need for cooling energy in conditioned buildings and making unconditioned buildings more comfortable.

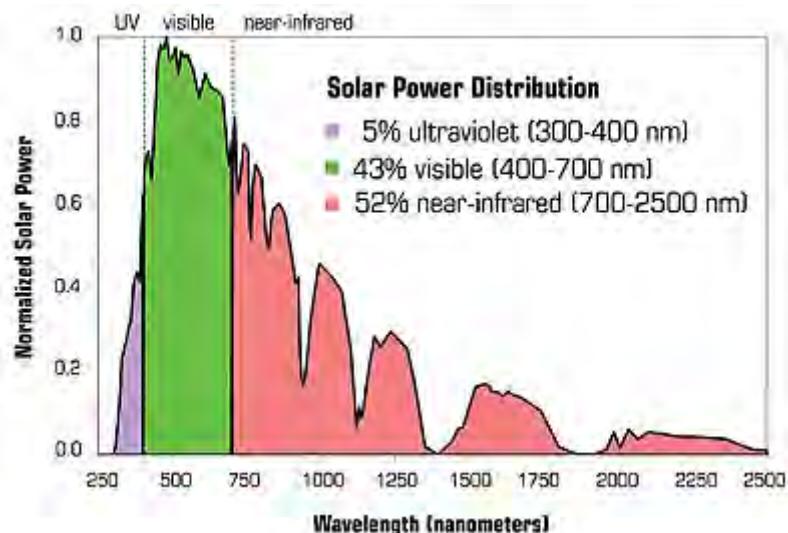


Figure courtesy of the Lawrence Berkeley National Laboratories, Berkeley, Calif.

**Figure 1: Peak-normalized solar spectral power—more than half of all solar power arrives as invisible, "near-infrared" radiation**

Cool, nonwhite roofing materials are expected to penetrate the roofing market within the next three years to five years. Preliminary analysis by LBNL and ORNL suggests the materials may cost up to \$1 per square meter more than conventionally colored roofing materials. However, this would raise the total cost of a new roof system only 2 percent to 5 percent.

### Cool, nonwhite colors

Developing the colors to achieve the desired solar reflectances involves much research and development. So far, LBNL has characterized the optical properties of 87 common and specialty pigments that may be used to color architectural surfaces. Pigment analysis begins with measurement of the reflectance— $r$ —and transmittance— $t$ —of a thin coating, such as paint film, containing a single pigment, such as iron oxide red. These "spectral," or wavelength-dependent, properties of the pigmented coating are measured at 441 evenly spaced wavelengths spanning the solar spectrum (300 nanometers to 2,500 nanometers).

Inspection of the film's spectral absorbance (calculated as  $1-r-t$ ) reveals whether a pigmented coating is "cool" (has low NIR



absorptance) or "hot" (has high NIR absorptance). The spectral reflectance and transmittance measurements also are used to compute spectral rates of light absorption and backscattering (reflection) per unit depth of film. The spectral reflectance of a coating colored with a mixture of pigments then can be estimated from the spectral absorption and backscattering rates of its components.

LBNL has produced a database detailing the optical properties of the 87 characterized pigmented coatings (see Figure 2). Its researchers are developing coating formulation software intended to minimize NIR absorptance (and maximize the solar reflectance) of a color-matched pigmented coating. The database and software will be shared with the consortium manufacturers later this year.



Figure courtesy of Lawrence Berkeley National Laboratories, Berkeley, Calif.

**Figure 2: Description of a red iron oxide pigment in the Lawrence Berkeley National Laboratory pigment database**

## Shingles

A new shingle's solar reflectance is dominated by the solar reflectance of its granules, which cover more than 97 percent of its surface. Until recently, the way to produce granules with high solar reflectance has been to use a coating pigmented with titanium dioxide (TiO<sub>2</sub>) white. Because a thin TiO<sub>2</sub>-pigmented coating is reflective but not opaque in NIR, multiple layers are needed to obtain high solar reflectance. Thin coatings colored with cool, nonwhite pigments also transmit NIR radiation. Any NIR light transmitted through the pigmented coating will strike the granule aggregate where it will be absorbed (typical dark rock) or reflected (typical white rock).

Multiple color layers, a reflective undercoating and/or reflective aggregate can increase granules' solar reflectances, thereby increasing shingles' solar reflectances.

Figure 3 shows the iterative development of a cool black shingle prototype by ISP Minerals Inc., Hagerstown, Md. A conventional black roof shingle has a reflectance of about 0.04. Replacing the granule's standard black pigment with a cool NIR-scattering black pigment (prototype 1) increases the solar reflectance of the shingle to 0.12. Incorporating a thin white sublayer (prototype 2) raises the shingle's solar reflectance to 0.16; using a thicker white sublayer (prototype 3) increases the shingle's reflectance to 0.18. The figure also shows an approximate performance limit (solar reflectance 0.25) obtained by applying 25-micron NIR-reflective black topcoat over an opaque white background.

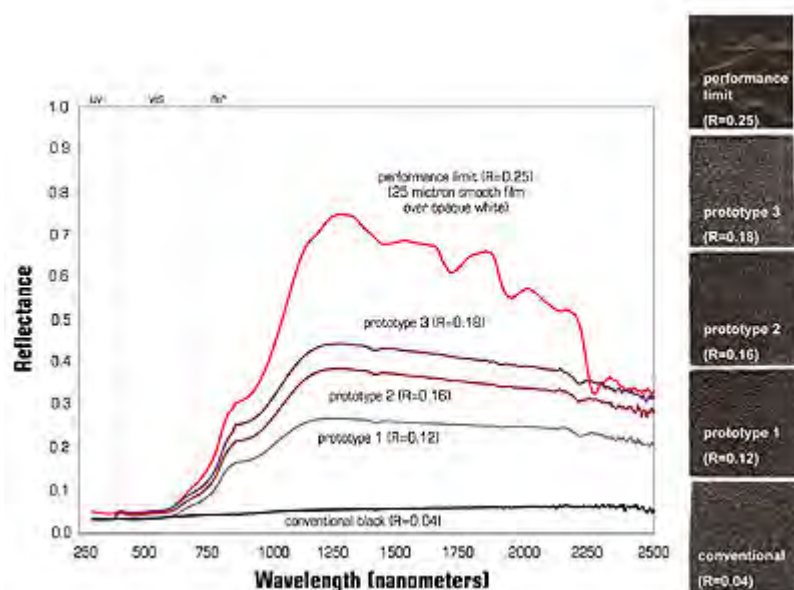


Figure courtesy of Lawrence Berkeley National Laboratories, Berkeley, Calif.

**Figure 3: ISP Minerals Inc., Hagerstown, Md., is developing a cool, black shingle. Shown are the solar spectral reflectances, images and solar reflectances (R) of a conventional black shingle; three prototype cool, black shingles; and smooth, cool, black film over an opaque white background.**

## Tile

There are three ways to improve solar reflectances of colored tiles: use clay or concrete with low concentrations of light-absorbing impurities, such as iron oxides and elemental carbon; color tile with cool pigments contained in a surface coating or mixed integrally; and/or include an NIR-reflective sublayer, such as a white sublayer, beneath an NIR-transmitting colored topcoat.

American Rooftile Coatings, Fullerton, Calif., has developed a palette of cool, nonwhite coatings for concrete tiles. Each of its COOL TILE IR COATINGS™ shown in Figure 4 has a solar reflectance greater than 0.40. The solar reflectance of each cool coating exceeds that of a color-matched, conventionally pigmented coating by 0.15 (terra cotta) to 0.37 (black).

## Metal

Cool, nonwhite pigments can be applied to metal with or without a white sublayer. If a metal is highly reflective, the sublayer may be omitted. The polymer coatings on metal panels are kept thin to withstand bending. This restriction on coating thickness limits pigment loading (pigment mass per unit surface area).

## Performance research

ORNL naturally is weathering various types of conventionally pigmented and cool-pigmented roofing products at seven California sites. Each "weathering farm" has three south-facing racks for exposing samples of roofing products at typical roof slopes. Sample weathering began in August 2003 and will continue for three years—until October 2006. Solar reflectance and thermal emittance are measured twice per year; weather data are available continuously. Solar spectral reflectance is measured annually to gauge soiling and document imperceptible color changes.

ORNL and the consortium manufacturers also are exposing roof samples to 5,000 hours of xenon-arc light in a weatherometer, a laboratory device that accelerates aging via exposure to ultraviolet radiation and/or water spray. ORNL will examine the naturally weathered samples for contaminants and biomass to identify the agents responsible for soiling. This may help manufacturers produce roofing materials that better resist soiling and retain high solar reflectance. Changes in reflectance will be correlated to exposure.

The labs and manufacturing partners also have established residential demonstration sites in California. The first, in Fair Oaks



(near Sacramento), includes two pairs of single-family, detached homes. One pair is roofed with color-matched conventional and cool-painted metal shakes supplied by Custom-Bilt Metals, South El Monte, Calif., and the other features color-matched conventional and cool low-profile concrete tiles supplied by Hanson Roof Tile, Charlotte, N.C. The second site, in Redding, is under construction and by summer will have a pair of homes roofed with color-matched conventional and cool asphalt shingles.

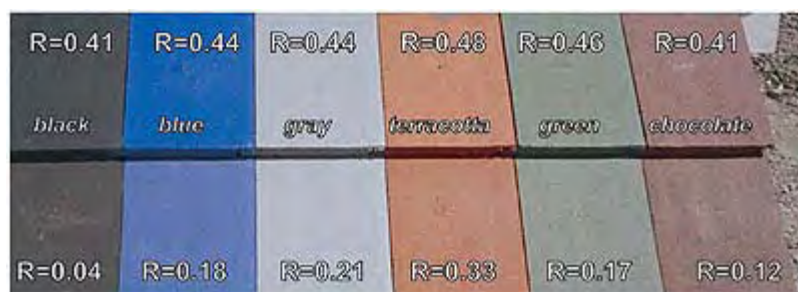


Figure courtesy of American Rooftile Coatings.

**Figure 4:** This is a palette of color-matched cool (top row) and conventional (bottom row) roof tile coatings developed by American Rooftile Coatings, Fullerton, Calif. Shown on each coated tile is its solar reflectance.

The homes in Fair Oaks are adjacent and share the same floor plan, roof orientation and level of blown ceiling insulation (19 hr•ft<sup>2</sup>•°F/Btu). The homes in Fair Oaks and Redding will be monitored through at least summer 2006.

One of the Fair Oaks homes roofed with low-profile concrete tile was colored with a conventional chocolate brown coating (solar reflectance 0.10), and the other was colored with a matching cool chocolate brown (an American Rooftile Coatings COOL TILE IR COATING™ with solar reflectance 0.41). The attic air temperature beneath the cool brown tile roof has been measured to be 3 K to 5 K cooler than that below the conventional brown tile roof during a typical hot summer afternoon (273.15 K equals 0 C).

The results for the pair of Fair Oaks homes roofed with painted metal shakes are just as promising. There, the attic air temperature beneath the cool brown metal shake roof (solar reflectance 0.31) was measured to be 5 K to 7 K cooler than that below the conventional brown metal shake roof.

These reductions in attic temperature are solely the result of the application of cool, colored coatings. The use of these cool, colored coatings also decreased the total daytime heat influx (solar hours are from 8 a.m.-5 p.m.) through the west-facing concrete tile roof by 4 percent and the south-facing metal shake roof by 31 percent (see Figure 5).

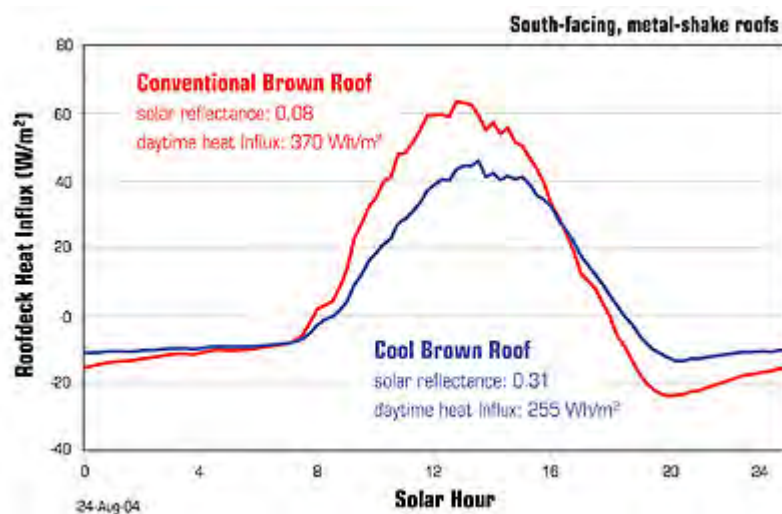


Figure courtesy of Oak Ridge National Laboratory, Oak Ridge, Tenn.

**Figure 5:** Heat flows through the roof decks of an adjacent pair of homes during the course of a hot summer day. The total daily heat influx through the cool brown metal shake roof (solar reflectance 0.31) between the solar hours of 8 a.m. and 5 p.m. is 31 percent lower than through the conventional brown metal shake roof (solar reflectance 0.08).

ORNL also is testing several varieties of concrete and clay tile on a steep-slope roof to further investigate the individual and combined effects of cool, colored coatings and subtile ventilation on the thermal performance of a cool roof system.

## Results to date

The two laboratories and their industrial partners have achieved significant success in developing cool, colored materials for

concrete tile, clay tile and metal roofs.

Since the inception of this program, the maximum solar reflectances of commercially available dark roofing products has increased to 0.25-0.45 from 0.05-0.25. Bi-layer coating technology (a color topcoat over a white or other highly reflective undercoat) is expected to soon yield several cost-effective cool, colored shingle products with solar reflectances in excess of the U.S. Environmental Protection Agency's ENERGY STAR® threshold of 0.25. Early monitoring results indicate using cool, colored roofing products measurably reduces heat flow into conditioned homes with code-level ceiling insulation.

As homeowners continue to seek energy-efficient products, the roofing industry's research into residential roofing products that offer energy-efficient features naturally will continue to evolve.

Provided energy-efficient products continue to perform satisfactorily, we expect cool, nonwhite metal, tile and shingle products to penetrate the roofing market within the next three to five years.

*Hashem Akbari leads LBNL's Heat Island Group. André Desjarlais leads ORNL's Building Envelope Group.*

**Editor's note:** Ronnen Levinson, scientist, Paul Berdahl, staff scientist, and Stephen Wiel, staff scientist, of LBNL; William Miller senior research engineer of ORNL; and Nancy Jenkins, program manager, Arthur Rosenfeld, commissioner, and Chris Scruton, project manager, of the California Energy Commission contributed to this article.

---

## Manufacturing partners

### 3M

St. Paul, Minn.

[www.scotchgard.com/roofinggranules](http://www.scotchgard.com/roofinggranules)

### Akzo Nobel

Felling, United Kingdom

[www.akzonobel.com](http://www.akzonobel.com)

### American Rooftile Coatings

Fullerton, Calif.

[www.americanrooftilecoatings.com](http://www.americanrooftilecoatings.com)

### BASF Industrial Coatings

Florham Park, N.J.

[www.ultra-cool.basf.com](http://www.ultra-cool.basf.com)

### CertainTeed Corp.

Valley Forge, Pa.

[www.certainteed.com](http://www.certainteed.com)

### Custom-Bilt Metals

South El Monte, Calif.

[www.custombiltmetals.com](http://www.custombiltmetals.com)

### Elk Corp.

Dallas

[www.elkcorp.com](http://www.elkcorp.com)

### Ferro Corp.

Cleveland

[www.ferro.com](http://www.ferro.com)

### GAF Materials Corp.

Wayne, N.J.

[www.gaf.com](http://www.gaf.com)

### Hanson Roof Tile

Charlotte, N.C.

[www.hansonrooftile.com](http://www.hansonrooftile.com)

### ISP Minerals Inc.

Hagerstown, Md.

### MCA Tile

Corona, Calif.

[www.mca-tile.com](http://www.mca-tile.com)

**MonierLifetile LLC**

Irvine, Calif.

[www.monierlifetile.com](http://www.monierlifetile.com)

**Owens Corning**

Toledo, Ohio

[www.owenscorning.com/around/roofing/Roofhome.asp](http://www.owenscorning.com/around/roofing/Roofhome.asp)

**Shepherd Color Co.**

Cincinnati

[www.shepherdcolor.com](http://www.shepherdcolor.com)

**Steelscape Inc.**

Kalama, Wash.

[www.steelscape-inc.com](http://www.steelscape-inc.com)

---

**Web-exclusive information** — [Study about the development of cool, colored roofing materials](#)

[© Copyright 2006 National Roofing Contractors Association](#)